INVESTIGATING POLLEN SIGNALLING NETWORKS TRIGGERED BY THE SELF-INCOMPATIBILITY RESPONSE IN *PAPAVER RHOEAS*

by

KATIE ANNE WILKINS

A thesis submitted to
The University of Birmingham
for the degree of
DOCTOR OF PHILOSOPHY

School of Biosciences
The University of Birmingham
Februaury 2013

UNIVERSITYOF
BIRMINGHAM

University of Birmingham Research Archive

e-theses repository

ABSTRACT

Self-incompatibility (SI) is a genetic mechanism which prevents self-fertilisation via the recognition and rejection of 'self' pollen. In the self-incompatible species *Papaver rhoeas* L., rejection of incompatible pollen is achieved through interaction of the female and male *S*-determinants, PrsS and PrpS, respectively. This interaction results in a Ca^{2+}-dependent signalling cascade in the 'self' pollen, which mediates programmed cell death (PCD). To date, many downstream effects of SI signalling cascade have been identified, including actin depolymerization, the formation of actin foci, and the activation of caspase-like activities. Work presented in this thesis identified the involvement of Reactive Oxygen Species (ROS) and Nitric Oxide (NO) in the SI response, and the temporal and spatial patterns were characterized. Other studies identified SI-induced cytosolic acidification as a key step in SI. Moreover, investigation of the role of ROS, NO and H^+ revealed that they all play a role in triggering key features of SI: actin foci formation and caspase-3-like activity. Other studies also provided the first evidence for vacuolar breakdown in SI in this species. Data presented also show the first documentation of SI-induced alterations in phospholipids. Together these data further our understanding of mechanisms involved in the complex SI signalling network.

DEDICATION

I lovingly dedicate this thesis to my wonderful Mum, Liz. Without her support, encouragement and unconditional love I would never have had the strength or determination to pursue my dreams and be the person that I am today.

ACKNOWLEDGEMENTS

TABLE OF CONTENTS

LIST OF FIGURES AND TABLES

CHAPTER 1: INTRODUCTION

CHAPTER 2: MATERIALS AND METHODS

CHAPTER 4: INVESTIGATING A POSSIBLE ROLE FOR PHOSPHOLIPID SIGNALLING DURING THE SELF INCOMPATIBILTY (SI) RESPONSE IN *PAPAVER RHOEAS* POLLEN TUBES

CHAPTER 5: ACIDIFICATION OF THE CYTOSOL OF SI-INDUCED POLLEN TUBES

CHAPTER 6: INVESTIGATING THE VACUOLE AS A POTENTIAL SOURCE OF SI-INDUCED ACIDIFICATION

CHAPTER 7: GENERAL DISCUSSION

APPENDIX I

ABBREVIATIONS

ADF: Actin depolymerising factor

BCECF AM: 2′,7′‑bis‑(2‑carboxyethyl)‑5‑(and‑6)‑carboxyfluorescein ester

BSA: Bovine serum albumin

CAP: Cyclase associated protein

c-DCFDA: 5-(and-6)-Carboxy-2',7'-dichlorofluorescein diacetate

CP: Capping Protein

c-PTIO: 2-(4-carboxyphenyl)-4,4,5,5- tetramethylimidazoline-1-oxyl-3-oxide

DAG: diacylglycercol

DGPP: diacylglycercol pyrophosphatase

DPI: Diphenyleneiodonium

F-actin: Filamentous actin (actin MFs)

FITC: Fluorescein isothiocyanate

G-actin: Globular actin (actin monomers)

GC: Generative cell

GM: Germination Medium

GroP glycerophosphoinositol

GroPP glycerophosphoinositol phosphate

InsP$_3$ or IP$_3$ inositol 1,4,5-trisphosphate

Jasp: Jasplakinolide

LatB: Latrunculin B

MAPK: Mitogen-activated protein kinase

NO: Nitric oxide

PA Phosphatidic acid

PAK Phosphatidic acid kinase

PC phosphatidylcholine

PCD: Programmed cell death

PE phosphatidyethanolamine

PG: phosphatidylglycerol

P_i: Inorganic phosphate

PI: phosphatidylinositol

PI 3-kinase: phosphatidylinositol 3-kinase

PIP: phosphatidylinositol monophosphate

PIP$_2$: phosphatidylinositol 4,5-bisphosphate

PPI: polyphosphoinositide

PLA: phospholipase A

PLC: phospholipase C

PLD: phospholipase D

PrpS: *Papaver rhoeas* pollen *S*

ROS: reactive oxygen species

Rh-Ph: rhodamine phalloidin

SI: Self-incompatibility

sPPase: soluble pyrophosphatase

TLC: thin layer chromatography

VN: Vegetative nucleus

CHAPTER 1: INTRODUCTION

1.1 PLANT SIGNALLING

The survival of a plant is dependent on their ability to respond to changes in their physiological status, changes in the environment, and the activity of others plants and pathogens. Over the last two decades many environmental, developmental, and defence signal transduction pathways have been characterized. The activation of specific signalling pathways occurs in response to specific stimuli, which may be a developmental, biotic or abiotic cue. These cues are detected by a receptor on the cell membrane, activating a specific pathway, and utilize a complex network of interactions to transduce the signal further downstream, orchestrating a biochemical and/or physiological response. Some of the signalling messengers employed, include the second messenger calcium (Ca^{2+}), changes in pH, increases in reactive oxygen species (ROS) and nitric oxide (NO), alterations in the actin cytoskeleton and alterations in phospholipid levels. In this thesis signal transduction pathways are of particular interest and will therefore be discussed further with reference to specific signalling messengers and their targets.

1.1.1 CALCIUM (Ca^{2+})

Ca^{2+} ions are well-established second messengers, which play an important role in controlling many cellular processes, such as apical tip growth in pollen and roots (Bibikova et al., 1998; Bibikova et al., 1997; Malho and Trewavas, 1996). In plant cells the basal cytosolic concentration of Ca^{2+}, ($[Ca^{2+}]_{cyt}$), is maintained at low nanomolar concentrations. However, the cell wall, vacuole, mitochondria and endoplasmic reticulum (ER) has a considerably higher concentration of Ca^{2+} (Kader and Lindberg, 2010). Stress can trigger a sudden increase

2

in $[Ca^{2+}]_{cyt}$, resulting in micromolar levels, which can be toxic to the cell. These changes in $[Ca^{2+}]_{cyt}$ are known to act as signal transducers with numerous targets, some of which include cell motility & cytoskeleton, exo- and endocytosis, and cell wall structure (Cheung and Wu, 2008).

Two key systems for studying calcium signalling are stomatal guard cell and pollen tubes, (pollen tubes will be discussed further in Section 1.4.1). The opening of guard cells can be stimulated by various cues including high light levels, low CO_2 concentrations, while abscisic acid (ABA) signalling and high CO_2 concentrations induce closure of guard cells. The treatment of the plant hormone ABA in guard cells, trigger multiple fluxes in Ca^{2+}, described as 'calcium signatures'. These calcium signatures are unique patterns of increases in $[Ca^{2+}]_{cyt}$ which are thought to determine the outcome of the final response (Hetherington and Brownlee, 2004; Hetherington et al., 1998; MacRobbie, 2000; Ng and McAinsh, 2003; Sanders et al., 1999).

Ca^{2+} signalling has also been studied in responses to many types of stress including salinity stress (Kader and Lindberg, 2010). Salinity stress is perceived at the cell membrane resulting in the increases of secondary messengers such as Ca^{2+} which triggers changes in channel activity or permeability of a membrane, the activation of specific MAPK, the induction or down-regulation of the specific genes and so on (Kader and Lindberg, 2010).

1.1.2 PROTONS (H$^+$)

Like Ca^{2+}, protons (H$^+$) are important for the regulation of growth in plant cells, and in the perception of environment and developmental cues. The intracellular pH of cells can be dynamically modulated, and thus serve as a second messenger to many stimuli, including root gravitropism, salinity stress and drought and during the hypersensitive response (Fasano et al., 2002; Felle, 2001; Kader and Lindberg, 2010; Roos et al., 2006; Schachtman and Goodger, 2008; Scott and Allen, 1999). In normal cellular conditions the cell plant cytosol has a pH of around 6.8-7.5, however organelles such as the vacuole and the apoplast have a much more acidic pH, reaching as low as pH 5.5 (Feijo et al., 1999; Katsuhara et al., 1989). During a gravitropic response, the Arabidopsis root cap apoplast modified its pH, acidifying to pH 4.5 from pH 5.5, simultaneously the cytoplasmic pH (pH$_c$) increased in columellar cells, (a tissue layer in the very tip of root tip) from 7.2 to 7.6. This pH change precedes changes in growth rates (Fasano et al., 2002; Fasano et al., 2001; Scott and Allen, 1999), and similar results were found in maize stem (Johannes et al., 2001). This modification of internal pH alters the gravitropic response resulting in advanced curvature, confirming the pHc plays an important role in plant signal transduction pathways during gravitropism (Fasano et al., 2001; Scott and Allen, 1999).

Changes in pH$_c$ also play an important signalling role during plant defense. A change in pH is necessary for triggering the biosynthesis of benzophenanthridine alkaloids, which are thought to act as phytoalexins (Dittrich and Kutchan, 1991). An influx of H$^+$ from the apoplast into the cytosol was reported for many plants during elicitation of the

4

hypersensitive response (Kader et al., 2007; Roos et al., 1998; Roos et al., 2006; Yamaoka et al., 2000). In Cultured cells of *Eschscholtzia californica* (Californian poppy) treatment with a yeast elicitor triggers an acidification of cytoplasmic and alkalinization of the vacuolar pH within minutes (Roos et al., 1998; Roos et al., 2006).

1.1.3 REACTIVE OXYGEN SPECIES (ROS) & NITRIC OXIDE (NO)

Reactive oxygen species (ROS) and Nitric Oxide (NO) are well known signalling molecules which are involved in numerous biological responses in both mammalian and plant systems. In plant cells, ROS is involved in hormone signalling in growth and development, cell cycle, stress, defense responses and PCD (several reviews describe ROS signalling; Apel and Hirt, 2004; Kwak et al., 2006; Laloi et al., 2004; Mittler et al., 2004). Furthermore, NO signalling has been associated with guard cell closure, abiotic stress and disease resistance (for reviews see Delledonne, 2005; Neill et al., 2003). Therefore, there is great interest in how active oxygen species (AOS) are perceived by signalling pathways and how they act as second messengers.

ROS

Research carried out by Foreman *et al.,* (2003), found that the addition of exogenous ROS to pollen tubes, replaced normal tip growth with isotropic growth, supporting the idea that ROS is involved in promoting polar growth. It is thought that ROS may control development by regulating cell growth (Gapper and Dolan, 2006). In Arabidopsis growing root hairs, and during Maize leaf expansion there is an accumulation of ROS at the tip of the root hair or the expansion zone in leaves, and it has been suggested that the gradient of ROS may be

involved in determining cell shape via mediating polar growth (Cardenas, 2009; Carol and Dolan, 2006; Foreman et al., 2003; Kwak et al., 2006; Liszkay et al., 2004; Rodríguez et al., 2002). Accumulation of ROS was associated with NADPH oxidase (NOX) activities, in which NOX generate the superoxide radical (O_2^-), using NADPH as an electron donor. In Arabidopsis, NADPH oxidase (NOX), genes are referred to as Arabidopsis respiratory burst oxidase homologues (Atrboh; Keller et al., 1998; Torres et al., 1998), and research in Arabidopsis has shown that ROOT HAIR DEFECTIVE2 (RHD2)/AtrbohC protein are required for root elongation. The los*S*-of-function *rhd2* mutation, results in decreased levels of ROS, and a reduction in root hair length compared to wild types (Foreman et al., 2003; Renew et al., 2005).

Although NOX has been implicated in root hair growth, there is increasing evidence for the role of Rho Of Plants (ROP) GTPases in the spatial regulation of ROS in roots (Carol et al., 2005; Jones et al., 2007). Studies showed there was an increase in ROS in ROP2 OX and constitutively active, *CA-rop2* expressing plants, and there was a reduction in ROS in *DN-rop2* plants. However, when the *CA-rop2* expressed in the NOX los*S*-of-function *rhd2-1* mutant, showed both ROS production and root hair growth was reduced, this suggested that RHD2 is required for ROPS2 dependent formation of ROS (Jones et al., 2007).

ROS signalling is also implicated during stress responses in plants, in particular during pathogen attack. ROS has several different roles during plant-pathogen responses. ROS is generated on the plasma membrane and can result in the cros*S*-linking of glycoproteins, strengthening the cell wall for protection against the pathogen (Bradley et al., 1992).

6

Increases in ROS during a hypersensitive response (HR) response are referred to as an oxidative burst. Several ROS are thought to be generated during a pathogen interaction, and from several different sources, e.g. from sub-cellular compartments, and the apoplast (Auh and Murphy, 1995; Grant et al., 2000). There is evidence for NOX function during apoplastic ROS production in response to recognition of a pathogen (Torres et al., 2006; Yoshioka et al., 2003). Furthermore, ROS can be utilised to activate Ca^{2+} channels to increase cytosolic Ca^{2+} levels, the activation of MAPK, microtubule depolymerization, defence gene activation, and cell death (Lecourieux et al., 2002; Levine et al., 1996; Levine et al., 1994; Rentel et al., 2004).

NO

NO is also used as a developmental regulator in many processes in plants including leaf extension, root growth, delaying fruit maturation and promoting seed germination (Kopyra and Gwózdz, 2003; Lombardo et al., 2006; Neill et al., 2003). In plants cells, sources of NO synthesis include the reduction in nitrite by nitrate reductase (NR) and oxidation of arginine to citrulline by nitric oxide synthase (NOS), (Bethke et al., 2004). However, it should be noted that NOS genes have yet to be identified in plants, although *NO ASSOCIATED1* (*NOA1*; formerly NOS1) partakes in NOS activity and pathogen-triggered NO burst (Asai et al., 2008; Asai and Yoshioka, 2008; Guo et al., 2003). Moreover, in other studies NR plays a role producing an oxidative burst during a pathogen response in *Nicotiana* leaves (Asai et al., 2008; Yamamoto-Katou et al., 2006). NO signalling has also been linked to the activation of

7

MAPK and the expression of defence genes such as *pathogenesiS-related proteins (*Pr) in Arabidopsis during pathogen attack (Clarke et al., 2000; Grun, 2006).

NO acts as a second messenger in many developmental events, such as seed germination and auxin signalling in root development (Beligni and Lamattina, 2000; Correa-Aragunde et al., 2004; Correa-Aragunde et al., 2008). In roots NO is an intermediate in the auxin-regulated signalling cascade which determines root morphology and physiology (Correa-Aragunde et al., 2004). In cucumber root development, NO is used to trigger cGMP production via guanylate cyclase activity, and furthermore NO activates a mitogen-activated protein kinase (MAPK) but in a c-GMP-independent pathway (Pagnussat et al., 2004). These targets are thought to be involved in mediate the formation of adventitious roots (AR) in response to auxin.

1.1.4 PHOSPHOLIPIDS

Membrane lipids contribute to the structural integrity of the cell, playing an essential role in maintaining chemical gradients between intracellular and extracellular environment and acting as a communication tool between external stimuli and the cell. Many phospholipids are involved in many signal transduction pathways (Munnik et al., 1998; Munnik and Nielsen, 2011; Munnik and Testerink, 2009), and several phospholipids have been identified as second messengers, such as phosphatidylinositol monophosphate (PIP), phosphatidylinositol bisphosphate PIP_2, phosphatidic Acid (PA) and diacylglycerol pyrophosphate (DGPP). In plants, there is a well-maintained system to regulate phospholipids, consisting of messengers and enzymes which are responsible for the production and degradation of

8

phospholipids (Figure 1.1). To date significantly more research has been carried out to investigate the role of PA during plant signalling and development than any other lipid messengers mentioned. PA is produced by numerous pathways, as demonstrated in Figure 1.1, using several different enzymes; phospholipase D (PLD), phospholipase C (PLC) and diacylglycercol kinase (DAG Kinase) (Munnik 2001; Wang 2002).
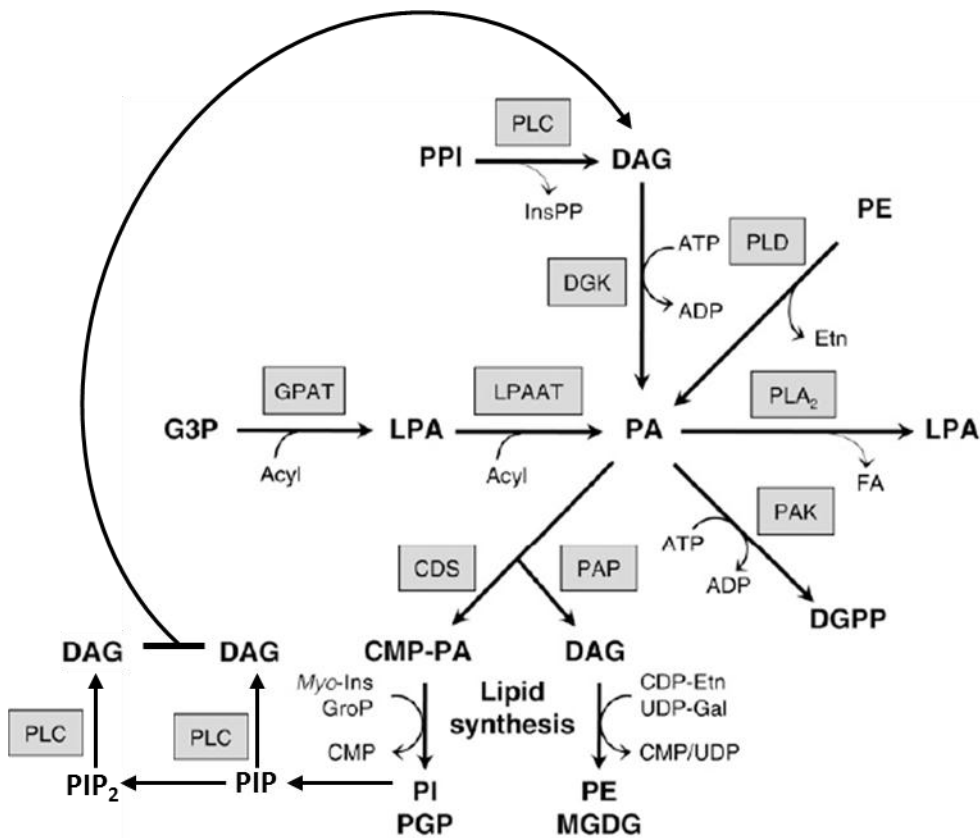
Figure 1.1. Model of PA synthesis pathways and PA-derived phospholipids

PA is formed through several pathways and is the source of many derivative signalling molecules. PA is formed through the acylation of G3P and LPA to produce glycerolipids. Furthermore, PA is also produced via the direct cleavage of PLD, and through a sequence of events which are catalysed by PLC/DGK. PA is also converted to cytidine monophosphate-phosphatidic acid (CMP-PA) by CMP-PA synthase (CDS) which leads to the synthesis of PI and PG(P). PE and MGDG is synthesised by the dephosphorylation of PA by PA Phosphatase (PAP), however it is to be noted during this process PA/DAG substrates are from different pool which are localized at the ER and plastidial envelope membrane, respectively. Secondary messengers PIP_2 and PIP are synthesised from PI and are later transformed in to DAG via PLC, whereas phosphatidic acid kinase (PAK) converted PA into DGPP. Adapted from Arisz & Munnik, 2011.

9

PA is known to act as a membrane localized signalling molecule, binding to downstream targets including a variety of protein kinases, phosphatases and specific proteins involved in vesicle trafficking or regulation of the actin cytoskeleton (Testerink and Munnik, 2011). In addition, PA is a structural membrane lipid and can affect the biophysical properties of the plasma membrane (Kooijman et al., 2003; Testerink and Munnik, 2011). PA also plays a role in development and is associated with triggering adventitious root (AR) formation in cucumber in response to auxin and NO signalling (Lanteri et al., 2008).

Furthermore, PA levels are elevated during a number of stress and developmental events, including leaf senescence and stomatal closing movement through PLD activities, and during ABA treatments (Mishra et al., 2006; Park et al., 2004). Interestingly, during leaf senescence there is an increase in PA through PLDα (Sang et al., 2001). Furthermore PLDα1 and PA have been shown to regulate a protein phosphatase 2C (PP2C), known as ABI1, which is a negative regulator of ABA responses in leaves (Zhang et al., 2004). PA produced by PLD α 1 binds to ABI1, reducing its migration to the nucleus by tethering it to the plasma membrane and therefore promoting ABA signalling, inhibiting stomatal closure (Mishra et al., 2006; Zhang et al., 2004). Moreover, research carried out by Park *et al.,* (2004), suggested that PA may activate a ROP-mediated ROS generation pathway which may lead to cell death in stress responses.

10

1.2 CELL DEATH

An example of a major plant signalling pathway is that of programmed cell death (PCD). Cell death is defined by the commitment of a cell to an irreversible pathway in which the cell goes past the 'point-of-no-return' resulting in the death of the cell. However, this pathway can vary depending on the stimuli and cell type (Kroemer et al., 2009). This highly conserved process, which is initiated by an intracellular signalling programme, is implicated in many developmental and immune responses in both mammalian and plant systems and is essential in many eukaryotes systems (van Doorn et al., 2011). Furthermore, cell death is not always a negative process, as it is a key part of many developmental processes, such as during lace leaf development (Gunawardena et al., 2004; Wright et al., 2009). Moreover, different categories of cell death can be defined upon the cellular morphological appearance, enzymological criteria or immunological characteristics.

Mammalian cell death is the most studied form of cell death and clear categories have been defined to characterise different types of cell death responses (For reviews see (Elmore, 2007; Kroemer et al., 2009). Although plant cell death differs from mammalian cell death in many ways there are still many similarities and key hallmarks which appear in both kingdoms and are therefore worth introducing. Mammalian cell death is defined into three main categories; necrosis, autophagic cell death and apoptosis.

11

1.2.1 NECROSIS

Necrosis is the result of cellular injury caused by external factors such as toxins or trauma, and may be associated with infection. This form of cell death is almost always detrimental to the host organism. Necrosis is usually characterised by key features such as an initial gain in cell volume, swelling of various organelles, early rupture of the plasma membrane and loss of intracellular content (Kroemer et al., 2009). It is also associated with alterations in mitochondrial membrane permeability, production of ROS and a drop in ATP levels. However, necrosis is still poorly understood and needs further investigation to determine whether this process is considered a 'programmed' process.

1.2.2 AUTOPHAGY

Autophagic cell death is carried out by the lysosomes of the cell and is termed 'self-eating'. Generally autophagy involves the delivery of portions of the cytoplasm to lysosomal vesicles where they are digested (Klionsky and Emr, 2000). There are different types of autophagy: micro-autophagy involves the sequestration of small portions of the cytoplasm at the lysosome surface. In macro-autophagy larger particles are sequestered in the cytoplasm, and form a unique double-membrane structure called the autophagosome. The autophagosome engulfs part of the cytoplasm with or without organelles and merges with a lysosomal (Otto et al., 2003; Yoshimori, 2004). The third type of autophagy is called mega-autophagy; this involves the permeabilization or rupture of the lysosome (which is a structure similar to the plant vacuole), resulting in the release of hydrolases, which degrade cellular components.

12

1.2.3 APOPTOSIS

Apoptosis is the most studied form of mammalian cell death. Cancer may occur as the result of oncogenic mutations which disrupt apoptosis, resulting in tumour initiation (Lowe and Lin, 2000). Apoptosis is described as the engulfment of the dying cell by a living one. The apoptotic cell fragments into apoptotic bodies; these bodies are then engulfed by phagocytes and are degraded by lysosomal enzymes. By engulfing all of the apoptotic bodies the cell prevents the leakage of its dead cell contents which could lead to inflammation and further infection in neighbouring cells. There are many cellular events or features that can be recognized as apoptosi*S*-induced. Key features include chromatin condensation, cell shrinkage, nuclear segmentation and plasma membrane blebbing. There are also other cell death features which are associated with apoptosis, although they are not specific to apoptotic cell death. These extra features include oligonucleosomal fragmentation of DNA and the activation of caspases.

1.2.3.1 CASPASES

A major hallmark of mammalian cell death is the presence and activation of family of intracellular cysteine-aspartic acid proteases known as caspases (Riedl and Shi, 2004). All caspases have cysteine amino acid in their active site, which cleaves target proteins at specific aspartic acids. Caspases are often referred to using the amino acid sequence of the substrate cleaved, for example caspase-3 has an optimal tetrapeptide recognition motif DEVD and is often called DEVDase. Tetrapeptide substrates and inhibitors based on the recognition motif of the caspases have been used to identify specific caspases involved in

13

particular pathways in mammalian cells. These substrates linked to fluorogenic indicators for caspase activities allow direct analysis of caspase-like activities. Using these tools, caspases have been identified as key initiators and executioners of many cell death pathways and are usually part of a cascade involving several caspases (Figure 1.2). As shown in Figure 1.2 there are two main pathways to trigger caspase-dependent cell death in mammalian cells.
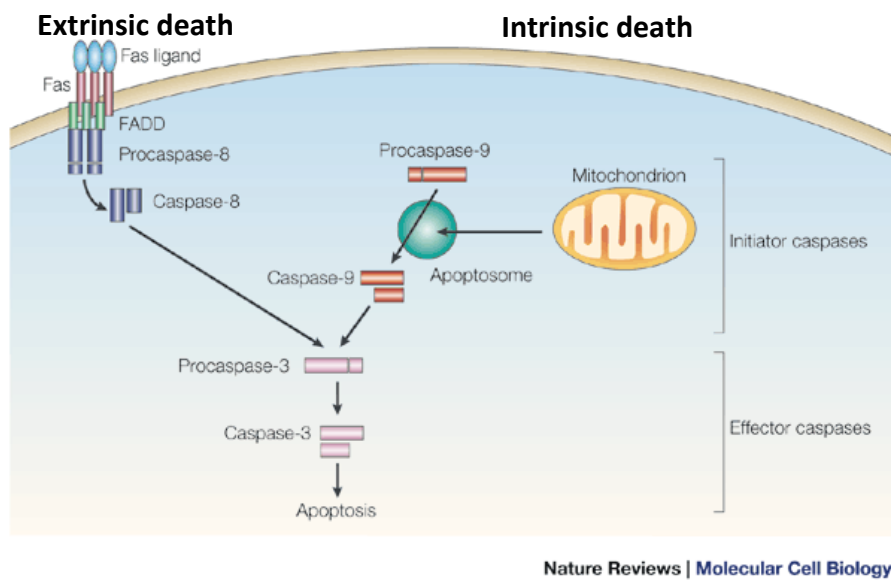
Figure 2.2 Caspase signalling cascade

Extrinsic death pathway is triggered by the interaction between a ligand (such as Fas ligand) and a receptor (such as Fas), this leads to the recruitment of adaptor molecule (FADD) resulting in the activation of caspase-8, and initiation of a caspase signalling cascade leading to cell death. Intrinsic death is triggered in response to damage of the mitochondria, which leaks cytochrome c leading the formation of the apoptosome, activating caspase-9, and similarly triggering caspases signalling cascade resulting cell death. Adapted from Holcik & Korneluk, 2001).

The extrinsic death pathway, specific ligands (such as FasL) cause death receptors (such as Fas) to oligomerize. This interaction results in the recruitment of adaptor molecules, (such as FADD), and the activation of initiator caspases, (such as caspase-8; Figure 1.2). Each caspase is produced as an inactive precursor (procaspase) which is activated by the cleavage of their aspartic acid, usually by another caspase. These caspases are regulated at a post-

translational level, ensuring that they can be rapidly activated in an amplifying proteolytic cascade, cleaving one another in sequence (Raff, 1998). Caspases are activated in a specific order; initiator caspases such as caspase*S*-6, -8, -9 and -10 are usually activated first. The initiator caspases proceed to activate downstream effector caspases such as caspase*S*-2, -3 and -7, ultimately resulting in cell death. Alternatively, cell death can occur as a result of intrinsic death stimuli (Figure 1.2). A stress response triggers cytochrome c release from the mitochondron, which a storehouse of key cell death-signalling proteins (Lam et al., 2001). This leads to the formation of the apoptosome, which consists of protease activating factor 1 (APAF-1), procaspase-9 and cytochrome c. Apoptosome-associated procaspase-9 self-activates which in turn, triggers a caspase signalling cascade by activation of downstream effector caspases 3 and/or 7. These caspases are responsible for ordering disassembly of the cell, and therefore apoptosis and cell death.

Caspases are involved in many cell death processes, such as cleaving proteins that support the nuclear membrane, thereby helping to dismantle the nucleus; they cleave DNAse inhibiting proteins, releasing the DNAse, to degrade the cell's DNA, resulting in the death of the cell (Enari et al., 1998). Caspase activity is very important in apoptosis, and failure of some caspases is one of the main contributors to tumour development as unwanted cells are not removed or dismantled (Wolf et al., 2001).

Another common feature of apoptosis that has also been linked to caspase activities is intracellular acidification. During apoptosis intracellular acidification occurs as pHi decrease approximately 0.3–1.4 pH_i units. This acidification occurs in response to multiple stimuli,

including staurosporine, arsenic, anti-Fas antibodies, and somatostatin (for review see (Matsuyama and Reed, 2000). Moreover, there is evidence that during somatostatin-induced apoptosis, caspase-8 mediates intracellular acidification, which is essential for the activation of activator caspases, such as caspase -9, -3, and -7 (Liu et al., 2000). The role of acidification in cell death is discussed further in Chapter 5.

There are no homologues of mammalian caspases present in the sequenced plant genomes (Woltering, 2004). However, caspase-like activities have also been identified in plants (Levine et al., 1996; van Doorn, 2005; van Doorn and Woltering, 2005; Watanabe and Lam, 2004), including in SI-induced *Papaver* pollen tubes (Bosch and Franklin-Tong, 2007). Caspase-like activities in plants will be discussed in more detail later in this chapter.

1.3 PLANT PROGRAMMED CELL DEATH (PCD)

Although less is known about plant cell death, programmed cell death (PCD) is being increasingly documented in plants and has been identified in response to many external factors such as abiotic and biotic stresses (Smart, 1994; Zhang and Klessig, 2001), plant-pathogen interactions (for review see Greenberg & Yao, 2004), and during plant development (Fukuda, 1997; Gunawardena et al., 2004; Pennell and Lamb, 1997; Vercher et al., 1987; Wright et al., 2009). As more evidence is emerging, apparent differences between plant and mammalian PCD have been documented. In plant PCD there are no phagocytic cells and there is no option for apoptotic bodies, as plant cells have a rigid cell wall (Van Doorn *et al., 2011*). Despite this, there are similarities between mammalian and plant cell

16

death systems, but plant PCD does not conform in full to the animal apoptosis type of cell death, and different plant PCD pathways may share only some features with apoptosis.

PCD in plants has recently been redefined according to morphological criteria (Van Doorn *et al., 2011*) and the term apoptotic cell death is no longer used to describe plant PCD. Two major categories in plant PCD have now been defined: vacuolar cell death and necrosis (Van Doorn *et al., 2011*), though there are other types of PCD that do not confirm to these two categories.

1.3.1 NECROTIC PCD

Like mammalian necrotic cell death, plant necrosis usually involves the swelling and bursting of a cell; spilling their contents over neighbouring cells, eliciting a damaging inflammatory response (Danon et al., 2000). Plant necrotic cell death is induced by numerous external stresses, including infection of plant pathogens (Greenberg and Yao, 2004). Some key markers for necrotic PCD have been identified. These include mitochondrial swelling, production of reactive oxygen species (ROS) and nitrogen species (NS), a reduction in mitochondrial membrane potential, a drop in ATP level and the permeabilization of the lysosomal membrane, which results in the release of cathepsin proteases (Kroemer et al., 2009). In addition, necrosis also results in the rupture of the plasma membrane, which leads to shrinkage of the protoplast. Necrosis can take from several minutes (toxic treatments) to several days (hypersensitive response (HR)) to complete (Levine et al., 1996).

17

1.3.2 VACUOLAR PCD

Plant vacuoles are diverse, dynamic structures, and they display a range of functions including the degradation of cellular components, maintenance of turgor pressure, sequestration of ions. They also act as a reservoir for the accumulation of proteins which may be required for germination or backup during starvation acting as a storehouse for proteins regulated for growth and development (Becker *et al.,* 2007; Marty *et al.,* 1999; Muntz 2007). To avoid repetition the vacuole will be discussed in more detail in Chapter 6, and only vacuolar cell death (VCD) will be discussed here.

VCD is the most common form of plant PCD, and has been documented in an array of systems, elicited by the cell or neighbouring cells as part of normal development or to prevent or contain infection or disease (for review see Hara-Nishimura and Hatsugai, 2011). In cells undergoing VCD, portions of the cytoplasm are transported in vesicles and delivered into the vacuole, where the vesicles fuse with vacuole, leading to swelling of the vacuole. As a result vacuoles undergo major rearrangement in shape and size that will require biogenesis or removal of tonoplast membranes. At this point the cargo is degraded in the vacuolar lumen. Major vacuolar reorganization and swelling occurs during elicitor-induced cell death (Higaki et *al., 2007*). However, vacuolar swelling is not the only vacuolar response during VCD. In some cells there is also loss of tonoplast stability, resulting in collapse of the vacuole. This results in the release of hydrolytic enzymes from the vacuole and the degradation of organelles such as the nucleus, protoplast and the cell wall (Bethke, 2004; Bozhkov et al.,

18

2003; Hara-Nishimura and Hatsugai, 2011; Hatsugai and Hara-Nishimura, 2010; Kuriyama, 1999; Obara et al., 2001; van Doorn, 2005; van Doorn and Woltering, 2005).

During the HR in tobacco leaves, cells undergo VCD. They exhibit features such as vacuolar reorganization and rupture. Higaki *et al.,* (2007) documented the breakdown of the vacuole during the HR in tobacco leaves treated with an elicitor from the oomycete *Phytophora cryptogea.* Initially the vacuole membrane formed bulb-like structures within the lumen, which coincided with the disruption and bundling of cortical microtubules and actin microfilaments. Soon after the cytoskeleton was completely disrupted and the bulb-like vacuolar structures disappeared, only small spherical vacuoles remained. Finally, the vacuolar membrane disintegrated resulting in death (Higaki *et al., 2007*). Vacuolar rupture is now commonly used as a key marker of cell death in many PCD pathways.

Vacuolar rupture also occurs in many developmental processes such as aerenchyma formation, suspensor degeneration, leaf perforations in the lace plant and petal senescence (Drew et al., 2000; Gunawardena et al., 2004; Pennell and Lamb, 1997; Rubinstein, 2000). Other morphological features of VCD include actin cable formation, nuclear envelope disassembly, and nuclear segmentation (Obara et al., 2001). This type of cell death can be a slow process taking up to several days, however, not all these features occur in all systems. A key example of VCD in plant development is that of tracheary element (TE) PCD, which occurs during xylem development (Pennell and Lamb, 1997). During this process cells, undergo formation of secondary cell walls and PCD, resulting in hollow dead cells (Fukuda, 1997; Fukuda, 2000; Groover et al., 1997; Obara et al., 2001). Ultrastructural observations

19

show TE differentiating cells undergo rapid and progressive degeneration of the nucleus, vacuole, plastids, mitochondria, and endoplasmic reticulum, followed by the removal of protoplasts, the plasma membrane, and parts of primary walls (Obara et al., 2001). It is assumed that many of these organelles and structures are degraded as a result of hydrolytic enzymes which are thought to accumulate in the vacuole of TEs (Obara et al., 2001). Thus, the collapse of the vacuole is a critical irreversible step to execute the degradation of various organelles (Fukuda, 1997; Groover et al., 1997). Obara *et al.,* has shown that nuclear degradation occurs only after the disruption of the tonoplast and that nucleic acids in the nucleus were degraded within 10 minutes of vacuolar rupture. Kuriyama *et al.,* (1999) suggested that the loss of selective permeability of the tonoplast may be responsible for the induction of PCD in TE cells.

1.3.2.1 PLANT CASPASE-LIKE ACTIVITIES

As previously discussed, caspases play an important role in mammalian cell death, and although there are no homologous genes in the plant genome, caspase-like activities have been identified in many plant processes (Bosch and Franklin-Tong, 2007; Levine and Kroemer, 2009; Sanmartín et al., 2005; van Doorn and Woltering, 2005; Watanabe and Lam, 2004; Woltering, 2004; Xu and Zhang, 2009). At present several distinct caspase-like activities have been identified in plants (for review see Xu and Zhang, 2009). Caspase-like activities documented in plant cells include YVADase (Belenghi et al., 2004; Bosch et al., 2010; Kuroyanagi et al., 2005), DEVDase, (Belenghi et al., 2004; Gao et al., 2008a; Thomas and Franklin-Tong, 2004), VEIDase(Bosch and Franklin-Tong, 2007), IETDase,(Bosch and

Franklin-Tong, 2007; Coffeen and Wolpert, 2004) VKMDase(Coffeen and Wolpert, 2004), LEHDase(Kim et al., 2003), TATDase and LEVDase activities (Bosch and Franklin-Tong, 2007). At present the most detailed characterization of plant caspase-like activities is of caspase-3/DEVD-like and caspase-1/YVADase-like activities.

Caspase-3/DEVDase-like activities have been documented during the development of seedlings in *Pisum sativum,* and microspore embryogenesis of barley (Belenghi et al., 2004; Rodríguez-Serrano et al., 2011), during stress responses such as during Ultraviolet C Overexposure, (Gao et al., 2008b; Zhang et al., 2009a) and during the Self-Incompatibility (SI) response in Papaver pollen tubes which will be discussed in section 1.5.3.2.9 (Bosch and Franklin-Tong, 2007). Furthermore, in *Arabidopsis* protoplasts recent research has shown that NO signalling maybe upstream of MPK6 a mitogen-activated protein kinase (MAPK) which is thought to mediates caspase-3-like activation during cadmium (Cd^{2+}) induced cell death (Ye et al., 2012). Recent research has shown that caspase-3/DEVDase-like activity also plays a role in secondary xylem development in *Populus tomentosa* (Han et al., 2012). Moreover, it was shown that the 20S proteasome was responsible for the caspase-3/DEVDase-like activities. During this process the inhibition of caspase-3/DEVDase-like activities with an inhibitor of DEVDase or a proteasome inhibitor prevent PCD in xylem development. Furthermore, in Arabidopsis, *Pseudomonas syringae* induced HR there is the activation of proteasome subunit PBA1, which has caspase-3/DEVDase-like activity (Hatsugai et al., 2009). Hatsugai et al., showed that during this response membrane fusion of the tonoplast with the plasma membrane is linked to the release of vacuolar antimicrobial proteins into the extracellular spaces, and therefore defence of the cell (Hatsugai and Hara-

Nishimura, 2010; Hatsugai et al., 2009). Moreover, the reduction in PBA1 activity abolished

the collapse of the vacuole during PCD (Hatsugai et al., 2009; Pajerowska-Mukhtar and Dong,

2009).

1.3.2.1.3 VACUOLAR PROCESSING ENZYME (VPE)

A key caspase-like protein in plant cell death is vacuolar processing enzyme (VPE), which is

used in systems which undergo vacuolar collapse and VCD. VPEs are usually localized in the

vacuole and possess the caspase-1 activity (YVADase), although it is structurally unrelated to

caspases (Hatsugai, 2004; Hatsugai et al., 2005).VPEs are members of the C13 family of

asparaginyl endopeptidases (also called legumains). They are highly conserved and have

been found in plants, fungi and animal cells (Hara-Nishimura et al., 2005; Hatsugai et al.,

2004; Kinoshita et al., 1999; Yamada et al., 2004). VPE is synthesized as an inactive

precursor, and is self-catalytically converted into the mature form under acidic conditions

(pH 5.5), (Kuroyanagi et al., 2002). VPE proteolytic activity was originally identified as a

processing enzyme in the maturation of seed storage proteins (Hara-Nishimura and

Hatsugai, 2011; Hara-Nishimura et al., 2005; Hara-Nishimura et al., 1991; Hara-Nishimura et

al., 1993), but it also plays a role in *Arabidopsis* seed coat development (Nakaune et al.,

2005; Nakaune et al., 2004). At present four VPE genes have been identified in Arabidopsis

genome, α, β, γ and δ, (Hara-Nishimura et al., 1991; Kinoshita et al., 1999; Nakaune et al.,

2005; Yamada et al., 2004).

VPEs are also activated during the cell death of *Nicotiana gossei* Domin ×*N. tabacum* L which

is lethal at the seedling stage. Cell death begins at the base of the hypocotyls and spreads

22

through the rest of the plant through the complete disintegration of the vacuolar membrane (Mino et al., 2007). VPE inhibitors suppress changes in the tonoplast and therefore cell death, and suggesting that VPE in triggering alterations in tonoplast stability (Mino et al., 2007). VPE activity was also reported in the up-regulation of cell death associated with leaf senescence and lateral root formation of Arabidopsis (Hara-Nishimura and Hatsugai, 2011; Kinoshita et al., 1999). Furthermore, a VPE has been identified in *Papaver* pollen, although its role is not yet known (Bosch et al., 2010)(discussed in section 1.5.3.2.9).

1.4 PLANT REPRODUCTION

Plant reproduction utilises a complex signal transduction network. At each stage of the reproduction process there are multiple environmental cues to interpret and respond to, which trigger numerous signalling pathways, some of which include recognition of compatible pollen (discussed further in section 1.5) and guidance signalling to an unfertilized ovule. Sexual plant reproduction is achieved by pollination and finally by the double fertilization process (fusion of two male with two female gametes). The pollination process begins with the release of pollen grains from the anthers until the delivery of the sperm cells (male gametes) into the ovule. Once the pollen grain lands on the stigmatic surface of the pistil, it hydrates and produces a pollen tube. The pollen tube, which contains the sperm cells, grows through the style towards the ovary following both internal and external stimuli. Once the pollen tube reaches the entrance to the ovary and an unfertilized ovule, the pollen tube will rupture, forcing the sperm cells out of the pollen tube and towards the ovule. Finally, double fertilization occurs in which one of the sperm cell fertilizes the central cell

23

and the other to the egg cell (female gametes). A fertilized ovule becomes a seed, which will give rise to a new seedling and will ensure the continued survival of the species.

Some plants (for example, *Arabidopsis thaliana*), are self-fertile and are therefore able to self-pollinate to produce offspring. However many sexually reproducing plants are non-self-fertile or self-incompatible (SI) (see section 1.5 SELF-INCOMPATIBILITY (SI).

1.4.1 THE POLLEN TUBE

The pollen tube has an essential role in sexual plant reproduction. It's sole purpose is to carry and deliver the male gametes to an ovule, where fertilization will take place. Furthermore, the pollen tube acts as a 'single cell', and has a rapid rate of tube formation and growth, and is therefore an excellent model system for studying cell processing involved cell polarity, signal transduction, channel and ion flux activity, cytoskeleton and cell-cell communication among others. Pollen tubes consist of four distinct zones: the apical growth zone (the tip region), the sub-apical zone, the nuclear zone and the zone of vacuolization and callose plug formation (Figure 1.3). The nuclear and vacuolized zones are referred to as the shank
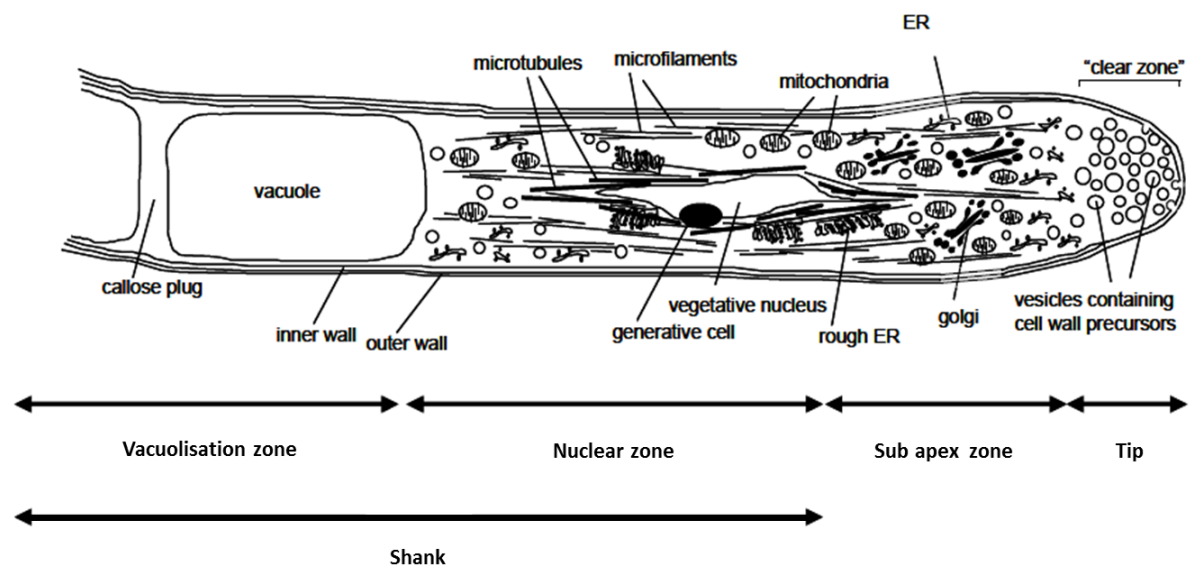
Figure 1.3. Diagram illustrating the intracellular organization of the pollen tube

The pollen tube consists of four sub sections known as the vacuolisation zone, the nuclear zone, the sub apex zone and the tip. The shank is comprised of the vacuolisation and nuclear zone, which contains the vacuole, major cytoskeletal structures, the vegetative nucleus and the generative nucleus. The sub apex zone contains the endoplasmic reticulum (ER), the golgi apparatus and mitochondria. The tip is fairly organelle free which on small vesicles containing cell wall precursors. Adapted from Franklin-Tong, 1999.

Actively growing pollen tubes possess a clear zone at their tips, which is free from organelles but is densely packed with secretory vesicles which are involved in the fusion of wall precursors to the tip (Franklin-Tong, 1999; Malhó, 2006; Malho et al., 2006). Behind this is the sub-apical zone, which consists of cytoplasm, numerous organelles including mitochondria and endoplasmic reticulum (ER) and a cytoskeleton network (Figure 1.3). The nuclear zone is where the vegetative nucleus (VN) and generative cell (GC) are located within the pollen tube and the vacuolar zone is the region which expands as the pollen tube grows. The vacuolar zone is interrupted by regular formation of callose plugs (Heslop-Harrison and Heslop-Harrison, 1985). More recent research in lily and *Arabidopsis* pollen tubes has shown that the vacuolar structure is actually more like network and not one large

central vacuole, typically shown in other plant cells (Hicks et al., 2004; Lovy-Wheeler et al., 2007), also see Chapter 6, for vacuolar structure in *Papaver* pollen.

An individual pollen tube must travel a great distance to fertilize an ovule, and so the rate which a pollen tube can grow is important. Unlike most plant cells in which growth occurs by modification of the existing cell wall and the insertion of new material throughout its surface, the highly polarised pollen tube extends exclusively by apical tip extension (Taylor and Hepler, 1997). The pollen tube is able to grow at speeds of up to 200-500 nm/s over a period of 15-50 s; this is the fastest growing cell on earth (Cheung and Wu, 2008; Pierson et al., 1996). The actin cytoskeleton has a crucial role in achieving these high growth rates through the regulation of cytoplasmic streaming, and the movement of vesicle containing cell wall components to the tip of the pollen tube.

Pollen tube growth is also stimulated by external factors such as electrical, mechanical and chemical guidance cues, triggering re-orientation and alterations in growth rates (Heslop-Harrison and Heslop-Harrison, 1985). For example, alterations in Ca^{2+} concentrations, or the presence of gamma-amino butyric acid (GABA), cysteine-rich attractant molecules LURES and transmitting-tissue-specific (TTS) proteins, secreted stylar tract proteins, are known to stimulate pollen tube growth, and direct pollen to unfertilized ovules (Cheung and Wu, 2008; Malho et al., 2006; Malho et al., 1994; Okuda et al., 2009), which is crucial for fertilization.

1.4.1.1 REGULATION OF POLLEN TUBE GROWTH

As discussed in section 1.1, ions are known to play a role in the regulation of many cellular processes and responses. Research suggests that oscillations of ionic concentrations and fluxes play a significant role in the regulation of pollen tube growth. Some of the key ions involved in pollen tube growth and regulation include calcium (Ca^{2+}) and protons (H^+). These will be discussed below.

1.4.1.1.2 CALCIUM (Ca^{2+})

Ratiometric Ca^{2+} indicator dyes have been used to measure intracellular Ca^{2+} ($[Ca^{2+}]_i$), and show an intracellular 'tip-focused' Ca^{2+} gradient in both lily and *Papaver* pollen tubes (Figure 1.4; (Franklin-Tong et al., 1997; Rathore et al., 1991).
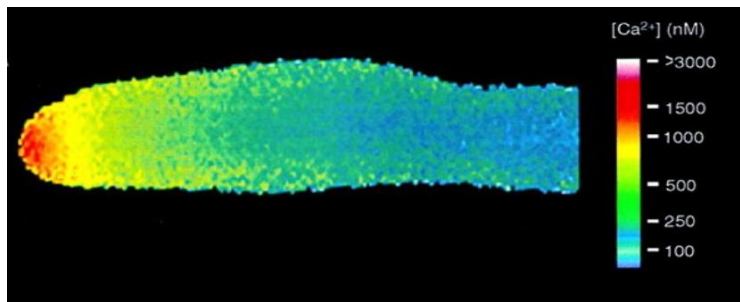
Figure 1.4 Imaging Cytosolic Calcium ($[Ca^{2+}]_i$) in Pollen Tubes.

Ratio imaging of $[Ca^{2+}]_i$ in a growing pollen tube of *Papaver rhoeas* microinjected with fura-2 dextran. Figure shows a typical pollen tube with a high apical $[Ca^{2+}]_i$ gradient. Adaption from Franklin-Tong *et al.,* 1997.

These $[Ca^{2+}]_i$ gradients are essential for pollen tube growth, and buffers such as BAPTA and caffeine have been used to block Intracellular Ca^{2+} increases in pollen tubes, resulting in the reversible inhibition of tube elongation (Feijo et al., 2001; Pierson et al., 1996; Straatman et al., 2001; Taylor and Hepler, 1997). Research has also shown that $[Ca^{2+}]_i$ oscillates at the

27

pollen tube tip. These oscillations can be between 750 - 3500 nM during growth (Pierson *et al.,* 1996), peaking 1-4 s after the peak in growth rate. It is thought that changes in $[Ca^{2+}]_I$ are the result of changes in growth rates and not *vice versa* (Holdaway-Clarke et al., 1997; Messerli and Robinson, 2003). It has been suggested that increase in growth rate leads to a mechanical deformation of the apical plasma membrane which leads to the opening of Stretch-Activated channels which allow Ca^{2+} influx (Hepler et al., 2012). Evidence from Pierson et al (1996) showed that in growing lily pollen tubes Ca^{2+} ion entry only occurs at the extreme apex of the pollen tube.

1.4.1.1.3 PROTONS (H+)

pH plays an important role in pollen tube growth. Pollen tubes are very sensitive to changes in both internal and external pH (Feijo et al., 1999; Fricker et al., 1997), which is unsurprising as pH can affect many biochemical processes, such enzyme activity. An acidic external pH is optimum for pollen tube growth, ~pH 4.5-6, with elongation being completely inhibited in media of ~pH 7 (Holdaway-Clarke et al., 2003). Intracellular proton concentrations ($[H^+]_i$) in pollen tubes have been monitored using ratiometric fluorescent indicators, although these results are controversial. Some groups have evidence that the pollen tube has an intracellular pH of 7.1 with no pH gradient in pollen tubes, suggesting that a pH gradient is not required for growth (Fricker et al., 1997). Other groups have shown that there is a pH gradient in pollen tubes consisting of a slightly acidic domain (~pH 6.8) at the extreme apex and an alkaline band (~pH 7.5) located along the clear zone (Feijo et al., 1999). This is more widely accepted. Furthermore, this theory is also supported by evidence from H^+-selective

vibrating probes. It has been suggested that there is an influx of H^+ at the apex of the pollen tube and efflux at the edge of the cell near the clear zone and alkaline band (Malhó, 2006).

Furthermore, $[H^+]_i$ oscillations have also been shown to play a role in pollen tube growth rates. During normal pollen tube growth, there is an increase in pH, reaching a maximum which plateaus before an increase in growth rate, this is followed by a sharp decrease in pH (Lovy-Wheeler et al., 2006; Messerli and Robinson, 2003). Recent research has shown that there is an increase in pH at the alkaline band in the pollen tube, which precedes growth (Lovy-Wheeler et al., 2006). This rise in pH could be controlled by a proton ATPase on the apical plasma membrane, and therefore could be a potential regulator of pollen tube growth (Feijo et al., 1999). Moreover, recent research in lily showed manipulation of intracellular pH, resulting in acidification, led to the destabilization of actin filaments, especially in the apical domain and resulting in inhibition of growth (Lovy-Wheeler et al., 2006). Again this highlights the importance of pH regulating in pollen tube growth.

1.4.1.1.4 REACTIVE OXYGEN SPECIES (ROS) and NITRIC OXIDE (NO)

ROS is also involved in the regulation of tip growth in both root hairs and pollen tubes (Potocký et al., 2007; Wang et al., 2010). ROS scavengers inhibited tip growth in pollen tubes, showing that ROS is essential for normal growth; the cessation of growth was recovered by the addition of H_2O_2 (Potocký et al., 2007). In addition Wang *et al.,* (2010), suggested that ROS production was disrupted during *S*-RNase-SI, and this disruption of ROS is involved in triggering actin depolymerization and DNA fragmentation.

NO is also involved in the re-orientation of *Lilium longiflorium* pollen tubes (Prado et al., 2008; Prado et al., 2004). It has also been implicated during a stress response in pollen tubes. Pollen subjected to ultraviolet-B radiation triggered in an increase NO levels in the grain and tube, which resulted in a reduction in germination and tube growth (He et al., 2007). Similar results have been found in *Arabidopsis* pollen treated with high levels of extracellular ATPγS (Reichler et al., 2009).

ROS and NO have also been associated with signalling during pollination in Arabidopsis and *Secencio squalidus* (McInnis et al., 2006). Evidence suggested that pollen had a high concentration of NO while stigmatic papillae had a high concentration of ROS. When a pollen grain adhered to papillae, ROS levels were reduced, suggesting cros*S*-talk between ROS and NO, and a potential important role in pollen-pistil interactions (McInnis et al., 2006).

1.4.1.1.5 THE ACTIN CYTOSKELETON

The actin cytoskeleton is at the heart of many essential processes in the pollen tube. Actin is an abundant protein in pollen. In *Papaver* pollen tubes, actin concentrations have been measured at 250 μM (Snowman et al., 2002). This high concentration of actin helps drive the fast growth of the pollen tube via cytoplasmic streaming and transport of secretory vesicles to the tip. It has been shown that without actin polymerization / turnover in the apical domain, pollen tube growth is inhibited (Gibbon et al., 1999; Vidali et al., 2009). More recently, Lovy-Wheeler *et al.,* (2005b), showed that lily pollen tubes have an actin collar towards the tip of the pollen tube (1-5 μm from the tip) which extends 5-10 μm into the cell cortex. Behind this region, actin cables are prominent and extend throughout the shank

region of the pollen tube. Studies have shown calcium channels can be regulated by F-actin (Wang et al., 2004). Using F-actin disrupting agents, such as cytochalasin D, cytochalasin B and latrunculin A, resulted in an inhibition of growth and an increase in calcium conductance, suggesting that an intact actin cytoskeleton is required to regulate the permeability of Ca^{2+} channels (Wang et al., 2004).

Ca^{2+} is also involved in regulation of the actin cytoskeleton in pollen. Pollen tubes microinjected with high concentrations of Ca^{2+} showed fragmentation of F-actin and inhibited cytoplasmic streaming. As previously mentioned, pollen tubes have a tip-focused Ca^{2+} gradient. In the tip, where $[Ca^{2+}]$ is at its highest, there is a 'clear zone' which is free from F-actin. It is thought that the high $[Ca^{2+}]$ is responsible for this, by preventing the polymerization of G-actin. There is also evidence of an actin 'fringe' just behind the clear zone at the tip of the pollen tube, this region is heavily populated with F-actin bundles (Lovy-Wheeler et al., 2006).

1.4.1.1.6 PHOSPHOLIPIDS

There is increasing evidence for the role of phospholipid signalling during pollen tube growth (Monteiro et al., 2005b; Pleskot et al., 2012; Potocký et al., 2003). Phosphatidic acid (PA) has been implicated in the regulation of cell polarity in tobacco pollen and tip-focused $[Ca^{2+}]_c$ gradient, suggesting the possibility that PA acts as a regulator of Ca^{2+} (Potocký et al., 2003). Multiple Ca^{2+} regulated PLD genes suggest there could be a feedback loop between PA and Ca^{2+} (Munnik, 2001). Furthermore, it has been shown that butanol treatments, which may disrupt PA formation (see Chapter 2 for more details). Such treatment have also been shown

31

to disrupt the transport and accumulation of vesicles to the apical region, suggesting they may actively participate in the control of endo- and exocytosis and interfere with the correct positioning of the actin cytoskeleton (Monteiro et al., 2005b). Huang *et al.,* (2006) showed that in Arabidopsis pollen, increases in PA stimulated uncapping of filament barbed ends, which leads to the extension of actin filaments, resulting in bundling of actin cables.

There are several pools of PA produced via different pathways. Work carried out by Pleskot *et al.,* (2012) have shown these different sources of PA have different roles in the pollen tube. PLD, DGKs and lipid phosphate phosphatases (LPPs) have all been shown to regulate PA levels in growing pollen tubes (Pleskot et al., 2012). Furthermore, it was shown that specific genes modulate different roles of PA. Using inhibitors, Pleskot *et al.,* (2012) showed that inhibition of PA production via inhibition of PLD (butanol treatments) or DGK activity resulted in the compromised membrane trafficking, disrupted tip-localised deposition of cell wall material and inhibited pollen tube growth. Furthermore, PLD disruption specifically affected the actin cytoskeleton, whereas DGK inhibition affected vacuolar dynamics (Pleskot et al., 2012; Pleskot et al., 2010). Prevention of attenuation of PA via inhibition of LPP activity resulted in stimulation of pollen tube growth. Thus, PA is known to play an important role in regulating pollen tube growth. Although PA is an important lipid involved in pollen growth, there is increasing evidence for the importance of some PA derivatives during plant signalling and communication and these will be discussed in more detail in Chapter 4.

1.5 SELF-INCOMPATIBILITY (SI)

As mentioned, plant reproduction involves multiple signal transduction pathways in response to many environmental signals. In some flowering plants complex mechanisms have been developed to ensure they reproduce efficiently, and protect their genetic diversity (Brewbaker and Shapiro, 1959). Populations which avoid self-fertilization generally have high levels of genetic polymorphisms, and so have the genetic variability required for withstanding a wide range of environmental challenges. Self-fertilization is prevented by various methods including selective maturation of reproductive organs (Davis et al., 1987) and the specific recognition and rejection of self-pollen via self- incompatibility (SI) (McClure, 2004). SI is a genetically controlled cell-cell recognition system. Interaction between the pollen tube and the stigma is very important in the recognition of self- genetic material, as it is at this point that a decision is made that pollen is either allowed to continue to grow or it is inhibited and programmed cell death (PCD) is induced. Self-pollen is recognized by the stigma as being genetically identical and therefore pollen tube growth is inhibited and non-self-pollen (compatible pollen) is permitted to grow and fertilize an ovule (Takayama and Isogai, 2005). It is estimated that some form of SI is present in ~60 % of all flowering plants (Hiscock and Kues, 1999). The interaction of the pollen tube and the stigma is a good model for cell-cell interaction and is therefore of great scientific interest.

There are several different types of SI in angiosperms. SI expected to have arisen independently multiple times, with SI in different plants utilising different recognition molecules and distinct pathways for the arrest of self-pollen tube growth (Takayama and

33

Isogai, 2005), although some species did lose SI over time and become self-compatible (SC) (Sage and Sampson, 2003). Most SI systems are characterized by a single highly polymorphic locus, the *S*-locus, although there are some exceptions, one being grasses (Poaceae) which have two loci; the *S*-locus and the Z-locus. The *S*-locus normally contains two tightly linked non-recombinant polymorphic genes, one controlling the pollen and the other the pistil identity (McCubbin and Kao, 2000; Silva and Goring, 2001). This multi-gene complex is known to be inherited as one segregating unit. There are many alleles of the *S*-locus, the variants are known as *S*-haplotypes.

The recognition of self or non-self operates at the level of protein-protein interactions between male and female components. Incompatible reactions occur when both *S*-determinants are derived from same *S*-haplotype, and result in the inhibition of the pollen tube. The recognition of self- and non-self-pollen can occurs at different stages of pollination and fertilization, depending on the species, it can be ovarian, pre zygotic or post zygotic (Sage and Sampson, 2003). For example, in *Papaver* SI death of self-pollen occurs very early in pollination and occurs on the stigma surface whereas in cocoa SI occurs much later, post-pollination (Ockendon, 2000).

There are two classes of SI; Gametophytic self-incompatibility (GSI) and Sporophytic self-incompatibility (SSI). SSI is controlled by the phenotype of the pollen grain's parent diploid genome. This allows the *S*-alleles to display dominant interactions in both pollen and pistil (Hiscock and McInnis, 2003; Hiscock and Tabah, 2003), which is discussed in more detail below. GSI, which is the abundant SI mechanism in flowering plants, is controlled by the

34

pollens own haploid genome. Furthermore, there are two distinct GSI systems; *S*-RNase-based (*Solanaceae, Rosaceae and Scrophulariaceae*) and Ca^{2+} -dependent (*Papaver*aceae), (which will be discussed in more detail later on).

1.5.1 SPOROPHYTIC SI

In Brassicaceae family, the female determinant was identified as a membrane-spanning stigmatic receptor kinase (SRK) which is specifically expressed in stigmatic tissues (Stein et al., 1991; Watanabe et al., 1994). SRK belongs to a large group of plant receptor-like kinases (RLK) and consists of a transmembrane domain and a cytosolic domain with serine/threonine kinase activity. Transgenic plants expressing SRK rejected self-pollen, showed that SRK is the sole female determinant required for SI in Brassica (Takasaki et al., 2000). Pollination bioassays and loss –and gain-of-function experiments have led to the identification of the male determinant, anther-specific gene *S*-locus protein 11 (SP11; Shiba et al., 2001; Suzuki et al., 1999; Takayama et al., 2001) / *S*-locus cysteine rich protein (SCR; Schopfer et al., 1999). SP11/SCR encodes a small cysteine-rich basic protein localized in the pollen coat.

SRK has been shown to physically interact with SCR/SP-11 via its extracellular domain, in a *S*-haplotype-specific manner (Chookajorn et al., 2004; Shimosato et al., 2007; Takayama et al., 2001). Based on structural characteristics, SRK and SCR/SP-11 SI interactions were thought to result in a phosphorylation cascade in the stigmatic papilla cell, leading to the rejection of self-pollen. The interaction of SCR/SP11, with SRK occurs at the stigmatic surface in an *S*-haplotype specific manner. The recognition of incompatible pollen results the

35

autophosphorylation of the transmembrane SRK domain (Figure 1.5), which activates a

signalling cascade resulting in the rejection of the pollen (Takayama et al., 2001). The

phosphorylation of SRK also activates ARC1 (Armadillo Repeat Containing protein) in a

phosphorylation-dependent manner (Samuel et al., 2006; Stone et al., 2003; Stone et al.,

1999). ARC1 is specifically expressed in the stigma and is an E3 ubiquitin ligase (Gu et al.,

1998; Stone et al., 2003). It is thought to be a positive effector of SI signalling by promoting

the ubiquitination and proteasomal degradation of stigmatic proteins which are required for

pollen tube growth (for review see; Takayama and Isogai, 2005).
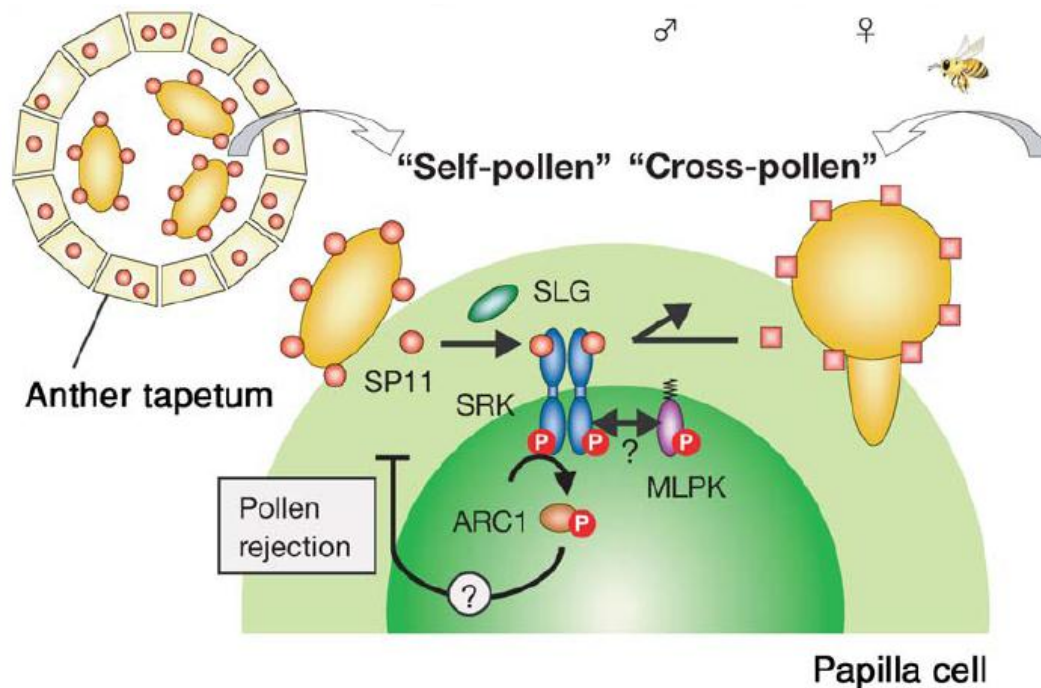
Figure 1.5. Molecular Model of Sporophytic Self-Incompatibility in Brassicaceae

Recognition of 'self' and therefore incompatible pollen occurs on the stigmatic surface. The SRK receptor kinase is the female determinant which is specifically localised to stigmatic tissue and papilla cells. SP11/SCR is the male determinant which is expressed in the anther tapetum and accumulates in the pollen coat during pollen maturation. The interaction of SP11/SRK results in the phosphorylation of SRK. This triggers a signalling cascade in which SRK activates ARC1, which is an E3 ubiquitin ligase. ARC1 is hypothesised to trigger the degradation of pollen positive effectors via the proteasome. Phosphorylated SRK also interacts with other molecules including MLPK and THL1 and THL2, although their roles are not yet fully understood. Ultimately interaction between incompatible SP11/SCR and SRK results in the death of the pollen tube. 'Cross' pollen interaction does not trigger the SP11/SRC-SRK signalling cascade and stigmatic proteins are not degraded and the pollen tube continued to grow. Figured taken from Takayama & Isogai 2005.

36

SRK-SP11/SCR stimulated signalling cascade also results in the activation of M locus protein kinase (MLPK) (see Figure 1.5). MLPK is a novel membrane-anchored cytoplasmic serine/threonine protein kinase which interacts directly with SRK to initiate SI signalling (Murase et al., 2004), it is suspected to be localized to the papilla cell membrane (Kakita et al., 2007). MLPK is thought to form a signalling complex with SRK that mediates the rejection response (Murase et al., 2004). The SRK kinase domain interacts with a range of intracellular proteins, including thioredoxin h-like proteins, THL1 (Bower et al., 1996). THL1 inhibits the autophosphorylation activity of SRK in the absence of SP11/SCR, and are therefore thought to be a negative regulator of SRK and SI (Cabrillac et al., 2001; Haffani et al., 2004). Ultimately the interaction between incompatible self-pollen results in the rejection of pollen (Takayama and Isogai, 2005).

1.5.2.1 *S*-RNASE BASED GAMETOPHYTIC SI

Solanaceae, Rosaceae and Scrophulariaceae families (tobacco, tomato, potato, apple, and snapdragon) share the same mechanism of SI. These families all have an *S*-RNase based system, which is the most phenogenetically widespread form of SI found in angiosperms (Xue et al., 1996). In *S*-RNase-based SI the female determinant is a stigmatic protein which exhibits ribonuclease activity, and thus is referred to as *S*-RNases (McClure et al., 2011; Murfett et al., 1994). *S*-RNases are expressed and secreted into the extracellular matrix (ECM) and along the path the pollen tube grows down the style (Xue et al., 1996). Both los*S*- and gain-of-function approaches were used to show *S*-RNase is the sole female determinant (Murfett et al., 1994), and that two His residues are important for ribonuclease activity and

37

are completely conserved in all S-RNases (Ioerger et al., 1991). The enzymatic activity of S-RNase is thought to play a role in degrading RNA, tracer experiments with ^{32}P-labelled pollen RNA showed that pollen rRNA are degraded in incompatible but not compatible pollen (McClure et al., 2011; McClure et al., 1990).

The male determinant is known as S-locus F-box protein (SLF; Sijacic et al., 2004) / S-haplotype-specific F-box protein (SFB; Lai et al., 2002). SLF/SFB are members of the F-box family of proteins, which function as a component of an E3-ubiquitin ligase complex. These proteins are involved in ubiquitin mediated protein degradation of non-self S-RNases and therefore permitting the survival of compatible pollen. Recent evidence has shown that in Petunia there are at least three types of SLF/SFB proteins encoded by several S-locus SLF/SFB genes which all function as the male determinant, but each recognises a different subset of non-self S-RNases (Kubo et al., 2010).

There is also evidence of a series of unlinked genes which also play a role in the mediation of S-RNase-SI (review by McClure, 2006; McClure et al., 2011; McClure et al., 2000). Although these modifier genes are not linked to the S-locus, their role is essential for SI, some of which are involved in the direct regulation of SI genes, and some have other roles in addition to their specific role in SI. In particular there is evidence for pistil modifier playing a role during S-RNase SI, Clone H-Top band protein (HT-B). HT-B, which is a small asparagine-rich protein. Downregulation of HT-B by anti-sense transformation and RNAi deprived transformants of the ability to reject self-pollen (McClure, 1999; O'brien *et al.,* 2002). Immunolocalisation experiments by Goldraij *et al.,* (2006) showed that HT-B localised in the membranes of

vacuoles and they directly interact with *S*-RNases. It has been hypothesized that HT-B is involved in destabilization of vacuoles (McClure and Franklin-Tong, 2006), and that in self-pollen tubes HT-B may facilitate *S*-RNase transport from an endomembrane compartment to the cytoplasm, where they could exert their cytotoxicity, leading to the arrest of the pollen tube growth.

S-RNase-SI is still under much debate, and several models have been developed over the years. However, at present there are two models which are widely accepted and supported. These are the degradation model and the compartmentalization model, and will be briefly described.

1.5.2.1.1 THE DEGRADATION MODEL

The degradation model is based on ubiquitylation and degradation of non-self-*S*-RNases. This model proposed that upon pollination, *S*-RNases are taken up into the pollen tube cytoplasm regardless of their *S*-haplotypes (Luu et al., 2000), where they interact with SLF/SFB to form a SLF/SFB-*S*-RNase complex (Figure 1.6). During a compatible interaction non-self *S*-RNase are marked for degradation by the 26S proteasome, and therefore the pollen RNA remains stable and growth continues (Figure 1.6; Kerscher et al., 2006; Qiao et al., 2004; Sijacic et al., 2004). In an incompatible reaction self-*S*-RNase are recognised, but not marked for degradation; *S*-RNase remain active and their cytotoxicity then results in RNA degradation and so incompatible pollen tube growth is inhibited (Figure 1.6; Hua and Kao, 2006; Qiao et al., 2004). Despite strong support for the degradation model, there is a great deal of evidence for additional factors playing a role in *S*-RNase SI which are not taken into account

39

in the degradation model, some of these are addressed in the next model; the

Compartmentalization model.

1.5.2.1.2 THE COMPARTMENTALIZATION MODEL

The Compartmentalization model proposes that all *S*-RNases, in addition to 120K and HT-B,

are taken up via endocytosis and sorted to the vacuole where they are isolated from the

cytoplasm (Figure 1.6). In a compatible reaction, HT-B is degraded by a hypothetical pollen

protein (PP) and the vacuole remains stable. Compatible *S*-RNases are compartmentalized

and therefore do not degrade the pollen RNA, and pollen tube growth continues (Figure 1.6).

It is proposed that some escaping *S*-RNases interact with SLF in the cytosol which led to the

recognition of compatible pollen. These *S*-RNases may be transported to the vacuole for

compartmentalisation. It is thought that a small percentage of *S*-RNases escape or leak into

the cytosol during an incompatible reaction, incompatible SLF and *S*-RNases interact and

form a complex. This *S*-RNase-SLF complex is hypothesised to block PP activity and in turn

prevent the degradation of HT-B. The vacuole is no longer stabilised by HT-B and the

vacuolar compartment containing *S*-RNases degrades (Figure 1.6). *S*-RNases are released

into the cytoplasm and RNA is degraded by its cytotoxic action, resulting in the inhibition of

pollen tube growth (McClure, 2006; McClure et al., 2011).
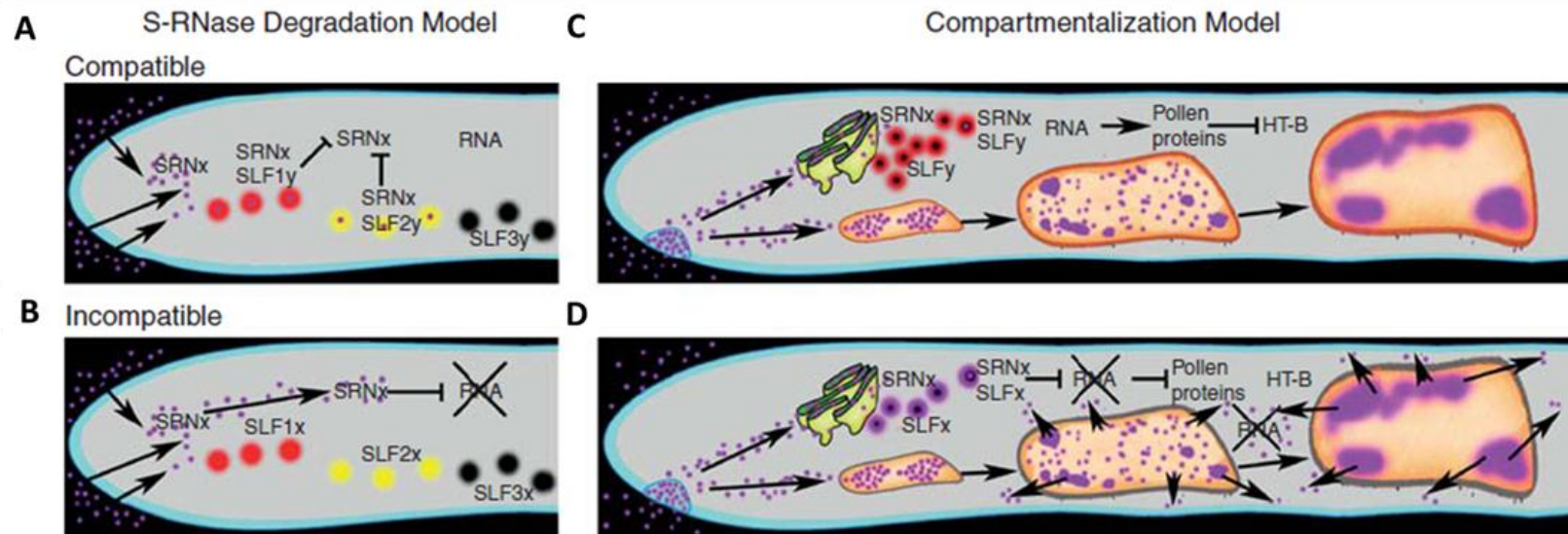
Figure 1.6 Models for *S*-RNase-Bases SI.

Model of *S*-specific pollen rejection. Pollen tubes are shown in the pistil ECM containing just one *S*-RNase, (SRN$_x$, purple), although it should be noted that in a typical *S*-heterozygote two *S*-RNases would be present. Compatible interaction: S$_y$-pollen and pistil is expressing S$_x$-RNase. Incompatible interaction: S$_x$-pollen and pistil is expressing S$_x$-RNase. A. *S*-RNase Degradation Model, compatible pollen tube. B. *S*-RNase Degradation Model, Incompatible pollen tube. C. Compartmentalization Model, compatible pollen tube. D. Compartmentalization Model, Incompatible pollen tube. A&B: The Degradation model: *S*-RNases from the stigmatic tissue enter the pollen tube (arrows). A. In a compatible interaction, *S*-RNases interact with multiple SLF/SFB (SLF1, red; SLF2, yellow; SLF3, black) and collaborate to cause inhibition of all *S*-RNase recognised by SLF/SFB as being different. This process marks *S*-RNases for degradation which is carried out by the proteasome, therefore preventing the degradation of RNA. B. During an incompatible interaction self *S*-RNases do not form a complex with SLF/SFB and *S*-RNases are free to degrade RNA of the self-pollen (cross), resulting in the inhibition of growth. C&D: The Compartmentalization Model: *S*-RNases from the stigmatic tissue enter the pollen tube via endocytosis (arrows), and sorted to the vacuole where they are isolated from the cytoplasm a small percentage of *S*-RNases are thought to remain in the cytosol where they interact with SLF. C. During a compatible reaction SLF recognises the *S*-RNases as being from 'cros*S*-pollen'. A hypothetical pollen protein, inhibits HT-B and the vacuole remains intact. *S*-RNases remain compartmentalised and pollen RNA remains stable, pollen tube growth continues. D. During an incompatible reaction SLF recognises the *S*-RNases as being from 'self-pollen', and *S*-RNases form a complex with SLF. This complex is thought to inhibit PP, and therefore HT-B is stable and the vacuole is degraded releasing *S*-RNases into the cytosol. The *S*-RNases in the cytosol degrade the pollen RNA (cross) and pollen tube growth is inhibited. Figure is adapted from McClure *et al.,* 2011.

1.5.3 GAMETOPHYTIC SI IN *PAPAVERACEAE*

Like the *S*-RNase gametophytic SI systems, *Papaver rhoeas* L. (field poppy) SI has a single *S*-locus (Lawrence, 1975). However, *Papaver* SI is induced via a unique gametophytic pathway, and many of its key features are different to that of other gametophytic systems, this includes the male and female determinants involved in the SI recognition.

The female determinant, *Papaver rhoeas* stigma S (PrsS) is a 15kDa hydrophilic protein which is developmentally controlled and secreted from female tissue (Foote et al., 1994). It has many haplotypes and cloning of several of these showed *S*-alleles share between 51.3 to 63.7% identity at the amino acid level. However, despite this high level of polymorphism they are expected to have very similar secondary structures (Foote et al., 1994; Kurup et al., 1998; Walker et al., 1996). Recombinant PrsS exhibiting *S*-specific biological activity can be produced and used in *in vitro* assays. These *in vitro* assays were used to induce SI-specific events in an *S*-specific manner, therefore confirming PrsS as the sole female determinant (Foote et al., 1994). Site-directed mutagenesis has shown that mutations of a hypervariable amino acid situated in the predicted hydrophilic surface loop 6 of PrsS, resulted in the loss of self-incompatibility and self-pollen continued to grow (Kakeda et al., 1998). This loop is thought to play a crucial role in pollen recognition and defining allelic specificity.

The male *S*-determinant, *Papaver rhoeas* pollen S (PrpS) is a novel 20 kDa protein which is expected to be a transmembrane protein which is associated with the plasma membrane (Wheeler et al., 2009). PrpS is a novel protein and is predicted to contain three to five putative membrane-spanning domains. PrpS also displays polymorphism typical of an *S*-locus

component and segregation analysis suggests co-segregation and linkage of *PrpS* and the

pistil gene *PrsS* (Wheeler et al., 2009).

1.5.3.1 INTERACTION BETWEEN PRSS AND PRPS

PrsS is thought to act as a signalling ligand which interacts with the pollen receptor, PrpS, in

an *S*-specific manner on the pollen tube surface. A 'Far western' approach was used to show

that specific amino acids on a predicted extracellular loop of PrpS interacted with PrsS

(Wheeler et al., 2009). To show whether PrpS mediated *S*-specific inhibition of pollen tubes

antisense- (a*S*-ODNs) or sense- (*S*-ODNs) oligonucleotides peptides based on the amino acids

suspected to be involved in the specificity of SI were used to knockdown expression of PrpS.

A*S*-ODNd gave recovery of SI treated pollen tubes, confirming PrpS is essential for SI

response and the cessation of the pollen tube growth (Wheeler et al., 2009).

1.5.3.2 MECHANISM OF *PAPAVER* SI

SI can be induced *in vitro* via the addition of recombinant PrsS to incompatible pollen, this

method has been used to identify many of the downstream events during SI, discussed in

more detail later on. An incompatible reaction results in a rapid Ca^{2+} dependent signalling

network which triggers the cessation of tube growth and ultimately triggers PCD of

incompatible pollen (Franklin-Tong and Franklin, 1993; Franklin-Tong et al., 1996; Franklin-

Tong et al., 1997; Franklin-Tong et al., 2002; Thomas et al., 2003; Thomas and Franklin-Tong,

2004).

43

1.5.3.2.1 CALCIUM (Ca²⁺) SIGNALLING MEDIATES *PAPAVER* SI

As discussed in section 1.1.1, calcium (Ca^{2+}) plays an important role in pollen tube growth. In *Papaver* pollen tubes there is a tip focused concentration gradient of 1-2 μM at the apex of the pollen tube and a mean basal levels of $[Ca^{2+}]_c$ in the shank of 210 nM (Franklin-Tong et al., 1997). Franklin-Tong *et al.,* (1993; 1997; 1995) showed incompatible stigmatic extracts and recombinant PrsS induce an almost instantaneous increase in intracellular $[Ca^{2+}]_{cyt}$ in the pollen tube. These SI-specific increases Ca^{2+} are characterized by a 'wave' which travelled away from the tip of the pollen tube in the shank, of the pollen tube; increases were not observed in the tip of the pollen tube (Franklin-Tong and Franklin, 1993; Franklin-Tong et al., 1997). These increases in cytosolic free $[Ca^{2+}]$ result in the immediate cessation of pollen tube growth. These studies helped sculpt the hypothesis that PrpS is a transmembrane receptor that interacts with PrsS is an *S*-specific manner, triggering a Ca^{2+}-dependent signalling cascade in incompatible pollen. Moreover, recent research has shown that SI triggers the activation of pollen grain protoplast plasma-membrane conductance(s) in an *S*-specific manner (Wu et al., 2011). The SI-activated conductance(s) are voltage sensitive, but do not require voltage for their activation. In addition it is permeable to divalent cations ($Ba^{2+} \geq Ca^{2+} > Mg^{2+}$) and the monovalent ions K^+ and NH_4^+. Wu *et al.,* (2011) proposed that the SI-induced conductance(s) may be a Non-Specific Cation Channel (NSCC), which allows both monovalent and divalent cations through. This adds to the growing evidence that PrpS may be an ion channel.

Ca^{2+} is a well-known second messenger, and it has been shown that these increases are important in signalling during SI. Over the past 20 years research has shown that there are many signalling targets downstream of the SI-specific increases in cytosolic Ca^{2+} in *Papaver* pollen tubes. Targets of SI-induced increases in Ca^{2+} will be discussed in the next section.

1.5.3.2.2 SOLUBLE INORGANIC PYROPHOSPHATASES (sPPases)

Rudd *et al.,* (1996) showed that SI-induced increases in cytosolic Ca^{2+} result in the phosphorylation of a soluble 26 kDa soluble inorganic pyrophosphatase (sPPase) 26 kDa; *Papaver rhoeaS*-p26.1 (Pr-p26.1). sPPases are important enzymes that are involved in the hydrolysis of inorganic pyrophosphates (PPi). During biopolymer synthesis PPi is generated, and sPPase hydrolysis of PPi generates inorganic phosphate (Pi), providing a thermodynamic pull, driving biosynthesis. The inhibition of sPPase activity leads to the inhibition of biosynthesis within the pollen tube, including essential cellular components involved in cell extension, growth, actin cytoskeleton and transport of materials.

Pr-p26.1 genes were cloned, and antisense oligonucleotides based on Pr-p26.1a/b sequences were produced in order to down-regulate Pr-p26.1 and analyse their importance in the SI response (de Graaf et al., 2006). The addition of antisense oligonucleotides resulted in the significant inhibition of pollen tubes growth (de Graaf et al., 2006). In SI-induced pollen tubes [PPi] increased. This provided good evidence of a functional link between alterations in sPPase activity & SI induction *in vivo* pollen tubes, suggesting SI could result in the phosphorylation of p26 which leads to the inhibition of pollen tube growth (de Graaf et al., 2006).

45

1.5.3.2.3 MITOGEN ACTIVATED PROTEIN KINASE (MAPK), p56

Mitogen activated protein kinases (MAPKs) are known to be key players in plant signalling

networks and are activated under both abiotic and biotic stress responses. They are

commonly part of Ca^{2+}-signalling cascade (Nakagami et al., 2005). SI activates the MAPK p56,

(Rudd et al., 2003). The SI-activated MAPK in turn activates a caspase-3/DEVDase-like

activity, a key player in PCD (Li et al., 2007; Rudd and Franklin-Tong, 2003; Rudd et al., 2003).

The activation of the MAPK p56 peaks 10 minutes after the induction of SI (Li et al., 2007;

Rudd et al., 2003), which is considered the initiation phase of SI. The MAPK cascade inhibitor

U0126, which blocks MAPK activity in both animals and plants, prevented the activation of

the SI-stimulated p56-MAPK. This alleviated SI-induced DNA fragmentation, and inhibited SI-

induced caspase-3-like/DEVDase activity and SI-induced loss of viability (Li et al., 2007).

These data suggests MAPK-p56 is involved in integrated SI signals.

1.5.3.2.4 CYTOCHROME C

Papaver SI triggers cytochrome c leakage within 10 minutes of induction (Thomas and

Franklin-Tong, 2004). The concentration of cytochrome c significantly increases in the first

two hours of the SI response. Research has also shown that increases in $[Ca^{2+}]_i$ stimulates

the release of cytochrome c into the cytosol during the SI response. Cytochrome c regulates

the activity of the inhibitor caspase, procaspase-9, in mammalian cells, but it is not known

what cytochrome c's target is in plants, but it could also be responsible for ordering

disassembly of the cell. Furthermore, in mammalian cells cytochrome c is released from the

46

mitochondria during stress response and therefore the mitochondria may also play a role in SI-induced release of cytochrome c.

1.5.3.2.5 DNA FRAGMENTATION

Jordan *et al.,* (2000) showed that DNA fragmentation occurred in an *S*-specific manner during the SI response. Data showed DNA fragmentation increases over time, and maximum levels were recorded at 12-14 hours after SI induction. DNA fragmentation is also discussed in section 1.5.3.2.7, with reference to the actin cytoskeleton.

1.5.3.2.6 SI INDUCED ALTERATION IN THE POLLEN TUBE CYTOSKELETON

SI triggers rapid depolymerization of F-actin bundles as early as 60 seconds after the induction of SI, which plays a role in the cessation of the pollen tube tip extension and growth (Geitmann et al., 2000; Snowman et al., 2002). This SI-induced depolymerization is mediated by increases in $[Ca^{2+}]_i$. Approximately 30 minutes of SI-induction, F-actin accumulates into 'punctate foci' (Geitmann et al., 2000; Snowman et al., 2002). These foci increase in size over time and their formation requires actin polymerization (Poulter et al., 2010). These foci are extremely stable and are resistant to actin depolymerizing drug, latrunculin B (Lat B), suggesting actin foci have very different properties to normal actin arrangements in pollen (Poulter et al., 2010).

The microtubule cytoskeleton is also a target of the SI response (Poulter et al., 2008). SI stimulates very rapid depolymerization of cortical microtubules, with cortical microtubules almost impossible to detect within 60 sec of SI induction . Lat B artificially depolymerizes

47

both actin filaments and microtubules, however Jasplakinolide, an F-actin stabiliser was

unable to prevent microtubule depolymerization in SI induced cells. In addition microtubule

depolymerization cannot trigger actin depolymerization, suggesting one-way cross talk. This

suggests that SI stimulates actin depolymerization and, as a consequence, triggers

microtubule depolymerization (Poulter et al., 2008).

1.5.3.2.7 THE CYTOSKELETON AND PROGRAMMED CELL DEATH (PCD)

The cytoskeleton is also involved in the activation of PCD during the SI response in

incompatible pollen (Snowman et al., 2002; Thomas et al., 2006). Thomas *et al.,* (2006) used

both Lat B and Jasplakinolide (Jasp) treatments to investigate the effects of actin

depolymerization and stabilization (Bubb et al., 1994), on DNA fragmentation in pollen

tubes. Lat B stimulated DNA fragmentation in a concentration-dependent manner. When SI-

induced pollen tubes were pre-treated with Jasp, which stabilizes F-actin, DNA

fragmentation was greatly reduced (Thomas et al., 2006). This shows that actin stabilization

alleviates SI-induced PCD, demonstrating that actin has a functional role in the initiation of

PCD in pollen tubes.

Further analysis of the cytoskeleton revealed the involvement of microtubules in PCD

(Poulter et al., 2008). As mentioned earlier, cortical microtubules rapidly depolymerize in SI-

induced incompatible pollen. Disruption of microtubules, with either stabilization or

depolymerizing drugs, did not trigger PCD in pollen tubes. Furthermore, microtubule

depolymerization does not disrupt the actin cytoskeleton. However, stabilization of

microtubules prior to SI-induction alleviated SI-induced caspase-3-like activities (Poulter et

al., 2008). These data suggest that disruption of the microtubule dynamics alone is not significant enough to induce PCD, but it is required for SI-induced PCD to progress, suggesting actin and microtubules work together to induce PCD (Poulter et al., 2008).

1.5.3.2.8 ACTIN BINDING PROTEINS (ABP) & SI

Actin binding proteins (ABPs) are involved in many cellular processes including the regulation of actin dynamics in pollen tubes (Staiger et al., 2010). SI-induces the formation of actin foci (Snowman et al., 2002), and recent work has shown that these foci are associated with the ABP cyclase-associated protein (CAP) and actin-depolymerizing factor (ADF), but not profilin and fimbrin (Poulter et al., 2010). In untreated pollen tubes CAP and ADF were not associated with F-actin, however after SI both rapidly co-localized with F-actin punctate foci. Mass spectrometry showed that not only CAP and ADF associated with actin in an *S*-specific manner, but other proteins may also associate with the punctate foci. These including 14-3-3 proteins, Ra*S*-like proteins, heat-shock proteins and chaperonins (Poulter et al., 2011). Although it is currently unclear how these proteins are involved in SI, it hints at further signalling networks.

1.5.3.2.9 CASPASE-LIKE ACTIVITIES

One of the key features of plant PCD is the activation of caspase-like activities (Levine et al., 1996; Sanmartín et al., 2005; van Doorn and Woltering, 2005; Watanabe and Lam, 2004; Woltering, 2004), as previously discussed in section 1.3.2.1. Caspase-like activities are also a key feature of SI response in *Papaver* pollen tubes. Pollen pre-treated with caspase inhibitors prior to SI induction reduced SI-induced DNA fragmentation, demonstrating the

49

significance of caspase-like activity during the SI response (Thomas and Franklin-Tong, 2004). Later on, Bosch & Franklin-Tong (2007) used fluorescent AMC-based caspase substrates to characterized caspase-like activities in more detail. Caspase-3-like/DEVDase and caspase-6-like/VEIDase activity was identified in the pollen tube cytosol in the first 1-2 hours after SI-induction peaking at 5 hrs (Bosch and Franklin-Tong, 2007). LEVDase activity was also identified in SI-induced pollen, but activity was much slower, peaking at 8hrs, when DEVDase and VEIDase activity was decreasing (Bosch and Franklin-Tong, 2007)). In addition, YVADase activity was also detected, but at very low levels. As mentioned, SI-induced pollen pre-treated with the caspase-3/DEVD inhibitor inhibited DNA fragmentation; however the caspase-1 inhibitor Ac-YVAD-CHO did not prevent DNA fragmentation (Thomas and Franklin-Tong, 2004). This indicated that caspase-3/DEVDase-like activities, but not caspase-1/YVADase-like activity is required for DNA fragmentation. This highlights the importance of caspase-3-like/DEVD activity in the mediation of SI-PCD (Thomas and Franklin-Tong, 2004).

Papaver rhoeas Vacuolar Processing Enzyme 1 (PrVPE1) has been cloned from *Papaver* pollen. VPE has YVADase activity, and unlike other VPEs it also has DEVDase and IETDase activities and does not need processing for activity (Bosch et al., 2010). PrVPE1 localizes to a reticulate compartment resembling the vacuole and requires an acidic pH for activity. However, YVADase activity in pollen tubes appears to be in the mitochondria. As it has been shown that YVADase activity is not required during the SI response in *Papaver* pollen tubes (Bosch & Franklin-Tong 2007; Thomas & Franklin-Tong 2004), it suggests that YVADase is not involved in PCD and might be involved in processing mitochondrial and vacuolar proteins. Moreover, the movement of YVADase activity into the cytosol during SI might be the result

50

of loss of integrity of mitochondria and vacuolar membrane. In addition, Bosch *et al.,* (2010) showed that PrVPE1 interacts with a DEVD motif, hinting that it could interact with DEVDase-containing substrate, although its function is unknown and requires further investigation.

1.5.3.2.10 SI-INDUCED POLLEN TUBE ACIDIFICATION

Recent work has shown that SI-induced caspase-like activities such as DEVDase and VEIDase have very narrow acidic pH optima of pH 5 (Bosch & Franklin-Tong, 2007). This suggests that caspase-like activities require an acidic environment to be functional. Normal healthy pollen tubes have a cytosolic pH of ~pH 6.8, within 160 minutes of the induction of SI, the cytosol rapidly acidifies to ~pH 5.6 (Bosch & Franklin-Tong, 2007). This acidification may be responsible for creating the optimal condition for caspase-like activity and may be vital for the initiation of PCD. Pollen tube acidification is discussed further in Chapter 5.

1.5.3.2.11 MODEL OF *PAPAVER* SI
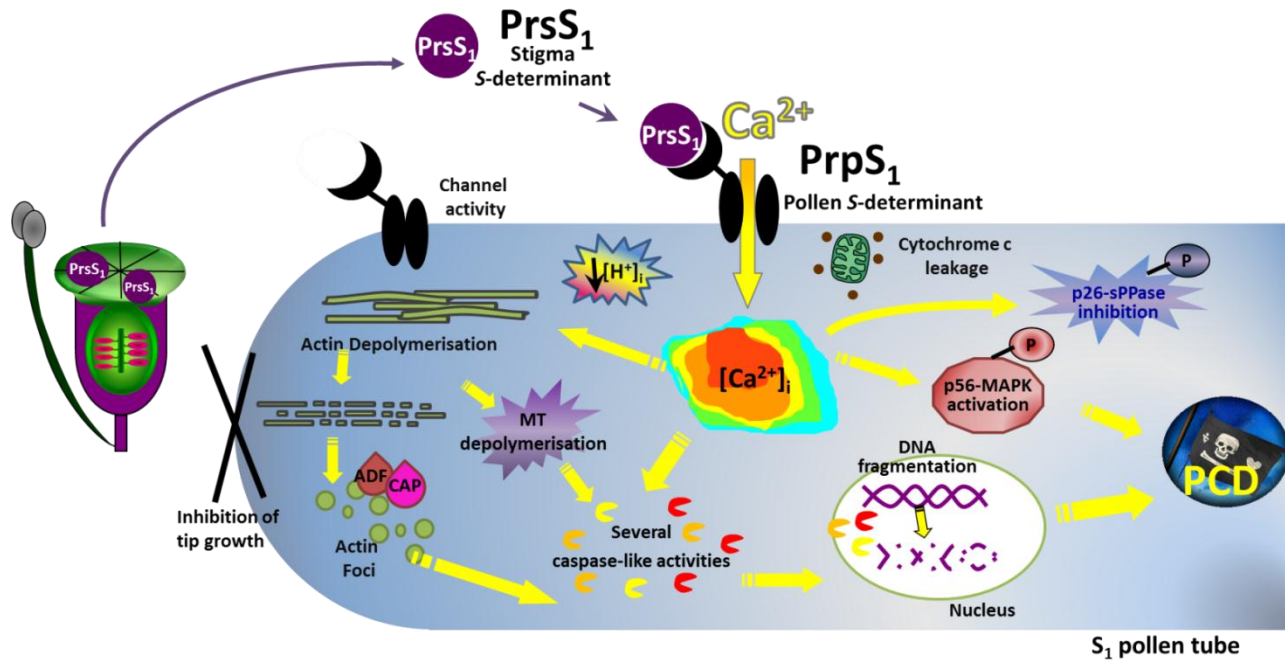
Figure 1.7. Model of Self-Incompatibility response in *Papaver rhoeas* pollen tubes

A proposed model for the self-incompatibility mechanism in *Papaver rhoeas*. During an incompatible interaction secreted stigmatic protein, *Papaver rhoeas* stigmatic S (PrsS), interacts with *Papaver rhoeas pollen* S (PrpS), pollen receptor in an S haplotype-specific manner, such as $PrsS_1$ binds to $PrpS_1$. This incompatible interaction triggers a rapid influx of Ca^{2+}, which induces a signalling cascade, resulting in the inhibition of tip growth. Increases in Ca^{2+} trigger dramatic alterations in the action cytoskeleton, including the depolymerization of F-actin, which is later followed by stabilization of F-actin into actin foci, which are decorated with actin binding proteins (ABPS), actin-depolymerizing factor (ADF) and cyclase-associated protein (CAP). Furthermore, the microtubule (MT) cytoskeleton undergoes depolymerization. Moreover, there are alterations in channel activity and acidification of the cytosol and the release of cytochrome c which is involved in programmed cell death (PCD). There is also the phosphorylation and inactivation of soluble inorganic pyrophosphatases (sPPases) Pr-p26.1a/b, and the phosphorylation and activation of mitogen activated protein kinases (MAPK) p56 which may signal to PCD. Furthermore, there is the activation of caspase-like activities which are known to translocate to the nucleus where DNA fragmentation occurs resulting in PCD, ensuring the incompatible pollen does not start to grow again.

1.6 AIMS OF THIS PROJECT

The work presented here investigated the signalling mechanisms involved in *Papaver rhoeas* SI. As shown in Figure 1.8 at the start of this project, key hallmarks such as actin foci formation, caspase-3/DEVDase-like activities and alteration in calcium concentration have been characterized. The following chapters represent new avenues of research previously unpublished (for a diagram showing the timeline of SI-induced events including those presented in this thesis see Chapter 7, Figure 7.1).

1. Investigating the role of reactive oxygen species (ROS) and nitric oxide (NO) as important signalling components during SI (Chapter 3).

   Research into mediators of lily and tobacco pollen tube growth had shown that ROS and NO play an important role in the key signalling pathways involved in maintaining polarised growth. We hypothesised that during the SI response in *Papaver* pollen tubes there must be alterations in these signalling molecules as growth is inihibted during such a response. Live cell imaging techniques were used to examine the temporal and spatial signals of both ROS and NO during SI. Inhibitors were used to block such signals to determine whether or not ROS and NO play a role in triggering key SI induced hallmarks such as alterations in the actin cytoskeleton and caspase-3-like activities. This work has now been published in Plant Physiology.
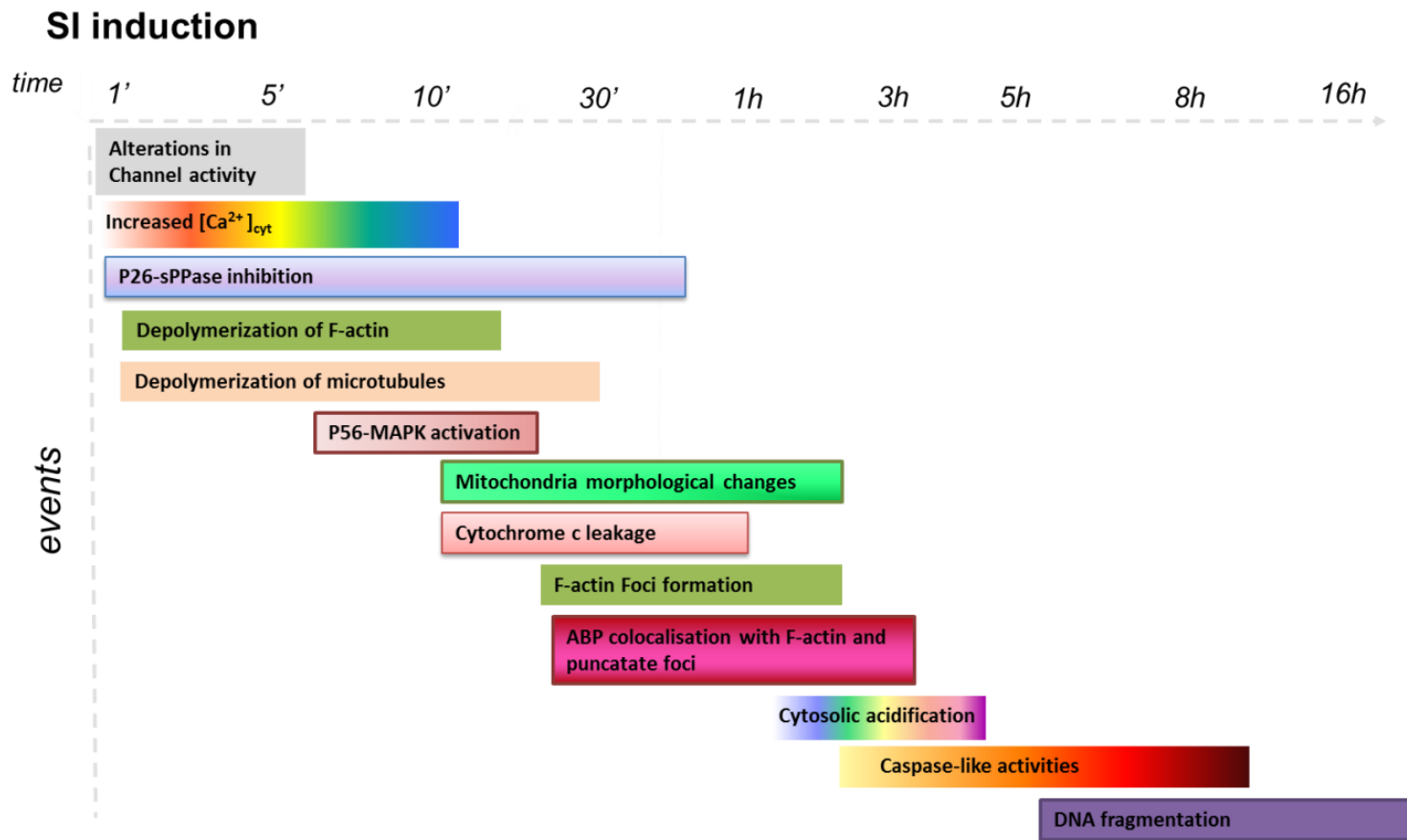
Figure 1.8. A timeline of SI-induced events characterised prior to research carried out in this thesis.

Figure shows the temporally SI-induced events in *Papaver* rhoeas pollen, identify upstream and downstream targets of SI-induced events discussed in Chapter one of this thesis.

2. Examining the possible involvement of phospholipids during the *Papaver* SI response (Chapter 4).

As previously discussed in this chapter, recent research has shown that alterations in the level of key phospholipids play a role in PCD events such as defence and stress responses. We therefore hypothesised that alteration in phospholipid levels also played a role in the SI response. Radiolabelling experiments were carried out to identify modifications in phospholipid levels during an *S*-specific interaction in *Papaver* pollen.

There was a significant alteration in the levels of the secondary messenger phosphatidic acid (PA), phosphatidylinositol monophosphate (PIP), a novel phospholipid diacylglycercol pyrophosphatase (DGPP) and an unidentified lipid PLX$_1$ during and SI response. Furthermore, we investigated whether the PA-producing enzyme phospholipase D (PLD) played a role in SI-induced increases in PA, through n-butanol treatments. The role of ROS and NO were investigated during SI-induced alterations in the levels of pollen tube phospholipids.

3. Investigating SI-induced cytosolic acidification (Chapter 5).

Previous studies identified an extreme acidification of the cytosol in SI-induced pollen tubes after 1-4 hr, which is thought to create optimal conditions for caspase-like activities, which are between pH 4.5-5.5 (Bosch & Franklin-Tong, 2007). This prompted further investigation of SI-induced acidification. The temporal and spatial analysis of SI-induced acidification was carried out through ratiometric imaging of a pH-dependent live cell probe. The analysis showed that acidification was a rapid

event. We hypothesised that this acidification would play a significant role in creating the optimal pH for caspase-like activities. Weak acids were used to manipulate the cytosolic pH of the pollen tube to investigate the role of pH on caspase-3/DEVDase-like activities *in vitro*. This technique was used to examine the role of pH on both caspase-3-like activities and actin foci formation, by both inducing acidification and blocking acidification in SI-induced pollen tubes.

4. Investigating the vacuole as a potential source of protons during SI-induced acidification events (Chapter 6).

Studies were carried out to identify possible causes of acidification. The acidic compartment, the vacuole, was investigated as a potential source of protons. Alterations in vacuolar morphology were characterized through live cell imaging of SI-induced pollen tubes. Such experiments identified extensive reorganization and breakdown of the vacuolar compartment during SI. Furthermore, inhibitors and ionophore were utilized to investigate potential upstream mediatiors of vacuolar breakdown, these included alterations in $[Ca^{2+}]_I$, alterations in cytosolic pH, and alterations in actin dynamics.

Work presented here broadens our understanding of the intimate signalling events involved in SI, and begins to identify the links between already established features, their relationship with each other, and discusses the similarities between *Papaver* SI-PCD and other PCD systems.

CHAPTER 2:

MATERIALS AND

METHODS

2.1 PLANT MATERIAL – *PAPAVER RHOEAS*

2.1.1 PAPAVER PLANT CULTIVATION

Seeds of *Papaver rhoeas* L. (Shirley) of both known and unknown *S*-genotype were sown into John Innes No. 1 potting compost pots, (3 seeds per pot) in a glasshouse at ~15 ˚C. Resultant plants were thinned to one plant per a pot after growing to a height of between 5 and 10 cm. At around 8 weeks in the greenhouse plants were allowed to harden outside for around 4 weeks and were then transplanted to a field in rows with approximately 50 cm between plants and 90 cm between rows.

2.1.2 DETERMINATION OF *S*-GENOTYPE

Plants with flowers 1-2 days prior to anthesis were emasculated on the plant using forceps sterilised in 70% ethanol. Emasculated flowers were covered with cellophane bags and tied using metal wire, to prevent pollination of flowers by insects. Stigmas were allowed to mature overnight and then examined for maturity. Mature emasculated stigmas were pollinated with pollen of a known genotype with a fine paintbrush directly onto the stigma surface. For example, a plant which has an expected genotype of S_1S_3 or S_1S_8, would be pollinated with pollen from a plant carrying either S_1 or S_3 pollen or S_1 or S_8 pollen.

After pollinations, the flowers were again covered in cellophane bags to protect them from contamination with other pollen, and were left overnight on the plant. Stigmas were harvested one day after pollination. The stigma was removed using a scalpel, placed in 20ml glass vials containing aniline blue and were left overnight to allow the stigmas to

58

soften. A sample of the stigma was removed, placed on a microscope slide and squashed using a cover slip. These were samples were then viewed under a microscope using UV illumination. All families grown were two-class families and thus were pollinated with two classes of pollen, one to provide a fully incompatible pollination and one to provide half-compatible pollination.

Those stigmas exhibiting fully incompatible pollination had pollen grains with very short pollen tubes which were identified by callose stained by the aniline blue solution (Figure 2.1b). Compatible pollinations had long pollen tubes with callose plugs at intervals along the length of the tube (Figure 2.1a). Those exhibiting half-compatible pollinations had 50% of pollen exhibiting long pollen tubes with callose plugs, whilst the remainder had no callose in the pollen grain.
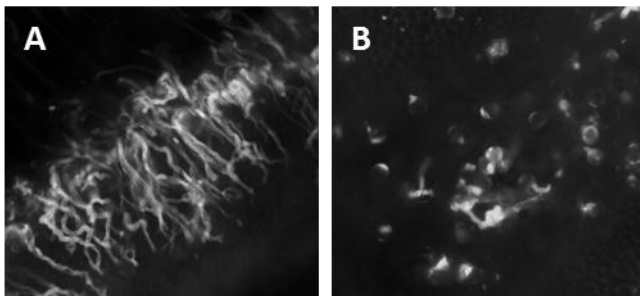
Figure 2.1: Images of pollinated stigma squashes

A fully compatible reaction (a) showing many long pollen tubes with callose plugs at regular intervals, and no callosic pollen grains. A fully-incompatible reaction (b) showing high amounts of callose in the pollen grains and very few pollen tubes.

Using this method, the genotype of the plant could be identified as shown in the Table below (Table 2.2).

Male Female	S$_1$ or S$_8$ pollen	S$_3$ or S$_8$ pollen	S$_2$ or S$_{12}$ pollen
S$_1$S$_8$	Incompatible	Half Compatible	Compatible
S$_3$S$_8$	Half compatible	Incompatible	Compatible
S$_2$S$_{12}$	Compatible	Compatible	Incompatible

Table 2.2. Genotyping of *Papaver rhoeas* plants

A punnett square to demonstrate the self-incompatiblility response in *Papaver* pollen. A compatible interaction occurs when neither *S*-haplotypes carried by the male pollen and the female stigma do not match, such as pollen of an S$_1$ or S$_8$ pollen interacting with a stigma of an S$_2$S$_{12}$ genotype. A half compatible interaction occurs when only one of the *S*-haplotypes match, and therefore half of the pollen would be incompatible and therefore rejected. A fully incompatible interaction occurs when both *S*-haplotypes match, and therefore all pollen will be rejected.

A female plant with a *S*-haplotype of S$_1$S$_8$ pollinated with pollen from a plant carrying S$_1$ or S$_8$ pollen resulted in an incompatible reaction, therefore identifying the female plant as having matching *S*-alleles to the parent of the pollen. However, if pollen from a plant carrying S$_3$ or S$_8$ alleles was used to pollinate the plant of a S$_1$S$_8$ haplotype, there will be a half compatible reaction as only the S$_8$ pollen will be incompatible and therefore growth will be inhibited, resulting in half of the pollen having long pollen tubes with multiple callose plugs and half with short inhibited pollen tubes. If the female plant with an S$_1$S$_8$ genotype is pollenated with pollen from a plant carrying S$_2$ or S$_{12}$ *S*-alleles, all pollen will be compatible and therefore none of the pollen will be inhibited, results in a fully

60

compatible reaction, indicating there are no matching alleles between the female and pollen donor plant.

2.1.3 PRODUCTION OF SEED

Plants of known *S*-genotype were used for the production of seed. Flowers were emasculated and were pollinated with pollen of known *S*-genotype. Pollinated flowers were covered in cellophane bags on the plants and left for approximately 6 weeks. After this time the seed was collected from seed pods and stored in paper bags at 4 °C.

2.1.4 COLLECTION OF POLLEN

Plants with at least three flower buds, 1 day prior to anthesis, were used for the collection of pollen. Multiple buds from the same plant, and therefore all of the same genotype, were cut from the plant 15 cm below the bud. Sepal and petals were removed and flowers were hung together upside down overnight in the cellophane bags in the glass house. Only flowers from the same plant were placed in the same cellophane bag. The following day, pollen was collected by vigorously shaking the cellophane bag and by tipping the pollen into gelatin capsules and labelled with the plant number. Capsules of pollen were stored in boxes containing silica gel to eliminate moisture and kept at -20 °C until required.

2.1.5 *PAPAVER RHOEAS* POLLEN TUBE GROWTH *IN VITRO*

Papaver pollen can be grown using several methods, although all are very similar there are some slight difference depending on the experiment type and volume of pollen required.

61

All methods require the pollen to undergo hydration prior to addition of growth medium as described; pollen was hydrated in a weighing boat, in a moist chamber at 28 ˚C for ~45 minutes. The shape of pollen grains was used to assess the state of hydration. When desiccated, pollen grains are elliptical, when hydrated they become spherical.

For all imaging experiments the following method for growth of pollen tubes was used; following hydration, pollen was resupended in liquid germination medium (GM) (13.5 % (w/v) sucrose, 0.01 % H_3BO_3, 0.01 % KNO_3, 0.01 % Mg $(NO_3)_2.6H_2O$,) and transferred to a 8 cm petri dish containing a solid GM (GM with 1.2 % agarose) base, as previously described in Snowman *et al.,* 2002. Pollen was grown at 10mg.ml^{-1} for ~45 min in a moist chamber at 28 ˚C, and assessed for percentage germination prior to experimentation.

For live cell imaging experiments 300 μL of the pollen sample was transfer to a 35mm glas*S*-bottom microwell culture dishes with a No. 1.5 coverglass (MatTek Corp. Ashland, MA, USA) coated with 0.001% (w/v) poly-l-lysine. Incubation with specific drugs, treatments or fluorescent indicators was carried out on these imaging slides. These slides were then used to image pollen tubes using either an inverted confocal microscope or an epi-fluorescent microscope.

For experiments such as the analysis of actin or caspase-like activities (where the extraction method was used), pollen was incubated with drugs or treatments on the 8 cm petri dish, pollen was allowed to grow for the desired amount of time at 28 ˚C on these dishes.

For experiments in which lipid extracts were analysed or the analysis of caspase-like activities in live cells, the pollen was grown using a slightly different method. Pollen was

62

hydrated and resuspended in liquid medium ensuring even mixing of the pollen and GM, as described above. This pollen sample was then aliquoted into 90 μL (lipid experiment) or 125 μL (caspase experiment) samples in wells of a 48 well plate. Pollen was grown at 10mg.ml^{-1} for ~45 min in a moist chamber at 28 ˚C in the plate. Treatments were introduced to pollen in the well 1:1 (lipid experiment), or made up to a final volume of 200 μL (caspase experiment), and pollen was grown in these wells at room temperature.

2.2 PRODUCTION OF PRSS

2.2.1 PRODUCTION OF RECOMBINANT *E.COLI*

Recombinant PrsS proteins were produced by using the nucleotide sequences specifying the mature peptide of the *S1*, *S3*, and *S8* alleles of the S gene (pPRS100, pPRS300, and pPRS800) cloned into the expression vector pMS119 as described previously (Foote *et al.,* 1994).

2.2.2 GROWTH OF *E.COLI* AND INDUCTION OF PRSS PROTEIN SYNTHESIS

Glycerol stocks of *E.coli* containing specific *S*-alleles, were streaked onto agar plates (50 μg ml^{-1} ampicillin with 15 g L^{-1} bacto-agar; LB Amp) and incubated overnight at 37 ^{o}C. The following day a single colony was isolated and incubated in 200 ml LB medium (LB medium with 15 g L^{-1} bacto-agar) plus 50 μm ml^{-1} ampicillin at 37 ^{o}C on a shaker overnight (200 rpm). The following day, 100 ml of the culture was transferred into a fresh 2 L flask with 100 mL of LB Amp. PrsS protein production was induced by adding IPTG to the concentration of 0.5 mM. The flasks were incubated for 4-6 h at 37 ^{o}C with 200 rpm

63

shaking. Cells were collected by centrifuging at 5000 rpm at 4 ^{o}C in a Beckman centrifuge for 10 min. The supernatant was discarded and the pellet of the cells was stored at -20 ^{o}C until needed. A sample of the pellet was used to check protein induction on SDS-PAGE at each step during the production of PrsS.

2.2.3 PURIFICATION OF INCLUSION BODIES

In order to extract PrsS from *E.coli*, the pellet was re-suspended in 200 mL of cold lysis buffer and centrifuged for 10 min at 5000 rpm, 4 ^{o}C. The supernatant was discarded, and the pellet was re-suspended in 20 mL of cold lysis buffer, to which 400 µl 10 mg ml^{-1} lysozyme (final concentration 0.2 mg mL^{-1}) and 100 µl of 50 mM PMSF (final concentration 0.25 mM) were added and incubated at 4 ^{o}C for 1.5 h. Following this, 26 mg sodium deoxycholate and 50 µl of 50 mM PMSF were added and the suspension was incubated for a further 30 min at 37 ^{o}C. The viscous solution was sonicated on ice, using a Soniprep 150 (Sanyo) at 10 amps for 5 x 30 sec pulses, with at least 30 s breaks on ice between rounds to allow cooling. The samples were centrifuged at 5000 rpm for 20 min at 4 ^{o}C. Following this the supernatant was discarded and pellet was washed in 20 mL of cold lysis buffer with 5 x 30 sec sonication on ice followed by a further centrifugation at 5000 rpm for 20 min at 4 ^{o}C, and the supernatant was discarded. This wash step was repeated 6 times. The clean inclusion bodies were stored at -20 ^{o}C until needed.

2.2.4 REFOLDING RECOMBINANT PRSS

The inclusion body pellet was re-suspended in 6 M guanidine hydrochloride and 500 mM cysteamine (2-mercaptoethylamine) on an orbital shaker for 4 h at room temperature.

Following solubilization, the insoluble mass was removed by centrifugation at 5000 rpm for 15 min at 20 ^{o}C and the supernatant was kept. The protein concentration was determined by Bradford assay (section 2.2.5). A sample was assessed by SDS-PAGE to determine purity of the PrsS protein.

PrsS was very slowly added to the 100 mL arginine folding buffer with the pipette immersed in the liquid with constant stirring, this whole process was carried out at 16 ^{o}C. The solution was left to renature at 4 ^{o}C overnight. The following day, the refolded protein solution was dialyzed against 5 L of the cold dialysis buffer in wide dialysis tubing with a molecular cut off of 12-14,000 Daltons (Medicell International Ltd.) at 4 ^{o}C. The buffer was changed at least 3 times, including one overnight period. Once the dialysis was complete the dialysis buffer was removed except ~100 mL. The tubing was then placed in a beaker with ~2 cm of dialysis buffer. PEG 6000 was sprinkled over the dialysis tubing containing the PrsS protein sample while shaking gently to concentrate the protein. Fresh PEG6000 was regularly added during the day until the sample had concentrated to ~10 % of its original volume. When the desired volume was reached, PEG was washed from tubes with SDW and the proteins were aliquoted into 1 mL microfuge tubes and snap-frozen in liquid nitrogen. The PrsS samples were stored at −80 ^{o}C until required.

2.2.5 ESTIMATION OF PROTEIN CONCENTRATION USING BRADFORD ASSAY

The protein concentration of a sample of PrsS was estimated through the Bradford assay (Bradford, 1976) according to manufacturer's instructions (BioRad, UK). The protein assay reagent (which contains Coomassie® Brilliant Blue G-250) was added to the diluted

protein samples, and its absorbance was measured at 595 nm with a spectrophotometer. Bovine serum albumin (BSA) was used as a standard.

2.3 TREATMENT OF POLLEN TUBES

In order to investigate the signalling events of *Papaver* SI, pollen was often treated with drugs to further our understanding of the relationship of specific messengers and targets of SI.

The method in which pollen was grown depended on the type of experiment and analysis required, this is described in more detail in section 2.1.5. In cases where a pre-treatment was carried out the drug would be added to pollen at the correct concentration for 10 minutes prior to the addition of PrsS. The addition of PrsS would also include the pre-treated drug at the correct concentration to compensate for the new higher volume of the sample.

2.3.1 IN VITRO INDUCTION OF SI

Recombinant PrsS (Kakeda *et al.,* 1998) was dialyzed over night at 4 °C into liquid GM using dialysis tubing with 12–14,000 K Da cut-off (Medicell International Ltd). The following day, PrsS was gently centrifuged and the protein concentration determined using the Bradford assay (Bradford, 1976). PrsS in GM was stored at 4 ^{o}C, and was active for ~5 days after dialysis.

To induce an SI response, PrsS proteins of the same *S*-genotype as the pollen were added to pollen at 10 μg.ml^{-1} (Snowman *et al.,* 2002), unless stated differently in the text. The

specificity of a response was tested with a compatible control. PrsS proteins with different S-alleles to the pollen were added, e.g. pollen with an S-genotype of S_2 or S_{12} were treated with PrsS recombinant proteins of an S_1 and S_8 genotype, result in a compatible interaction. This was used to show whether a response is due to a S-specific interaction.

2.3.2 PROPIONIC ACID

In order to manipulate the cytosolic pH of *Papaver* pollen tubes, propionic acid (sodium propionate in sterile distilled water; SDW) of a known pH was added to pollen growing on a solid GM plate or directly to a glass imaging slide, by holding the plate at an angle and gently pipetting the propionic acid on the dish/slide. A final concentration of 50 mM propionic acid was used. The sample was gently swirled in order to ensure thorough mixing. The pollen was then analysed for either changes in pH, actin, the vacuole or caspase-like activities (see later for methodology).

2.3.3 LATRUNCULIN B (LAT B)

Latrunculin B (Lat B) is a natural toxin derived from marine sponges, including the genus *Latrunculia*. Lat B reversibly binds to actin monomers and prevents them from polymerizing. When administered *in vivo* Lat B disrupts the actin filaments of the cytoskeleton (Snowman et al., 2002; Yarmola et al., 2000). Pollen was treated with 1 μM Lat B (10 mM stock made up in DMSO and stored in aliquots at $-$ 20 °C), pollen was then either fixed and then either labelled with rhodamine phalloidin (Rh-Ph) to analyse actin organization, or the cytosolic pH was measured, or vacuolar organization was monitored or lipid levels were analysed (see later for methodologies).

67

2.3.4 JASPLAKINOLIDE (Jasp)

Jasplakinolide (Jasp) is a drug isolated from the marine sponge *Jaspis johnstoni*. It is a non-fluorescent, cell-permanent F-actin drug which induces the polymerization and stabilization of actin into filaments (F-actin). Jasp binds to F-actin competitively with phalloidin and is an irreversible probe.

Pollen was treated with 0.5 μM Jasp (1 mM stock solution prepared in DMSO stored in aliquots at $-$ 20 °C). Pollen was then either fixed and labelled with rhodamine phalloidin (Rh-Ph) to analyse actin organization or the cytosolic pH was measured or vacuolar organization was analysed accordingly (see later for detailed methodologies).

2.3.5 A23187 (CALCIMYCIN)

A23187 is a mobile ion carrier that forms stable complexes with divalent cations. A23187 is used to increase intracellular Ca^{2+} levels in cells (i.e. it acts as a calcium ionophore). It is also known to inhibit mitochondrial ATPase activity. 10-50 μM A23187 (10 mM stock solution prepared in DMSO stored in aliquots at $-$ 20 °C) was used to increase intracellular $[Ca^{2+}]$ in *Papaver* pollen tubes. After the addition of A23187 to growing pollen tubes, the pollen was either fixed and labelled with rhodamine phalloidin (Rh-Ph) to analyse actin organization or the cytosolic pH was measured or vacuolar organization was analysed accordingly, or ROS and NO levels were monitored using live cell imaging (see later for methodologies).

2.3.6 LANTHANUM (La^{3+})

Lanthanum (La^{3+}) is a calcium channel blocker and was used to prevent intracellular increases in Ca^{2+}. 500 μM La^{3+} (10 mM stock solution prepared in DMSO stored in aliquots at – 20 °C) was added to pollen growing on a solid GM plate or directly to a glass imaging slide (as described in section 2.1.5) and then ROS or NO or cytosolic pH was monitored in SI-induced cells (see section 2.3.1 for detailed methodologies).

2.3.7 DIPHENYLENEIODONIUM (DPI)

Diphenyleneiodonium (DPI) is an inhibitor of flavin-linked oxidases, including NADPH oxidase (Banks, 1966). DPI was used to inhibit ROS production in *Papaver* pollen tubes. Pollen was treated with 400 μM DPI and ROS / NO / pH was monitored accordingly.

2.3.8 TEMPOL

Tempol is a membrane-permeable ROS scavenger. Tempol was used to scavenger ROS in *Papaver* pollen tubes at 2 mM. This treatment was used in conjunction with caspase and lipid analysis.

2.3.9 2-(4-CARBOXYPHENYL)-4,4,5,5-TETRAMETHYLIMIDAZOLINE-1-OXYL-3-OXIDE (cPTIO)

2-(4-carboxyphenyl)-4,4,5,5- tetramethylimidazoline-1-oxyl-3-oxide (cPTIO) is a nitric oxide scavenger and was therefore used to scavenge NO in *S*-induced pollen tubes. c-PTIO was used at 400 mM and then NO or ROS was monitored.

69

2.3.10 HYDROGEN PEROXIDE

Hydrogen peroxide (H_2O_2) was used to artificially trigger increases in reactive oxygen species in the pollen tube. Furthermore this treatment was used at 2.5 mM to test the ability of the probe CM-H_2DCF-DA to monitor alterations in ROS in pollen tubes.

2.3.11 N-BUTANOL

During phospholipid analysis, n-butanol can be used to as a competitive substrate for the transphosphatidylation activity of Phospholipase D (PLD; Munnik et al. 1995). This occurs at the expense of phosphatidic acid (PA) formation, resulting in the formation of phosphatidyl butanol (P-But). The formation of P-But via PLD activity can be monitored using ^{32}P-labelling of pollen extracts (see section 2.7). 0.5% n-Butanol was used during such experiments.

2.4 VISULAISATION OF F-ACTIN IN *PAPAVER* POLLEN TUBES

Pollen was grown and treated using the required treatment as described above, and fixed with 400 μM 3- maleimodobenzoic acid N-hydroxysuccunumide ester (MBS; Pierce. 10 mM stock in DMSO) for 6 min at room temperature, followed by 2 % paraformaldehyde for 1 h at 4 °C. Both these fixatives were slowly dripped into the growing pollen tubes in a petri dish tilted to evenly distribute the chemicals. Pollen tubes were collected using a pipette tip which had the tip cut off to enlarge the opening, limiting damage to pollen tubes during their transfer into a fresh microfuge tube. To remove the fixative the pollen was centrifuged at 4,000 rpm for 1.5 minutes, the supernatant was discarded and 1 ml of 1x Tris buffered saline, pH 7.6 (TBS) was added the microfuge tube. The centrifugation

was repeated and this wash step was repeated twice more, and the pollen pellet was finally re-suspended in 100 µl of TBS.

Actin was stained using 66 nM Rhodamine Phalloidin (Rh-Ph), wich only binds F-actin, not G-actin. The fixed pollen samples were incubated with Rh-Ph for at least 30 minutes at 4 °C, but usually left overnight to ensure good levels of staining.

2.5 PROGRAMMED CELL DEATH (PCD) ASSAY

As discussed in the Chapter One, programmed cell death (PCD) can be defined by several key markers. These studies have used caspase-3-like activity as a marker of PCD during the SI response in *Papaver* pollen tubes. Caspase-3/DEVDase-like activities can be monitored using several different methods. During this thesis two methods were used for the analysis of caspase-3-like activities in pollen tubes. Firstly activities were monitored through the incubation of pollen extracts to the caspase substrate Ac-DEVD-AMC and cleavage activity was detected with a fluorescence plate reader. Secondly caspase-like activities were monitored with the ImageiT Live Caspase 3 & 7detection Kit, which allows the imaging of caspase-like activities in live pollen tubes. Both techniques are described in more detail below.

2.5.1 CASPASE ACTIVITY ASSAY - Ac-DEVD-AMC

The fluorogenic caspase-3 substrate Ac-DEVD-AMC is used to establish whether caspase-3-like activity, and therefore PCD, is present in pollen tube treated with drugs and/or during SI response. This fluorescent caspase activity assay is based on the cleavage of 7-amino-4-methylcoumarin (AMC) from the C-terminus of the fluorogenic substrate (Ac-

71

DEVD-AMC) by a caspase-like enzyme, which is measured by an increase in the fluorescence intensity at 460 nm. This caspase substrate has the amino acid recognition sequence DEVD which is generally cleaved by caspase-3 in mammalian cells. The fluorogenic caspase-3 substrate Ac-DEVD-AMC gives off a fluorescent signal when cleaved to DEVDase (caspase-3-like) activity which can be monitored by a fluorescence plate reader.

Pollen was prepared as stated under section 2.1.5. Pollen tubes were treated with various stimuli/drugs for 5 hours at room temperature (as this time period gives the highest caspase activity if PCD is occurring [Bosch & Franklin-Tong, 2007]). Following this treatment stage, the pollen tubes were collected from the petri dish by scraping the pollen with a bacterial spreader made from a glass pipette. Using a plastic pipette with a cut tip, the pollen sample was transferred into a 1.5 mL microfuge tube. Pollen was then centrifuged in a micro-centrifuge for 1 min at 13,200 rpm. The supernatant was discarded. 160 µl of caspase extraction buffer (50 mM sodium acetate, 10 mM L-cysteine, 0.01% CHAPS and 10% glycine, pH 6), was added to the pollen pellet. The samples were then roughly homogenized using a pellet pestle. At this point pollen could be snap-frozen in liquid nitrogen and stored at -20 $^{\circ}$C. The pollen samples were then subjected to 4-5 rounds of sonication at 10 amps for 10 seconds, and kept on ice during and after sonication to prevent overheating. This was followed by centrifugation for 30 min at 13,200 rpm (max. speed) at 4 $^{\circ}$C. The supernatants containing extracted proteins were removed and were frozen at -20 $^{\circ}$C until required.

The protein concentration of the pollen protein extraction samples was measured using the Bradford Assay as described in section 2.2.5. The protein concentration was then adjusted to 1 µg µl^{-1} by diluting in caspase extraction buffer. If the protein concentration was below 1 µg µl^{-1}, the appropriate volume of extract was added to the well to make up 10 µg. 10 µg of total protein was incubated with 50 µM Ac-DEVD-AMC in sodium acetate (NaOAc) buffer (50 mM sodium acetate, 10 mM L-cysteine, 0.01% CHAPS and 10% glycine, pH 5.0) at 27°C, total volume 100µl per well in a 96 well plate. The other samples were made up to the maximum volume of extract with pH 6 sodium acetate extraction buffer, so all the samples had equal volumes of protein extract and pH 6 extraction buffer. An additional sample was set up, in which Ac-DEVD-CHO, an inhibitor of caspase 3 & 7 activity, was used to ensure authentic caspase-like activity was being monitored by the caspase detection probe, Ac-DEVD-AMC, during these caspase detection assays. Fluorescence was monitored at 460 nm using a time-resolved fluorescence plate reader (FLUOstar OPTIMA; BMG LABTECH) every 15 min over a time period of 5 h. The caspase activity for each sample was calculated by subtracting the fluorescence reading of the first cycle from the final (21st) cycle reading. The results were presented as percentage caspase activity relative to the untreated control or the SI-induced sample. Each assay was performed on at least 3 independent samples, and was measured in duplicates. P-values were calculated using ANOVA.

2.5.2 CASPASE ACTIVITY ASSAY- IMAGE-IT ™ LIVE GREEN CASPASE-3 AND -7 DETECTION KIT

In order to monitor caspase activity in living growing pollen tubes the cell permeant ImageiT Live Caspase 3 & 7 detection Kit (Invitrogen) was used. This kit contains a FAM-DEVD-FMK FLICA regent which is associated with a fluoromethyl ketone (FMK) moiety which can react covalently with a cysteine, with a caspase- specific amino acid sequence. This recognition sequence is aspartic acid-glutamic acid-valine-aspartic acid (DEVD / caspase 3 & 7), furthermore a carboxyfluorescein group (FAM) is attached as a reporter.

FAM-DEVD-FMK was prepared as a 30x stock in DMSO fresh on the day of use and was used at 0.1x in GM. Pollen tubes were incubated with the FAM-DEVD-FMK for 60 min wrapped in aluminium foil, to protect the probe from light, before being transferred to a glass bottomed imaging dish, and the pollen tubes were washed twice in fresh GM. Pollen tubes were then imaged using an epifluorescence microscope using FITC filters. Only fluorescence in pollen tubes was scored; pollen which did not produce a tube was not scored due to the high levels of auto-fluorescence in the grain. Fluorescence was used to indicate the presence of caspase 3 & 7 activity in the cell. 50 pollen tubes were scored per a treatment and at least 3 independent replicates were performed for each treatment.

2.6 FLUORESCENCE MICROSCOPY

2.6.1 EPIFLUORESCENCE IMAGING

Epifluorescence images were collected with a Nikon Eclipse TE300 microscope attached to a charged coupled device (CCD) camera supplied by Applied Imaging, UK. Fluorescence

74

was detected using filters fluorescein isothiocyanate (FITC) filter (excitation, 492 nm, emission 519 nm; Chroma Technology) or Texas Red (excitation, 577 nm, emission 620 nm; Chroma Technology) configured by Applied Imaging, UK. Capture and analysis of images was achieved with Nikon Elements imaging software. Images were saved as TIFF files and then analyzed using ImageJ or Microsoft PowerPoint. This system was used to collect images and data from cells labelled with either a ROS, NO or mitochondrion live imaging probe (as discussed below), genotyping of *Papaver* plants and F-actin analysis.

2.6.2 CONFOCAL LASER SCANNING MICROSCOPY

Confocal microscopy was carried out using a Leica SP2 Inverted Confocal with a controlled environmental chamber. The system is equipped with at 488nm, 458nm, 405nm and lasers. Lasers used for each experiment are stated in each individual experimental procedure. This equipment was used for live cell imaging of *Papaver* pollen tubes labelled with a vacuolar compartment probe and the measurement of cytosolic pH. It was also used to image fixed pollen tubes stained with rhodamine phalloidin (Rh-Ph).

2.6.3 VACUOLAR LABELLING

1 µM 5-(and-6)-Carboxy-2',7'-dichlorofluorescein diacetate(c-DCFDA; Invitrogen) was used for vacuolar visualization. c-DCFDA is colourless and non-fluorescent until its acetate groups are cleaved by intracellular esterases which results in it's fluorescent form.

Pollen was grown in petri dishes as described in section 2.1.5. Pollen was either pre-treated on imaging slides with drugs etc before the addition of the vacuolar probe c-DCFDA or afterwards depending on the time point required, as the signal of the probe

decreases after ~35 minutes of labelling; therefore multiple pollen tubes had to be imaged to document later time points. Pollen was labelled between 15-30 minutes in darkness with c-DCFDA and then imaged using a confocal microscope (see section 2.6.2), exciting with 488nm lasers and emission was collected with a 500-550 nm band pass filter.

2.6.4 REACTIVE OXYGEN SPECIES & NITRIC OXIDE IMAGING IN POLLEN TUBES

Pollen was grown in petri dishes as described in section 2.1.5. A sample of the pollen was transferred onto an imaging dished prior to the addition of fluorescent indicators for reactive oxygen species (ROS) or nitric oxide (NO). For the visualisation of ROS in *Papaver* pollen tubes, the cell permeable dye CM-H2DCF-DA (2 µm Invitrogen) was incubated with pollen for 30 min in the dark. NO was monitored using the probe DAF-FM-DA (10 µm; Invitrogen). Pre-grown pollen tubes were incubated with the probe for 10 minutes, in the dark. After the appropriate incubation with either the ROS or NO probe, pollen was imaged prior to the addition of treatments and thereafter to monitor the effects of treatments on either nitrogen species in the pollen tubes using an epi-fluorescent microscope (see section 2.6.1). This is described in more detail in Chapter 3.

2.6.5 MEASURING CYTOSOLIC pH OF POLLEN TUBES

Intracellular pH (pHi) was monitored in living pollen tubes with acetoxymethyl ester of the pH-sensitive fluorophore 2′,7′‑bis‑(2‑carboxyethyl)‑5‑(and‑6)‑carboxyfluorescein (BCECF; Invitrogen), using a Leica DM IRE2 confocal microscope (see section 2.6.2). BCECF

has a pK_a of ~ 6.98, and is therefore ideally matched to the normal range of cytoplasmic pH (pH 6.8-7.4). BCECF AM is an ester derivative which is uncharged and is therefore membrane permeable and therefore does not need to be injected like BCECF dextran. Once inside the cell the lipophilic blocking groups are cleaved by intracellular esterases, turning the non-fluorescent BCECF AM into a charged fluorescent form. BCECF is excited at 488 nm and emits ~550 nm.

Pollen tubes were grown according to section 2.1.5, and then transferred on to glass bottomed imaging dishes coated with 0.01% poly-lysine prior to treatments or labelling with BCECF AM. As BCECF AM has a tendency to be sequestered into pollen tube organelles after ~25 min incubation, newly labelled pollen tubes must be imaged for each time point. As a result, pollen was treated with drugs either before or after labelling with BECEF AM, depending on the time point required.

Pollen tubes were loaded with 2 μM BCECF for 3.5 min, followed by a 100 μl wash with GM plus treatment to the same concentration as the sample (i.e. if the treatment final concentration was 1 μM then the wash was also 1 μM so as to ensure that the sample was not diluted). Samples were only imaged within 5-10 minutes after the addition of BCECF, as this timeframe allowed accurate reporting of cytosolic pH. Samples could not be used after this 10 minute period, due to dye sequestration by organelle compartments.

Images were taken sequentially using the following microscope settings. The first image was taken under the following conditions: excitation at 488 nm, 7% power and emission were collected at 510–550 nm. The second image was captured using excitation at 458

77

nm, 12% power, and emission 510-550. Both images were captured using the following settings: 512x512 frame size, scan average 1x, 400x scan speed, 3x zoom. Each pair of images (488 and 458 nm) was imported into Image J software as a 'stack', layering the images on top of each other. A box was drawn in the pollen tube of a known size (a 50 x 50 pixel box, 4 boxes per tube) and the mean intensity of that area was measured. A measurement was taken from each pollen tube image (488 nm and 458 nm image) in exactly the same position on each image. Four pairs of measurements were collected for each tube. Each pair of measurements was used to create a ratio (pH-dependent: pH independent ratio; 488 nm : 458 nm). The ratio from all the pairs of measurements was averaged to give one ratio value per pollen tube. These mean ratio values were then used to determine the pH of the pollen tube using a reference calibration curve based on a pseudocytoplasm calibration set. A calibration curve was carried out for each individual imaging session.

In vitro calibration was performed using 40 μM BCECF free acid (2',7'-(carboxyethyl)-5-(and-6)-carboxyfluorescein; Invitrogen) in a pseudocytosol (100 mM KCl, 10 mM NaCl, 1 mM MgSO$_4$, 10 mM MES, 10 mM Hepes, adjusted to desired pH). 200 μl of pseudocytosol was added to a glass bottomed imaging dish. 40 μM BCECF free acid was added to the slide and mixed using a pipette away from direct light. Imaged were taken sequentially using the same microscope settings as those used for *in vitro* pollen tube measurements (488 nm, 458 nm). A pair of images was taken at each of the following pH values to create a calibration curve: pH 5, 5.5, 6, 6.5, 7, 7.5, 8. Using image J software, average intensities were measured for each pair of images and a ratio value calculated. These ratios were

then plotted to give a calibration curve pH: ratio. This calibration curve was then used to calculate the pH of individual pollen tubes in the presence of various stimuli.

2.7 PHOSHOLIPID ANALYSIS

2.7.1 PHOSHOLIPID LABELLING WITH ^{32}P

Papaver pollen was hydrated at 28 °C for 1 hour as described in section 2.1.5. Pollen was suspended in liquid GM (10 mg.ml^{-1}). Pollen was then treated with 50 µCi ^{32}PO$_4^{3-}$ (Amersham ^{32}PO$_4^{3-}$, carrier free), and aliquot into 90 µL samples in a 48 well plate and incubated for 4 hours at room temperature.

2.7.2 POLLEN TREATMENTS OF ^{32}P LABELLED POLLEN TUBES

After 4 hours labelling with 50 µCi ^{32}P, pollen treatments were administered 1:1 with pollen extracts. Treatments included: addition of PrsS, A23187, La^{3+}, DPI, c-PTIO, Jasp, Lat B and n-butanol. All are described in the pollen treatments section (section 2.3).

2.7.3 LIPID EXTRACTION

At specific times, ^{32}P-labelled pollen tube samples were stopped by the addition of 20 µL 50% perchloric acid (PCA, 5% final concentration). After mixing, samples were removed from 48 well plate and transferred to a 2 mL 'safe lock' Eppendorf and vortexed for 5 minutes. Samples were centrifuged for 1 minute, 13,000 rpm and further treated with 750 µL of CMH solution (CHCl$_3$/MeOH/HCl (50:100:1)), which was followed by 5 minute on a vortex shaker. Samples were centrifuged once more at 13,000 rpm for 1 minute. The water was then removed from the lipid sample by the addition of 400 µL of chloroform

(CHCl$_3$) followed by 100 µL of 0.9 % NaCl, and vortexed on shaker for 5 minutes. After another centrifugation at 13,000 rpm for one minute the upper phase (aqueous free label) of the sample was removed and discarded. The lower phase was transferred to a clean tube containing 400 µL theoretical upper phase (TUP; CHCL$_3$:MeOH:1M HCL, 3:48:47 v/v). Samples were vortexed for 5 minutes on shaker and centrifuged at 13,000 rpm for 1 minute. The upper phase was once again removed and discarded. 20 µL of cold iso-propanol was added to each sample. Lipid extracts were then dried by vacuum centrifugation (~45 minutes, heated to 54 °C). Once samples had dried they were dissolved in 100 µL CHCl$_3$ and samples were stored at -20°C (under N$_2$ gas) or used immediately for TLC analysis.

2.7.4 THIN LAYER CHROMATOGRAPHY (TLC)

In order to analyse phospholipid activity, lipid extracts were separated using a thin layer chromatography (TLC) using several different solvent systems. For standard analysis 20 µL of each lipid extract was loaded onto a potassium oxalate (KOX) coated Silica 60 TLC plate. Samples were loaded at least 3 cm away from the edge of the plate and 2 cm from the bottom of the plate. All samples were pre-incubated in an alkaline solvent system (CHCl$_3$, MeOH, 25 % NH$_4$OH, H$_2$O; 90:70:4:16 (v/v/v)) tank for 30 minutes before separation by TLC for 1.5 hours using the alkaline solvent system as described by Munnik et al.,(1994a).

In experiments in which n-butanol was used to monitor PLD activity in ^{32}P-labelled pollen tubes, lipid extracts were loaded on to standard Silica 60 TLC plates, and lipids were separated in an EtAc solvent system comprising Eythl acetate/Iso-octane/Formic

acid/H_2O (120:Iso-octane:30: 100)) for 1 hr. Radio-labelled phospholipids were detected using either autoradiography or phosphorimaging (Molecular Dynamics).

2.7.5 PHOSPHOR-IMAGER ANALYSIS

In order to quantify alterations in lipid extracts, phosphorimages of the samples run on TLC were analysed. Individual lipid spots were quantified using a Typhoon FLA 7000 PImager (General Electric) and analysed using Image Quant software (General Electric).In addition the background for each lane was calculated and the lipid spots were then presented as a percentage of total labelled lipids, or as otherwise stated. In most cases lipids were identified by using a tobacco BY2 cell extract as a standard.

2.7.6 IDENTIFICATION OF PLX$_2$

Tobacco BY2 cells were used as a standard for the identification of labelled lipids in *Papaver* pollen extracts. However on specific occasions, further analysis was required to confirm the identity of some lipids, this included lipids labelled as PLX$_1$ and PLX$_2$. For the preparation and purification of ^{32}P-labeled PLX$_1$ and PLX$_2$ a two-dimensional TLC system was used. Lipid extracts from pollen treated with PrsS for 120 min were loaded on to a KOX TLC plate at the far right hand side of the plate. The extract was run in an alkaline solvent system (as described above) for 1.5 hr in the first dimension. The plates were then air dried and the plate was turned on its side and chromatography carried out in a second dimension using an acidic solvent solution ($CHCl_3$/pyridine/formic acid (35:30:7, v/v/v) for 1 hr. PLX$_1$ and PLX$_2$, phosphatidic acid (PA) and lysophosphotidic acid (lysoPA) were isolated using a scalpel and placed in individual Eppendorf to be dried in a vacuum centrifuge.

81

PLX$_2$ was expected to be Diacylglycerol Pyrophosphate (DGPP). Therefore, following the Munnik *et al.* (1994a) protocol ^{32}P-Labeled PLX$_2$ was taken through a deacylation process in which lipids were deacylated with monomethylamine at 53°C for 30 min as described in Munnik *et al.* (1994a), if PLX$_2$ was DGPP a this process would result in a glyceropyrophosphate (GroPP). The PLX$_2$ was then dried by vacuum centrifugation and dissolved in H$_2$O.

Furthermore PLX$_2$ was further treated with n-butanol/petroleum ether 40-60° /ethyl formate (20:4:1) to remove fatty acids. The upper organic phase was removed and discarded, the lower phase was washed once more with a n-butanol: petroleum ether 40-60° : ethyl formate (20:4:1) solution and vacuum centrifuged until dry. At this point half of the PLX$_2$ sample was taken through a mild acid treatment in which the potential GroPP would be hydrolyzed to phosphate (P$_i$) and glycerophosphate (GroP). This was carried out via the treatment with 4 M formic acid for 10 min at 100°C.

Samples were spotted on polyethyleneimine (PEI) cellulose anion-exchange TLC polygram sheets, and GroP, Pi, and GroPP were separated using a mixture of 0.5 M ammonium formate and 0.2 M formic acid as a solvent (Munnik et al., 1994). ^{32}P-labeled Pi standard was from Amersham Corp. Radioactive spots were detected by autoradiography.

CHAPTER 3: REACTIVE OXYGEN SPECIES AND NITRIC OXIDE MEDIATED ACTIN REORGANIZATION AND PCD IN THE SI RESPONSE OF *PAPAVER*

3.1 INTRODUCTION

As mentioned in Chapter 1, Reactive oxygen species (ROS) and Nitric Oxide (NO) which are well known signalling molecules are involved in numerous biological responses in both mammalian and plant systems (see Apel and Hirt, 2004; Kwak et al., 2006; Laloi et al., 2004; Mittler et al., 2004 for reviews). ROS and NO play a considerable role in plant PCD, and in particular during pathogen attack. Both ROS and NO have been implicated in the formation of an oxidative burst which is used to combat infections. Moreover, during hypersensitive response (HR) ROS has been associated with increases cytosolic Ca^{2+} levels, the activation of MAPK, microtubule depolymerization, and cell death (Lecourieux et al., 2002; Levine et al., 1996; Levine et al., 1994; Rentel et al., 2004). Furthermore, NO signalling has been linked to the activation of defence genes during a pathogen-induced HR (Romero-Puertas et al., 2004).

As discussed in Chapter 1, ROS is also involved in cell development and the regulation of many processes, including the regulation of tip growth in both root hairs and pollen tubes (Potocky *et al.,* 2007; Wang *et al.,* 2010). It has been demonstrated that ROS scavengers inhibit tip growth in pollen tubes, showing that ROS is essential for normal growth; the cessation of growth was recovered by the addition of H_2O_2 showing that H_2O_2 may be responsible for regulating pollen tube growth (Potocky *et al.,* 2007). Although NO is known to have a role in plant development, such as triggering seed germination (Kopyra et al, 2003) and root hair formation (RHF) (Lombardo *et al.,* 2005), it has not yet been directly associated with regulating tip growth. However, there is evidence that NO is involved in the re-orientation of *Lilium longiflorium* pollen tubes (Prado *et al.,* 2004,

84

2008). More recent research has suggested that the NO signalling pathway is involved in mediating the suppression of pollen germination and pollen tube elongation by extracellular nucleotides in Arabidopsis pollen tubes, in response to high levels of extracellular ATPγS (Reichler et al., 2009). In addition, NO has been implicated during a stress response to ultraviolet-B radiation in *Paulownia tomentosa* pollen tubes. Ultraviolet-B radiation triggered a reduction in pollen germination and tube growth, which was associated with an increase in NO levels in the pollen grain and tube (He *et al.,* 2007).

ROS and NO have also been associated with signalling during pollination in *Arabidopsis* and *Sececio squalidus* (McInnis *et al.,* 2006). Evidence suggested that pollen had a high concentration of NO while stigmatic papillae had a high concentration of ROS. When a pollen grain adhered to papillae, ROS levels were reduced, suggesting cros*S*-talk between ROS and NO, and a potential important role in pollen-pistil interactions. More recent work has suggested that ROS production is disrupted during *S*-RNase-SI in *Pyrus*, which is linked to actin depolymerization and DNA fragmentation (Wang et al., 2010).

In summary, ROS and NO are important second messengers during PCD and pistil-pollen interactions. PCD is a key feature of the SI response in *Papaver* pollen tubes, and although ROS and NO have been implicated in plant reproduction there are limited studies involving physiologically relevant stimuli. However, since this the work presented in the chapter commenced, a group working on SI in olive (*Olea europaea*) have also discovered that both $O_2^{\cdot-}$ and NO are essential for triggering PCD in self-incompatibility.

Furthermore, it was suggested that SI triggers PCD through a peroxynitrite, which is involved in protein nitration (Serrano et al., 2012).

In this chapter, both ROS and NO were investigated in *Papaver* pollen tubes during SI. Investigations were carried out to establish whether ROS and/or NO were essential for SI, and also investigate what was up or downstream of the ROS/NO response. Furthermore, we investigated whether ROS and/or NO were involved in the SI-PCD pathway. This work was published in Plant Physiology (www.plantphysiol.org):

K.A. Wilkins, J. Bancroft, M. Bosch, J. Ings, N. Smirnoff, and V.E. Franklin-Tong (2011). ROS and NO mediate actin reorganization and programmed cell death in the Self-Incompatibility response of *Papaver*. *Plant Physiology*, **156**, 404-16.

(Copyright American Society of Plant Biologists)

In summary, this paper identified distinct patterns in increases in both ROS and NO triggered by the SI response. We established that Ca^{2+} increases are upstream of ROS and NO and that ROS/NO scavengers alleviated both the formation of SI-induced actin punctate foci and the activation of a DEVDase/caspase-3-like activity implicated in being involved in SI-PCD. This work demonstrated the importance of ROS and NO during *Papaver* SI events and highlighted their role in triggering alterations in key SI markers, including signalling to PCD.

I investigated the functional role of ROS and NO increases in *Papaver* pollen tubes (Figure 5-7) and provided images for supplemental data (Supplemental Figures 2-6). This included identifying Ca^{2+} as a mediator of ROS and NO in SI-induced *Papaver* pollen tubes. I also investigated ROS and NO signalling during SI-stimulated formation of actin punctate foci and the activation of caspase-like activities (DEVDase). Furthermore I contributed

data in the form of controls and repeats experiments of SI-induced alterations in ROS and NO in pollen tubes (Figure 3 &4). In addition, I also carried out analysis on all the data presented in the paper, including statistical analysis and the production of figures and supplemental movies. I also contributed to the writing of the results section of the functional data and was involved in editing draft manuscripts.

I was not the only person to contribute to the manuscript and the other authors contributions are as follows: James Bancroft was an undergraduate student in the Franklin-Tong lab and also undertook an undergraduate Summer Studentship from the Wellcome Trust. James carried out all the preliminary ROS and NO imaging and established that SI stimulated ROS and NO. He contributed to the following figures: Figure 1-4 and Supplemental Figure S1.

Maurice Bosch was a post-doc in the Franklin-Tong lab and supervised James Bancroft, and contributed to the writing of the manuscript and editing. James, Maurice and I contributed equally to the paper.

Jennifer Ings worked in the Franklin-Tong lab as an undergraduate project student under my supervision. She worked with me to learn many of the techniques used here and independently contributed some of the caspase activity data (Figure 6).

Nicholas Smirnoff was involved in the discussion of ideas and editing of the manuscript. Noni Franklin-Tong is my supervisor and so had overall control of the project and was responsible for the writing of the manuscript.

3.2 THE PUBLISHED PAPER

CHAPTER 4: INVESTIGATING A POSSIBLE ROLE FOR PHOSPHOLIPID SIGNALLING DURING THE SELF INCOMPATIBILTY (SI) RESPONSE IN *PAPAVER RHOEAS* POLLEN TUBES

4.1 INTRODUCTION

As previously discussed in Chapter 1, phospholipid signalling is becoming a popular topic of research in plant biology. In recent years, phosphatidic acid (PA) has been identified as a secondary messenger (Munnik, 2001; Testerink and Munnik, 2005; Testerink and Munnik, 2011), associated with a wide range of important cellular processes such as MAPK activation (Lee et al., 2001; Yu et al., 2010), K$^-$ channel activity (Jacob *et al.,* 1999), and actin organization (Lee *et al.,* 2003). Furthermore, PA signalling plays an important role in plant signalling during biotic and abiotic stress responses, including pathogen attacks (Laxalt and Munnik, 2002; Laxalt et al., 2007; van der Luit et al., 2000; Yamaguchi et al., 2005; Young et al., 1996), wounding (Bargmann et al., 2009a; Lee et al., 2001), and hyperosmotic stress (Bargmann et al., 2009b; Meijer et al., 2001; Munnik and Meijer, 2001; Zonia and Munnik, 2004).

As mentioned in Chapter 1, PA signalling has been documented during pollen tube growth in several species, and has been implicated in the regulation of cell polarity in tobacco pollen and tip-focused $[Ca^{2+}]_c$ gradient (Potocký *et al.,* 2003). Furthermore, PA signalling has also been implicated in triggering alterations in cytoskeleton dynamics in mammalian (Ha and Exton, 1993; Zhou et al., 1995) and plant cells (Dhonukshe et al., 2003; Gardiner et al., 2003; Gardiner et al., 2001). In particular, PLD activity has been associated with microtubule rearrangement in Arabidopsis roots (Gardiner *et al.,* 2001). Addition of 1-butanol, which inhibits PA production via PLD activity, disrupted the organization of cortical microtubules, suggesting that PA through the PLD pathway, is required for normal regulation of the microtubule cytoskeleton and therefore growth

(Gardiner *et al.,* 2003). Research has also shown that PA triggers actin alteration through the modulation of actin binding proteins (ABP), and in particular Capping Protein (CP) (Huang *et al.,* 2006). Huang *et al.,* (2006) found that the presence of PA results in the inhibition of the ability of CP to block the barbed end of actin filaments, leading to significant increases in filamentous actin in both Arabidopsis suspension cells and *Papaver* pollen grains. Moreover, PA treatments in soyabean suspension-cultured cells, resulted in significant increases in filamentous actin within 30 minutes of treatment. It is also suspected that a Ca^{2+}-dependent protein kinase may transduce the PA signal (Lee *et al.,* 2003).

PA has been shown to accumulate in response to several Pathogen Associated Molecular Patterns (PAMPs), including xylanase, flagellin, n-acetylchitooligosaccharide, and chitosan in tomato, alfalfa, and rice cells (Bargmann et al., 2006; den Hartog et al., 2003; Raho et al., 2011; van der Luit et al., 2000). Treatment of tomato cell cultures with the fungal elicitor xylanase resulted in increases in PA via phospholipase C (PLC) and diacylglycercol kinase (DGK) pathway. Furthermore, this response results in an accumulation in nitric oxide (NO), which is involved in inducing cell death (Laxalt and Munnik, 2002; Laxalt et al., 2007). PA signalling has also been linked to both upstream and downstream increases in reactive oxygen species (ROS) during cell death in plants (Park et al., 2004; Sang et al., 2001; Zhang et al., 2003; Zhang et al., 2009b). In ABA signalling in guard cells, PA production via PLD α1, is involved in triggering increases in ROS through the stimulation of NADPH oxdase activity RbohD (RbohD; respiratory burst oxidase homolog D) and RbohF (Zhang et al., 2009b).

91

As discussed in Chapter 1, there is increasing evidence for phospholipid signalling during pollen tube growth. Alterations in PA levels have been shown to be involved in hypo-osmotic or hyperosmotic stress responses in tobacco pollen tubes (Zonia and Munnik, 2004). Furthermore, during hyperosmotic stress there is an increase in phosphatidylinositol phosphate (PIP) levels, and the pollen tube apical region increased by 46% in cell volume. These increases in PA were generated by PLD activities. Salt-induced hyperosmotic stress in pollen tubes triggers a reduction in PA levels and an increase in phosphatidylinositol bisphosphate (PIP_2) isomers. These data highlight the involvement of specific PA 'signature' during specific stresses.

As previously discussed (Chapter 1), the SI response in *Papaver rhoeas* triggers a complex signalling pathway in incompatible pollen mediated by increases in cytosolic Ca^{2+}, which results in Programmed Cell Death (PCD). As PA signalling has been linked to many key targets which are involved in the SI in *Papaver*, such as cytosolic Ca^{2+}, and alteration is the cytoskeleton (Dhonukshe et al., 2003; Li et al., 2009). Furthermore, data presented in Chapter 3, also identified ROS and NO key signalling components during the SI response, and as discussed above ROS and NO play a key role in many PA-mediated responses during the HR. We therefore investigated the role of phospholipids during the SI in *Papaver rhoeas* pollen tubes by examining changes in phospholipid levels. SI-induced alterations in phospholipid levels were identified as early as 20 minutes after the induction of SI, resulting in alterations in PA, and PIP. Furthermore, a novel phospholipid identified as diacylglycercol pyrophosphatase (DGPP) also underwent significant increases. In addition, treatments with 1-butanol showed during an SI response there is a significant up-regulation of PLD activity.

We also investigated the potential role of upstream mediators during SI-induced alterations in phospholipid levels. As actin depolymerization occurs within 2 minutes of SI induction, the role of actin dynamics was also investigated as a potential upstream mediator of SI-induced alterations in phospholipids. Moreover, as ROS and NO play an important role in the SI response, we therefore investigated whether increases in ROS or NO play a role in triggering specific SI-induced phospholipid alterations.

4.2 RESULTS

4.2.1 ^{32}P INCORPORATION IN *PAPAPVER RHOEAS POLLEN*

In order to monitor phospholipids in *Papaver* pollen, the lipids were labelled with radioactive orthophosphate (^{32}PO$_4{}^{3-}$). To ensure a suitable amount of pollen lipids were incorporated with the radioactive ^{32}P, healthy pollen tubes were grown in the presence of ^{32}PO$_4{}^{3-}$ for different time periods and a lipid extraction subsequently carried out on the samples. Lipid extracts were analysed using thin layer chromatograph (TLC; see materials and methods for details). Structural lipids such as phosphatidylethanolamine (PE) and phosphatidylcholine (PC) labelled within 30 minutes, however labelling of smaller lipids such as phosphatidic acid (PA) and phosphatidylinositol monophosphate (PIP) took much longer (see Figure 4.1). Four hours of labelling led to suitable levels of ^{32}P incorporation of all major lipids, therefore this length of time was selected for all further radiolabelling experiments.
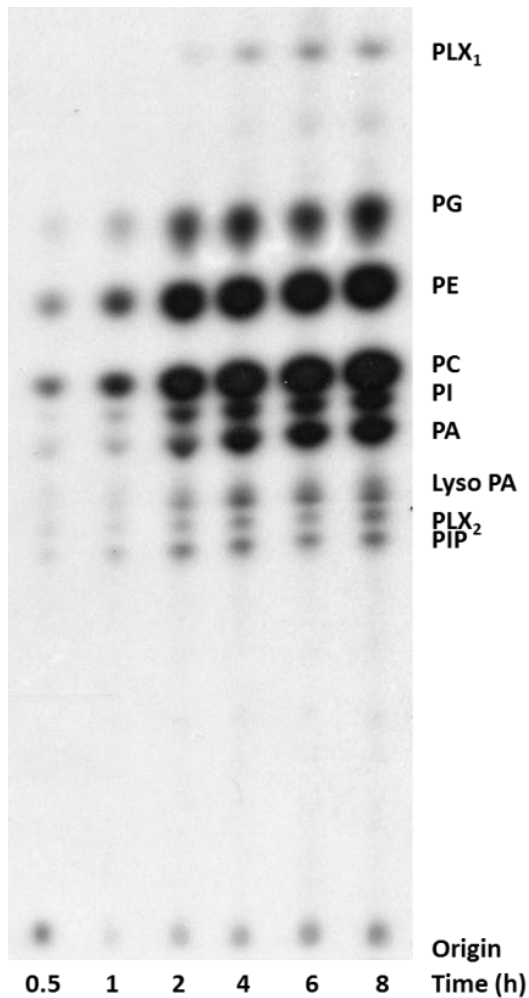
Figure 4.1. *Papaver rhoeas* pollen ^{32}P incorporation

Papaver rhoeas pollen was hydrated and grown in liquid growth medium in the presence of ^{32}P. Samples were taken at set intervals, between 0.5 and 8 hrs, and a lipid extraction was carried out. All samples were loaded on to a KOX TLC and run in an alkaline solvent tank. The TLC was exposed on to autoradiograph film to establish a suitable time for ^{32}P incorporation into *Papaver rhoeas* pollen. PLX$_1$, unknown phospholipid X$_1$; PG, phosphatidylglycerol; PE, phosphatidylethanolamine; PC, phosphatidylcholine; PI, phosphatidylinositol; PA, phosphatidic acid; lyso PA, Lysophosphatidic acid; PLX$_2$, unknown phospholipid X$_2$; PIP, phosphatidylinositol monophosphate.

4.2.2 SI INDUCED ALTERATIONS IN PHOSPHOLIPID LEVELS IN *PAPAVER* POLLEN TUBES

Having established a suitable labelling period, growing pollen tubes were labelled with ^{32}P for 4 hours and treated with PrsS to test whether Self-Incompatibility (SI) induced specific alterations in lipids (Figure 4.2). Treatments were stopped between 2.5 and 120 minutes

95

after SI induction and a lipid extraction subsequently carried out on the samples. Lipid extracts were analysed as before using TLC. Figure 4.2 shows that SI-induced pollen tubes undergo significant alteration in levels of phospholipids compared to untreated pollen. As shown in Figure 4.2A, untreated pollen undergoes little alterations in phospholipid levels over a 120 minute period, and this is shown in Figure 4.2 B,C & D, which show quantitative values for specific phospholipids. However, the addition of PrsS resulted in a significant change in the levels of some phospholipids, indicated by the arrows in Figure 4.2A. These include PLX_1, PA, PLX_2 and PIP (see Figure 4.2A).

Quantification of phospholipid levels during the SI response are shown in Figure 4.2 B-D; (see materials and methods for methodologies). As shown in the Figure 4.2B there was a specific in increase in phosphatidic acid (PA) levels in SI-induced *Papaver* pollen. PA levels in SI-induced pollen significantly increase in the percentage of lipids with $^{32}P_i$ incorporated from 5.0 % at 0 minutes to 15.5 % within 120 minutes (***, p= 0.008, Figure 4.2B). Levels of PA in SI-induced samples significantly differed to pollen treated with growth medium for 120 minutes (*, p=0.047, Figure 4.2B). Furthermore, there was an increase in $^{32}P_i$ labelling of an unidentified lipid, PLX_2 after SI induction (Figure 4.2C). PLX_2 levels increased from 0.5 % to 0.8 % within 20 minutes SI induction (**, p= 0.031, Figure 4.2C).

96
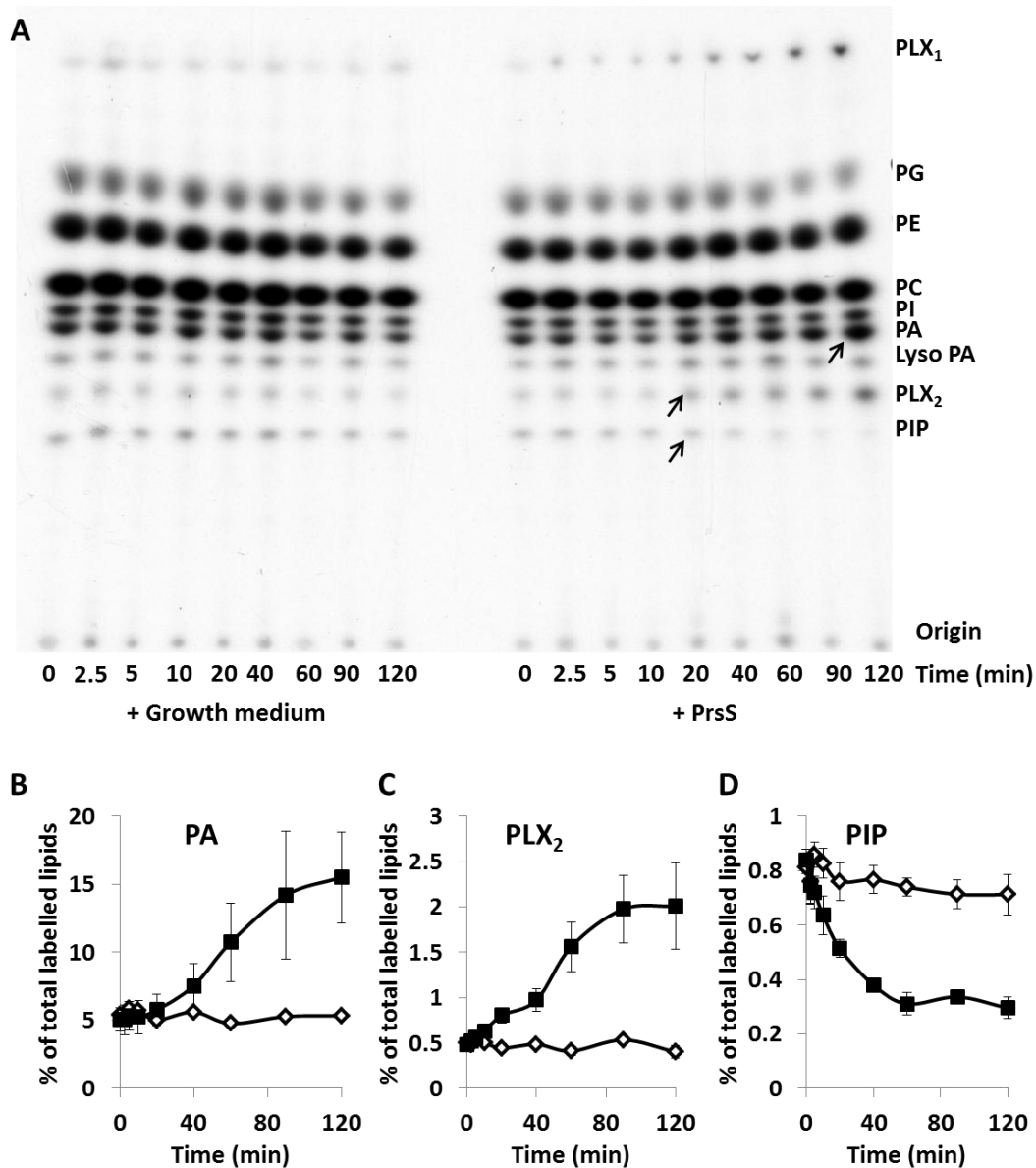
Figure 4.2 SI Induced changes in *Papaver rhoeas* pollen phospholipid levels

Pollen was grown for 4 hours in the presence of ^{32}P after which pollen was treated with either growth medium (untreated samples) or 10 μg.ml^{-1} PrsS to induced SI. At regular intervals samples were stopped and a lipid extraction was carried out. Pollen samples were then loaded on the TLC and run in an alkaline solvent system. TLC was exposed on to autoradiograph film. A. A representative image of an autoradiograph of pollen treated with either growth medium or PrsS at several time points. Arrows indicate phospholipids which undergo significant changes during the SI response. B. Graph of levels of phosphatidic acid (PA) in pollen treated with growth medium (open diamond symbols) or PrsS (closed square symbols). C. Graph of levels of PLX$_2$ in pollen treated with growth medium (open diamond symbols) or PrsS (closed square symbols). D. Graph of levels of phosphatidylinositol monophosphate (PIP) in pollen treated with growth medium (open diamond symbols) or PrsS (closed square symbols). Data shown in the graphs is n= 5.

This was significantly different from levels in untreated pollen incubated with growth medium for the same period of time (**, p= 0.009, Figure 4.2C). Levels of PLX$_2$ remained

97

significantly different to those treated with growth medium for 120 minutes (*, p= 0.029, Figure 4.2C), where 2.0 % of total lipids incorporated with ^{32}P was PLX$_2$, compared to untreated samples in which only 0.4% of total lipids was PLX$_2$. This lipid was investigated further (see section 4.2.3).

There was also a significant change in phosphatidylinositol monophosphate (PIP) levels in SI-induced cells (Figure 4.2D). Within 20 minutes of SI treatment there was a small but significant decrease in PIP levels, from 0.8 % at time 0, to 0.5 % (***, p= 4.95 E^{-04}). This 20 minute SI treatment resulted in significantly different levels of PIP compared to pollen treated with growth medium for the same period of time (*, p=0.012, Figure 4.2D). The levels of PIP continued to decrease over time, and after 40 min, PIP levels in SI-induced pollen were 0.4 % of total lipids incorporated with ^{32}P, compared to 0.8 % in untreated pollen PIP levels (***, p=4.245 E^{-04}, Figure 4.2D). After 120 minutes PIP levels in SI-induced pollen decreased to 0.3 % of total ^{32}P incorporated lipids. This was significantly different to untreated pollen at the same time point, (0.71 % of total labeled lipids, **, p= 0.008, Figure 4.2D). These data show that during the SI response there are significant alterations in PIP levels, occurring within 20 minutes of SI induction.

To establish whether this response was *S*-allele specific, compatible pollen was also treated with PrsS. Two samples of pollen, one pollen of a S$_1$ or S$_3$ genotype (incompatible), and one with pollen of a S$_2$ or S$_6$ genotype (compatible) were treated with PrsS$_1$ and PrsS$_3$ or growth medium for up to 120 minutes. Pollen with *S*-alleles matching the PrsS would undergo a SI response (incompatible), pollen with different *S*-alleles would not undergo SI and are therefore classed as compatible. Figure 4.3 A-D shows a

98

TLC of lipid extracts of pollen samples of either a S_2 or S_6, or S_1 or S_3 genotype, treated with either $PrsS_1$ and $PrsS_3$ or growth medium. PA, PLX_2 and PIP levels were quantified and plotted into graphs (Figure 4.3 E-G respectively). Both pollen samples, S_1S_3 or S_2S_6, treated with growth medium for 120 minutes showed no significant increase in PA levels compared to time 0 (N.S, p= 0.202, and N.S, p= 0.146, respectively, Figure 4.3E). As shown in Figure 4.3E there was an increase in PA in SI induced pollen (incompatible). Quantification showed that at time 0, PA levels in SI induced pollen were 101.9 % of untreated pollen of the same *S*-genotype; this significantly increased to 207.6 % within 60 minutes (*, p= 0.050; Figure 4.3E).

PA levels in incompatible pollen continued to increase over time. 120 minutes after SI induction PA levels increased by 183.37 % compared to untreated pollen of the same genotype, this was significantly different pollen at time 0, (***, p=3.740 E^{-04}, Figure 4.3E). This supports data presented in Figure 4.2, in which data showed PrsS triggers increases in PA levels in incompatible pollen over time. Importantly, data presented in Figure 4.3E shows that addition of PrsS to pollen of a different *S*-genotype (compatible) does not induce an increase in PA (Figure 4.3E). Quantification revealed that after 120 minutes treatment, compatible pollen PA levels were 100.70 % of untreated compatible pollen, and were not significantly different from pollen at time 0 (N.S, p= 0.584, Figure 4.3E). However, PA levels for compatible and incompatible SI treatments for 120 minutes were highly significantly different (***, p=0.000904, Figure 4.3E). This demonstrates that PA increases are due to an *S*-allele specific interaction, only occurring in incompatible SI induced pollen.

99
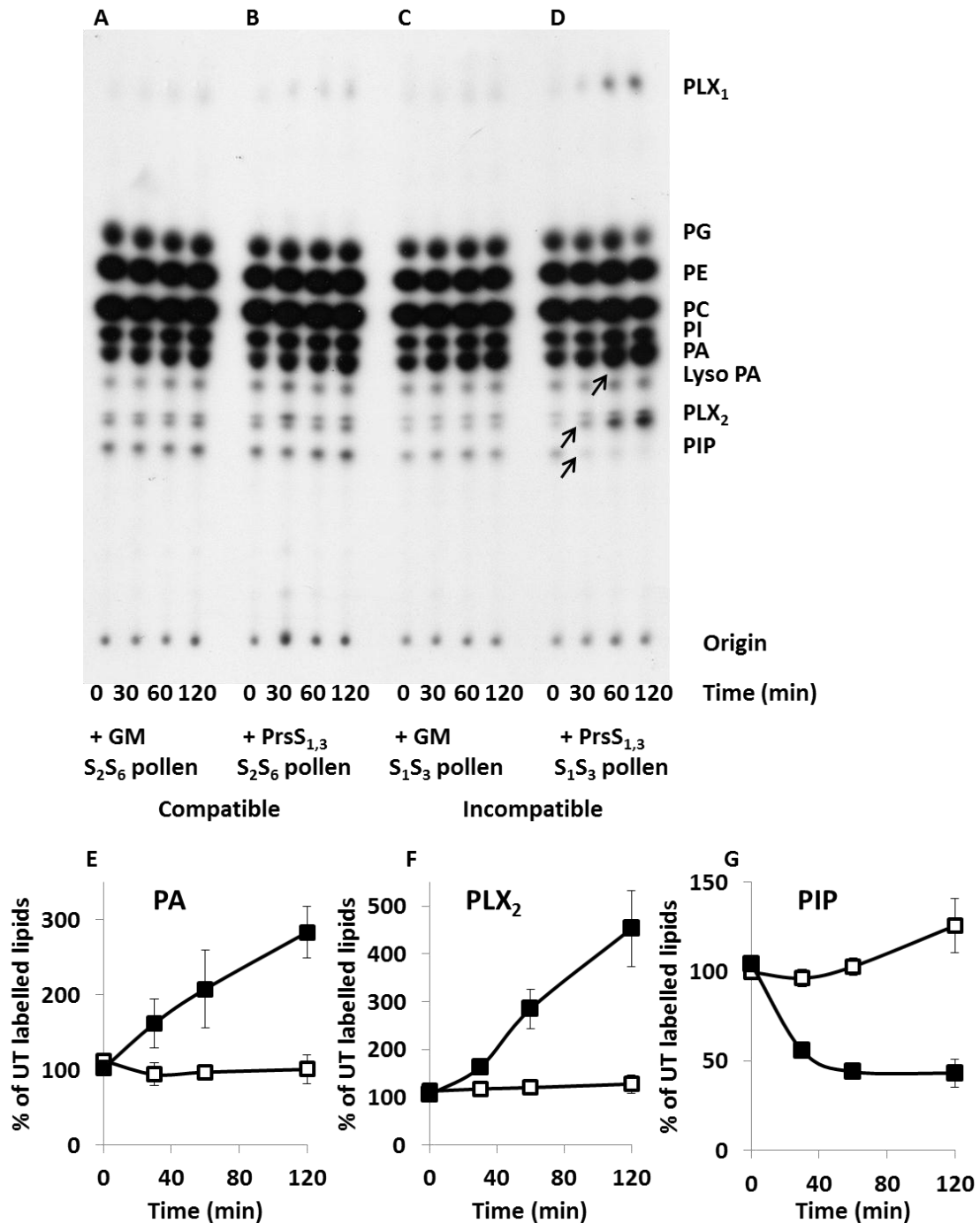
Figure 4.3. Phospholipid alterations are SI-specific

[32]P labelled pollen of a either a S_1 or S_3, or S_2 or S_6 genotype were treated with either $PrsS_{1,3}$ or growth medium (GM). If the *S*-alleles match there is an incompatible response (Incompatible; black squares), if the *S*-alleles different there is a compatible response (Compatible; white squares). At specific time points lipid extractions were carried out and samples were loaded on to TLC and labelled lipids were visualised by phor-imager and autoradiograph. A. Autoradiograph of S_2S_6 pollen treated with growth medium. B. Autoradiograph of S_2S_6 pollen treated with $PrsS_{1,3}$, resulting in a compatible response. C. Autoradiograph of S_1S_3 pollen treated with growth medium. D. Autoradiograph of S_1S_3 pollen treated with $PrsS_{1,3}$, resulting in an incompatible response. E-G Quantification of samples from TLC shown in A, samples are expressed as a % of untreated controls for each pollen. Solid squares are Incompatible pollen and therefore undergoing SI response, open squares Compatible pollen, as the alleles are different to that of PrsS. Plot of levels of phosphatidic acid (PA; E), PLX_2 (F) and phosphatidylinositol monophosphate (PIP; G), n=6.

Quantitative analysis of PLX_2 levels showed similar alterations (Figure 4.3F). Both pollen samples, S_1S_3 or S_2S_6, treated with growth medium for 120 minutes showed no significant increase in PLX_2 levels compared to time 0 (N.S, p=0.921, and N.S, p= 0.956, respectively, Figure 4.3F). PLX_2 levels increased from 105.2 % at time 0 to 453.1 % of untreated PLX_2 levels, which was a highly significantly difference (***, p=0.001, Figure 4.3F). Furthermore, at 120 minute of treatment with PrsS, in an incompatible challenge, there was a significant difference in PLX_2 levels compared to pollen undergoing a compatible SI challenge, 127.44 %, compared to 453.10 % in pollen undergoing an SI response (**, p=0.003, Figure 4.3F). Compatible pollen did not have significantly different levels of PLX_2 at time 0 compared to 120 minutes of treatment with PrsS (N.S, p= 0.584, Figure 4.3F). These data confirm that an incompatible SI induction triggers significant changes in levels of PLX_2, and moreover, demonstrate that these changes in PLX_2 are S-specific and do not occur in compatible pollen challenged with the same PrsS proteins. Thus, these alterations are triggered specifically by the SI response.

Analysis of PIP levels showed that in both pollen samples, S_1S_3 or S_2S_6, treated with growth medium for 120 minutes, there was no significant increase in PIP levels compared to time 0 (N.S, p= 0.799, and N.S, p= 0.869, respectively, Figure 4.3G). Further analysis of PIP levels in incompatible pollen treated with PrsS showed that SI-induction resulted in a significant reduction in PIP levels (Figure 4.3G). After 60 minutes treatment with PrsS in incompatible pollen there was a significant decrease in PIP levels, from 104.04 % at time 0 to 43.99 % within 60 minutes of treatment (***, p= $6.16E^{-08}$, Figure 4.3G). PIP levels continued to drop over time and at 120 minutes after treatment there was a highly significant difference in PIP levels in compatible and incompatible pollen treated with

PrsS. Treatment with PrsS in pollen with a different *S*-genotype for 120 minutes, a compatible response, resulted in significantly different levels of PIP compared to pollen undergoing an incompatible response, 125.67 %, and 43.15 %, respectively (***, p=6.780 E^{-04}, Figure 4.3G). These data confirm that decreases in PIP is due to a *S*-specific response in pollen, only occurring in SI-induced pollen, and pollen treated with PrsS in a compatible manner do not trigger the decrease in PIP levels.

Figure 4.2A also shows an increase in a phospholipid labelled at PLX_1. Unfortunately due to experimental difficulties we did not see the spot labelled as PLX_1 at the beginning of the study and therefore quantification analysis was not carried out at the time. As this work was carried out during a visit to the University of Amsterdam we were unable to extract this data as yet. As quantification of lipid levels is calculated as a percentage of total lipid levels it is difficult to interpret PLX_1 data without full quantification analysis, and as a result quantitative and statistical analysis of this PLX_1 will not be presented in thesis.

In summary, these data show that alterations in PA, PLX_1, PLX_2 and PIP are due to an *S*-specific interaction, and only occur when the *S*-genotype of the pollen matches that of PrsS resulting in an incompatible response. All following experiments used pollen of an 'incompatible' genotype to test the role of specific lipids during the SI response in *Papaver* pollen.

4.2.3 IDENTIFICATION OF PLX_2

As previously mentioned, an SI-induced increase in a lipid labelled as PLX_2. Tobacco BY2 cells were used as a standard for the identification of labeled lipids in *Papaver* pollen tube

102

extracts, and this allowed unequivocal identification of several phospholipids; phosphatidylglycerol (PG); phosphatidylethanolamine (PE); phosphatidylcholine (PC); phosphatidylinositol (PI); phosphatidic acid (PA); lysophosphatidic acid (lyso PA); phosphatidylinositol monophosphate (PIP). However, further analysis was required to confirm identity of certain lipids, including those identified as PLX_1 and PLX_2. Unfortunately we were unable to identify PLX_1, and therefore this results section will focus on the identification of PLX_2. Research carried out by Munnik *et al.,* (1996), showed *Chlamydomonas* cells treated with mastoparan triggered an increase in a lipid which ran below PA and above PIP, this was identified as diacylglycercol pyrophosphate (DGPP) (Munnik *et al.,* 1996). Furthermore, as mentioned in the introduction chapter, DGPP is known be involved in signalling in plant species and increases in DGPP levels occur during treatments with the mastoparan and during pathogen attack (Munnik et al., 2000; van der Luit et al., 2000). PLX_2 identified in this chapter ran in a similar position to the DGPP identified in *Chlamydomonas* cells and therefore PLX_2 was thought to be a DGPP. As illustrated in Figure 4.4, if PLX_2 is a DGPP, deacylation of PLX_2 should result in the formation of glycerophosphoinositol phosphate (GroPP). Furthermore, when GroPP was incubated with a mild acid treatment, GroPP show form a glycerophosphoinositol (GroP) and a phosphate group (P_i).
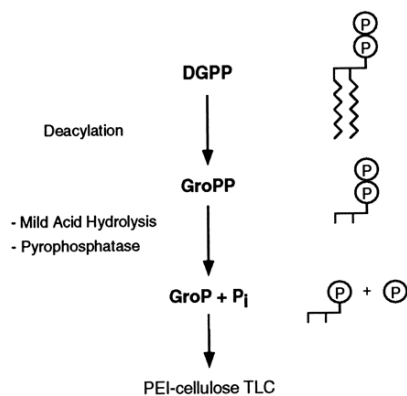
Figure 4.4. Scheme to identify PLX₂ as DGPP

To confirm the identity of a Diacylglycercol pyrophosphates (DGPP) a series of treatments can be carried out. The deacylation of DGPP with result in the removal of the fatty acid chains resulting in the formation of a glycerol pyrophosphates (GroPP). Furthermore if this GroPP is treated with a mild acid treatment, the GroPP will hydrolyse to produce a glycerol phosphatase(GroP) and inorganic phosphate (Pi). These samples can then be run on a PEI-cellulose with the addition of key phosphate marker to confirm the identity of the DGPP. Adapted from Munnik *et al.,* 1996.

Therefore, following the Munnik et al. (1994a) protocol, pollen was treated with PrsS to induced SI for 120 minutes prior to lipid extraction. For the preparation and purification of ³²P-labeled PLX₂, a two-dimensional TLC was used (see materials and methods for details). Figure 4.5A shows an autoradiograph of the 2D TLC, with key lipids labelled, including PLX₂, PA and lyso PA. These lipids were removed and taken through a deacylation process, followed by acid treatments (Munnik *et al*. 1994a). Samples were then spotted on to PEI cellulose anion-exchange TLC PolyGram sheets and positions of the standards were visualized by phosphate stain (Figure 4.5B). This show that the removal of the fatty acid chains of PLX₂ resulted in the formation of glycerol pyrophosphates (GroPP). Furthermore, mild acid treatment, lead to the hydrolysis of the GroPP a glycerol phosphatase (GroP) and a phosphate group (Pi). This confirms that PLX₂ is a DGPP. In addition, as lysoPA was very close to the PLX₂ spot in Figure 4.5A, lysoPA was also taken through the deacylation process to remove the fatty acids. This did not result in the formation of a GroPP, as with PLX₂, but instead lysoPA forms a GroP, confirming that the spots labelled as 2 and 3 in Figure 4.5A are different phospholipids.

104
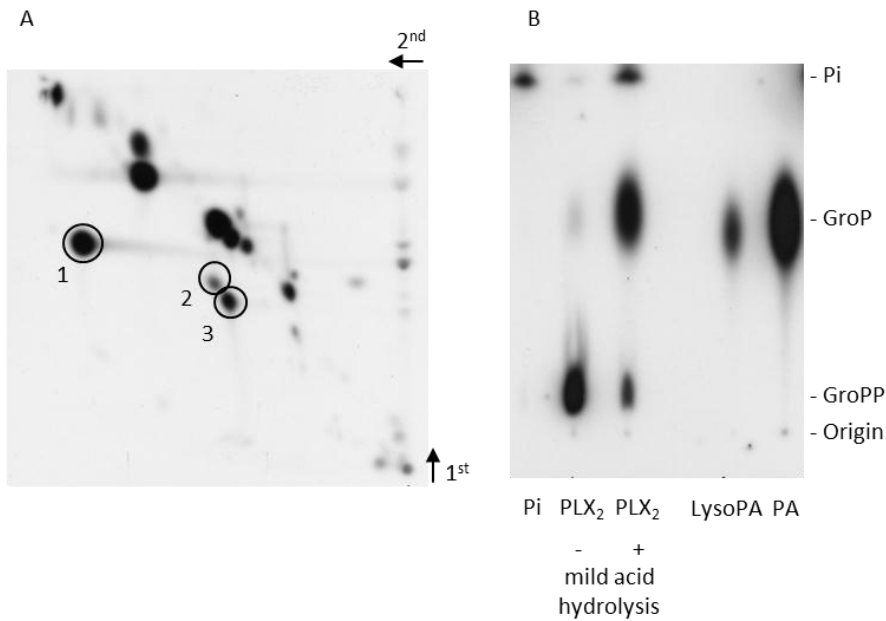
Figure 4.5. Identification of PLX$_2$

Lipids were extracted from pollen treated with PrsS to induced SI response. A) Samples were separated by two-dimensional TLC, and visualized by autoradiography. Labelled lipids (circled) are identified as follows 1.phosphatidic acid (PA), 2. Lysophosphatidic acid (lysoPA), 3.PLX$_2$. B) ^{32}P-Labeled diacylglycercol pyrophosphate (DGPP) was isolated, and the fatty acids were removed by deacylation with monomethylamine. The water-soluble head group, presumed to be glycerolpyrophosphate (GroPP), was subsequently treated for 10 min with 4 M formic acid at 100°C or kept on ice as a control. Samples were chromatographed with a mixture of 0.5 M ammonium formate and 0.2 M formic acid on PEI cellulose together with nonradioactive P$_i$ and GroP. The positions of the standards were visualized by phosphate stain.

4.2.4 THE SI RESPONSE TRIGGERS THE UPREGULATION OF PHOSPHOLIPASE D (PLD) ACTIVITY IN *PAPAVER* POLLEN TUBES

Data presented here has shown that PA production is stimulated by the SI response. As discussed in Chapter 1, PA can be generated through several different pathways and has been associated with stress responses such as H$_2$O$_2$-induced cell death during oleate treatment of Arabidopsis (Zhang *et al.,* 2003), and aluminium-induced cell death in tomato cells (Yakimova *et al.,* 2007).

A key pathway in which PA is made is through the activity of phospholipase D (PLD). PLD has several different roles, including membrane tethering, and acting as a catalyst for the conversion of structural phospholipids, such as phosphatidylcholine, into PA. PLD activity

105

is also upregulated during several stress responses such as osmotic stress in the green alga *Chlamydomonas moewusii* and cell-suspension cultures of tomato (Munnik *et al.,* 2000). We therefore decided to investigate whether PLD activity plays a role during the SI response in *Papaver* pollen tubes. In order to monitor PLD activity, n-butanol can be used to as a competitive substrate for the transphosphatidylation activity of Phospholipase D (PLD; Munnik *et al.,* 1995). This occurs at the expense of PA formation, resulting in the formation of phosphatidyl butanol (P-But, see Material and Methods). Pollen was pre-labelled with ^{32}P, and treated with either incompatible PrsS to induce SI, or growth medium (control), and with or without 0.1% n-butanol to monitor PLD activity. Pollen was treated for up to 120 minutes and extracts were made at specific time points, and analysed using a TLC.

Figure 4.6A shows a TLC of lipid extracts of pollen treated with either PrsS or growth medium, with and without 0.1% n-butanol. Data shows there was a significant increase in PA levels in pollen treated with incompatible PrsS for 120 minutes (Figure 4.6C). Quantification showed that 14.87 % total labelled lipids were comprised of PA, compared to untreated pollen of which only 5.00 % of total lipids were PA, (**, p= 0.003, Figure 4.6E). The addition of n-butanol for 120 minutes resulted in a significant difference in PA levels compared to untreated pollen medium for the same period of time (8.15 % & 5.00 % respectively, *, p=0.040, Figure 4.6E). However, despite this increase in PA in butanol-treated pollen it was still significantly different to PA levels in SI-induced pollen, after 120 minutes of treatment, 8.15 % and 14.87 % respectively (**, p=0.004, Figure 4.6E). This increase in PA levels in the presence of butanol, suggests that this could be due to the stimulation of PLD activities.

106
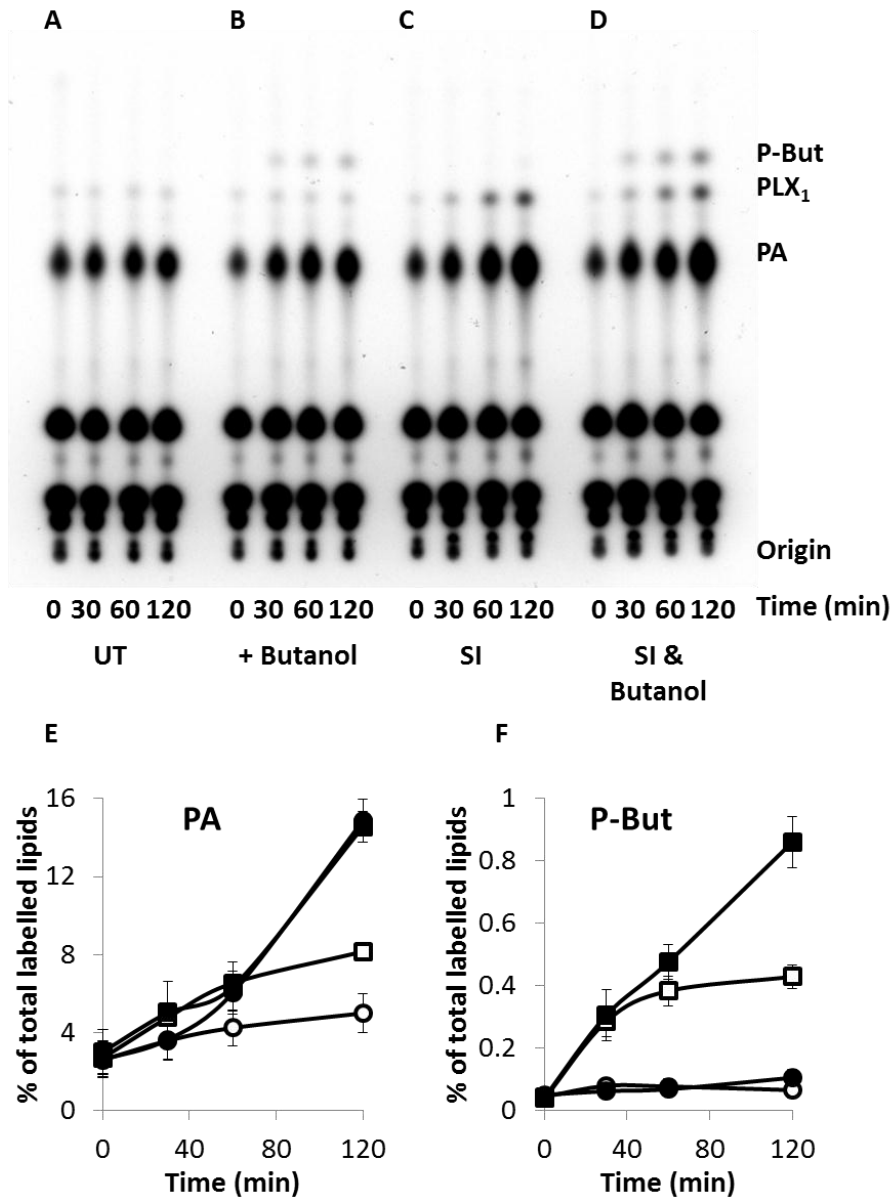
Figure 4.6. Investigating PLD activity during the SI response

Pollen was grown for 4 hours in the presence of ^{32}P after which pollen was treated with either growth medium (UT) or 10 µg.ml^{-1} PrsS to induced SI (SI), growth medium & 0.1 % n-Butanol (+ Butanol) or PrsS & 0.1% n-Butanol (SI & Butanol). At regular intervals samples were stopped and a lipid extraction was carried out. Pollen samples were then loaded on the TLC and run in an EtAc solvent system. TLC was exposed on to autoradiograph film. A-D, A representative image of an autoradiograph of pollen treated with either growth medium or PrsS at several time points. A. Pollen treated with growth medium, B, Pollen treated with growth medium & 0.1% butanol, C, SI-induced pollen, D, SI-induced pollen & 0.1% butanol. E&F, specific phospholipid spots were quantified and are expressed at as % of total labelled lipids for each lane, graphs represent 3 independent experiments. Treatments are labelled as follows; SI; closed circlee symbol, SI-B; closed square symbol, UT; open circle symbol) UT-B; open square symbol. E. Graph of phosphatidic acid (PA) levels in lipid extracts. F. A Graph of levels of P-butanol (P-But) levels in lipid extracts.

There was an increase in P-but levels in pollen tubes treated with n-butanol compared to just those treated with growth medium. In untreated pollen tubes there were very low levels of P-but, as shown in Figure 4.6F, representing <0.1 % in all samples not treated with butanol, which were considered as background. When 0.1 % n-butanol was added to pollen there was a significant increase in P-but levels. After 120 minutes, n-butanol treated cells had P-but levels of 0.43 % of total labelled lipids, which is an increase of 0.36%. This was significantly different to untreated pollen at the same time point (***, p=0.001, Figure 4.6F). As the formation of P-but is used as a marker for PLD activity, these data suggest PLD activities are involved in normal pollen tube growth.

Pollen treated with n-butanol & PrsS for 120 mins had P-but levels of 0.86 % of total labelled lipids, which was significantly different to P-but levels of pollen treated with n-butanol for the same time period (**, p=0.009, Figure 4.6F). The level of P-but was doubled in SI treated pollen compared to untreated pollen. It is generally thought the n-butanol should attenuate PA formation, however data presented here show there is no significant difference in PA levels in pollen treated with either PrsS or n-butanol & PrsS for 120 minutes, 14.87 % and 14.55 respectively (N.S, p=0.823, Figure 4.6E). Furthermore, there was an increase in PA compared to untreated and butanol treated. Therefore, although there was an increase in PLD activity, butanol treatments did not attenuate PA, and P-but formation did not appear to be at the expense of PA. It is possible be that another pathway which prevents the conversion of PA to another product is inhibited and therefore maybe responsible for the same levels of PA with the addition P-But via the transphosphatidylation activity of Phospholipase D.

As there was no reduction in PA levels, we wondered whether other lipids had been affected by the formation of P-But instead of the signalling molecule PA. Therefore, we decided to investigate whether the PLD pathway played a role in triggering other SI-induced alterations in phospholipid levels. We hypothesised that if pollen was treated with n-butanol during an SI response, if the PA from the PLD pathway was essential for the formation of DGPP, the conversion to P-But would inhibit this action, prevent DGPP formation, resulting in a reduction in DGPP levels compared to normal SI-induced pollen. Therefore the same pollen extracts as shown in Figure 4.6 were run on a TLC in an alkaline solvent solution (see Materials and Methods; Figure 4.7A-D). Figure 4.7A show phospholipid levels of pollen treated with growth medium or PrsS, both with and without butanol, and PA, PIP and DGPP levels were analysed using a phosphor-imager (Figure 4.7E-G). Quantitative analysis of PA levels showed similar results to those shown in Figure 4.6. There was a significant difference between SI-induced and untreated pollen PA levels after 120 minutes of treatment, 21.44 % and 8.63 % respectively (***, p= 3.43 E^{-04} , Figure 4.7). Although PA levels were higher in all samples when run in an alkaline solvent system, when compared to PA levels when the samples were run in an EtAc solvent system as shown in Figure 4.6. However, there was no significant difference between PA levels in SI-induced pollen and SI with n-butanol for 120 minutes (N.S, p= 0.769, Figure 4.7E). There was a significant difference between DGPP levels in pollen which were SI induced and untreated for 120 minutes (**, p=0.006, Figure 4.7F). In pollen treated with n-butanol and PrsS compared to pollen treated with just PrsS for 120 minutes, there was no significant difference in DGPP levels (N.S, p=0.987). These data show that similar levels are DGPP are formed, despite the presence of n-butanol. Therefore, the higher levels of

P-but, despite the normal levels of PA, are likely not to be due to the inhibition of DGPP formation, which is normally produced from PA via the enzyme phosphatidic acid kinase (PAK). Furthermore, there were no significant changes in PIP levels in pollen treated with PrsS and PrsS with n-butanol. This suggests that n-butanol does not affect the decrease in PIP levels triggered by an incompatible interaction. These data suggest that PLD is activated during normal pollen growth, and that there is an activation of PLD in response to SI-induction. Furthermore, the formation of P-But does not appear to affect PA levels or DGPP and PIP levels, suggesting that another pathway could be compensating for the reduction in PA through the formation of P-But.
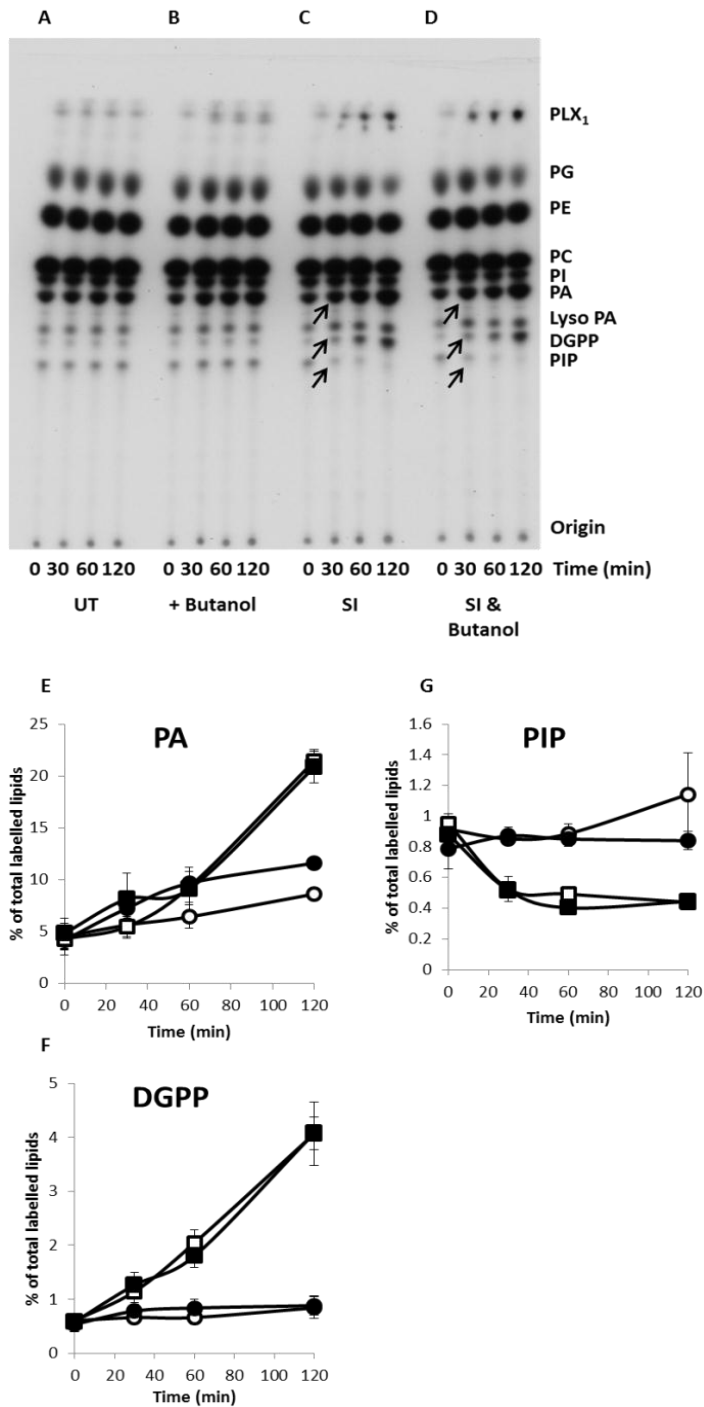
Figure 4.7. PLD activity in SI-induced cells

Pollen was grown for 4 hours in the presence of ^{32}P after which pollen was treated with either growth medium (UT) or 10 μg.ml^{-1} PrsS to induced SI (SI), growth medium & 0.1 % n-Butanol (UT-B) or PrsS & 0.1% n-Butanol (SI-B). At regular intervals samples were stopped and a lipid extraction was carried out. Pollen samples were then loaded on the TLC and run in an Alkaline solvent system. TLC was exposed on to autoradiograph film. A-D, A representative image of an autoradiograph of pollen treated with either growth medium or PrsS at several time points. A. Pollen treated with growth medium, B, Pollen treated with growth medium & 0.1% butanol, C, SI-induced pollen, D, SI-induced pollen & 0.1% butanol. E-G, specific phospholipid spots were quantified and are expressed at as % of total labelled lipids for each lane, graphs represent 3 independent experiments. Treatments are labelled as follows; SI; open square symbol, SI & Butanol; closed square symbol, UT; open circle symbol) + Butanol; solid circle symbol. E. Graph of phosphatidic acid (PA) levels in lipid extracts. F. Graph of diacylglycercol pyrophosphate (DGPP) levels in lipid extracts. G. Graph of phosphatidylinositol monophosphate (PIP) levels in lipid extracts.

111

4.2.5 ALTERATIONS IN ACTIN DYNAMICS ARE NOT UPSTREAM OF SI-INDUCED ALTERATIONS IN PHOSPHOLIPID LEVELS *PAPAVER* POLLEN

Another key feature of SI response in *Papaver* pollen is the dramatic alterations in the actin cytoskeleton (Geitmann et al., 2000; Snowman, 2000; Snowman et al., 2002) . As mentioned in chapter 1 and 3, during the SI response, actin depolymerization occurs within 1- 2 minutes of SI induction. This is followed by a period of polymerization during in which very stable punctate foci are formed (Poulter *et al.,* 2010). Moreover, these actin alterations have been associated with Programmed Cell Death (PCD) via the activation of caspase-like activities and DNA fragmentation during an incompatible SI response (Thomas *et al.,* 2006). We therefore decided to investigate whether actin alterations are upstream of the alterations in phospholipid levels during SI. Our approach was to treat pollen tubes with either 0.5 μM Jasplakinolide (Jasp) an actin stabilising agent or 1 μM Latrunculin B (Lat B) an actin depolymerizing drug, to investigate whether triggering alterations in the actin cytoskeleton was sufficient to induce alterations in phospholipid levels, similar to that documented during SI response in pollen tubes. Pollen tubes were also pre-treated with Jasp prior to the addition of PrsS to see if actin stabilization prior to SI-stimulated actin depolymerization is sufficient to rescue SI-induced pollen from alterations in key phospholipids PA, DGPP and PIP.

Figure 4.8A shows a TLC of lipid extracts from pollen treated with either growth medium, PrsS, Jasp, Lat B or pre-treated with Jasp prior to SI induction. Quantification of data showed there was a highly significant difference in PA, DGPP and PIP levels in SI-induced pollen tubes at 120 minutes compared with untreated pollen at the same time point (**,

p=0.008, ***, p=1.430 E^{-04},***, p=7.700 E^{-04} respectively, Figure 4.8B-D). There was no

significant difference in PA, DGPP and PIP levels in pollen treated with growth medium
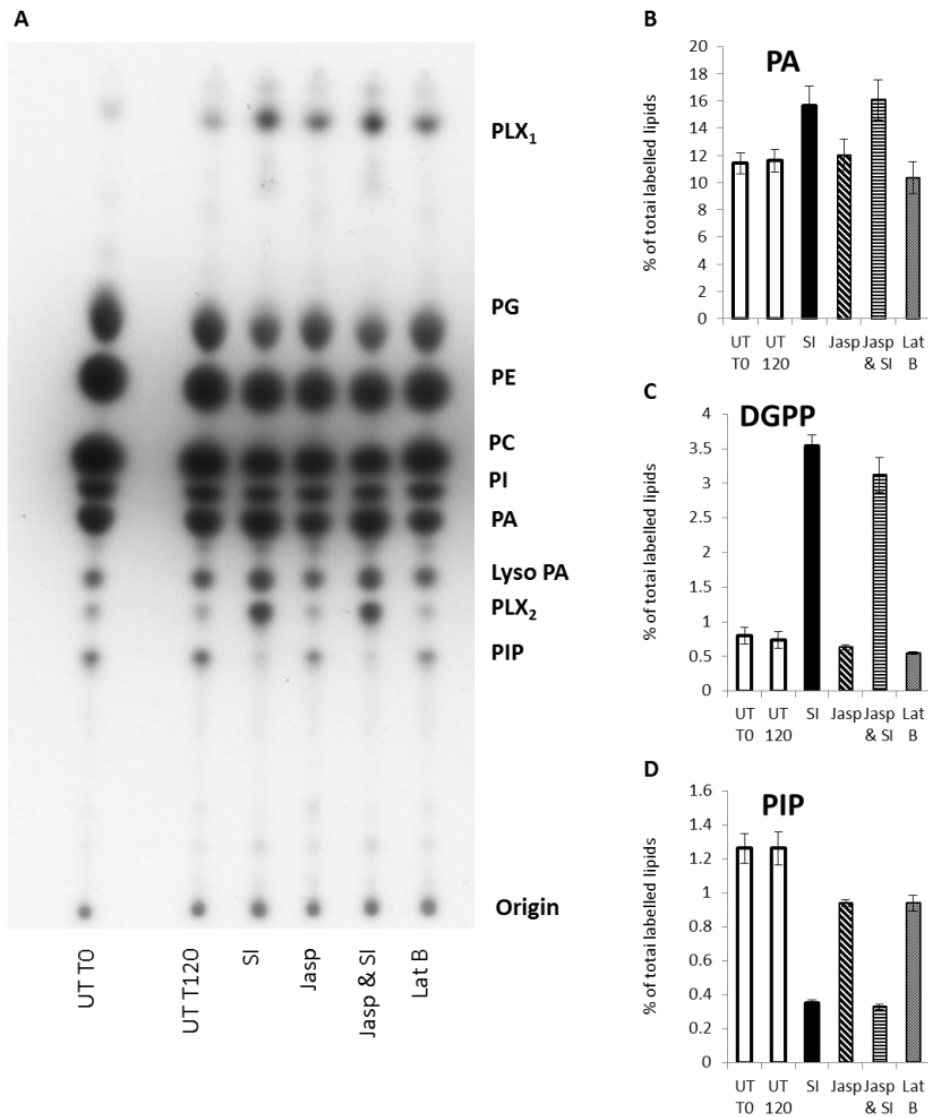
Figure 4.8. Actin stabilization and depolymerization do not trigger alterations in *Papaver* phospholipids

Pollen was grown for 4 hours in the presence of ^{32}P after which pollen was treated with either growth medium (UT), 10 µg.ml^{-1} PrsS to induced Self-Incompatibility (SI),), 0.5 µM Jasplakinolide (Jasp), O.5 µM Jasp & SI or 1 µM Latrunculin B (Lat B). Samples were stopped and a lipid extraction was carried out at 120 minutes of treatment, however a sample for untreated pollen was taken at Time 0 and 120. Pollen samples were loaded on the TLC and run in an alkaline solvent system. TLC was exposed on to autoradiograph film. A, A representative image of an autoradiograph of pollen treated with either growth medium, PrsS, Jasp, Jasp & SI, and Lat B, and are plotted in graphs B-D. B-D, specific phospholipid spots were quantified and are expressed at as % of total labelled lipids for each lane, graphs represent 3 independent experiments. Treatments are labelled as follows; SI; Solid black bar, Jasp; white bar with black diagonal stripes, Jasp & SI; white bars with black horizontal stripes, Lat B; solid grey bars, and UT; white bars. B. A Graph of levels of phosphatidic acid (PA) levels in lipid extracts. C. Graph of diacylglycercol pyrophosphate (DGPP) levels in lipid extracts. D. Graph of phosphatidylinositol monophosphate (PIP) levels in lipid extracts. N=3.

at time 0 with 120 minutes of treatment (N.S, p=0.871063, p=0.710559, p=0.995651 respectively, Figure 4.8B-D). However, it should be noted that the PA, DGPP and PIP levels were higher in untreated pollen in these experiments compared to previous (for example see, Figure 4.2). As previously discussed, this could be due to sub-optimal growing conditions, however as SI-induced alteration in phospholipid levels were similar to that of previous experiments it suggests that the pollen is still responding to the addition of PrsS.

Pollen tubes treated with Jasp did not have significantly different PA levels from untreated pollen (12.04% & 11.61% respectively, N.S, p=0.774, Figure 4.8A&B), however they were not significantly different from SI-induced pollen either (15.63%, N.S, p=0.064, Figure 4.8B). These data suggest that Jasp treatments had little effect on PA levels in *Papaver* pollen tubes. Moreover, pollen was pre-treated with Jasp for 10 minutes prior to SI induction to examine if it prevented SI-induced depolymerization, by stabilizing actin filaments with Jasp, could prevent SI-induced alterations in phospholipid levels. This pre-treatment had little effect on PA levels in SI-induced cells and there was no significant difference between SI-induced pollen tubes and those pre-treated with Jasp (N.S, p=0.839, Figure 4.8B). These data suggest that preventing actin depolymerization does not prevent SI-induced increases in PA levels. Pollen was also treated with Lat B for 120 minutes to test whether actin depolymerization could trigger alterations in phospholipids levels similar to those observed during an SI response. Lat B treatments had little effect on PA levels compared to untreated pollen of the same time point (N.S, p=0.435, Figure 4.8B). Furthermore, there was a significant difference in PA levels between pollen treated with Lat B compared to SI-induced pollen (*, p=0.050, Figure 4.8B). These data suggest

that like the Jasp treatments, Lat B treatment, and therefore actin depolymerization, is not sufficient to trigger alterations in PA levels similar to that of SI-induced pollen tubes.

Pollen treated with Jasp did not have significantly different levels of DGPP compared to untreated pollen of the same time point (N.S, p=0.439, Figure 4.8C). Furthermore, pollen tubes treated with Jasp had highly significantly different levels of DGPP to those of SI-induced pollen, (***, p=5.83 E^{-05}, Figure 4.8C). Moreover, in pollen that was pre-treated with Jasp for 10 minutes prior to SI induction, therefore preventing SI-induced depolymerization of actin filaments, did not affect DGPP levels, as there was no significant difference between SI induced and pre-treated pollen (N.S, p=0.227, Figure 4.8C). These data suggests that preventing actin depolymerization does not inhibit SI-induced increases in DGPP levels. Pollen was also treated with Lat B for 120 minutes to test whether actin depolymerization could trigger alterations in phospholipids levels similar to those observed during an SI response. Lat B treatments had little effect on DGPP levels compared to untreated pollen of the same time point (N.S, p=0.189, Figure 4.8C). Furthermore, there was a significant difference in DGPP levels between pollen treated with Lat B compared to SI-induced pollen (***, p=4.98E^{-05}, Figure 4.8C). These data suggest that alterations in actin dynamics do not play a role in triggering SI-induced alterations in DGPP levels in *Papaver* pollen tubes.

PIP levels were also monitored in Jasp treated pollen tubes. Jasp treatments did trigger significantly different levels of PIP compared to untreated pollen of the same time point (N.S, p=0.032, Figure 4.8D). Furthermore, pollen tubes treated with Jasp had highly significantly different levels of PIP to those of SI-induced pollen, (***, p=2.94 E^{-05}, Figure

4.8D). This suggests actin stabilization does not play a role in triggering SI-induced decrease in PIP levels. Moreover, pollen was pre-treated with Jasp for 10 minutes prior to SI induction to examine if prevent SI-induced depolymerization, by stabilizing actin filaments with Jasp, could prevent SI-induced alterations in phospholipid levels. This pre-treatment did not affect PIP levels, as there was no significant difference between SI induced and pre-treated pollen (N.S, p=0.454, Figure 4.8D). This suggests that preventing SI-induced actin depolymerization does not play a role in triggering a decrease in PIP levels. Treatment with Lat B triggered a significant difference in PIP levels compared to untreated pollen (*, p=0.040, Figure 4.8D). Furthermore, there was a significant difference in PIP levels between pollen treated with Lat B compared to SI-induced pollen (***, p=2.840 E^{-04}, Figure 4.8D). These data suggest that actin depolymerization can trigger a decrease in PIP levels, and therefore actin depolymerization may play a role in triggering SI-induced decreases in PIP levels.

4.2.6 INVESTIGATING THE ROLE OF ROS AND NO DURING SI-INDUCED ALTERATIONS IN PHOSPHOLIPID LEVELS IN *PAPAVER* POLLEN

As shown in Chapter 3, ROS and NO play an important role in triggering caspase-like activities and the formation of actin foci (Wilkins *et al.,* 2011). We wondered whether ROS or NO might play a role in modulating phospholipids in the SI response in *Papaver* pollen. As previously discussed, ROS is involved with phospholipid signalling networks. For example research carried out by Park *et al.,* (2004) has shown that PA induced leaf cell death led to increases in ROS in whole leaf and single cells of Arabidopsis. Moreover, there is increasing evidence for the role of PLD in ROS production in Arabidopsis leaves

(Sang *et al.,* 2001). More recently, evidence is emerging for the role of NO during auxin-induced adventitious root formation in cucumber, in which NO was shown to trigger increases in PA levels via PLD activity (Lanteri *et al.,* 2008).

To examine a possible role of ROS or NO, our approach was to treat pollen with c-PTIO, a NO scavenger, and DPI, an NADPH inhibitor (ROS), to investigate whether either species plays a role in triggering the SI-induced phospholipid signalling in *Papaver* pollen. Figure 4.9A shows pollen lipid extracts that were treated with either growth medium, PrsS (SI), or with the NO scavenger c-PTIO, or the NADPH oxidase inhibitor, DPI or with or without the addition of PrsS. As shown earlier, comparing PA, DGPP or PIP levels in untreated pollen at time 0 and after 120 minutes of growth medium treatment there were no significant differences (N.S, p=0.696, p= 0.828, p=0.698, respectively, Figure 4.9B-D). There was a significant difference in PA, DGPP and PIP levels between untreated pollen at 120 minutes compared to levels in SI induced pollen of the same time point in (**, p=1.908 E^{-03}, **, p=9.145 E^{-03}, *, p= 0.0136 respectively, Figure 4.9B-D). Pollen treated with the NO scavenger c-PTIO, had significantly different PA levels compared to untreated pollen at the same time point (***, p= 7.10 E^{-04}, Figure 4.9B). These levels were not significantly different to those of SI-induced pollen (N.S, p= 0.137, Figure 4.9B). These data show that scavenging NO has an effect on PA levels in normal pollen tubes, therefore suggesting interfering with normal NO levels in the pollen tubes triggers a PA response. Pollen tubes were also treated with the NADPH oxidase inhibitor DPI. This also induced a significant increase in PA, when compared to untreated pollen of the same time point (*, p=0.049, Figure 4.9B).
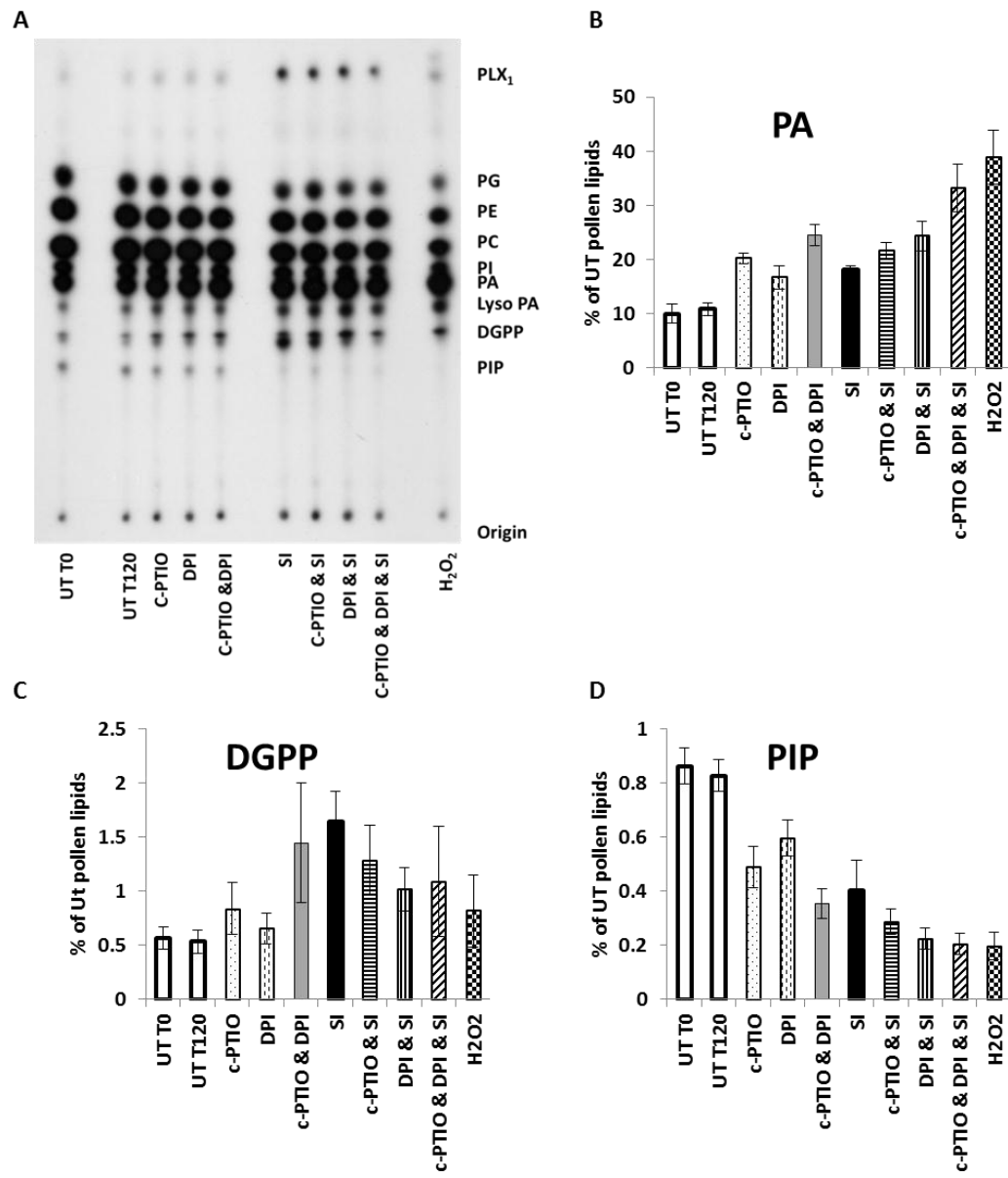
Figure 4.9. Investigating the role of ROS & NO during SI-induced alterations in phospholipid levels in *Papaver* pollen

Pollen was grown for 4 hours in the presence of ^{32}P after which pollen was treated with either growth medium (UT), 10 µg.ml^{-1} PrsS to induced Self-Incompatibility (SI), 400 mM c-PTIO (c-PTIO), 400 µM DPI (DPI), c-PTIO & DPI together, c-PTIO & SI, DPI & SI, c-PTIO & DPI & SI and 2.5 mM H$_2$O$_2$. Samples were stopped and a lipid extraction was carried out at 120 minutes of treatment, however a sample for untreated pollen was taken at Time 0 and 120. Pollen samples were loaded on the TLC and run in an alkaline solvent system. TLC was exposed on to autoradiograph film. A, A representative image of an autoradiograph of pollen treated with either growth medium, SI, c-PTIO, DPI, c-PTIO & DPI, c-PTIO & SI, DPI & SI, c-PTIO & DPI & SI and H$_2$O$_2$, are plotted in graphs B-D. B-D, specific phospholipid spots were quantified and are expressed at as % of total labelled lipids for each lane, graphs represent 3 independent experiments. Treatments are labelled as follows; UT; white bars, SI; Solid black bar, c-PTIO; white bar with black dots, DPI; vertical dash, c-PTIO & DPI, grey bar, c-PTIO & SI; white bar with horizontal black lines, DPI & SI; white bar with vertical black lines, c-PTIO & DPI & SI; white bar with diagonal black lines and H$_2$O$_2$; black and white checker bars. B. A Graph of levels of phosphatidic acid (PA) levels in lipid extracts. C. Graph of diacylglycercol pyrophosphate (DGPP) levels in lipid extracts. D. Graph of phosphatidylinositol monophosphate (PIP) levels in lipid extracts. n=3.

118

There was no significant difference in PA levels in pollen tubes treated with DPI compared to SI-induced pollen (N.S, p=0.573, Figure 4.9B), suggesting the inhibition of NADPH oxidase resulted in an increase in PA in *Papaver* pollen tubes.

Moreover, pollen treated with c-PTIO and DPI together had significantly different levels of PA to untreated pollen (***, p=9.1 E^{-04}, Figure 4.9B), and PA levels were significantly higher compared to SI-induced (*, p= 0.0220, Figure 4.9B). PA levels in simultaneously treated c-PTIO & DPI cells were not significantly different to pollen treated with c-PTIO alone (N.S, p=0.090, Figure 4.9B), suggesting that the addition of c-PTIO may of had a damaging effect on the pollen. In summary interfering with ROS or NO levels in *Papaver* pollen tubes induced an increase in PA levels.

Furthermore, pollen was pre-treated with c-PTIO or DPI or both, prior to the addition of PrsS to test whether inhibition of ROS or NO has an effect on SI-induced phospholipid alterations. As expected, both individual pre-treatments of either DPI or c-PTIO did not rescue cells from SI-induced alterations in PA (N.S, p= 0.075 and p=0.022 respectively, Figure 4.9B). These data suggest that inhibition of either NO or ROS signalling does not prevent SI-induced alterations in PA levels in *Papaver* pollen tubes. However, previous work has shown that during the SI response ROS and NO act in concert, for example both ROS and NO inhibition was required to prevent caspase-3/DEVDase-like activity during the SI induced pollen tubes (Wilkins *et al.,* 2011). We therefore tested whether the inhibition of ROS and NO together, had a stronger impact on phospholipid than individual treatments. Pollen pre-treated with c-PTIO and DPI prior to SI-induction had significantly higher levels of PA compared to untreated pollen tubes after 120 minutes of treatment

(**, p= 0.002.760 E^{-03}, Figure 4.9B), and had significantly higher levels of PA compared to SI-induced pollen tubes (*, p= 0.015, Figure 4.9B). These data show that the addition of c-PTIO, DPI and PrsS triggers a stronger PA response than just SI-induction alone, suggesting blocking both ROS and NO do not prevent SI-induced increase in PA levels.

To investigate whether a ROS is responsible for SI-induced increases in PA levels, pollen was treated with the ROS, H_2O_2. Addition of H_2O_2 resulted in significant increases in PA levels compared to untreated pollen (**, p=1.680 E^{-03}, Figure 4.9B). These PA levels were also significantly higher than that of SI-induced pollen (**, p=6.739 E^{-03}, Figure 4.9B). These data show that a ROS treatment triggers an increase in PA levels

DGPP levels were also monitored to assess whether NO or ROS inhibitors trigger alterations in DGPP levels similar to of SI-induced pollen (Figure 4.9C). The addition of c-PTIO to pollen resulted in a slight but not significant increase in DGPP levels compared to untreated pollen at 120 minutes of treatment, (N.S, p=0.285, Figure 4.9C). There was a significant difference in DGPP levels in SI-induced cells compared to pollen treated with c-PTIO (*, p=0.034, Figure 4.9C). These data suggest that inhibition of NO signalling in normal pollen tubes does not trigger alterations in DGPP levels, unlike SI-induced pollen. Treatment with DPI, the ROS inhibitor, did not trigger significant increases in DGPP levels, when compared to untreated pollen of the same time point (p=0.507, Figure 4.9C), and there was a significant difference in DGPP levels between pollen treated with DPI and SI-induced pollen (*, p=0.018, Figure 4.9C). Furthermore, when both ROS and NO was inhibited, DGPP levels of pollen tubes were not significantly different to untreated pollen or SI-induced pollen (N.S, p=0.158, p=0.762 respectively, Figure 4.9C). Therefore these

data are difficult to interpret, and require further investigate to conclude whether inhibition or normal ROS and NO signalling in *Papaver* pollen tubes is sufficient to trigger alterations in DGPP levels.

ROS and NO scavengers were also used to block ROS and NO signalling during the SI response to investigate their importance during SI-induced increases in DGPP. Pre-treatment of pollen with c-PTIO prior to SI-induction, resulted in increases in DGPP compared to untreated pollen tube of the same time point, but this was not significantly different SI-induced pollen (N.S, p= 0.426, Figure 4.9C). These data suggest this concentration of c-PTIO does not affect DGPP levels in SI-induced pollen tubes. However, there was just a significant difference in DGPP levels in pollen that were pre-treated with DPI prior to SI-induction compared the normal SI-induced pollen (*, p=0.050, Figure 4.9C). This suggests inhibition of NADPH oxidase prevented some of the DGPP formation in SI-induced pollen tubes and therefore ROS signalling could play an important role in triggering DGPP formation during the SI response.

As previously mentioned, inhibition of both ROS and NO signalling during the SI response had a significant impact on SI-induced increases in caspase-3-like activities in *Papaver* pollen tubes (Wilkins *et al.,* 2011); see chapter 3). Therefore, pollen was pre-treated with c-PTIO and DPI prior to SI-induction. Pollen pre-treated with c-PTIO and DPI together did not have significantly different DGPP levels compared to SI-induced pollen (N.S, p=0.653, Figure 4.9C). However, as pre-treatment with DPI did result in a significantly lower level of DGPP in SI-induced cells, these data suggest that c-PTIO may have a negative effect on pollen, as there was no rescue when DPI was used in conjunction with c-PTIO in SI-

induced pollen tubes. Furthermore, as DPI treatment, a NADPH oxidase inhibitor, resulted in a reduction in DGPP this suggests a ROS could be responsible for mediating SI-induced alterations in levels of DGPP. Moreover, as NADPH oxidase is known to mediated production of hydrogen peroxide in several stress related responses in plants (Elmayan and Simon-Plas, 2007; Yang and Chung, 2012). We decided to test whether the addition of H_2O_2 could trigger increases in DGPP levels similar to that of SI-induced pollen tubes. However, results show that pollen treated with H_2O_2 did not have significantly different levels of DGPP compared to untreated or SI-induced pollen (N.S, p=0.446 and p=0.105 respectively, Figure 4.9C). Therefore, suggesting H_2O_2 is not responsible for triggering SI-induced alteration in DGPP levels, and perhaps another form of ROS could play a role.

PIP levels were also monitored during treatments with c-PTIO and DPI. Pollen treated with c-PTIO had significantly lower levels of PIP compared to untreated pollen tubes (0.83 % & 0.49 % respectively, Figure 4.9D). This decrease in PIP level was significantly different to untreated pollen, but not significantly different to SI-induced pollen (*, p=0.012, N.S, p=0.542 respectively, Figure 4.9D). These data suggests that the inhibition of NO in pollen tubes triggers a decrease in PIP comparable to that of SI-induced pollen tubes, and therefore NO signalling may play an important role in triggering SI-induced decrease in PIP levels.

Furthermore, there was a significant decrease in PIP levels in pollen treated with DPI compared to untreated pollen (*, p=0.038, Figure 4.9D). This decrease was not significantly different to SI-induced cells (N.S, p=0.178, Figure 4.9D). These data show that the inhibition of NADPH oxidase resulted in a significant decrease in PIP levels that was

comparable with that of SI-induced pollen tubes. Moreover, pollen treated with c-PTIO and DPI together had significantly different levels of PIP than untreated pollen and not significantly different levels compared to SI-induced pollen (***, p=9.80 E^{-04} and N.S, p=0.689 respectively, Figure 4.9A&D). These data suggest that inhibition of ROS and/or NO has a significant effect on PIP levels in normal pollen tubes and therefore could play an important role in general regulation or growth of the pollen tube, and maybe involved in triggering SI-induced alterations in PIP levels.

As expected both individual DPI and c-PTIO pre-treatments, and simultaneous treatments did not rescue pollen tubes from SI-induced alterations in PIP (N.S, p=0.171 and p=0.358, p=0.134 respectively, Figure 4.9D). Therefore, these results are difficult to interpret as during the SI response there are increases in both ROS and NO, and decreases in PIP. Therefore if ROS and/or NO play a role in SI-induced alterations in PIP, their inhibition would perhaps be expected to prevent SI-induced alterations. However, just as the addition of the inhibitors triggered a decrease in PIP similar to that of SI-induced pollen, it is difficult to ascertain whether ROS or NO really play a role in this response. Pollen was treated with H_2O_2, a type of ROS, to further investigate whether the increases in ROS could trigger SI-induced decreases in PIP. The addition of H_2O_2 resulted in significant decrease in PIP levels compared to untreated pollen (**, p=1.680 E^{-03} and p=1.800 E^{-04} respectively, Figure 4.9D), which were not significantly different from SI-induced pollen (N.S, p=0.105). These data suggest that increases in ROS might play a role in triggering SI-induced reduction in PIP levels.

123

In summary, these data show that both the addition of a ROS in the form of H_2O_2 and the inhibition of ROS and NO in SI-induced pollen tubes resulted in an increase in PA levels in *Papaver* pollen tubes. These data suggest that alterations in normal ROS signalling may play a role in triggering increases in PA, as both the inhibition and addition of ROS stimulated PA production. Furthermore the inhibition of ROS and NO also induced a reduction in PIP levels, mimicking SI-induced decreases. The addition of H_2O_2 also trigger significant reduction in PIP levels, again suggesting that perhaps alterations in normal ROS and NO signalling may play a role in regulating PIP levels in *Papaver* pollen tubes. Inhibition of ROS in SI-induced pollen tubes also resulted in a reduction in SI-induced increases in DGPP levels, however addition of ROS in the form of H_2O_2 did not trigger an increase in DGPP levels. These data suggest that ROS signalling may play a role in triggering alterations in DGPP levels, however perhaps H_2O_2 is not responsible, and another form of ROS may be involved, as H_2O_2 treatments did not stimulate an increase in DGPP levels similar to SI-induced pollen tubes.

4.2.7 ROS DOES NOT TRIGGER SI-INDUCED INCREASES IN PLD ACTIVITIES

Previous data has shown that the inhibition of NADPH oxidase, by means of DPI treatment, during an SI response resulted in lower levels of DGPP than normal SI-induced pollen (Figure 4.9). PLD activities are an important enzyme in PA production, furthermore PLD activity have been implicated in many stress responses where ROS is a key signalling component (Li et al., 2004; Sang et al., 2001; Zhang et al., 2003). Data shown in Figure 4.6 show there were significant increases in PLD activity in SI-induced pollen tubes (Figure 4.6). We therefore wanted to investigate whether blocking ROS production resulted in a

reduction in PLD activity. As previously discussed, butanol is used as a competitive substrate for the transphosphatidylation activity of Phospholipase D (PLD; (Munnik *et al.,* 1995), therefore monitoring the formation of P-But can be used to assess PLD activity. Therefore, to investigate the role of ROS during PLD activity during SI-induced pollen, pollen was pre-treated with DPI and was treated with either butanol or butanol and PrsS (Figure 4.10). Figure 4.10A shows a TLC of pollen lipid extracts treated with growth medium, growth medium and n-butanol, DPI and n-butanol, PrsS and n-butanol and DPI, PrsS and n-butanol for 120 minutes. Quantification of the lipids are shown in Figure 4.10B,C, where P-but and PA levels were monitor. As shown in Figure 4.10B, there were significant increases in P-But, and therefore PLD activity, in pollen treated with DPI and butanol compared to butanol alone (***, p=0.001, Figure 4.10B), moreover this increase in P-but in DPI and butanol treated cells was not significantly different to P-But levels in SI-induced pollen tubes (N.S, p=0.052, Figure 4.10B). There is no significant difference in P-But levels of pollen pre-treated with DPI prior to SI induction and butanol treatment, compared to normal SI-induced pollen (N.S, p=0.448, Figure 4.10A&B). These data suggest the inhibition of ROS production by DPI, does not have a significant effect of P-But formation and therefore PLD activity during the SI response.
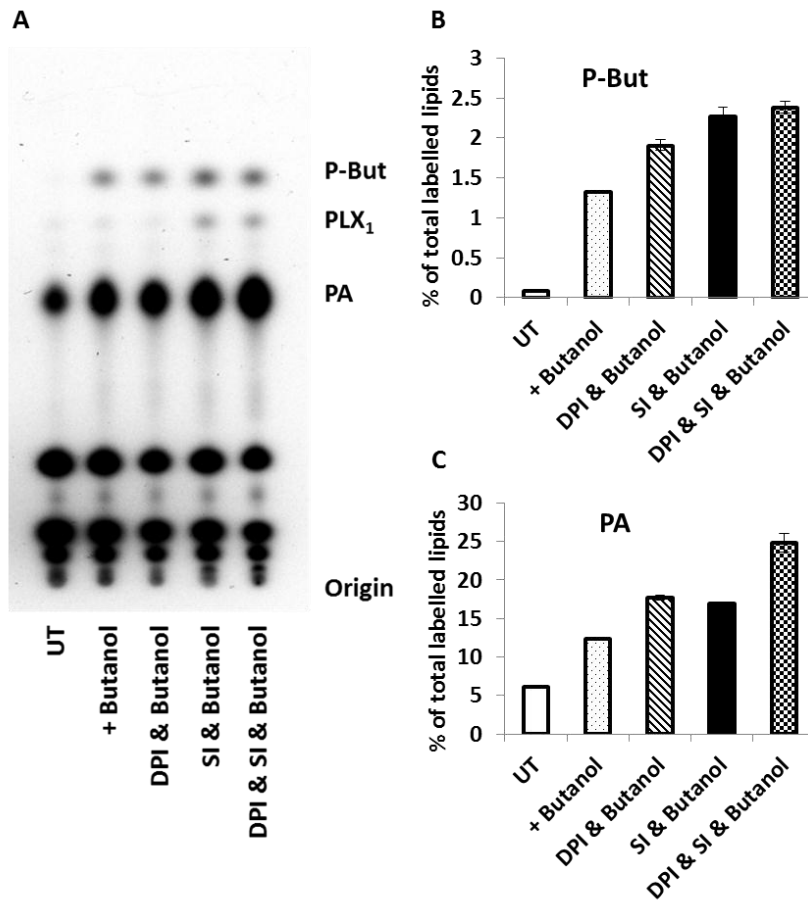
Figure 4.10 Investigating the role of PLD during ROS signalling in SI-induced alterations in phospholipid levels in *Papaver* pollen tubes.

Pollen was grown for 4 hours in the presence of ^{32}P after which pollen was treated with either growth medium (UT) or growth medium & 0.1 % n-Butanol (+ Butanol), DPI & 0.1% n-Butanol (DPI & Butanol), PrsS & 0.1% n-Butanol (SI & Butanol), or DPI & PrsS & 0.1% n-Butanol (DPI & SI & Butanol). After 120 minutes of treatment samples were stopped and a lipid extraction was carried out. Pollen samples were then loaded on the TLC and run in an EtAc solvent system. TLC was exposed on to autoradiograph film. A-C, A representative image of an autoradiograph of pollen treated with either growth medium (UT), butanol, DPI & butanol, SI & Butanol or DPI & SI & Butanol. B&C, specific phospholipid spots were quantified and are expressed at as % of total labelled lipids for each lane, graphs represent 3 independent experiments. Treatments are labelled as follows; UT; white bar, Butanol; white bar with black spots; DPI & Butanol; White bar with black diagonal lines, SI & butanol; black bar, DPI & SI & butanol; white and black checkered bar. B. A Graph of levels of P-butanol (P-But) levels in lipid extracts. C. Graph of phosphatidic acid (PA) levels in lipid extracts.

However, despite the presence of n-butanol there was a significant increase in PA in pollen treated with DPI and n-butanol, and growth medium with n-butanol, (***, p=6.95 E^{-05}, Figure 4.10C). Furthermore, data presented in Figure 4.10 show similar results to those shown in Figure 4.6 and Figure 4.10. There is a significant increase in PA levels in SI-induced and butanol treated pollen compared to pollen treated with growth medium and

126

butanol (***, p=6.00 E^{-05}, Figure 4.10A&C). As previously discussed, these data suggest that perhaps another PA-pathway could be up-regulated to compensate for a decrease in PA through the PA-PLD pathway, due to the presence of butanol and therefore P-but.

Furthermore, to ensure DPI treatment also had an inhibitory effect on DGPP formation in the presence of butanol, the samples shown in Figure 4.10 were also run in an alkaline solvent solution to visualise DGPP lipid spots (Figure 4.11A). Figure 4.11B showed quantitatively that pollen treated with DPI & butanol do not have significantly different levels of DGPP compared to pollen treated with just butanol (N.S, p=0.418306, Figure 4.11). Furthermore, there was a highly significant difference between pollen treated with DPI & SI & Butanol compared those treated with just SI & Butanol (**, p=2.413 E^{-03}, Figure 4.10C). These data show that DPI treatment inhibits SI-induced increases in DGPP, even in the presence of butanol, therefore suggesting the presence of butanol, and therefore the inhibition of PA formation through the transphosphatidylation function of PLD, does not interfere with DGPP formation. Moreover, these data suggests that SI-induced increases in DGPP levels in *Papaver* pollen tubes may not be formed through the PLD pathway.
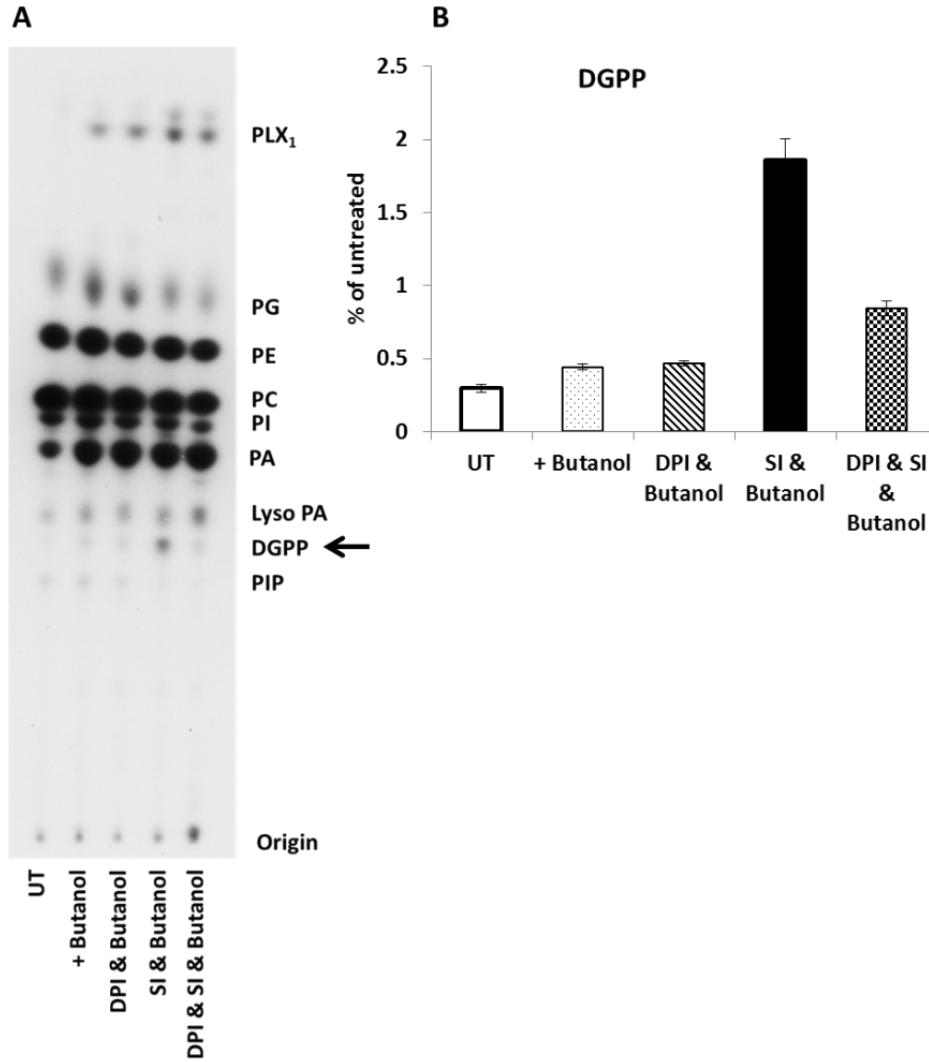
Figure 4.11. Inhibition of ROS signalling during the SI response in *Papaver* pollen tubes results in a reduction in PLD activities

Pollen was grown for 4 hours in the presence of ^{32}P after which pollen was treated with either growth medium (UT) or growth medium & 0.1 % n-Butanol (+ Butanol), DPI & 0.1% n-Butanol (DPI & Butanol), PrsS & 0.1% n-Butanol (SI & Butanol), or DPI & PrsS & 0.1% n-Butanol (DPI & SI & Butanol). After 120 minutes of treatment samples were stopped and a lipid extraction was carried out. Pollen samples were then loaded on the TLC and run in an alkaline solvent system. TLC was exposed on to autoradiograph film. A representative image of an autoradiograph of pollen treated with either growth medium (UT), butanol, DPI & butanol, SI & Butanol or DPI & SI & Butanol. Arrow indicates DGPP lipid spots. B. Diacylglycercol pyrophosphate (DGPP) spots were quantified and are expressed at as % of total labelled lipids for each lane, graph represent 3 independent experiments. Treatments are labelled as follows; UT; white bar, Butanol; white bar with black spots; DPI & Butanol; white bar with black diagonal lines, SI & butanol; black bar, DPI & SI & butanol; white and black checkered bar.

128

4.3 DISCUSSION

This chapter has described the first steps in identifying phospholipids as a target during the SI response in *Papaver* pollen tubes. As yet phospholipids have not been investigated during the SI response in any species. However, phospholipids have been identified as key signalling components during normal pollen tube growth. The most notable is phosphatidic acid (PA) signalling, which has an important role in regulating the apical tip growth of pollen tubes (Monteiro et al., 2005a; Monteiro et al., 2005b; Pleskot et al., 2012; Potocký et al., 2003). Despite the increasing amount of evidence for the role of phospholipid signalling in pollen tubes, there are few studies in which physiologically relevant stimuli was used. Here we have used biochemical approaches to identify alterations in three major phospholipid levels during a SI-specific response in *Papaver* pollen: PA, phosphatidylinositol monophosphate (PIP) and a phospholipid X_2 (PLX_2), which we later identified as the novel diacylglycercol pyrophosphate (DGPP). Furthermore there appears to be an increase in an unidentified lipid PLX_1, however due to experimental difficulties were not able to quantify these changes in this study. We have shown that during SI there is a significant increase in phospholipase D activities, which is known to transform structural lipids into the signalling messenger PA. Alterations in the actin cytoskeleton do not appear to play a significant role in signalling upstream of SI-induced alterations in phospholipids. Furthermore, data suggest that a ROS may be involved in triggering SI-induced increases in DGPP.

4.3.1 SI TRIGGERS ALTERATIONS IN THE LEVELS OF SPECIFIC PHOSPHOLIPIDS

As previously discussed, intracellular PA levels increase under various biotic and abiotic stress conditions, including pathogen attack (van der Luit et al., 2000; Yamaguchi et al., 2005; Young et al., 1996), wounding (Lee *et al.,* 2001) and hyperosmotic stress (Munnik et al., 2000; Zonia and Munnik, 2004).

During the SI response there were significant increases in PA and decreases in PIP levels, in addition to evidence for the up-regulation of PLD activities. Like SI-induced alterations, during hypo-osmotic stress, there were significant increases in PA and a reduction PIP levels, which was accompanied by stimulation of PLD activity and increases in the pollen tube apical cell volume (Zonia and Munnik, 2004). During the SI response there are significant alterations in channel activity and increase in Ca^{2+}, which will affect the homeostasis of the pollen tube and this may account for a similar response to osmotic stress in tobacco pollen tubes.

Althought data has shown that there are alterations in both PA and PIP levels during osmotic stress and the SI response in *Papaver* at present their role in these responses are not yet know and this is something that will be discussed in Chapter 7.

During osomotic stress in tobacco cells, decreases in PIP levels did not result in an increase in PIP_2 levels, which is usually associated with PIP kinase activities (as shown in Figure 1.1 in Chapter 1). Therefore these results suggest that the decrease in PIP maybe due to the inhibition of it synthesis, or perhaps there could be an up-regulation of its hydrolysis by PLC activities to form DAG or other products (Zonia and Munnik, 2004). In

130

Papaver pollen tubes, both untreated and SI-induced, PIP_2 was not visible, suggesting very low levels with little turnover, and therefore SI-induced decrease in PIP could be due to an increase in PLC activity or by the inhibition of a PIP kinase, similar to a hypo-osmotic response. In a scenario where SI resulting in an increase in PLC activity this would suggest that PLC actiuvities may also be involved in increasing PA levels, as PLC is part of the PLC/DAG pathway which is responsibility for production PA (Chapter 1, Figure 1.1). Furthermore, the PLC/DAG pathway is already known to be activated in certain stress conditions, such as during a pathogen attack (de Jong et al., 2004; Testerink and Munnik, 2005). However, as PLC activities were not monitored during this study, their role during the SI response is only speculative and should be investigated further in future studies.

Research has shown that the inhibition of a PI kinase in guard cells results in a reduction in PIP levels, which play a role in inhibiting ABA-induced cytosolic Ca^{2+} increases and stomatal closure in guard cells (Jung et al., 2002; Lee et al., 1996). Franklin-Tong *et al.,* (1996) showed that IP_3 maybe be involved in releasing of Ca^{2+} stores during the SI response. The hydrolysis of PIP through PLC activities could produce IP_3 during SI, and therefore play a role in triggering increases in cytosolic Ca^{2+}. Moreover, PI kinase has been shown to be important for vacuole organization during pollen development, suggesting PIP decreases could result in the reorganization of organelles (Lee et al., 2008a; Lee et al., 2008b). This is something which could be investigated in the future to fully understand the role of PIP signalling during the *Papaver* SI response.

Furthermore, during the SI response there was significant increase in PLD activities. Although PLD activities are notable for their role in PA production, they are also a pH-

sensitive membrane tethering-associated enzyme, which play a role in membrane tethering during plant PCD (Fan *et al.,* 1997). Therefore PLD activities could also potentially be involved in regulation of organelle structure and localization during SI response. PLD activities will be discussed in more detail later on with reference to specific signalling pathways in Chapter 7.

Unfortunately the role of PA was not investigated during this chapter, however one of the most documented targets of PA signalling is protein and lipid kinases (Lee et al., 2001; Meijer and Munnik, 2003; Munnik, 2001; Munnik et al., 1998). In soybean (*Glycine max*), wounding induces the activation of a MAPK. Furthermore, the activation of the wounding MAPK could be trigger by treatments with exogenous PA, and inhibition of PA production prevented MAPK activation. Therefore this PA signalling is implicated in the activation of MAPK during wounding(Lee *et al.,* 2001). Furthermore, recent research has shown that these in increases in PA utilize this MAPK to modulate actin polymerization during wounding, which is a common stress response in plants (Lee *et al.,* 2003). During the SI response in *Papaver* pollen tubes there is the activation of a 56 kDa MAPK, p56, which is in turn activates a caspase-3/DEVD-like activity, a key player of PCD (Rudd *et al.,* 2003). However, p56 activity peaks just 10 minutes after SI induction, and PA increases are observed after 40 minutes of SI induction this suggests that PA may not play role in activation of p56 during the SI response.

Furthermore as described in this chapter within 20 minutes of the SI response there is an SI-specific increase in a lipid originally labelled as PLX_2. This was later identified as diacylglycercol pyrophosphatase (DGPP). DGPP is a novel phospholipid found in both

132

plants and yeast, but not in higher animals. DGPP is formed through the phosphorylation of PA by PA kinase activity (Munnik et al., 1996; Wissing and Behrbohm, 1993). PA kinases had been associated with the plasma membrane, however a gene for PA kinase has yet to be identified in plants. DGPP can be dephosphorylated back to PA by an enzyme called DGPP phosphatase (DPP). Four genes encoding DPPs have been identified in *Arabidopsis thaliana*, called AtLPP1–4 (Jeannette *et al.,* 2010). In yeast DPP1 is associated with the vacuole membrane, although the role of DGPP is still unknown (Han *et al.,* 2004). In plants cells DGPP signalling has been associated with various abiotic and biotic stresses (de Jong et al., 2004; den Hartog et al., 2001; den Hartog et al., 2003; Munnik et al., 2000; Pical et al., 1999; van der Luit et al., 2000) and during plant signalling (Zalejski et al., 2006; Zalejski et al., 2005). In the green alga *Chlamydomonas*, mastoparan treatments lead to increases in PA through both PLD and PLC pathways, and increases in DGPP (Munnik et al., 1995; Munnik et al., 1996). In addition, in *Vicia sativa* seedlings treated with mastoparan there were significant increases in phosphatidic acid (PA) and diacylglycerol pyrophosphate (den Hartog et al., 2001; den Hartog et al., 2003). Treatment with Nod factor had similar effects, although less pronounced, and PA was produced through both the PLD pathway and the PLC/DGK pathway.

In addition to SI-induced pollen tubes, DGPP accumulation coincides with a rise in PA levels in several plant species subjected to either hyperosmotic stress, or dehydration (Munnik et al., 2000; van der Luit et al., 2000). At present very little is known about the role of DGPP during stress responses, however during ABA signalling DGPP is thought to play a role in Ca^{2+} mediated regulation of gene expression (Zalejski et al., 2006; Zalejski et al., 2005). However traditionally DGPP was thought to play a role in attenuate the PA

signal, implying that DGPP is just an inactivated form of PA. However, as there is a

relatively low level in untreated cell, and during a stress response there is a rapid

accumulation, suggests that DGPP could be a signalling molecule itself. DGPP is discussed

more with respect to ROS signalling later on.

Data also suggested there was an *S*-specific increase in the unidentified lipid PLX_1. PLX_1

did not identify with any of the standard lipid markers, which suggests this lipid may have

a novel role in the SI response. Continued research to identify and characterise this lipid

may reveal more details regarding the role of phospholipids during the SI response.

4.3.2 THE ROLE OF THE ACTIN CYTOSKELETON IN TRIGGERING SI-INDUCED ALTERATIONS IN PHOSPHOLIPID LEVELS IN *PAPAVER* POLLEN TUBES

During the SI response in *Papaver* pollen there is rapid depolymerization of the actin

cytoskeleton (Snowman et al., 2002). This depolymerization is followed by actin

stabilization in punctate actin foci. These foci are detectable within 30 minutes of SI

induction and very prominent within 1 hr. Moreover, these actin foci are decorated with

ABPs actin-depolymerizing factor ADF and cyclase-associated protein (CAP). We therefore

wanted to investigate whether alterations in actin dynamics were involved in triggering

SI-induced alterations in phospholipid levels. Data presented in this chapter shows that

both actin depolymerization and stabilization did not alter levels of PA or DGPP,

suggesting that SI-induced increases in PA and DGPP are likely to be downstream of these

signals. This is not surprising given the late time of PA and DGPP alterations. However,

134

data suggested that actin depolymerization and stabilization, may play a minor role in triggering decreases in PIP levels, as there was a significant decrease in PIP levels when treated with either Jasp or Lat B. At present there is no evidence for the role of F-actin in modulating PIP levels in plants. However, there is much evidence suggesting phospholipid signalling is involved in regulating downstream actin dynamics, although there is no evidence for this presented here, the role of phospholipid signalling on actin dynamics during the SI response in *Papaver* pollen tubes could be examined in future studies, see Chapter 7 for further discussion.

Evidence from other groups have shown that, similar to mammalian cells, increases in PA promote actin polymerization in plants (Ha and Exton, 1993; Lee et al., 2003). Moreover in soybean it is though that PA mediates actin polymerization through a 54 kDa Ca^{2+}-dependent protein kinase (Lee *et al.,* 2003). PA has also been shown to mediate alterations in actin status through the inhibition of ABPs such as capping protein (CP) (Huang, 2006; Huang et al., 2003). At present the role of CP has not been investigated in SI-induced actin foci formation in pollen tubes, however other evidence suggest that other phospholipids such as PIP_2 interacts with other ABPs such as profilin (Drobak *et al.,* 1994) and ADF/cofilin (Gungabissoon *et al.,* 1998), which may also play a role in regulating SI-induced actin alterations. Research has also shown that PLD activities play a role in regulating microtubule dynamics in plant cells. Moreover, in algae (*Silvetia compressa*), PLD activity has been shown to regulate microtubule organization but does not appear to regulate actin arrays or endomembrane trafficking directly (Peters *et al.,* 2007). PLD activities have also been linked to microtubule reorganization in Arabidopsis and tobacco cells, interestingly PA treatments did not induced similar results (Dhonukshe

et al., 2003; Gardiner et al., 2003).As discussed in Chapter 1, during the SI response in *Papaver* pollen tubes microtubule depolymerization occurs within 2 minutes of SI induction. Therefore temporally PLD activities may be downstream, however the earliest time point in which PLD activities were monitored during the SI response was 30 minutes, so at present we cannot say that PLD activities do not occur prior to 30 minutes. Therefore, in the future the role of PLD activities on the microtubule cytoskeleton in *Papaver* pollen tubes may be of interest for future work.

4.3.3 ROLE OF ROS AND NO IN SI-INDUCED ALTERATIONS IN PHOSPHOLIPID LEVELS

Data presented in chapter 3 showed during the SI response there is a significant increase ROS signalling within 6 minutes of SI induction, which is followed by an increase in NO levels, peaking within 25 minutes. During SI, both ROS and NO signalling was implicated in actin foci formation and caspase-3-like activities (Chapter 3; (Wilkins *et al.,* 2011). We therefore decided to test whether ROS and NO signalling was also involved in SI-induced alterations in phospholipid levels. Data presented in this chapter showed that scavenging NO during the SI response had no effect on PA, DGPP or PIP levels, and therefore NO is not implicated in triggering alterations in phospholipid levels during the SI response. As SI increases in NO begin within 15 minutes and peak approximately 25 minutes after SI induction, increases in NO maybe downstream of alterations in phospholipid levels which change within 20 minutes of SI induction.

Furthermore, pollen treated with the NADPH oxidase inhibitor, which inhibits ROS production, in SI-induced pollen tubes did not rescue SI-induced increases in PA or SI-

induced decreases in PIP. This suggests that both phospholipids may be upstream of ROS, however as ROS increases are documented as early as 6 minutes after SI induction, it suggest there are not involved in the same pathway. However, the inhibition of NADPH oxidase during the SI response rescued some DGPP formation. This decrease in DGPP also coincided with an increase in PA, although this increase was significantly different to SI-induced levels of PA, it suggest that blocking NADPH oxidase activity may prevent the conversion of PA to DGPP. Therefore these results suggest that ROS signalling may be involved in mediating PA kinases, which is responsible for converting PA to DGPP. As previously mentioned a PA kinase has yet to be identified in plant cells, and therefore little is known about the regulation of DGPP. Surprisingly, when pollen was treated with the ROS, H2O2, there was no significant increase in DGPP, but there was a significant decrease in PIP, and a significant increase in PA. These data suggested H_2O_2, but not an NADPH oxidase-ROS could be involved in triggering the alterations in PA and PIP during SI response, and another type of ROS perhaps via a NADPH oxidase pathway may be involved in DGPP signalling during SI response.

ROS signalling is implicated in several phospholipid-related signalling pathways. It has been suggested that PLDδ is activated by H_2O_2, whereas PLDα1 and PA are involved in the production of ROS (Wang, 2005). It is thought that PLDδ is involved in mediating plant stress tolerance by signalling resistance to damages inflicted by ROS, decreasing H_2O_2-promoted programmed cell death (Li et al., 2004; Zhang et al., 2003). Furthermore, there is evidence that PLDδ and PA play a role in H_2O_2-induced activation of MAP kinase cascades (Zhang *et al.,* 2003). However, ROS may also play another role in manipulating phospholipids. In both mammalian and plant cells, ROS is known to participate in

137

oxidizing phospholipids to hydroperoxides, forming truncated phospholipids such as azelaoyl phosphatidylcholine (Az-PC). Az-PC are known to rapidly enters cells to damage mitochondrial integrity and initiate intrinsic apoptosis (Bhattacharjee, 2012; Latchoumycandane et al., 2012). Therefore, perhaps ROS may play a role in triggering cell death through its oxidising capabilities rather than signalling pathways, however as increases in ROS in SI-induced pollen are transient and not sustained this is unlikely.

Despite there being some evidence for ROS playing a role up-stream of phospholipids, there is much evidence to suggest that ROS is downstream of phospholipid signalling in some systems (Leshem et al., 2007; Sang et al., 2001; Tuteja and Sopory, 2008). As previously discussed, PA is known to trigger ROS production through the stimulation of NADPH oxidase activities. At present we do not know what the source of ROS is during the SI response, however live cell imaging of ROS during the SI response suggested that ROS does not originate from the plasma membrane, which is the site of NADPH oxidases in many plant species (Chapter 3). Furthermore, imaging suggests that ROS may originate from organelles, such as the mitochondria as ROS 'hotspots' resembles mitochondria (as shown in (Bosch et al., 2010).

4.3.4 SUMMARY

Data presented in this chapter has shown that during the SI response in *Papaver* pollen tubes there are significant increases in 3 known phospholipids; PA, PIP, and DGPP(Figure 4.12). Data also suggested there is an *S*-specific increase in an unidentified lipid PLX_1. Furthermore, research has shown that during the SI response there is a significant increase in PLD activities. In addition alterations in actin dynamics may play a role in SI-

induced decrease in PIP, and ROS may be involved in DGPP formation (Figure 4.12). At present phospholipid signalling has not been investigated during the SI response, and therefore data presented here is of significant interest. Although we did not investigate the role of these alterations in phospholipids levels during this SI response, the research presented here is be the basis for a new avenue of research in understanding the signalling mechanisms involved in the SI response and PCD systems in plant cells.
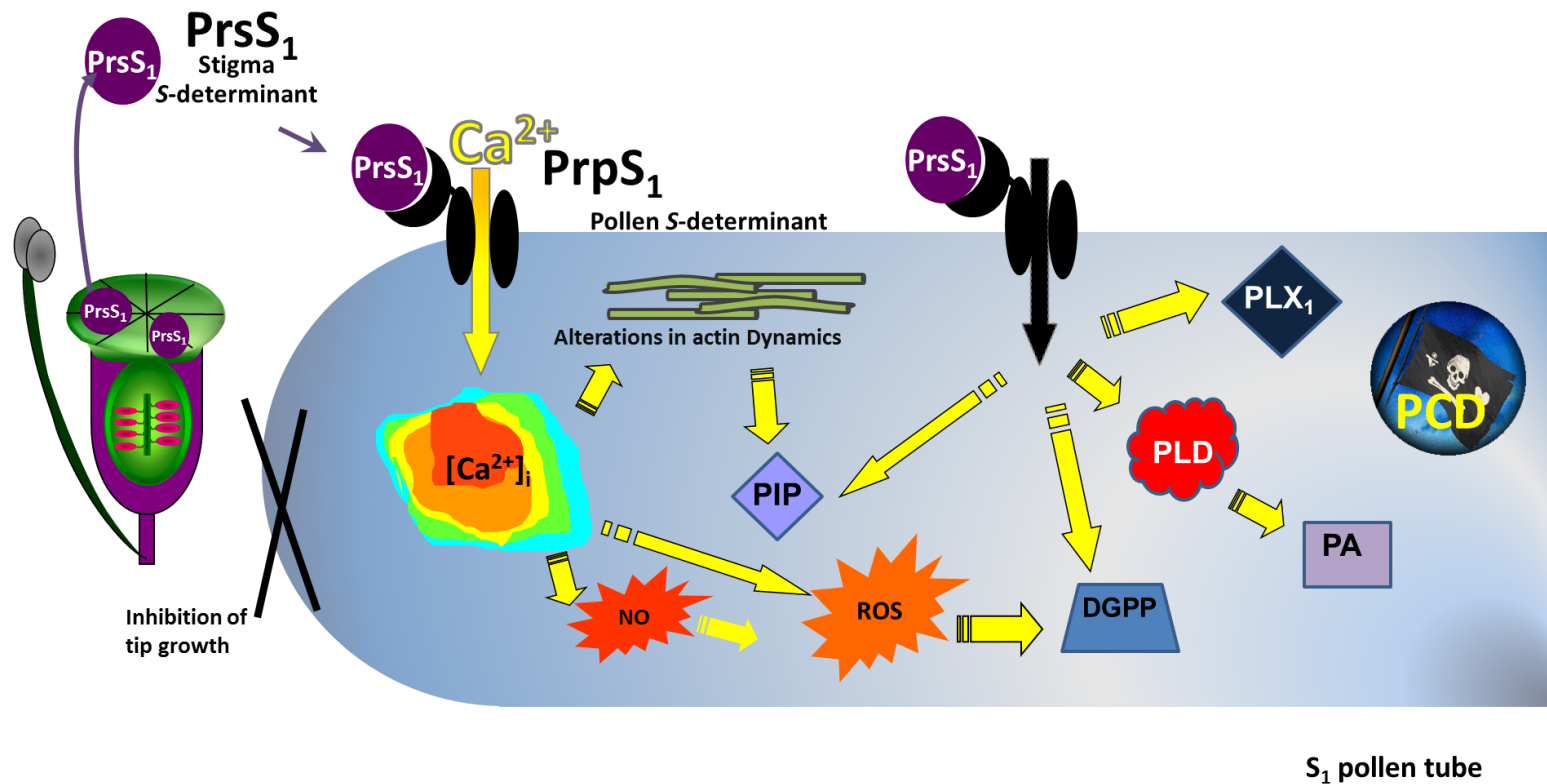
Figure 4.12 A model of SI-induced alterations in phospholipid levels in *Papaver* pollen tubes.

A proposed model for the self-incompatibility mechanism in *Papaver rhoeas* highlighting data present in this chapter. During an incompatible interaction secreted stigmatic protein, *Papaver rhoeas* stigmatic S (PrsS), interacts with *Papaver rhoeas pollen* S (PrpS), pollen receptor in a S haplotype-specific manner, such as $PrsS_1$ binds to $PrpS_1$. This incompatible interaction triggers a rapid influx of Ca^{2+}, which induces a signalling cascade, resulting in the inhibition of tip growth. Increases in Ca^{2+} trigger transient increases in Reactive Oxygen Species (ROS) and Nitric Oxide (NO) (see chapter 3 for details). Increases in these signalling molecules also lead to dramatic alterations in the action cytoskeleton, including the depolymerization of F-actin, which is later followed by stabilization of F-actin into actin foci, and Programmed Cell Death (PCD). Data presented in this chapter showed that during the SI response there are significant increase in phosphatidic Acid (PA) and diacylgycerol pyrophosphate (DGPP). PA increases are mediated through the enzyme phospholipase D. Moreover ROS is is involved in mediating increases in DGPP. There are also significant decreases in phosphatidylinositol monophosphate (PIP) levels, which maybe mediated through alterations in actin dynamics. A self-incompatible reaction also results in the increase in a currently unidentified lipid PLX_1.

CHAPTER 5: ACIDIFICATION OF THE CYTOSOL OF SI-INDUCED POLLEN TUBES

5.1 INTRODUCTION

As discussed in Chapter 1, many cellular processes are regulated by both internal and external pH. Alterations in intracellular pH can result in the modification of enzymes (Guern *et al.,* 1991), protein synthesis (England *et al.,* 1991), alterations to the structure and activity of actin-binding proteins and therefore the cytoskeleton (Gungabissoon et al., 1998; Lovy-Wheeler et al., 2006). Furthermore, alterations in cytosolic pH have been heavily associated with mammalian PCD (Gottlieb, 1996; Meisenholder et al., 1996). BCECF, a pH indicator originally developed by Tsien (1982), has been used by many groups to measure cellular pH in both mammalian and plant cells. This dye has been used to monitor the pH of pollen tubes in several different species including *Nicotiana tabacum* L., which has a cytosolic pH of 7 (Matveeva *et al.,* 2003), *Lilium longiflorium* pollen, pH 7.11 (Fricker *et al.,* 1997; Lovy-Wheeler 2006; Feijó 1999) and *Papaver rhoeas* pollen has a cytosolic pH of 6.9 (Bosch & Franklin-Tong *et al.,* 2007).

The regulation of cytosolic pH is an important factor in pollen tube growth, as discussed in Chapter 1. Some data suggests there is a pH gradient in pollen tubes, with an acidic tip of ~pH 6.8 and an alkaline band at pH 7.5 which correlates with the actin collar, furthermore it has been suggested that this gradient is part of a complex pH network (Feijo et al., 1999; Michard et al., 2009). At present there is some conflicting evidence surrounding the importance of pH gradients during pollen tube growth, and although it has been shown that the pH is an integrate part of apical tip growth. However, there is still some debate over whether pH gradients are a result of growth or whether they regulate growth itself.

To investigate the role of pH in both mammalian and plant cells, including pollen, weak acids have been used to artificially manipulate cellular pH (Matveenva *et al.,* 2003; Becker *et al.,* 2004; Crawford *et al.,* 1994; Westhoff *et al.,* 2002; Papuga *et al.,* 2010; Tournaire-Roux *et al.,* 2003; Lovy-Wheeler *et al.,* 2006). Weak acids such as propionic acid and sodium acetate, cross the cell membrane in their protonated forms and dissociate in the cytosol, resulting in a decrease in intracellular pH. These compounds may also be transported across membranes via ion channels and exchangers (Westhoff 2002; Bertl & Felle 1985; Roper 2007). Sodium acetate was used to look at the effects of acidification on actin organization in lily pollen tubes (Lovy-Wheeler *et al.,* 2006). Artificial acidification to pH 6.3 resulted in the inhibition of growth and the destabilization of the actin collar.

Propionic acid has been used to investigate the role of pH in pollen tube germination in *Nicotiana tabacum* L. (Matveeva *et al.,* 2003), roots hairs (Herrmann and Felle, 1995), and *Pelvetia* rhizoids growth (Gibbon and Kropf, 1994; Guern and Frachisse 1988). Addition of propionic acid resulted in the inhibition of growth in all mentioned cell types and diminished the pH gradient in rhizoid cells of Pelvetia embryos. Propionic acid has also been used to investigate molecular mechanism of aquaporin in root cells (Tournaire-Roux *et al.,* 2003) and to analyse the regulation of LIMs (LIM domain-containing proteins), which are associated with protein-protein interactions, in *A. thaliana* and lily pollen tubes (Papuga et al., 2010; Wang et al., 2008). Data suggested that LIMs, specifically PLIM2c localised to actin bindles at low pH, pH 6.2, however at pH 7.4 PLIM2c was inhibit. These data suggest that alterations in pH play a significant role in manipulating the actin cytoskeleton through regulation of LIM proteins.

As discussed in Chapter 1, cytosolic acidification is a common event during mammalian apoptosis (Matsuyama and Reed, 2000). A typical drop in pH in mammalian cells during apoptosis has been recorded as ~ 0.3-1.4 pH units (Matsuyama and Reed, 2000; Nilsson et al., 2006; Nilsson et al., 2004; Thangaraju et al., 1999a), which can be caspase-dependent or –independent (Matsuyama *et al.,* 2000; Furlong *et al.,* 1997; Zanke *et al.,* 1998). During TNF-α induced apoptosis in U937 cells, the cytosolic pH acidifies from pH 7.2 to 5.8, which coincided with an increase in pH in lysosomes from pH 4.3 to 5.2. These data suggest that apoptotic-induced acidification may be due to the release of protons from the lysosome (Nilsson et al., 2006; Nilsson et al., 2004). Furthermore, during apoptosis in the IL-3 dependent cell line BAF3, cytosolic acidification resulted in the activation of interleukin-1 β convertase (ICE)-like protease and DNA fragmentation (Furlong *et al.,* 1997). In addition, increasing extracellular pH reduces ICE-like protease activation and DNA fragmentation suggesting pH plays an important role in regulating cell death during this response. Furthermore, in human promyelocytic leukaemia cells (HL60) cells, the cytosolic acidification resulted in increased levels of DNA fragmentation and cellular degradation (Park *et al.,* 1996). Cytosolic acidification has been shown to signal for mitochondrial translocation of Bax, a pro-apoptotic Bcl-2 protein, triggering drug-induced apoptosis of tumour cells (Ahmad *et al.,* 2004).

In plant cells evidence of dramatic alterations in cytosolic pH during normal plant development and stress events are rare, although it is often assumed to occur, particularly during PCD. Once such example is during tracheary element (TE) differentiation, in which the cells undergo PCD in order to create the water bearing xylem. During this process the acidic vacuole ruptures, releasing cytotoxic enzymes into

144

the cytosol which contribute to the degradation of the cell. It is assumed that the breakdown of the acidic vacuole results in cytosolic acidification. However, as yet this acidification has not been measured (Obara 2001; Rotari *et al.,* 2005).

One of the few examples in which plant acidification has been measured is during gravitropism in Arabidopsis roots. The surface of roots has a highly dynamic pH pattern (Monshausen et al., 2007; Monshausen et al., 2011). Within 3 minutes of manipulation of the root position, there is acidification of the upper flank of the root by 2.8 pH units. Concurrently the surface pH of the lower flank increased 3.0 pH units. This process results in the initiation of gravitropic curvature, and therefore reorientation of the root growth. Moreover, these events have been shown to be triggered by auxin redistribution, which is thought to play a role in regulating plasma membrane proton pump activity. Which in turn is thought to contributing to the acidification of the upper flank of the root, resulting in faster growth on that side of the root (Monshausen *et al.,* 2011).

Previous studies by Bosch and Franklin-Tong*,* (2007) have shown that SI-induced *Papaver* pollen tubes undergo a substantial change in cytosolic pH. Untreated healthy pollen tubes have a cytosolic pH of ~pH 6.9. 1-4 hours after inducing SI, the pollen cytosolic pH acidifies to ~pH 5.5. This was the first documentation of SI-PCD-associated cytosolic acidification in plants. As previously described in Chapter 1, a key feature in SI-induced *Papaver* pollen tubes is the activation of caspase-like activities. Bosch & Franklin-Tong *et al.,* (2007) carried out studies to establish the temporal and spatial activation of caspase-like activities in SI-induced pollen. Activities identified included DEVDase activity (caspase-3/DEVDase-like activity, a known executioner caspase in apoptosis) and shown

145

to be involved in SI-mediated PCD (Thomas and Franklin-Tong, 2004; Thomas et al., 2006). Bosch & Franklin-Tong (2007) showed that these caspase-like activities peaked at ~5 hr. after SI-induction, and the study also showed that these activities required an acidic pH, with activity optimal at pH 5. In particular caspase-3/DEVD-like activity was significantly lower in all other buffers outside of the pH 4.5-5.5 range, showing there is a very narrow pH window for their activity. As SI-induced acidification of the cytosol had occurred at 1-4h post-SI, which is temporally prior to the peak of the caspase-3/DEVDase-like activity at 5 h, this suggests pollen tube acidification could play a vital role in creating optimal conditions for these activities in SI-induced pollen tubes. Although these studies established the induction of caspase-like activities and extreme cytosolic acidification during SI, the temporal and spatial examination of the changes in pH were not examined. This chapter investigates SI-induced acidification in much more detail. Specifically, we wished to know how fast cytosolic acidification occurs during the SI response, whether pH 5.5 is the most acidic pH obtained, and whether there is any recovery of intracellular pH. Furthermore, we wished to establish if SI-induced acidification is required for the induction of caspase-3/DEVDase-like activities, and if any of the other key hallmarks of SI response, such as actin alterations, are a consequence of acidification. Data presented here show SI-induced acidification is a rapid response, in which acidification occurs within 10 minutes of SI induction and continues for up to 60. To investigate the role of SI-induced acidification in *Papaver* pollen tubes, weak acids were used to manipulate the cytosolic pH of the pollen tube to either a neutral or acidic pH. Addition of propionic acid pH 5.5 resulted in the rapid acidification of *Papaver* pollen tubes, and resulted in reorganization of F-actin and the formation of actin foci. In addition artificial acidification

resulted in significant increases in caspase-3/DEVDase-like activities. Moreover, inhibition of SI-induced acidification by propionic acid pH 7 prevented actin foci formation and strongly inhibited caspase-like activities, highlighting the importance of pH during the SI response. Data presented in this chapter also show that Ca^{2+} increases are upstream of pH alterations. In summary, this chapter provides the first detailed studies investigating the role of acidification during the SI response in *Papaver* pollen.

5.2 RESULTS

5.2.1 MEASUREMENT OF CYTOSOLIC PH IN *PAPAVER* POLLEN TUBES

Pollen tubes were labelled with the ratiometric pH indicator BCECF AM to measure their cytosolic pH. The ratiometric pH indicator BCECF is available as both an ester (AM) and a dextran forms. The dextran form must be microinjected or bombarded into cells, as the dextran conjugate is membrane impermeable. In this study the ester form was used, as it is membrane permeable, eliminating the need for time consuming microinjection techniques. However, the ester form of BCECF presents some disadvantages. The ester probe was sequestered to organelles and other compartments if incubated for ~30 minutes, and no longer indicated the pH of the cytosol (See supplemental Figure 1). To avoid this problem, pollen tubes were incubated with BCECF AM for only a short period of time prior to imaging to prevent sequestering of the probe (5 minutes incubation prior to imaging, and images were only taken within 10 minutes of loading to ensure that cytosolic pH was being measured).

The cytosolic pH of *Papaver* pollen tubes was measured using confocal ratiometric

imaging of BCECF AM. A ratio was calculated between two images which were collected

with different excitation wavelength pollen tubes loaded with the dye BCECF AM (488 nm

/ 458 nm; Figure 5.1) and the pH value was calculated using a calibration curve based

upon measurements taken from BCECF acid-labelled pseudocytosol solutions (see

Chapter 2 for more details; Figure 5.1).
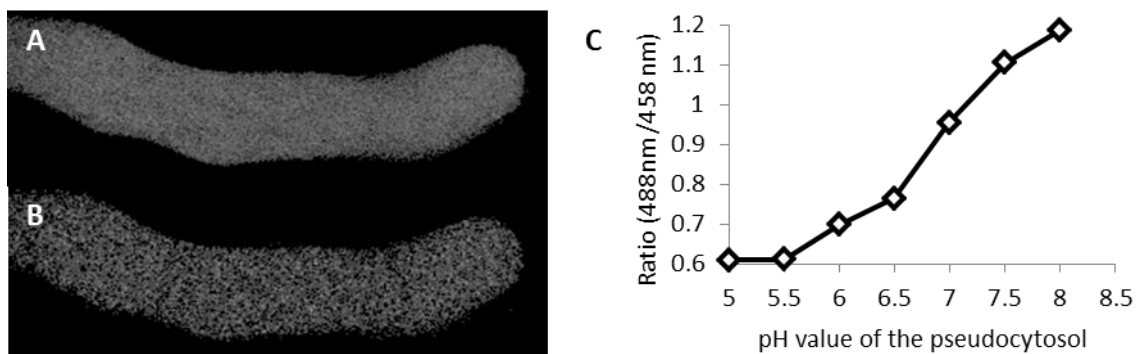
Figure 5.1 Measuring the cytosolic pH of *Papaver* pollen tube with the pH indicator BCECF AM

A healthy pollen tube was labelled with BCECF AM for 5 minutes prior to ratiometric imaging with a confocal microscope. A. This image shows BCECF AM signal when excited at 488 nm. B. This shows the BECEF AM signal when excited at 458 nm. Both images were collected at 500-550 nm using confocal microscopy. A ratio value was made of the two images using Image J; this ratio would then be used to determine the pH of the pollen tube cytosol using a calibration curve (C), also collected during the same experiment. The pollen tube presented here has a cytosolic pH of 6.8. C. Pseudocytosol solutions which mimic the cytosol of the pollen tube were labelled with BCECF free acid and a confocal image was taken excitation 488nm and then 458nm, both were collected at 510-550 nm, a ratio of these two images was calculated and was plotted in a graph Ratio: pH values. This was carried out for pseudocytosol solutions at pH 5-8, at approximately 0.5 intervals.

The images of the pollen tube shown in Figure 5.1 are representative of an untreated

healthy pollen tube. Pollen tubes had a fairly uniform labelling with BCECF AM, with no

distinct compartments or variations in pH levels, verifying that the dye has not been

sequestered into organelles. Figure 5.1A shows the pH-dependent image (excitation 488

nm, emission collection 510-550 nm) and Figure 5.1B shows the pH-independent image

(excitation 458 nm, emission collection 510-550 nm). Figure 5.1C shows a typical

calibration curve constructed using seven different pH pseudocytosol calibrations buffers.

A calibration graph similar to that shown in Figure 5.1C, was used to calculate the cytosolic pH ($[pH]_{cyt}$) of BECEF-AM labelled pollen tubes by reading the ratio of the pollen tube across to the curve. A fresh calibration was carried out for each experiment. The untreated pollen tube in Figure 5.1 has a $[pH]_{cyt}$ of pH 6.8. This therefore supports Bosch & Franklin-Tong (2007) findings that *Papaver* pollen tubes have a fairly neutral cytosolic pH.

5.2.2 SI-INDUCED ACIDIFICATION OF THE CYTOSOL

Previous research has shown that acidification of the cytosol occurs in SI-induced pollen tubes (Bosch and Franklin-Tong, 2007). This acidification could play an important role in creating the right environment for activation of the SI-induced caspase-like proteins. However, a detailed account of the temporal alterations in pH of SI-induced pollen tubes had not yet been carried out. It was therefore decided to investigate SI-induced intracellular pH concentration ($[pH]_i$) changes between zero and three hours after SI induction. At each time point several pollen tubes' cytosolic pH was measured. As the pH indicator BCECF AM tends to sequester into organelles after prolonged incubation, pollen tubes were labelled with the probe only for a very short period of time and a 'snap-shot' was taken at each time point using different pollen tubes (i.e. the same pollen tube pH could not be monitored over the full 3 hr. period; see Materials and Methods for full details).

The cytosolic pH of pollen tubes measured at the beginning of the experiment (T=0) for all datasets was relatively constant, ranging from ~pH 6.8- 7.05 (n=100), with a mean of pH 6.8 (Figure 5.2A). Furthermore, there was no significant difference between the $[pH]_i$

of untreated pollen tubes (UT) and SI induced (N.S, p=0.171, Figure 5.2A), or untreated

and compatible pollen tubes at this time point (N.S, p=0.871, Figure 5.2A). In untreated

pollen tubes, the pH remained high and did not change significantly from $[pH]_{cyt}$ at time 0

over a period of 3 hr. (N.S, p= 0.060; Figure 5.2A). Representative untreated pollen tubes

are shown in Figure 5.2B&C, which had a pH of pH 7.1 at the beginning of the treatment

(Figure 5.2B) and a pH of 7.15 at 60 minutes after the addition of growth medium (Figure

5.2C). In these untreated pollen tubes there was little change in the distribution of signal

between time 0 and 60 minutes, which supports the idea that pH does not normally vary

much in normal growing pollen tubes. Pollen treated with PrsS in an incompatible

combination (Figure 5.2A) showed a rapid decrease in cytosolic pH within 10 minutes of

SI-induction, reaching an average cytosolic pH of 6.39 (n=11), which is highly significantly

different from the pH at time 0, *** p= 3.253 E^{-07}, Figure 5.2A). A representative image is

shown in Figure 5.2D, pH 6.4. Here the pollen appears to more acidic toward the cell wall,

perhaps indicating an influx of protons at the site, however this could also be an artefact

edge effect. The $[pH]_{cyt}$ of the SI-induced pollen tube was significantly different to that of

untreated pollen tubes after 10 minutes of treatment (***, p=0.0001; Figure 5.2A). After

30 minutes SI induction, the $[pH]_{cyt}$ was even more acidic, at pH 6.02, which is highly

significantly different to untreated pollen tubes at the same time point (***, p= 0.0003,

Figure 5.2A). A representative image of the BCECF labelling of a pollen tube treated with

PrsS for 30 minutes is shown in Figure 5.2E. This shows that the cytosol was much more

acidic in than untreated pollen tubes, with the cytosolic signal appearing more uneven.

The acidification of the cytosol continued for 60 minutes, when it reached its most acidic

point, ~pH 5.5 (n=16). This was highly significantly different to [pH]$_{cyt}$ of untreated pollen

tubes at 60 minutes (***, p=8.3236 E^{-06}, Figure 5.2A).
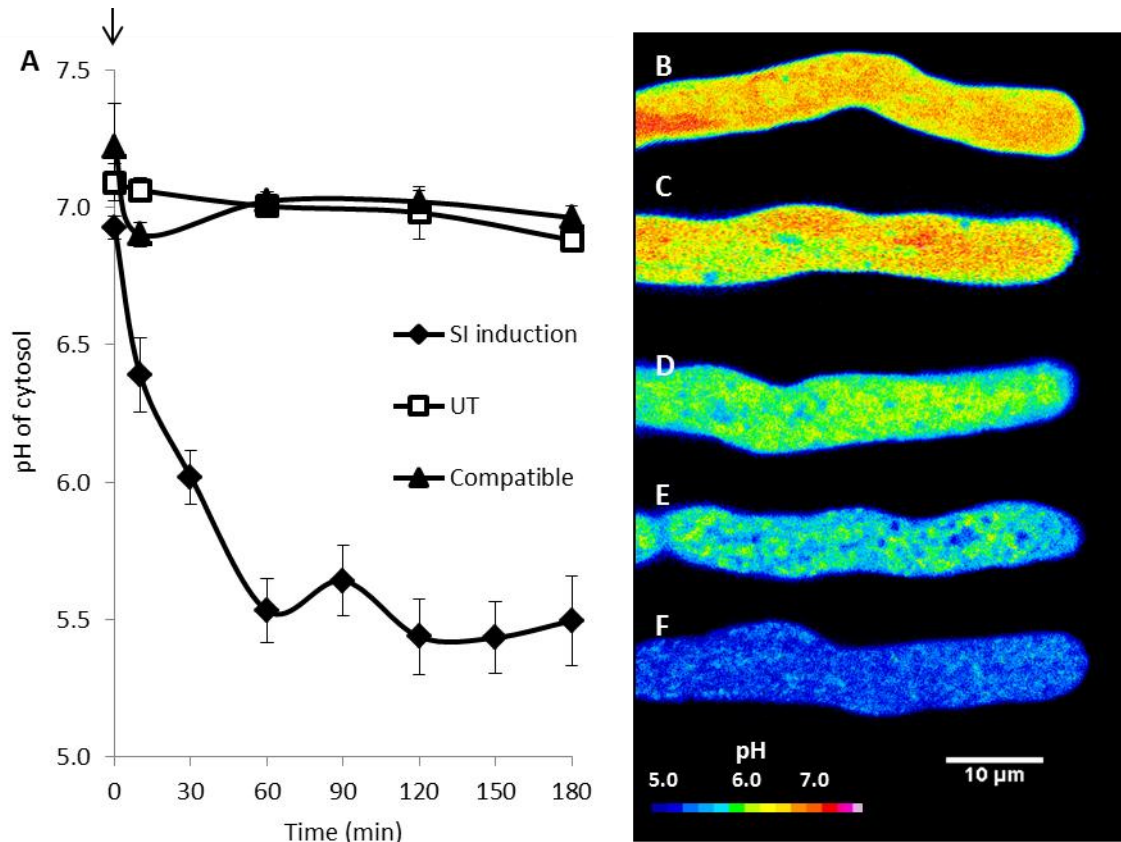
Figure 5.2. SI-induced pollen tubes undergo rapid acidification of the cytosol.

Pollen was labelled with the ratiometric pH indicator BECEF AM to determine the cytosolic pH at time intervals after the addition of PrsS to induced SI (arrow indicates addition of PrsS). A. Pollen tubes were treated with either PrsS to provide an incompatible response (SI induction; closed diamond symbol) or PrsS to provide a compatible response, where the pollen *S*-genotype matches PrsS (Compatible; closed triangle symbol), and growth medium used a control (untreated, UT; Open square symbol), n=263. pH of cytosol was determined (see materials and methods), in which the mean pH was calculated within the first 25 μm of the region within the pollen tube tip. B-F. Images were collected during ratiometric imaging of the pH indicator BECEF AM, images displayed are from the pH-dependent image (488 nm excitation and 510-550 emission). Background was subtracted and images were pseudocoloured in the image analysis software ImageJ (see material and methods for details). Images B & C are representative of untreated pollen tubes at T0, pH 7.1 and T60 pH 7.15 respectively. D-F. Representative pollen tubes pseudocoloured to show typical alterations in cytosolic pH during the SI response. D. Pollen tube 10 minutes after addition of PrsS, cytoplasmic pH 6.4. E. Pollen tube 30 minutes post induction of SI response, cytoplasmic pH 6.1. F. Pollen tube 60 minutes after addition of PrsS, cytoplasmic pH 5.5. Calibration of the cytosolic pH is indicated by the inset colour scale. Scale bar 10 μm.

A representative image of an SI-induced pollen tube of 60 minutes is shown in Figure

5.2F. These data show that the cytosol has become very acidic, and this was confirmed by

ratiometric analysis of this pollen tube which show the cytosolic pH was pH 5.5, (Figure 5.2F). There was no significant difference between the cytosolic pH of SI-induced pollen tubes at 60 minutes of treatment compared to those with 180 minutes of treatment (N.S, p=0.105, Figure 5.2A), suggesting that the pollen tubes have reached an equilibrium by ~60 minutes post SI. Furthermore, at this 180 minute period there was a highly significant difference between the cytosolic pH of untreated pollen tubes and SI induced pollen tubes (*** p= 1.571 E^{-04}, Figure 5.2A).

To ensure the acidification was an SI-specific response, compatible pollen was also treated with the same PrsS as used to induce SI in incompatible pollen. As the pollen has a different genotype to the PrsS administered, SI will not be triggered (see Material & Methods). As shown in Figure 5.2A, compatible pollen did not exhibit the same response as incompatible pollen and acidification of the cytosol did not occur, remaining at pH 6.96 at 180 minutes after the addition of PrsS (n=8). Furthermore, compatible pollen cytosolic pH at 60 minutes was not significantly different to untreated pollen of the same time point (p=0.673) or at 180 minutes of treatments (p=0.168). Moreover, compatible pollen treated with PrsS was significantly different to the cytosolic pH of incompatible pollen at both 60 and 180 minutes of treatment (***, p=1. 828 E^{-04}; ***, p= 3.79 E^{-04}, respectively).

Overall, these data show that the cytosol of SI-induced pollen tubes acidifies rapidly during the initial SI response, and the pH of the cytosol stabilises at ~ 60 minutes, remaining very acidic thereafter at an average of ~5.84 $\pm$ SEM (n=67). Moreover, this is an *S*-specific event.

5.2.3 WEAK ACIDS ACIDIFY THE CYTOSOL OF *PAPAVER* POLLEN TUBES

To investigate the importance of acidification, weak acids were used to mimic the cytosolic acidification induced in pollen tubes by the SI response. In order to achieve this, weak acids were added to the growth medium of healthy pollen tubes. Preliminary experiments used 100 mM sodium acetate at pH 5.5 to artificially acidify pollen tubes (see supplemental Figure 2). However, most studies used the cell permanent weak acid, propionic acid, to manipulate the pH of *Papaver* pollen tube cytosol. Concentrations of 10 mM to 100 mM of propionic acid were tested. 10 mM PPA was not sufficient to stably reduce the cytosolic pH of pollen tubes (data not shown), and therefore a higher concentrations (50 mM) were used (Figure 5.3).

The cytosolic pH of pollen tubes were measured using BCECF AM at T=0, 10, 60 & 120 minutes after the addition treatments including growth medium as a control, PrsS to induced SI, propionic acid pH 5.5 to mimic SI-induced acidification, propionic acid pH 7 as a control, and propionic acid pH 7 & PrsS, in which pollen was pre-treated with propionic acid for 10 minutes prior to the addition of PrsS, to investigate whether propionic acid pH 7 could be used to prevent SI-induced acidification (see Chapter 2 for details; Figure 5.3).
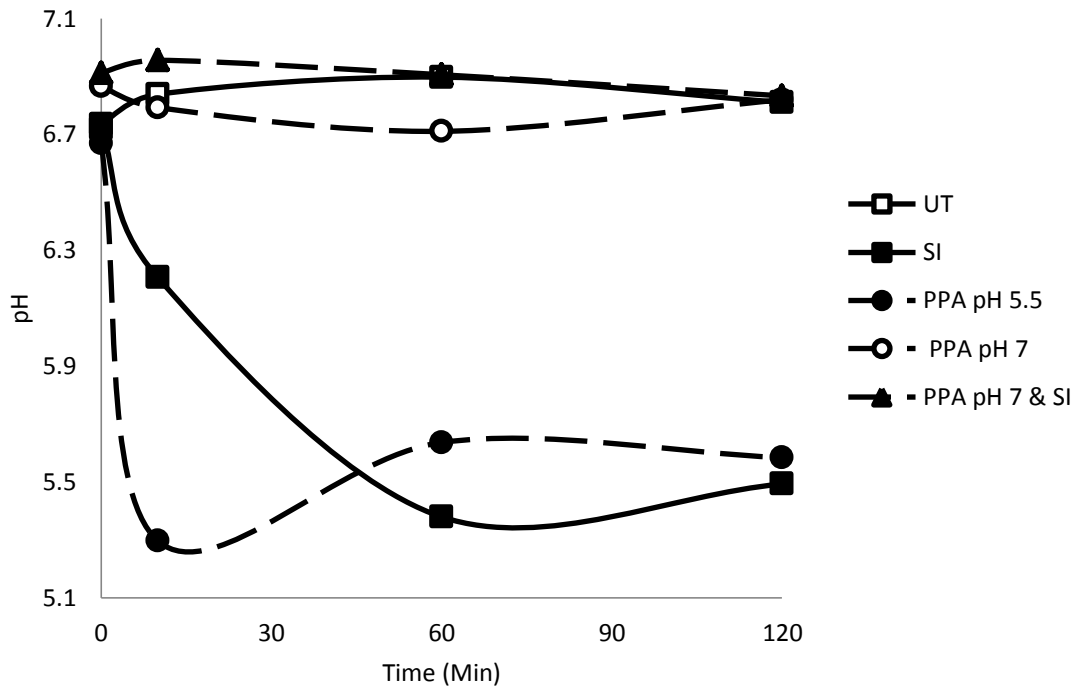
Figure 5.3. 50 mM Propionic acid can be used to manipulate cytosolic pH of pollen tubes to mimic SI-induced acidification, and prevent SI-induced acidification

Papaver pollen was incubated at T = 0 with either growth medium (untreated, UT; open square symbol, solid black line), PrsS (SI; closed square symbol, solid black line), 50 mM propionic acid pH 7 (PPA pH 7; open circle symbol, dashed line), 50 mM propionic acid pH 5.5 (PPA pH 5.5; solid circle symbol, dashed line) or pre-treated with 50 mM propionic acid pH 7 for 10 minutes prior to addition of PrsS (PPA pH 7 & SI; solid triangle symbol, dashed line). Pollen was labelled with BECEF AM and ratiometrically imaged to determine the cytosolic pH of the pollen tube at T0, 10, 30, 60 and 120 minutes after addition of treatments. N=176.

Addition of PrsS resulted in rapid acidification of the cytosol similar to that shown in

Figure 5.2. Pollen treated with PrsS for 120 minutes were highly significantly different to

untreated pollen at the same time point (***, p= 1.000 E^{-04}, Figure 5.3). The addition of

growth medium had no effect on cytosolic pH, and there was no significant difference

between untreated pollen at T0 and T120 minutes (N.S, p=0.853, Figure 5.3).

The addition of 50 mM propionic acid pH 5.5 resulted in rapid acidification of the cytosol,

within 10 minutes of addition the cytosol was pH 5.30 (n=17) with was highly significantly

different to untreated cells at 10 minutes (*** p= 1.49 E^{-07}, Figure 5.3). However, after

the pollen tubes' initial dramatic acidification, there was a period of slight cytosolic pH

154

recovery. Pollen tubes incubated with 50 mM propionic acid pH 5.5 for 60 minutes had a pH of 5.64 (n=19), and continued to remain near this pH, thereafter pollen tubes after 120 minutes had a cytosolic pH of pH 5.58 (n=16, Figure 5.3). This latter cytosolic pH was significantly different to that of untreated pollen at this time point (*** p= 4.8134 E^{-06}), and not significantly different to SI induced pollen tubes (N.S, p= 0.691, Figure 5.3).

However, perhaps not unexpectedly, pollen tubes treated with propionic acid pH 5.5 had different temporal profile for intracellular acidification than SI induction. Pollen tubes treated with propionic acid pH 5.5 reached pH 5.3 (n=17) within 10 minutes incubation whereas SI induced pollen tubes only acidified to pH 6.21 (n=8), and therefore there is a significant difference in pH at this time point (**, p=0.002, Figure 5.3). However, as the later time points are not significantly different, this demonstrates that propionic acid pH 5.5 can be used to induce the same level of acidification as SI induced cells.

To investigate whether change in $[pH]_{cyt}$ was due to the presence of propionic acid itself or whether the actual pH of the propionic acid played a role in the buffering of cytosolic pH of the pollen tubes, pollen was treated with a propionic acid at pH 7. The pH of pollen tubes incubated with 50 mM propionic acid pH 7 did not change considerably over 120 minutes (Figure 5.3). For example pollen tubes treated with propionic acid pH 7 for 10 minutes had a cytosolic pH of 6.79, there was no significant difference after 120 minutes of incubation, at which point the pollen tube has a cytosolic pH of 6.82 (N.S, p= 0.875, Figure 5.3). Furthermore, the cytosol of pollen tubes treated with propionic acid at pH 7 for 120 minutes was not significantly different from untreated pollen at the same time point (N.S, p=0.890, Figure 5.3). Moreover there was a highly significant difference

155

between pollen treated with propionic acid pH 5.5 and propionic acid pH 7 for 120 minutes (*** p= 9.57 E^{-04}, Figure 5.3). These data suggest that the pH of the buffer, rather than the addition of the propionic acid itself, was the significant factor in the manipulation of cytosolic pH of the pollen tubes. Pollen tubes treated with propionic acid pH 7 continued to display cytoplasmic streaming, although tip elongation was inhibited in all pollen treated with propionic acid at all pHs. This has been previously reported in propionic acid treated *Neurospora* hyphae and *Agapanthus* pollen tubes (Parton *et al.,* 1997). Moreover, as acidification only occurs in cells treated with propionic acid pH 5.5 this suggests that these buffers can be used to suitably buffer the cytosolic pH of the pollen tube and propionic acid pH 7 can be used as a suitable control of the presence of propionic acid in pollen tubes.

We decided to test if we could block SI-induced events in *Papaver* pollen tubes by inhibiting the acidification using propionic acid pH 7. This would provide important data as to whether acidification was a key step required for SI events. Results shown in Figure 5.3, showed that pollen pre-treated with propionic acid pH 7 for 10 minutes prior to SI induction, did not undergo acidification of the cytosol. Pollen pre-treated with propionic acid pH 7 for 10 minutes, (labelled as T0 in figure 5.3), pollen had a cytosolic pH of 6.91 (n=4) which was not significantly different to the pollen after SI induction of 120 minutes (post-propionic acid pre-treatment), pH 6.83 (n=9; N.S, p= 1.000, Figure 5.3). Furthermore, the pH of cells treated with propionic acid pH 7 & SI for 120 minutes were not significantly different to untreated pollen at the same time point (N.S, p= 0.705), or pollen treated with just propionic acid pH 7 for 120 minutes (N.S, p=0.947, Figure 5.3). However, there was a highly significant difference between pollen treated with propionic

acid & SI induced pollen with no pre-treatment at the same time point (***p=5.32 E^{-04}, Figure 5.3). These data demonstrate that propionic acid pH 7 can be used to block SI-induced acidification in *Papaver* pollen tubes

In summary, these data show that propionic acid pH 5.5 can be used to mimic SI-induced acidification. Furthermore, propionic acid pH 7 can be used to prevent acidification in SI-induced pollen tubes. Therefore propionic acid can be used to manipulate the pH of the cytosol in pollen tubes to investigate the role of acidification during the SI response and to identify whether acidification is a key step required for downstream SI events.

5.2.4 ACIDIFICATION OF POLLEN TUBES TRIGGERS CASPASE-LIKE ACTIVITIES

As previously mentioned, Bosch *et al.,* (2007) demonstrated that *in vitro* caspase-3-like activities require an acidic environment to be functionally active, and are only active within a very narrow range of pH ~4.5 to 5.5. The experiments described earlier show that propionic acid can be used to artificially acidify pollen tubes to similar pH as that of SI-induced pollen tubes and to prevent acidification by buffering. It was of particular interest to investigate whether caspase-3-like activities could be induced by artificial acidification of the cytosol with propionic acid in *Papaver* pollen tubes, as this might reveal whether acidification played a role in SI-induced caspase activities *in vivo.*

Pollen was treated with either propionic acid pH 5.5, PrsS to induce SI, growth medium (untreated) or propionic acid pH 7 as controls. A further treatment was conducted in which pollen was pre-treated with propionic acid pH 7 for 10 minutes prior to the addition of PrsS to investigate whether blocking acidification prevents caspase-3-like

activities during the SI response. Caspase-3-like activities were scored 5 hr. after addition

of the treatments using a caspase-3 FAM-DEVD-FMK FLICA substrate (see Material &

Methods for details).

Figure 5.4 shows that, as expected SI-induced pollen tubes had very high levels of

caspase-3-like activities (97.33 %), whereas untreated pollen tubes had only background

levels of caspase-3-like activities (3.33 %) and were therefore highly significantly different

from SI-induced pollen (***, p=4E^{-10}, Figure 5.4).
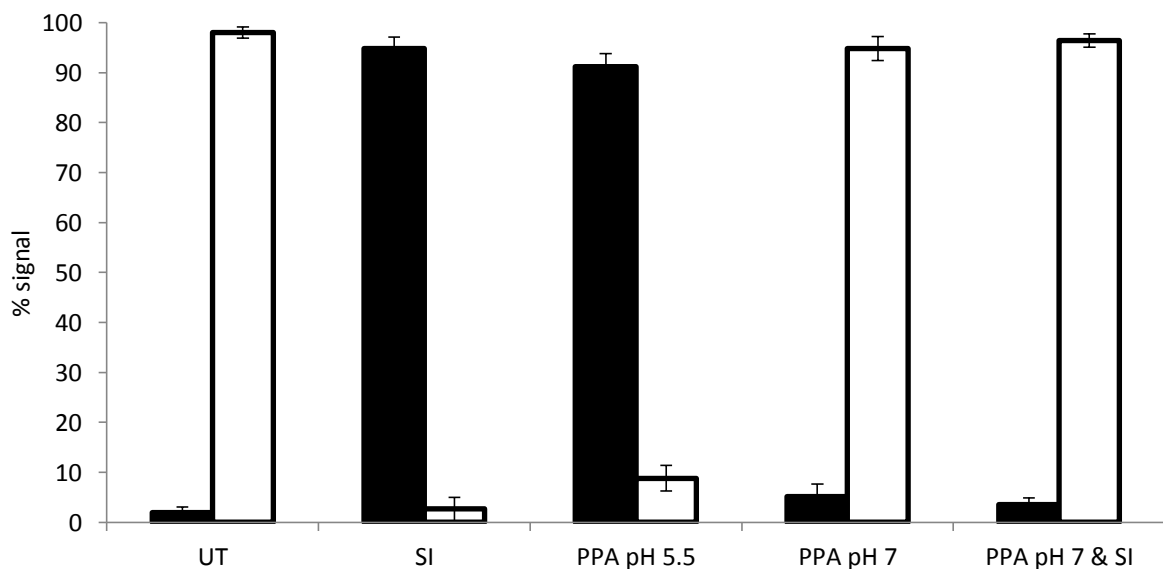
Figure 5.4. Manipulation of pollen tube cytosolic pH can be used to trigger or block caspase-3-like activities

Pollen was pre-grown for 1 hr prior to the addition of treatments; Growth medium (UT), PrsS (SI), 50 mM PPA pH 5.5 (PPA pH 5.5), 50 mM PPA pH 7 (PPA pH 7) and a 10 min pre-treatment with 50 mM PPA pH 7 followed by the addition of PrsS (PPA pH 7 & SI). Pollen was incubated for 5 hr prior to scoring for caspase-like activity using the ImageiT live caspase 3&7 detection Kit (Invitrogen). Fluorescence was counted as a positive for DEVDase (caspase-3-like) activity (black bars) and no fluorescence (no caspase-3-like activity) is shown in the white bars. Each pollen tube was scored for either having caspase-3-like activity or no activity, n=150.

These data confirmed previous reports that SI triggers significant increases in caspase-like

activities (Bosch & Franklin-Tong, 2007). Addition of propionic acid pH 7 only gave 8.00 %

of pollen tubes with caspase-3-like activities, which was not significantly different to untreated cells (N.S, p=0.262, Figure 5.4), and significantly different to SI-induced cells (***, p=4.2E^{-09}, Figure 5.4). The addition of propionic acid pH 5.5, which mimicked SI-induced acidification, resulted in high levels of caspase-3-like activities (87.33 %, Figure 5.4). These levels of caspase-3-like activities were not significantly different to SI-induced caspase-3-like activities (N.S, p= 0.331, Figure 5.4), and were significantly different to untreated and propionic acid pH 7 treated pollen tubes levels (***, p= 1.00 E^{-09} and, ***, p= 8.7 E^{-09} respectively, Figure 5.4). Furthermore, blocking SI-induced acidification by buffering pollen tubes with propionic acid pH 7 prior to SI induction prevented the SI-induced activation of caspase-3-like activity, with only 4.67 % of pollen tubes giving a positive signal (Figure 5.4). These caspase-3-like activities in pollen tubes pre-treated with propionic acid pH 7 , prior to SI induction were significantly different to that of SI-induced cells and those treated with propionic acid pH 5.5 (***, p= 6.00 E^{-10}, and ***, p= 1.6 E^{-09} respectively, Figure 5.4). Moreover, these activities were not significantly different to untreated and propionic acid pH 7 treated cells (N.S, p= 0.380, and N.S, p= 0.578 respectively, Figure 5.4). These data demonstrate that the acidification to ~pH 5.5 is essential for the activation of caspase-3-like activities in *Papaver* pollen tubes. Furthermore, blocking SI-induced acidification prevented caspase-3-like activities, confirming the essential role of pH during caspase activation in SI.

5.2.5 THE ACTIN CYTOSKELETON IS A TARGET OF CYTOSOLIC ACIDIFICATION

The actin cytoskeleton plays an important role in pollen tip growth and is a key target in the *Papaver* SI response (Snowman *et al.,* 2002; Poulter *et al.,* 2008, 2010, 2011; Thomas *et al.,* 2006). Depolymerization of F-actin occurs very rapidly after the induction of the SI response and is therefore implicated in mediating downstream events such as PCD (Thomas *et al.,* 2006). Studies carried out in lily pollen tubes show that actin alterations can be mediated by changes in pH (Lovy-Wheeler *et al.,* 2006). SI-induced depolymerization of F-actin occurs within 2 minutes of the induction. We therefore wondered whether these alterations could be involved in mediating the acidification of the cytosol, which begins within 10 minutes of SI induction, but takes 60 minutes to reach is most acidic point. To investigate whether actin alterations are upstream of the SI-induced acidification, the actin depolymerizing drug Latrunculin B (Lat B), and actin stabilising agent Jasplakinolide (Jasp) were used to alter actin dynamics in *Papaver* pollen

tubes, during which the pH of the cytosol was monitored.
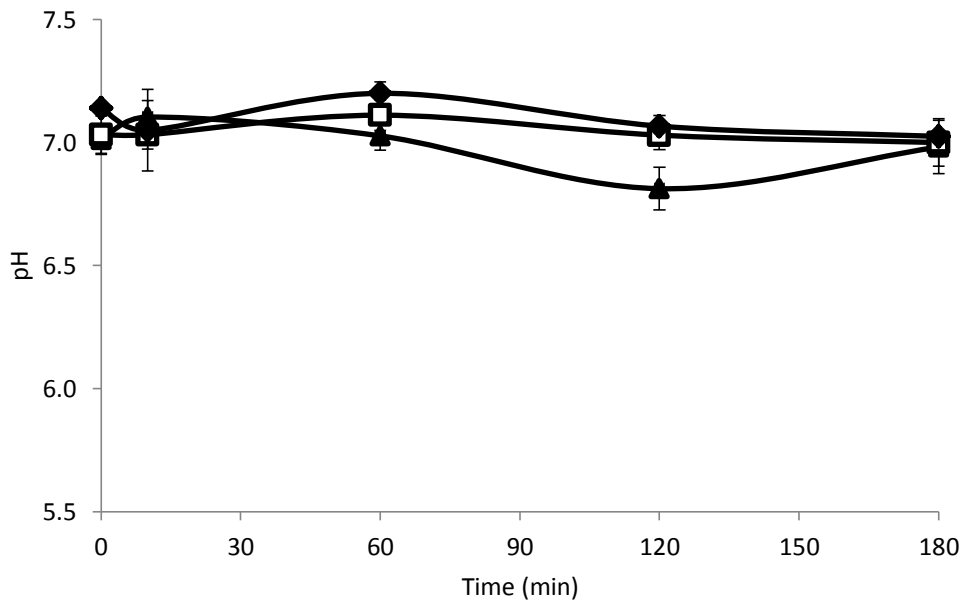
Figure 5.5. Actin alterations are not responsible for SI-induced acidification of the cytosol

Pollen tubes were treated with Latrunculin B (Lat B; solid triangle symbol), an actin depolymerizing agent, Jasplakinolide (Jasp; solid diamond symbol), an F-actin stabiliser or growth medium (untreated, UT; open square symbol), for up to 180 minutes. The pH of treated cells was monitored with the pH indicator BECEF AM at specific time points. N=139 pollen tubes.

As shown in Figure 5.5, neither Lat B nor Jasp treatments resulted in the rapid cytosolic acidification associated with SI response. There was no significant difference in cytosolic pH between Jasp and Lat B treatments compared to untreated pollen tubes (p= 0.212; p= 0.260, respectively, Figure 5.5). These data suggest that neither actin depolymerization nor stabilization is responsible for the acidification of the cytosol in *Papaver* pollen tubes. Therefore, actin alterations could be downstream of SI-induced cytosolic acidification.

We decided to investigate whether SI-induced acidification was upstream of actin alterations. As mentioned above, during the SI response F- actin depolymerizes, another key feature of the SI response is the stabilization of F-actin to actin foci. Actin foci form within 1 hr of SI induction, however after 3 hrs, much larger F-actin foci are evident

161

(Snowman *et al.,* 2002). In order to investigate the relationship between pH alterations and actin foci formation, propionic acid was used to manipulate the cytosolic pH of pollen tubes. Pollen tubes were treated with either 50 mM propionic acid pH 5.5, PrsS to induce SI, growth medium (untreated), 50 mM propionic acid pH 7, or with a 50 mM propionic acid pH 7 pre-treatment followed by the addition of PrsS. After 3 hours incubation with treatment, pollen was fixed and labelled for F-actin (see Materials & Methods). Pollen tubes were scored for actin filaments, foci or intermediates (which have both some filaments and foci in the same cell; Figure 5.6).
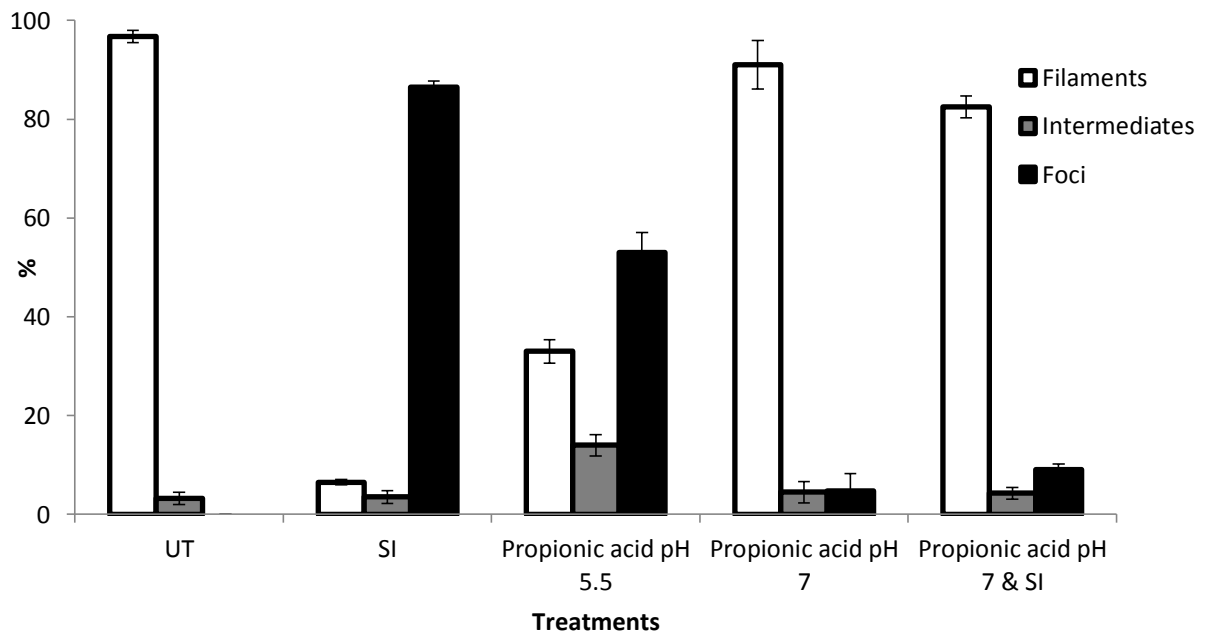
Figure 5.6. Manipulation of cytosolic pH of *Papaver* pollen tubes triggers actin foci formation, in a pH-dependent manner.

Papaver pollen tubes were incubated with 50 mM propionic acid pH 5.5, PrsS and growth medium (untreated, UT) and 50 mM propionic acid pH 7 were used for controls. In addition pollen was pre-treated with 50 mM propionic acid pH 7 for 10 minutes prior to the induction of SI. All pollen was treated for 3 hrs. Pollen was then fixed and labelled with Rh-PH for F-actin visualisation. 50 pollen tubes were scored in each treatment for actin foci, filaments or intermediates using an epi-fluorescent microscope. Data suggest foci form in a pH-dependent manner. N = 2,400.

162

Figure 5.6 shows that both normally growing pollen tubes (UT) and propionic acid pH 7 treated pollen tubes had predominately F-actin filaments (96.75 % & 94.5 % respectively), and very low levels of foci (0.00 % & 4.75 %, respectively). Pollen tubes treated with propionic acid pH 5.5 had high levels of foci (53.00 %, Figure 5.6). These were significantly greater than foci levels in UT pollen (0 %; ***, p= 0.000958) and propionic acid pH 7 treated pollen (4.75 %, ** p=1.412 E^{-03}, Figure 5.6).

SI induced pollen had high levels of actin foci, 86.50 %, similar to those shown in Chapter 3 (Wilkins *et al.,* 2010). However, pollen tubes treated with propionic acid pH 5.5 had lower levels of foci than those of SI induced pollen tubes (***, p= 1.380 E^{-03}, Figure 5.6). This suggests that although acidification of the cytosol triggers a significant amount of actin foci, this may not be the only trigger required for actin foci formation in *Papaver* pollen tubes.

Pollen pre-treated with propionic acid pH 7 followed by addition of PrsS, had highly significantly different levels of actin foci compared to those treated with PrsS (9.00 %, 86.5 %, ***, p= 4.25 E^{-07}, Figure 5.6). Moreover, pollen tubes treated with propionic acid pH 7 and PrsS, had levels of actin foci formation not significantly different to that of pollen treated with just propionic acid pH 7 (N.S, p=0.114, Figure 5.6). However, there was a significant different between the levels of foci formed in propionic acid pH 7 and SI compare to untreated pollen (*, p= 0.01822, Figure 5.6), suggesting there could be a mild response from the addition of propionic acid. Comparisons between untreated pollen and those treated with propionic acid pH 7 show there was a significant difference in actin foci levels between the two treatments (p=0.004017, Figure 5.6), which supports this

idea. These data suggest that blocking the acidification of pollen tubes, prevented pollen tubes from forming actin foci, highlighting the importance of pH alterations during the SI response in *Papaver* pollen tubes. In addition, there was also a significant difference between pollen treated with propionic acid pH 5.5 and pollen treated with propionic acid pH 7 & SI (***, p= 5.99 E^{-04}, Figure 5.6). These data demonstrate that the pH of the cytosol is a major factor required for in actin foci formation, although it is not the only one.

In summary, data presented here show that lowering the cytosolic pH of pollen tubes resulted in a significant increase in actin foci, which are a typical feature of the SI response. Furthermore, the blocking of acidification in SI-induced pollen tubes prevented actin foci formation. This suggests that acidification plays an important role in the formation of actin foci during the SI response in *Papaver* pollen tubes.

5.2.6 CA^{2+} INCREASES ARE UPSTREAM OF CYTOSOLIC ACIDIFICATION

Previous data has shown that almost immediately after the induction of the SI response there are significant increases in $[Ca^{2+}]_{cyt}$ (Franklin-Tong *et al.,* 1993; 1995; 1997). More recent work has shown that SI results in rapid alterations in plasma-membrane conductance(s) with Ca^{2+} influx occurring (Wu *et al.,* 2010). Therefore, it was of interest to test whether acidification of the cytosol was downstream of these Ca^{2+} alterations. In order to investigate this, pollen tubes were treated with the Ca^{2+} ionophore, A23187, and pH of the cytosol was monitored using the pH indicator BECEF AM.

As shown in Figure 5.7, addition of A23187 results in the rapid acidification of the pollen tube cytosol. Comparison with previous data (Figure 5.2A & 5.3) show the acidification

164

observed in A23187-treated pollen tubes is similar to that of SI-induced pollen tubes.

Furthermore, within 30 minutes of treatment there is a significant difference in cytosolic

pH of A23187 treated pollen tubes compared to untreated pollen tubes (*, p=0.043).

Moreover, after 120 minutes of treatment with A23187 there was still a highly significant

difference to untreated pollen tubes of the same time point (***, p= 9.81 E^{-04}). These

data demonstrate that Ca^{2+} increases trigger acidification of the pollen tube cytosol and

therefore are implicated in triggering SI-induced acidification.
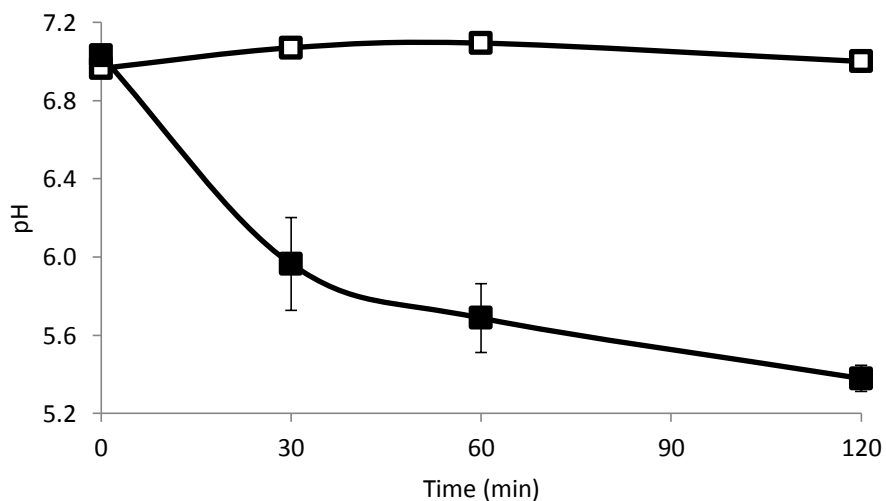
Figure 5.7. Ca^{2+} ionophore A23187 can be used to trigger cytosolic acidification of *Papaver* pollen tubes

Pollen tubes were treated with 50 µM A23187 (A23187; solid symbols) or growth medium (UT; open symbols) and pH was monitored with the pH indicator BECEF AM, as described in methods and materials (Ch. 2). n=52.

165

5.3 DISCUSSION

Previous work has shown that SI-induction in *Papaver* pollen tubes result in caspase-3- & -6-like activities, which peak 5 hours after induction. Furthermore, these caspase-3-like activities require an acidic environment to be functionally active (Bosch and Franklin-Tong, 2007). Many authors have recently reported plant caspase-1, 3 and 6-like activities have a preference for an acidic pH (Korthout *et al.,* 2000; He and Kermode, 2003; Danon *et al.,* 2004; Rotari *et al.,* 2005; Lombardi *et al.,* 2007, Bosch & Franklin-Tong 2007). This has led to the assumption of there must be acidification of the cell to create the acidic environment required for these caspase-like activities. This chapter has investigated the role of pH in *Papaver* SI in some depth. Here we have established the temporal patterns of SI-induced acidification and shown that artificial acidification of pollen tubes can be induced with the weak acid propionic acid. Using this approach we have shown that artificial acidification of pollen tubes resulted in the formation of punctate actin foci, a typical hallmark of *Papaver* SI, and the induction of caspase-3-like activities. Moreover, SI-induced acidification is mediated by increases in cytosolic Ca^{2+}. These data demonstrate that acidification of the cytosol is a key event in *Papaver* SI response and one which is necessary for these key downstream events.

5.3.1 SI-INDUCED ACIDIFICATION OF *PAPAVER* POLLEN TUBES

In *Papaver* pollen tubes SI-induced acidification of the cytosol was rapid, with no recovery. As mentioned, SI-induced acidification of pollen tubes had been previously revealed by Bosch & Franklin-Tong (2007), and results presented here support their findings. The new temporal analysis of SI-induced acidification presented here show that

acidification begins within 10 minutes of SI induction and after one hour the pollen has already reached it most acidic point, ~pH 5.5. This pH change is extremely acidic. During mammalian apoptosis cytosolic acidification is a common early event, in which a typical acidification can range from 0.3 to 1.4 pH units (Matsuyama and Reed, 2000; Nilsson et al., 2006; Nilsson et al., 2004; Thangaraju et al., 1999a; Thangaraju et al., 1999b). In comparison, SI-induced acidification is very near the extreme end of mammalian acidification, which occurs during TNF-α induced apoptosis in U937 cells. This extreme acidification has been associated with caspase-3 & 8 activities (Nilsson *et al.,* 2006), which were also shown to be induced in acidified *Papaver* pollen tubes.

In mammalian cells, acidification has major links with apoptosis. The activation of some endonucleases, which are known to be involved in DNA fragmentation during apoptosis, are believed to require intracellular acidification for their activity (Goossens et al., 2000). During ionomycin-induced apoptosis and the inhibition of protein isoprenylation lovastatin in HL-60 cells, which also results in apoptosis, there was a correlation between DNase II activity and acidification (Barry and Eastman, 1992; Pérez-Sala et al., 1995). Moreover, the activation of the Na^+/H^+ antiporter induced an increase in pH which was sufficient to prevent or arrest DNA digestion and therefore apoptosis. This suggests that intracellular acidification during apoptosis has a role in triggering DNA fragmentation, and intracellular acidification maybe due to alterations in channel activities in mammalian apoptosis. At present DNA fragmentation has not been investigated in response to acidification in *Papaver* pollen tubes. However as discussed in Chapter 1, significant DNA fragmentation does occur in SI-induced pollen tube, and therefore acidification of the cytosol could also play a role in this event.

In drug induced apoptosis in Jurkat T-lymphoblasts and Chinese hamster ovary (CHO) cells the overexpression of the proto-oncogene *B-cell lymphoma 2 (Bcl-2),* which prolongs cell survival and suppresses apoptosis, attenuates acidification and prevents cell death (Meisenholder et al., 1996; Palissot et al., 1998; Reynolds et al., 1996; Simon et al., 1994). This suggests that proto-oncogene maybe responsible for preventing acidification in healthy cells. In addition, in breast tumour cells, apoptosis induced by staurosporine treatments, is associated with intracellular acidification. This acidification was prevented with the pan-caspase inhibitor zVAD-FMK or by expression of Bcl-2 (Wolf and Eastman, 1999). Furthermore, zVAD-FMK treatment showed a concentration-dependent protection from PARP (poly-ADP ribose polymerase) cleavage and DNA digestion and early changes in membrane permeability (Wolf *et al.,* 1997). These data suggest that intracellular acidification is a key process in apoptosis in mammalian cells and is involved in the regulation of DNA fragmentation, via endonuclease, however these data suggest that acidification could be both upstream and downstream of specific caspase activities in mammalian apoptosis.

Changes in intracellular pH are reported during developmental events in plants, such as root tip growth (Feijo et al., 1999; Gibbon and Kropf, 1994; Robson et al., 1996), as previously discussed. In plants PCD-associated acidification has not been widely reported, however it is assumed to occur in many developmental events where PCD plays a role (Bollhöner et al., 2012; Fukuda, 2000; Morimoto and Shimmen, 2008). One of the few studies to monitor pH alterations during PCD in plants is a recent study by Young *et al.,* (2010), who used the mammalian pro-apoptotic gene BAX to induce PCD in onion epidermal cells. The pH of PCD-induced onion epidermal cells, and cells undergoing

tracheary element (TE) differentiation in Arabidopsis, was monitored by measuring the loss of fluorescence of the pH-sensitive YFP probe (Young et al., 2010a). Results suggested BAX induces acidification and PCD in onion cells. Unfortunately this method did not quantify the acidification in terms of pH units, and cells were only measured 30 minutes after they were bombarded with the YPF probe. However, as there was a loss of fluorescence in both cell types and treatments, this suggested that acidification occurred in these systems.

In plant cells acidification has also been linked to plant defence. In barley coleoptile cells a decline in cytoplasmic pH has been associated with an increased resistance to the pathogenic fungus *B. graminis* (Yamaoka *et al.,* 2000). *Nitellopsis obtusa* cells treated with salt are one of the few examples in which acidification of the cytosol has been measured and has been shown to play a role in cell death (Katsuhara *et al.,* 1989). The cytoplasmic pH dropped from pH 7.2 to pH 7.0, furthermore there was an alkalization of the vacuole of 0.3 pH units after one hour exposure to salt stress. The authors suggest this feature of salt stress could be due to the inhibition of H^+-pumps on the vacuolar membrane (tonoplast). Data suggested a PPi-dependent H^+ pump is probably inhibited by the changes in ion distribution is induced by the salt treatment.

This is clearly an area for further future investigation, as there are currently only a few examples of cytosolic acidification in plant cells make it difficult to interrupt the role of acidification in plant development and defence.

5.3.2 ROLE OF ACIDIFICATION IN PCD

5.3.2.1 ACTIVATION OF CASPASE-LIKE ACTIVITIES

As discussed in Chapter 1, a key example of caspase-like activity in plants is Vacuolar

Processing Enzyme (VPE), which has caspase-1/YVADase-like activities. VPE is essential for

a viruS-induced hypersensitive response that involves PCD (Hatsugai *et al.,* 2004) and the

maturation of seed storage proteins (Hara-Nishimura *et al.,* 2000). During these

processes it is known that VPE is self-catalytic, activated from their inactive precursors.

Furthermore it has been postulated that this activation occurs in the acidic environment

of the vacuole. A common feature of VPE-cell death is the disruption of the tonoplast,

and it has been suggested that the release of VPE during this rupture leads to the

processing of cytosolic material and is therefore involved in PCD execution (Sanmartín *et

al.,* 2005). This is similar to animals cell cathepsins, which are lysosomal proteases, which

are released from damaged lysosomes, resulting in the activation of caspase cascades in

the cytosol, triggering apoptosis (Ferri and Kroemer, 2001; Rojo et al., 2004). VPE has

been identified in *Papaver* pollen tubes, however its activity does not increase during the

SI response, suggesting it does not play a role in this type of PCD. Despite this it was

shown that VPE does require an acidic environment to be functionally active (Bosch et al.,

2010).

In mammalian cells there are data that suggest there is a link between caspase activation

and acidification during mammalian apoptosis. In Michigan Cancer Foundation – 7 (MCF-

7) breast cancer cells, apoptosis induction via treatment with somatostatin (SST) leads to

caspase-8/IETDase -mediated acidification (Liu *et al.,* 2000), and the prevention of

acidification by pH clamping inhibited its ability to induce apoptosis (Sharma and Srikant, 1998; Thangaraju et al., 1999a).

Data presented in this chapter, suggest that acidification is important for SI-induced caspase-3-like activation. Artificial acidification of *Papaver* pollen tubes with propionic acid pH 5.5 led to similar levels of caspase-like activities to SI-induced cells. Moreover acidification was prevented in pollen pre-treated with propionic acid pH 7 prior to SI induction, which prevented SI-induced caspase-3-like activities. These data suggest they require an acidic pH for activation, similar to mammalian caspases and the caspase-like activities in plants, despite the absence of mammalian caspase genes in plant genome, pH is of great importance to caspase activity.

5.3.2.2 ACIDIFICATION TRIGGERS FORMATION OF ACTIN FOCI

As previously mentioned, during the SI response the actin and microtubule cytoskeleton undergoes major alterations (Poulter et al., 2011; Poulter et al., 2010; Poulter et al., 2008; Thomas et al., 2006). This includes the depolymerization of F-actin filaments, followed by stabilization to form actin foci. Actin depolymerization occurs within 2 min of SI induction and is therefore implicated in early signalling events, and has been shown to be involved in triggering PCD in *Papaver* pollen (Thomas *et al.,* 2006). Data presented here show that artificial acidification of the pollen tube cytosol with propionic acid triggered actin foci formation, moreover blocking SI-induced acidification with propionic acid pH 7 prevented SI-induced actin foci formation. These data suggest that cytosolic acidification is upstream of SI-induced actin alterations and plays an important role in modulating the formation of actin foci in *Papaver* pollen tubes.

171

In lily pollen tubes it has also been shown that pH plays a role in mediating the actin cytoskeleton. Lovy-Wheeler *et al.,* (2006) showed artificial acidification of the cytosol by 1 pH unit for 30s was sufficient to trigger the breakdown of actin bundles, the loss of the apical actin fringe, which localize with the alkaline band, and inhibit pollen tube growth. However, actin foci were not seen in lily pollen tubes acidified to pH 6, suggesting that perhaps a more acidic pH is required for actin foci formation, but mild acidification maybe responsible for increased actin depolymerization. As the actin cytoskeleton in *Papaver* pollen tubes was not imaged during the early stages of artificial acidification, this is perhaps something to investigate further in the future, as a mild acidification, for example to pH 6.5, maybe responsible for the initial depolymerization of actin filaments during the SI response.

Structures which appear to be similar to actin foci have been identified in mammalian and yeast cells, although at present this has yet to be confirmed. In yeast, actin patches (bundles of F-actin) are associated with endocytosis (Young *et al.,* 2004), during periods of starvation yeast form actin bodies which are thought to be a reserve of actin that can be immediately mobilized for actin cables and patches formation upon re-entry into a proliferation cycle (Sagot *et al.,* 2006). In animal and Dictyostelium cells Hirano bodies are formed during stress or disease events (Hirano, 1994; Maselli et al., 2002). As yet, little is known how these actin structures are formed or regulated, and present it is not known if pH plays a role in regulating these structures.

An acidic environment could play a role in triggering a change in activity of specific actin-binding proteins such as ADF/cofilin which manipulate the organization of the

cytoskeleton (Allwood, 2002; Bernstein et al., 2000; Carlier et al., 1997; Gungabissoon et al., 1998; Yonezawa et al., 1987). Hawkins *et al.,* (1993) showed that the human actin binding protein, actin depolymerizing factor (ADF), is pH-sensitive. At pH 8 ADF bound G-actin therefore preventing actin polymerization. However, at a pH below pH 7 ADF binds F-actin. Similar results were found in mouse fibroblasts (Swiss 3T3 cells)(Bernstein *et al.,* 2000). Lowering intracellular pH resulted in the co-localization of ADF with actin filaments, and when the pH was increased, ADF resumed it depolymerizing role and partitioned more with monomeric actin. Furthermore, in maize cells, Gungabissoon *et al.,* (1998) showed that under alkaline environment (pH 9.0) ADF show a greater ability to depolymerize F-actin, however under acidic conditions (pH 6.0) filaments were adorned with ZmADF3. pH-sensitive ADF is of significant interest to understanding SI-induced events. Poulter *et al.,* (2010), has shown that within 10 minutes of induction of the SI response in *Papaver* pollen tubes there was significant co-localization of ADF with highly polymerized F-actin foci. Data presented in this chapter show that within 10 minutes of SI response the cells have already acidified to pH 6.4, and pH 6.0 within 30 minutes. In maize cells pH 6 was sufficient to induce co-localisation of ADF and F-actin bundles, therefore suggesting that SI-induced acidification may play a role in triggering the association of ADF with *Papaver* actin foci. Therefore these data suggest that alterations in cytosolic pH in both plant and mammalian cells, during stress responses, may be used to regulate the actin cytoskeleton, suggesting a similar mechanism maybe conserved.

At present the role of acidification on ABPs has not been investigated during the SI response and further studies on this topic in the future may help us to understand how actin foci form and their role in the SI response in *Papaver* pollen tubes.

173

5.3.3 SOURCES AND MEDIATORS OF SI-INDUCED ACIDIFICATION

Although we have shown that SI-induced acidification plays an important role in the activation of caspase-3-like activities and the formation on punctate actin foci, at present we do not know the source of acidification. Potential sources of SI-induced acidification could be (i) extracellular; through the influx of protons from external media, through the pollen tube plasma membrane or alterations in channel activities (ii) or intracellular through the leakage of an acidic organelle. Research has found that increases in Ca^{2+} (A23187) can trigger acidification of *Papaver* pollen tubes and therefore role of Ca^{2+} in SI-induced acidification and other potential sources of protons will be discussed further in this section.

5.3.3.1 CALCIUM

Increases in Ca^{2+} are a significant early event in SI-induced pollen tubes, major increases occur almost instantaneously during an SI response (Franklin-Tong et al., 1997; Franklin-Tong et al., 2002). Increases in Ca^{2+} have been linked to actin alteration and PCD in *Papaver* pollen tubes. Ca^{2+} increases induced by A23187, resulted in the rapid acidification of the cytosol, suggesting that acidification of the cytosol could be downstream of Ca^{2+} signals. Studies in soylipid lipsome have shown that the addition of a Ca^{2+} ionophore resulted in an increase in proton influx (Jyothi *et al.,* 1994). Moreover, in rat aortic vascular smooth muscle cells, treatments with agonists that increase Ca^{2+} trigger intracellular acidification as a result of Ca^{2+}/H^{+} exchange across the plasma membrane (Daugirdas *et al.,* 1995).

Several studies in mammalian cell have suggested there could be a feedback loop between H^+ and Ca^{2+} in signalling pathways. For example, in DAOY medulloblastoma cells, extracellular acidification triggers Ca^{2+} release from Ca^{2+} stores via a Phospholipase C-Sensitive Pathway (Huang *et al.,* 2008). Moreover, in human airway smooth muscle cells (ASMCs), extracellular acidification stimulates IL-6 production and Ca^{2+} mobilization through proton sensing OGR1 receptors (Ichimonji *et al.,* 2010). Unfortunately in studies presented here it was difficult to monitor pH alterations within the first 10 minutes of SI induction, and therefore we are unable to determine exactly how fast acidification occurs beyond the 10 minute time point. Ideally we would artificially trigger pH changes and monitor Ca^{2+} levels in the pollen tube, to investigate whether there is a feedback loop between increases in $[Ca^{2+}]_{cyt}$ and intracellular acidification during the SI response. However, at present we were unable to perform these studies during this thesis and this may be the focus of future studies, in order to further our understanding of the mechanisms involved in triggering cytosolic acidification.

5.3.3.2 PROTON PUMPS AND ALTERATIONS IN CHANNEL ACTIVITIES MAY PLAY A ROLE IN SI-INDUCED ACIDIFICATION

As discussed, results presented here show Ca^{2+} influx is upstream in SI-induced acidification. In animal cells, Ca^{2+}-mediated acidification has been linked to alterations in Ca^{2+}/H^+ exchange across the plasma membrane, which results in the increase in protons in the cytosol (Daugirdas *et al.,* 1995). These data suggest that acidification in animal cells may be due to the movement of external protons into the cytosol. The external growth

medium in which the *Papaver* pollen tubes are grown is ~pH 5.5, therefore this could be a potential source of protons during SI-induced cytosolic acidification. Furthermore, this would suggest that there could be alterations to plasma membrane integrity and/or alterations in the channel activity during this response. Research carried out by Wu *et al.,* (2010) has already shown that during *Papaver* SI response there are alterations in plasma-membrane conductance(s) in an *S*-specific manner. Furthermore, they suggested that SI-induced conductance(s) may be a non-specific cation channel (NSCC). They showed that both monovalent cations and divalent cations Ba^{2+}, Ca^{2+}, Mg^{2+} and NH_4^+ are involved in SI. However H^+ was not tested. This work added to the growing evidence suggesting that PrpS might act as an ion channel, and supports the idea that channel activity could be responsible for the rapid acidification we have monitored.

Although we have not identified the source of protons responsible for the acidification of the cytosol in SI, some studied have been carried out in guard cells to begin to identify the source of protons in their system. Stomatal closure is associated with alterations in cytosolic pH. Acidification of the cytosol coincided with changes in membrane potential, which were thought to play a role in determining the direction and capacity of ion transport in subsidiary cells (Grabov and Blatt, 1997; Chen, 2001; Wang *et al.,* 2001; Mumm *et al.,* 2011). In addition, during plant-pathogen defence the cytosol of infected host cells undergo cytoplasmic acidification, and alkalinization of the apoplast, via an influx of external protons (Lapous *et al.,* 1998; He *et al.,* 1998; Mathieu *et al.,* 1991; Kuchitsu *et al.,* 1997; Mathieu *et al.,* 1996; Roos *et al.,* 1998). Furthermore, the inhibition of proton pump triggers rapid cell death in tumour cells, due to the resulting intracellular acidification, caspase activation and early accumulation of reactive oxygen species (Fais,

2010). These examples suggest that alterations in membrane potential and channel activities could be responsible for both developmental and stresS-induced cytosolic acidification, and therefore such alterations could also play a role in SI-induced acidification. Therefore future studies should investigate further the role of SI-induced channel activities and membrane potentials to help identify the source of protons during this response.

However, the movement of protons from the extracellular sources is not the only source of protons during cytoplasmic acidification. In elicitor-treated California poppies (*Eschscholtzia californica)* cells, cytoplasmic acidification was frequently observed (Roos *et al.,* 1998). During this reaction lysophosphatidylcholine (LPC) was generated by phospholipase A_2 at the plasma membrane, which lead to the activation of a tonoplast H^+/Na^+ antiporter and a transient increase of the vacuolar pH (Viehweger *et al.,* 2002). Furthermore, in many plants during elicitation of the hypersensitive response there is an influx of H^+ from the apoplast into the cytosol (Roos et al., 2006).

Another mechanism potentially involved in SI-induced acidification is the activation of protein kinases. Pathogen-induced cytosolic acidification in tobacco cells was prevented by treatment with protein kinase inhibitors (Mathieu *et al.,* 1996). These results suggested that proton influx could be preceded and controlled by protein phosphorylation-dephosphorylation. During *Papaver* SI the MAPK p56 is activated within 10 minutes of SI induction (Rudd *et al.,* 2003). However, as SI-induced acidification is already in progress within 10 minutes of SI induction it suggests that the activation of p56 may not play a role in SI-induced cytosolic acidification.

177

5.3.3.3 ORGANELLES AS A POTENTIAL SOURCE OF PROTONS

5.3.3.3.1 MITOCHONDRIA

Mitochondria play a significant role in apoptosis by releasing caspase activators, including cytochrome C. Furthermore research has shown that mitochondrial fragmentation leads to intracellular acidification in *Caenorhabditis elegans* and mammalian cells (Johnson and Nehrke, 2010). It has been suggested that mitochondrial fragmentation may cause acidification through two separate processes: oxidative signalling and lactic acidosis.

Drug-induced apoptosis in tumour cells resulted in intracellular acidification triggered by mitochondrial-derived hydrogen peroxide (Hirpara *et al.,* 2001). Furthermore, it is though that hydrogen peroxide triggered this acidification through the translocation of Bax to the mitochondria which is involved in triggering mitochondrial alkalinization, leading to the acidification of the cytosol. Moreover, this acidification lead to the release of cytochrome c release, caspase activation and mitochondrial swelling and depolarization (Ahmad et al., 2004; Matsuyama and Reed, 2000). As the activation of mammalian caspases by cytochrome C *in vitro* is minimal at neutral pH, but maximal at acidic pH, this suggests that mitochondria-induced acidification of the cytosol may be important for caspase activation.

As previously discussed in Chapter 1, cytochrome c leakage from the mitochondria into the cytosol is detected as early as 10 minutes after SI induction in *Papaver* pollen tubes, suggesting within 10 minutes the mitochondria membrane integrity is compromised (Thomas and Franklin-Tong. 2004). Furthermore, within 1 h of SI induction there were significant alterations in the morphology of mitochondria, including swelling and blebbing

(Bosch and Franklin-Tong, 2008; Geitmann et al., 2004a; Geitmann et al., 2004b). Within 10 minutes of SI-induction some cytosolic acidification has occurred, therefore protons may be leaking from the mitochondria into to the cytosol contributing to cytosolic acidification during the SI response. Moreover, data presented in Chapter 3 & 4 also suggested the role of ROS during SI-induced cell death. During live cell imaging of ROS signals in SI-induced pollen tubes, ROS signal localised with organelles that resembled mitochondria. These data implicate the role of the mitochondria in alterations both ROS and cytosolic acidification, and therefore should be investigated further in the future.

5.3.3.3.2 VACUOLE

As discussed in Chapter 1, the vacuole plays and important role in plant PCD. The rupture of the acidic vacuole is associated with cell death in many systems and is important in many developmental events, such as xylem differentiation (Fukuda, 2000; Obara et al., 2001). Furthermore, the rupture of the acidic vacuole may also play a role in cytosolic acidification and therefore is of significant interest during SI-induced events. This prompted studies to investigate the role of the vacuole during the SI response, and will be discussed in more detail in Chapter 6 to prevent repetition.

5.3.4 SUMMARY & MODEL

Data presented in this chapter characterised SI-induced acidification in *Papaver* pollen tubes. Figure 5.8 shows a model of SI-induced events in *Papaver* rhoeas pollen incorporating previously published data and new data presented in this chapter. Interaction between the secreted stigmatic protein, *Papaver* rhoeas stigmatic S (PrsS), with *Papaver* rhoeas pollen S (PrpS), pollen receptor in a S haplotype-specific manner,

such as PrsS$_1$ binds to PrpS$_1$, results in an incompatible reaction which triggers a rapid

signalling cascade in *Papaver* pollen (Figure 5.8). SI triggers an almost instantaneous

alterations in channel activities and a significant increase in cytosolic Ca^{2+} (Franklin-Tong

et al., 1997; Franklin-Tong et al., 2002; Wu et al., 2011). Data presented in this chapter

has shown that both SI and increases in cytosolic Ca^{2+} triggering acidification of the

cytosol within 10 minutes of SI induction, and reaching it most acidic point, pH 5.5 within

60 minutes. Furthermore, during this chapter propionic acid has been used to manipulate

the pH of the pollen tube to investigate the relationship between pH and caspase-like

activities and actin alterations. Artificial acidification of the cytosol triggered both

caspase-like activities and actin foci formation (Figure 5.8). Moreover, blocking SI-induced

acidification prevented both caspase-3-like activities and actin foci formation. These data

suggest that acidification of the cytosol is essential for both caspase-3-like activities and

actin foci formation and therefore plays a significant role in SI events (Figure 5.8).

Furthermore, previous research has shown that caspase-3/DEVDase-like activities that

translocate to the nucleus are involved in DNA fragmentation (Bosch and Franklin-Tong,

2007; Bosch et al., 2008). Therefore, as discussed acidification of the cytosol may also

play a role in triggering other SI-induced events such as DNA fragmentation resulting in

programmed cell death (PCD) (Rudd and Franklin-Tong, 2003; Rudd et al., 2003), and this

is something that should be investigated in the future to full understand this significance

of Si-induced acidification. As mentioned at present we do not know the source of

protons responsible for SI-induced acidification although several potential sources have

been identified, the mitochondria and vacuole, which are also included in this model

(Figure 5.8).
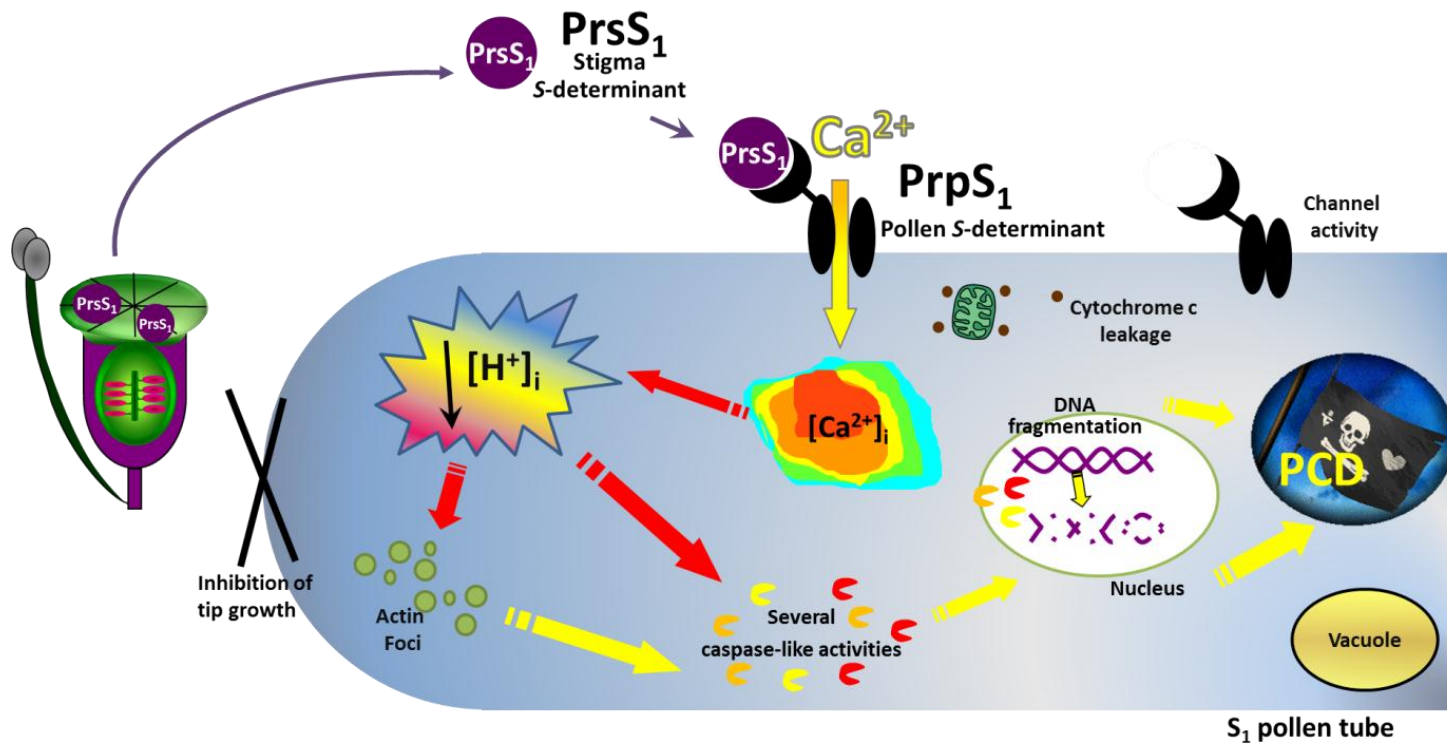
Figure 5.8. Model of the role of SI-induced acidification in *Papaver* pollen tubes

A proposed model for the self-incompatibility mechanism in *Papaver rhoeas* highlighting data present in this chapter (indicated by red arrows). During an incompatible interaction secreted stigmatic protein, *Papaver rhoeas* stigmatic S (PrsS), interacts with *Papaver rhoeas pollen* S (PrpS), pollen receptor in a S haplotype-specific manner, such as $PrsS_1$ binds to $PrpS_1$. This incompatible interaction triggers a rapid influx of Ca^{2+}, which induces a signalling cascade, resulting in the inhibition of tip growth. Increases in Ca^{2+} trigger dramatic alterations in the actin cytoskeleton, including the depolymerization of F-actin, which is later followed by stabilisation of F-actin into actin foci. Furthermore, increases in Ca^{2+} trigger rapid acidification of the cytosol which is also associated with actin foci formation. In addition acidification of the cytosol is also essential for caspase-3-like activities which are known to translocate to the nucleus where DNA fragmentation occurs resulting in programmed cell death (PCD), ensuring the incompatible pollen does not start to grow again. Moreover, there are alterations in channel activity and alterations in mitochondria, both of which may be a potential source of protons responsible for SI-induced acidification of the cytosol. Furthermore, the vacuole may also be a source of protons (which is investigated in Chapter 6).

181

As mentioned both organelles are suspected to play a role in SI-induced acidification and are therefore of significant interest for future studies; particularly the vacuole. The vacuole is a very acidic organelle which has been implicated in several forms of PCD in plants cells. Therefore, we decided to investigate the role of the vacuole during the SI response. Data is presented in Chapter 6.

CHAPTER 6: INVESTIGATING THE VACUOLE AS A POTENTIAL SOURCE OF SI INDUCED ACIDIFICATION

6.1 INTRODUCTION

Chapter Five showed that during the SI response there was rapid acidification of the cytosol in *Papaver* pollen tubes. Acidification was observed as early as 10 minutes after SI induction, and continued to acidify for approximately an hour, when it reached its lowest intracellular pH, ~pH 5.5. Weak acids were used to manipulate the cytosolic pH of the pollen tube and demonstrate that acidification was sufficient to induce actin foci formation and an increase in a DEVDase/caspase-3-like activities. These data demonstrated that SI-induced acidification is an important phenomenon during SI events. One potential source of protons in *Papaver* pollen tubes is the acidic compartment; the vacuole. As discussed in the introduction chapter, the vacuole plays an important role in maintaining the homeostasis of healthy plant cells. During salt stress the vacuole plays a vital role in compartmentalizing excess Na^{2+} and H^{+} ions, through the regulating the expression and activity of Na^{+} transporters and H^{+} pumps, which generate the driving force for transport on ions across the tonoplast (Zhu, 2003). However, as discussed in introduction chapter, the vacuole also plays a major role in plant cell death (Hatsugai and Hara-Nishimura, 2010). The collapse of the vacuole and the release of the hydrolytic enzymes, which are usually involved in the degradation of unwanted particles and nutrient recycling, through pathways such as autophagy (Hanaoka et al., 2002), have been shown to play a key role in PCD many different species. Examples include developmental events such as senescence and suspensor degeneration (Gahan *et al.,* 1982; Obara *et al.,* 2001; Filonova *et al.,* 2002). Moreover, during *Lathyrus undulatus* PCD of the tapetum, a nutritive tissue within the anther, the breakdown of the tonoplast lead to the collapse of the vacuole, releasing hydrolytic enzymes resulting in the degradation

184

of cell components (Vardar and Unal, 2012). Furthermore, vacuolar rupture is also a key feature of treachery element (TE) differentiation, which involves the breakdown of cells in order to create xylem systems to transport water (Obara et al., 2001). Moreover, there is evidence that nuclear degradation occurs immediately after the collapse of the vacuole in *Zinna* TE differentiation, and it has been suggested this may be due to the release of vacuolar hydrolytic enzymes, therefore suggesting the vacuole plays a major role in this type or PCD (Obara 2001; Rotari *et al.,* 2005).

During SI-induced PCD there is rapid acidification of the cytosol, currently there is limited documentation of PCD-induced acidification in other types of plant cells, although this process is presumed to occur in many types of plant PCD, as discussed in Chapter Five (Bollhöner et al., 2012, Fukuda, 2000, Morimoto and Shimmen, 2008). Where acidification occurs during PCD there is often an association with the vacuole, as shown by Katsuhara et al., (1989). During their investigation of salt stress in *Nitellopsis obtusa* cells they found that the cytoplasmic pH dropped from pH 7.2 to pH 7.0 was coupled with an increase in pH in the vacuole, suggested salt stress maybe result in the inhibition of a H^+-pumps on the vacuolar membrane (tonoplast) resulting in a loss of protons in to the cytosol. Moreover, in elicitor-treated cells of Californian poppy, cytosolic acidification correlated with a shift in the pH in the vacuole, suggesting there is movement of proton between the cytosol and the vacuole (Roos et al., 1998). These examples implicate the vacuole as a potential source of protons during plant PCD-induced acidification events.

Furthermore, another key feature of the elicitor triggered HR which also occurs during in the SI response are increases in $[Ca^{2+}]_{cyt}$ (Franklin-Tong et al., 1997; Jordan et al., 2000;

Wilkins et al., 2011). During the hypersensitive response of tobacco to *Pseudomonas syringae pv syringae*, increases in Ca^{2+} have been shown to mediate intracellular acidification, and a net uptake of H^+ from the extracellular medium (Atkinson *et al.,* 1985, 1990; Baker *et al.,* 1987). As mentioned earlier this acidification maybe due to the rupture of the vacuole and therefore could be mediated by a Ca^{2+} signal.

As discussed in the introduction chapter, the cytoskeleton plays an important role in SI-induced PCD (Bosch et al., 2008; Poulter et al., 2011; Poulter et al., 2008; Thomas et al., 2006). In Tobacco BY-2 cells and various Arabidopsis cells, there is evidence that the cytoskeleton plays an important role in vacuole morphogenesis (Higaki et al., 2006; Kutsuna and Hasezawa, 2002; Mathur et al., 2003). The artificial disruption of F-actin bundles by the application of actin polymerization inhibitors facilitated the disintegration of the bulb-like vacuolar structures and the formation of smaller vacuolar compartments (Higaki et al., 2006; Sheahan et al., 2007). Furthermore, in *Physcomitrella patens* (Moss), the depolymerization of microtubules dramatically affected the structure and movement of vacuoles (Oda et al., 2009b). In addition, pharmacological experiments have shown that actin and microtubules are essential for vacuolar membrane maintenance and nuclear positioning in synchronized tobacco BY-2 cells(Kutsuna and Hasezawa, 2002). Although there is evidence for the role of the cytoskeleton in organelle organization, to date, little is known about the relationship between the cytoskeleton and vacuole during plant PCD, mainly because vacuolar structures are easily disrupted by chemical fixation (Wilson 1990) and little is known about the mechanics of vacuolar rupture. Despite this work carried out by Higaki *et al.,* (2007) showed that during the PCD in Tobacco BY-2 cells, vacuolar reorganization is associated with the actin cytoskeleton. The inhibition of

actin polymerization facilitate the disappearance of bulb-like vacuolar membrane structures and induction of cell death (Higaki et al., 2007). Thus, as the cytoskeleton has a key role in SI, it could also be involved in the maintenance and potential breakdown of the vacuole, which could lead to acidification of the cytosol during the SI response in *Papaver* pollen tubes.

In this chapter, the role of the vacuole in the SI response has been investigated. As discussed the vacuole is a very acidic organelle and vacuolar rupture is a key feature in many PCD systems (Hatsugai *et al.,* 2004; Higaki *et al.,* 2011). Furthermore, as shown in chapter 5 during SI-PCD there is rapid acidification of the cytosol, suggesting that perhaps vacuolar rupture might also play a role in the acidification observed during SI, and therefore play a role in the induction of PCD. Briefly, the studies included in this chapter documented the spatial and temporal reorganization and disintegration of the vacuole in SI-induced pollen. Furthermore, possible triggers for vacuolar breakdown were investigated, identifying increases in intracellular Ca^{2+} as an upstream mediator of vacuolar reorganization and breakdown. However, alterations in actin cytoskeleton triggered reorganization of the vacuole but not breakdown. Artificial acidification of pollen tube cytosol triggered the reorganization and disintegration of the vacuole, but blocking SI-induced acidification prevented vacuolar breakdown, suggesting acidification itself may trigger breakdown of the vacuole.

6.2 RESULTS

6.2.1 VISUALIZATION OF THE VACUOLE IN *PAPAVER* POLLEN TUBES

Untreated *Papaver rhoeas* pollen tubes were labelled with the vacuolar marker carboxy-DCFDA (carboxy-5-(and-6)-carboxy-2',7'-dichlorofluorescein diacetate) (Figure 6.A). The pollen vacuole shows a reticulate structure predominately in the shank of the pollen tube, which appears to be absent from the very tip of the pollen tube. To be confident carboxy-DCFDA was visualising the vacuole, a vacuolar membrane marker, δ-TIP-GFP (Hicks et al., 2004), was also utilized (Figure 6.1B). δ-TIP-GFP gave a slightly different signal to that of carboxy-DCFDA , displaying a much "thinner" labelling, as expected with a membrane marker, but it showed a similar reticulate pattern similar to c-DCFDA, (Figure 6.B). Thus, we can be confident that c-DCFDA is reporting the vacuole in these pollen tubes.
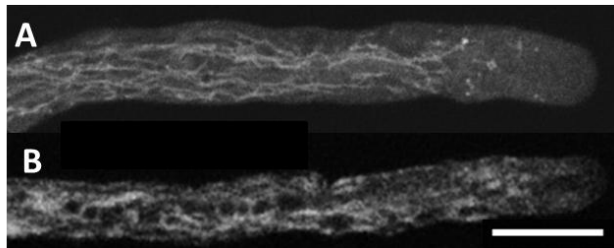
Figure 6.1. Visualisation of vacuole in *Papaver* pollen tubes

A. Untreated pollen labelled with c-DCFDA vacuolar marker. B. Untreated pollen tube expressing δ-TIP-GFP, image was taken by Maurice Bosch. Both images show a distinct reticular structure predominately in the area behind the clear zone. Scale bar = 10 µM.

6.2.2 SI STIMULATES RAPID REORGANIZATION AND THE BREAKDOWN OF THE VACUOLE

To investigate whether SI induction stimulated vacuolar alterations in *Papaver* pollen tubes, SI-induced pollen expressing a δ-TIP-GFP construct or labelled with c-DCFDA were imaged. Figure 6.2 shows that prior to SI induction (time=0) pollen tubes had a reticulate structure similar to that in Figure 6.1. SI-induced pollen tubes displayed vacuolar reorganization within 19 minutes, although very small alterations in vacuolar structure were noticeable after 7 minutes of induction (Figure 6.2). As the SI response progressed the vacuolar network appeared to form shorter, more globular compartments and began to lose its typical reticulate structure (Figure 6.2). Within 37 minutes of SI induction, long strands of labelled vacuolar structure appeared to have broken down into shorter bundles of signal. Within 66 minutes of SI, the bundles vacuolar signal had aggregated together into tight pockets with lower levels signal being visible, suggesting the vacuolar signal was being released into the cytosol suggesting the vacuolar compartment was breaking down. After ~80 minutes the vacuole had almost completely broken down and there was very little structure intact, only very small brightly stained bundles of vacuolar material remained (Figure 6.2). Pollen treated with PrsS for 118 minutes showed similar breakdown of vacuolar signal with barely any signal remaining, and the vacuolar staining remained similar thereafter for several hours, certainly up to 4.5 hours (data not shown).

Pollen expressing δ-TIP-GFP was also treated with PrsS to induced SI (Figure 6.2). Untreated pollen (time=0), had a similar vacuolar organization to that of pollen shown in Figure 6.1B, with long reticulate vacuolar structure. After 48 minutes of SI induction, the

189

vacuolar membrane began to aggregate and form small pockets of signal. After 89

minutes of treatment there was very little intack signal remaining, with lots of very small

bundles of signal. Although there is more signal remaining in pollen expressing δ-TIP-GFP

than c-DCFDA after SI induction, both sets of images suggest that the reorganization and

breakdown of the vacuolar compartment occur.

C-DCFDA labeled

δ-TIP-GFP expressing
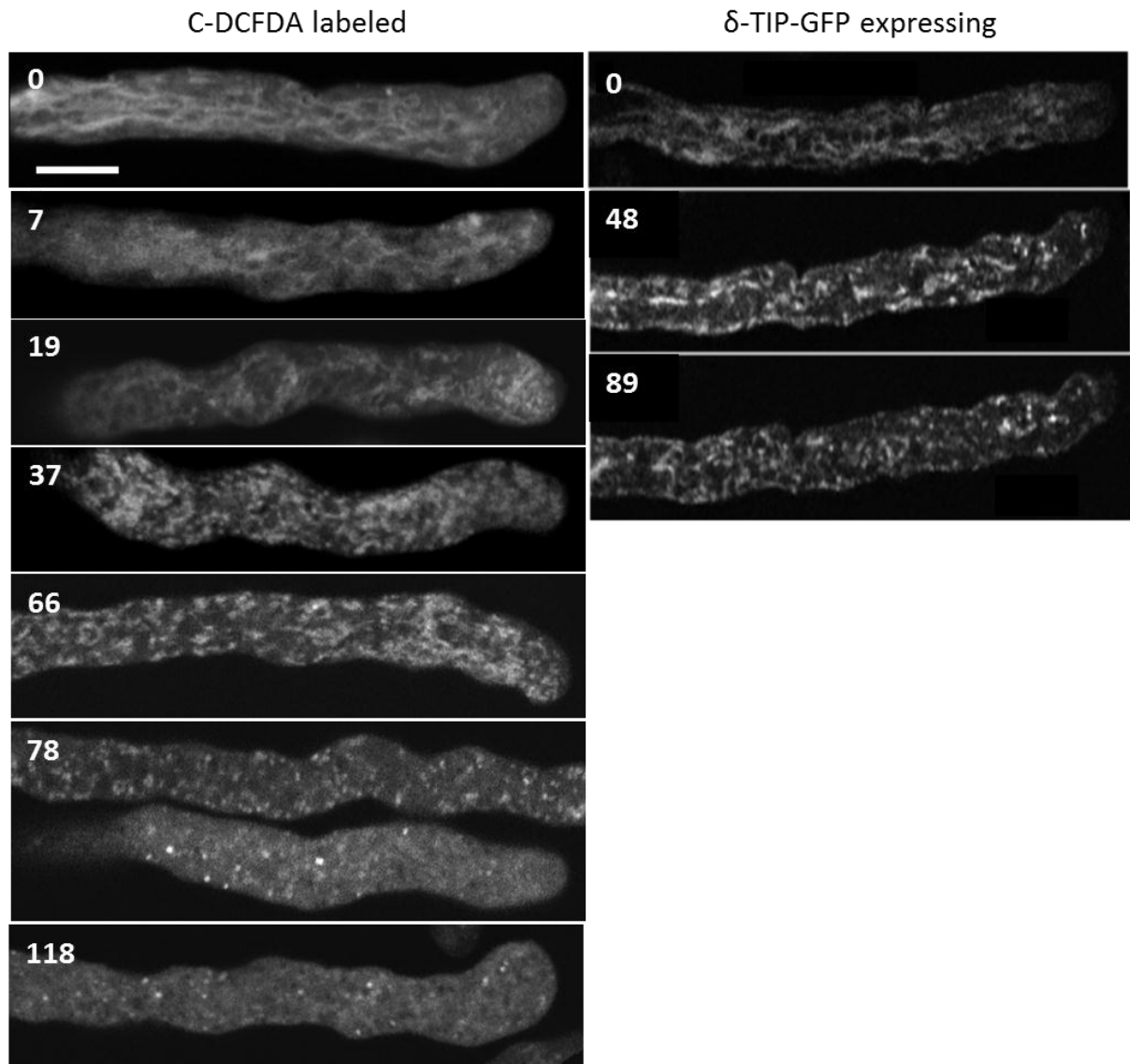
Figure 6.2. SI triggers vacuolar reorganization and disintegration

Pollen tubes were stained with 1µM c-DCFDA, challenged with PrsS to stimulate SI, and imaged using a Leica confocal microscope

c-DCFDA: Typical untreated pollen tube with a tubular vacuole organization, T=0. Apparent vacuolar reorganization within 7 minutes, this continues as shown at 19 min after the addition of PrsS. At 37 minutes after SI induction there is further reorganization of the vacuole, shorter stands of vacuole with a tendency to aggregate together were observed. At 66 min after SI induction there is further reorganization, showing less defined tubular structure and apparent degradation of the vacuole. At 78 minutes after addition of PrsS there is apparent degradation of the vacuole, with small bright spots of signal remaining. 118 min after SI induction vacuole tubular structure is completely disrupted and much has disintegrated; only small reticular bundled vacuole spots remain.

δ-TIP-GFP: A typical untreated pollen tube expressing δ-TIP-GFP, which localised to the tonoplast of the vacuole, labelling is similar to untreated pollen labelled with c-DCFDA (0), a reticular structure, but with a thinner signal, as only the membrane is labelled in δ-TIP-GFP expressing pollen. SI induced-pollen tubes expressing δ-TIP-GFP, 48 minutes post SI induction, the signal became more dispersed, as SI progressed the signal became very apparent disrupted without the tight reticular structure, 89 minutes. Together these data demonstrate that vacuolar collapse is a dramatic and relatively early event in during the SI response. Scale bar= 10 µM.

6.2.3 QUANTIFICATION OF VACUOLAR ALTERATIONS REVEAL RAPID REORGANIZATION AND BREAKDOWN OF THE VACUOLE

SI-induced pollen vacuolar images (c-DCFDA labelled pollen tubes) taken over a 160 minute period were analyzed and pollen were assigned to different categories based upon visual morphology (n=214). The following categories were used; (i) a clear reticulate vacuolar network, (ii) reorganization and (iii) extensive breakdown and with little or no intact vacuole remaining. Data in Figure 6.3 shows that a large proportion of SI-induced vacuolar reorganization is very rapid. Approximately 80 % of all pollen tubes observed between 5 < 15 minutes after SI-induction were undergoing reorganization of the c-DCFDA vacuolar signal.
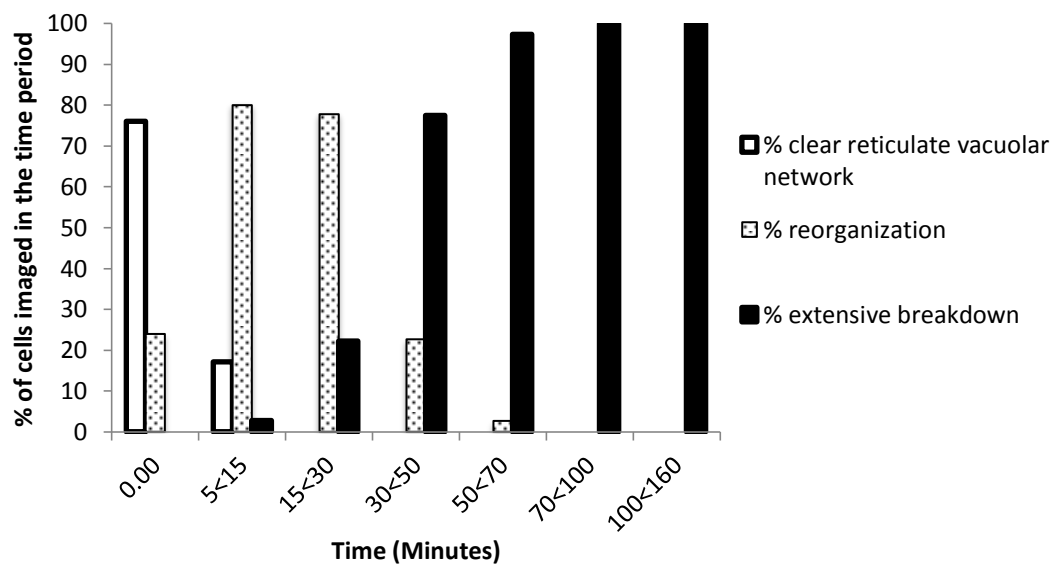
Figure 6.3. SI-induced alterations in vacuolar morphology

Pollen was treated with PrsS to induce an incompatible reaction; pollen was labelled with the vacuolar marker c-DCFDA. Pollen tubes were then assigned to one of four categories referring to vacuolar morphology. These categories includes; (i) clear reticulate vacuolar network, (ii) reorganization and (iii) extensive breakdown with no distinct shapes. N=214.

Of the remaining 20 % of pollen, 17 % exhibited a normal, clean, reticulate vacuolar

structure as observed in untreated pollen. The remaining 3 % pollen had extensive

breakdown of their vacuolar structure. These data suggest that alterations in the vacuolar

structure were a very rapid response during the SI response. Between 15<30 minutes

after SI induction there is was no significant difference in the levels of pollen exhibiting a

state of reorganization, accounting for 78% of pollen observed during this time point

(Figure 6.3). However, there was a shift in the remaining 22 % of pollen; there was no

longer any pollen exhibiting a clear reticulate vacuolar structure, and instead the

remaining 22 % of pollen exhibited extensive breakdown of vacuolar compartments

(Figure 6.3). This is a trend which continued throughout the remaining time points,

gradually over time less pollen exhibited a state of reorganization and within 70<100

minutes of SI-induction all pollen, 100 %, exhibited extensive breakdown of the vacuolar

signal, in which there are no distinct shapes or compartments remaining (Figure 6.3).

Therefore these data suggest that vacuolar breakdown is a dramatic and rapid response.

6.2.4 CALCIUM IS A KEY MEDIATOR IN VACUOLAR BREAKDOWN

As mentioned earlier, increases in cytosolic Ca^{2+} concentration ($[Ca^{2+}]_{cyt}$) are essential for

triggering SI in *Papaver* pollen tubes (Bosch and Franklin-Tong, 2008; Franklin-Tong et al.,

1997; Jordan et al., 2000). Rapid alterations in $[Ca^{2+}]_{cyt}$ are known to be upstream of many

of the major hallmarks of SI (Jordan et al., 2000; Snowman et al., 2002; Wilkins et al.,

2011), which is unsurprising as Ca^{2+} is well known secondary messenger which is

important in many plant PCD systems (White and Broadley 2003; van Doorn et al., 2011).

Furthermore, as mentioned earlier, there are many similarities between the

hypersensitive response and SI. During the hypersensitive response of tobacco to

Pseudomonas syringae pv syringae (Atkinson *et al.,* 1985, 1990; Baker *et al.,* 1987), an

increases in Ca^{2+} have been shown to mediate intracellular acidification. Furthermore,

during a viru*s*-induced hypersensitive response in tobacco there is extensive rupturing of

the vacuolar (Higaki *et al.,* 2007), which may induce acidification of the cytosol. These

studies suggest that Ca^{2+} could potentially mediate the acidification of the cytosol, and

that the acidification of the cytosol could be due to the rupture of the vacuole.

We therefore decided to investigate whether these increases in $[Ca^{2+}]_{cyt}$ play a role in SI-

induced vacuolar breakdown, which may be responsible for acidification of the cytosol.

Pollen tubes were treated with 10 μM A23187, a calcium ionophore, which has been

used extensively to mimic the increases in $[Ca^{2+}]_{cyt}$ triggered during SI response in

Papaver pollen tubes (Franklin-Tong et al., 1996; Franklin-Tong et al., 1997; Wilkins et al.,

2011). Pollen was subsequently labelled with the vacuolar marker c-DCFDA and the

vacuole was monitored by confocal microscopy. Within 7 minutes of the addition of

A23187 the vacuole had already started to undergo some reorganization, the tight

reticulate structure of untreated pollen had started to reorganize and vacuolar

bundles/strands were less defined (Figure 6.). Within 25 minutes of SI induction, the

vacuole had undergone extensive reorganization, forming short bundles and bright spots

of signal, suggesting the vacuole was breaking up into smaller compartments and the

signal had moved into the tip, which was not observed in untreated pollen tubes (Figure

6.). In addition, the background fluorescence had increased, suggesting that the c-DCFDA

dye was leaking from the vacuole into the cytosol, due to rupture of the tonoplast. After

46 minutes there was very little vacuolar structure remaining, with only a few small spots

194

visible, and at 77 minutes almost all of the vacuole appeared to have disintegrated with only an occasional spot of c-DCFDA signal remaining (Figure 6.). The A23187 stimulated breakdown of the vacuole appears to be rather similar to the alterations observed in SI-induced pollen tubes although at a much faster rate (Figure 6.). Untreated pollen tubes had no observed vacuolar breakdown for the same time points.
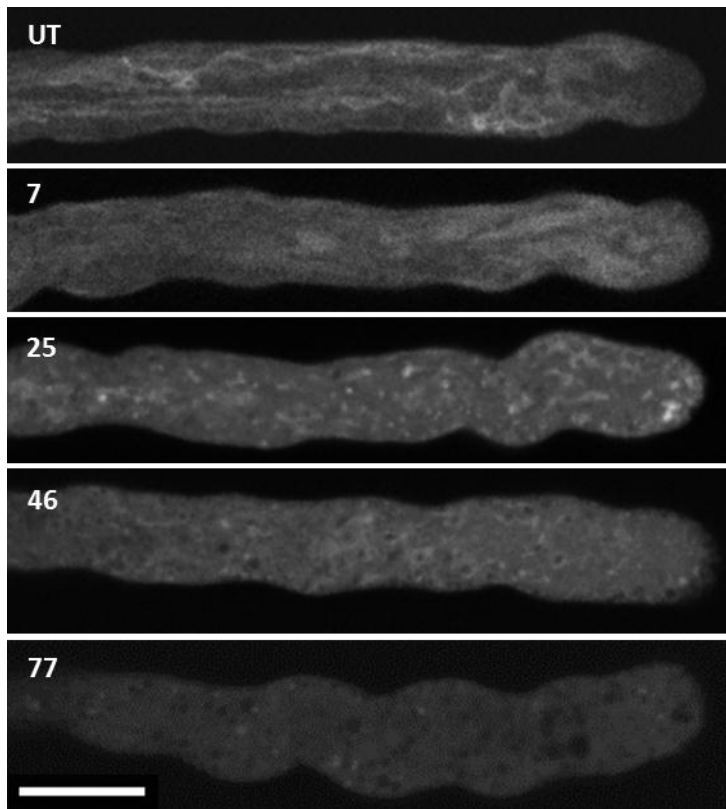
Figure 6.4. Pollen tubes treated with calcium ionophore show vacuolar reorganization and breakdown.

Papaver pollen tubes treated were treated with 10 μM A23187, a calcium ionophore, and then labelled with c-DCFDA to visualise the vacuole. A typical untreated pollen tube exhibits a reticulate structure with fine vacuolar strands visible throughout the pollen shank (UT). Numbers refer to the length of time in which SI was induced. 7 minutes after the addition of A23187 the vacuole appears to have undergone some reorganization. 25 minutes post A23187 addition, the vacuole has undergone major reorganization, small bundles have formed and the background signal in the cytosol increases suggesting vacuolar rupture and leakage of the vacuolar marker. 46 minutes after addition of A23187 there is very little vacuolar signal and aggregated spots of signal have become smaller. 77 minutes after the addition of A23187 the vacuolar structure appears to of almost complete disintegrated, with only a few bright spots of c-DCFDA signal remains, suggesting extensive breakdown of the vacuolar compartment. Scale bar = 10 μM.

195

These data demonstrate that increases in $[Ca^{2+}]_{cyt}$ can trigger the breakdown of the vacuole, and therefore vacuolar breakdown is implicated in SI-induced acidification which is also triggered by increases in Ca^{2+}.

6.2.5 ACTIN ALTERATIONS STIMULATE VACUOLAR REORGANIZATION, BUT NOT BREAKDOWN

As previously discussed, the cytoskeleton plays and important role in SI induced PCD (Thomas *et al.,* 2006; Poulter *et al*, 2008; Bosch & Franklin-Tong, 2008). Furthermore, as the actin cytoskeleton has been implicated in vacuolar maintenance and organization, the actin cytoskeleton may also play a role in the breakdown of the vacuole, which could lead to acidification of the cytosol. To investigate whether the actin cytoskeleton plays a role in the SI-induced vacuolar breakdown, pollen tubes were treated with Latrunculin B (Lat B), an actin depolymerizing drug, or Jasplakinolide (Jasp), an actin polymerizing drug. Pollen was labelled with c-DCFDA to visualise the vacuole during these treatments, using confocal microscopy. In Lat B treated pollen tubes the vacuole underwent extensive reorganization as early as 16 minutes after the addition of the treatment (Figure 6.), however unlike the SI-induced vacuolar breakdown (Figure 6.2), the vacuole was not broken down into very short bundles of c-DCFDA signal, but it appears to aggregate into large pockets of vacuolar signal which are connected by cables of signal (Figure 6.2). After 56 and 73 minutes of treatment with Lat B, the pollen vacuolar signal continued to aggregate into large bundles of signal, resulting in large areas of the cytosol which were free of any signal (Figure 6.5). The aggregation of c-DCFDA signal appeared to be more

severe, as only very bright tight bundles of vacuolar signal away from the tip of the pollen tubes remained, as shown at 107 and more so at 153 minutes of Lat B treatment (Figure 6.5). These data suggest pollen treated with Lat B, the actin depolymerization drug, resulted in the reorganization of the vacuole. However actin depolymerization did not result in the vacuolar breakdown observed in SI-induced pollen tubes, suggesting actin status may play a role in the organization of the vacuolar structure, but does not appear to be involved in triggering vacuolar breakdown during SI.

197
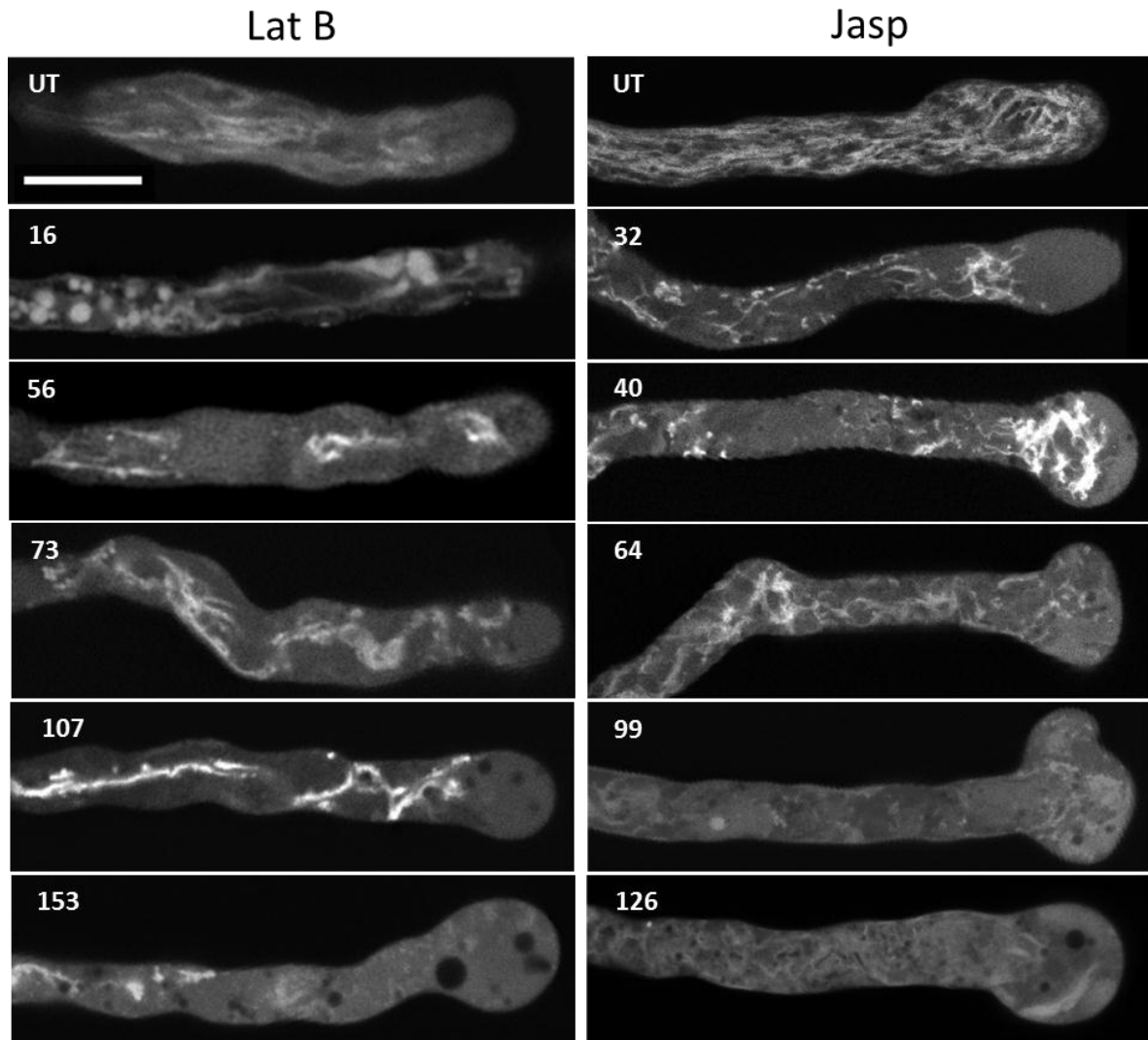
Figure 6.5. Actin Alterations trigger vacuolar reorganization but not breakdown

Untreated healthy pollen tubes labelled with 1 µM c-DCFDA (A & G) displaying typical vacuolar organization. Pollen tubes treated with 1 µM Lat B (left hand column of images) and 0.5 µM Jasp (right hand column of images) and labelled with 1 µM of the vacuolar marker c-DCFDA.

16 minutes treatment with Lat B induced rapid reorganization of the vacuole, with large vacuolar compartments with limited reticular structure. The vacuole continues to aggregate together with some vacuolar leakage in to the cytosol (56 & 73 minutes after the addition of Lat B). 107 minutes Lat B treatment, vacuolar signal appears to moving away from the tip of the pollen tube and there vacuole in the shank has aggregated together in tight bundles. 153 minutes post-Lat B, there is very little vacuolar signal in compartments towards the tip of the pollen tube, although there are some tight bundles towards the back, and a high signal in the cytosol. 32 minutes treatment with Jasp pollen reorganises in to bundles away from the tip. 40 min of Jasp treatment, a bulbous tip is forming which is typical of Jasp treatment, the vacuole continues to aggregate around the base of the bulbous tip form a concentrated region of signal. 64 and 99 minutes post-Jasp the bright vacuolar signal is decreasing and the background fluorescence is increasing suggesting leakage of the vacuolar marker from the vacuole into the cytosol. 126 min post-Jasp, the vacuolar signal is decreasing and there are no defined vacuolar structures which resemble the reticular structure of untreated pollen tube vacuoles. Scale bar = 10 µm.

Pollen treated with Jasp also triggered the reorganization of the vacuole. Within 32 minutes of the treatment, the vacuole had aggregated into short bundles, predominately towards the tip of the pollen tube (Figure 6.5). After 40 minutes of Jasp treatment, pollen tubes were forming a bulbous tip, which is a typical symptom of Jasp treatments, and the vacuolar signal continued to aggregate around the base of the bulbous tip, forming very tight bundles which appeared to be connected by thin strands of vacuolar signal (Figure 6.5). After 64 minutes of treatment, the concentrated vacuolar signal had decreased and the bundles and strands appear to have moved away from the tip of the pollen tube (Figure 6.5). Furthermore, the tight bundles observed around 40 minutes after addition of Jasp appear to be looser by 64 minutes of treatment and the c-DCFDA signal appeared to be spreading out, but not as uniformed as the vacuolar structure of untreated pollen tubes. Furthermore, after 99 and 126 minutes of treatment with Jasp, the pollen tube vacuolar signal appeared to change very little, the vacuolar signal consisted of thicker strands and compartments throughout the pollen tube and no longer aggregating into tight bundles which were seen at the beginning of the treatment with Jasp, at 32 & 40 minutes. These data suggest that the initial treatment with Jasp resulted in the reorganization of the vacuolar structure into tight bundles, which overtime relaxed into thicker strands and compartments which occupy all regions of the pollen tube. However, these structures appear to differ somewhat from the vacuolar structure of untreated pollen tubes, which appear to be more organized, with a thinner more reticulate structure than the later stages of Jasp treatment. Therefore Jasp treatments resulting in actin stabilization, does not trigger the vacuolar breakdown observed in SI-induced pollen tubes, and therefore does not appear to play a role in this aspect of the SI response.

199

Although the actin cytoskeleton does appear to play a role in the organization of the vacuole, actin alterations alone do not trigger the breakdown of the vacuole observed in SI-induced and A23187 treated pollen tubes (Figure 5.2 & 5.3), suggesting that actin alterations alone do not trigger the breakdown of vacuole.

6.2.6 ARTIFICAL ACIDIFICATION THE CYTOSOL OF *PAPAVER* POLLEN TUBES CAN BE USED TO INVESTIGATE THE EFFECT OF PH ON VACUOLAR BREAKDOWN

Data presented in this chapter has shown that vacuolar reorganization and breakdown occurs rapidly during the SI response (Figure 6.2). In Chapter 5, data showed SI-induced rapid acidification of the cytosol, which was also mediated by increases in Ca^{2+} and not actin alterations. Furthermore, data presented showed that the acidification of the cytosol occurs within 10 minutes of SI induction. Data shown in Figure 5.2 also showed that ~10 minutes after SI induction the vacuole undergoes reorganization, prior to rupture. As discussed earlier the vacuole is a major source of protons, and its rupture could be contributing to the rapid acidification observed during the SI response. Therefore these data raise the question; 'is the vacuolar rupture resulting in the acidification of the cytosol or is there some acidification prior to vacuolar breakdown?' At present, the role of the vacuole in cytosolic acidification during SI has not been investigated in any system, and unfortunately we currently do not have the tools to directly trigger that breakdown of the vacuole and look at the effect on cytosolic pH, to investigate whether the breakdown of the vacuole could be a direct cause of cytosolic acidification in *Papaver* pollen tubes. However, results in Chapter 5 showed that weak

acids could be used to manipulate the cytosolic pH of pollen tubes, and therefore we could test whether a change in cytosolic pH had an effect on the vacuole, to try to establish the sequence of events during the SI response. Therefore pollen was treated with either growth medium (UT), PrsS to induce SI (SI), propionic acid pH 7, propionic acid pH 5.5 to mimic SI-induced acidification, or pollen was pre-treated with propionic acid pH 7 for 10 minutes prior to SI induction to block SI-induced acidification (propionic acid pH 7 & SI). Pollen was subsequently labelled with the vacuolar marker c-DCFDA and imaged using a confocal microscope to investigate whether alterations in pH are upstream of SI-induced vacuolar reorganization and breakdown (Figure 6.6).

Figure 6.6 shows over a period of approximately 80 minutes there is no reorganization or disruption of the vacuole in pollen treated with growth medium. Pollen treated with PrsS undergo rapid and extensive reorganization and breakdown of the vacuole, data shown in Figure 6.6 is that same as that in Figure 6.2, and therefore will not be discussed again. Pollen tubes treated with propionic acid pH 7 underwent some reorganization within the first 14 minutes, in which the typical reticulate structure is not as well defined as untreated pollen tubes and the vacuolar structure was pushed in to the tip of the pollen tube. After 28 minutes of treatment there was major reorganization of the vacuole, which strongly aggregated together in to bundles of vacuolar signal. This aggregation continued thereafter, and after 65 and 72 minutes of treatment with propionic acid pH 7, the vacuole no longer resembles the reticulate structure of untreated pollen, but instead aggregated into large pockets of vacuolar signal which is connected by strands of vacuolar signal. .

201
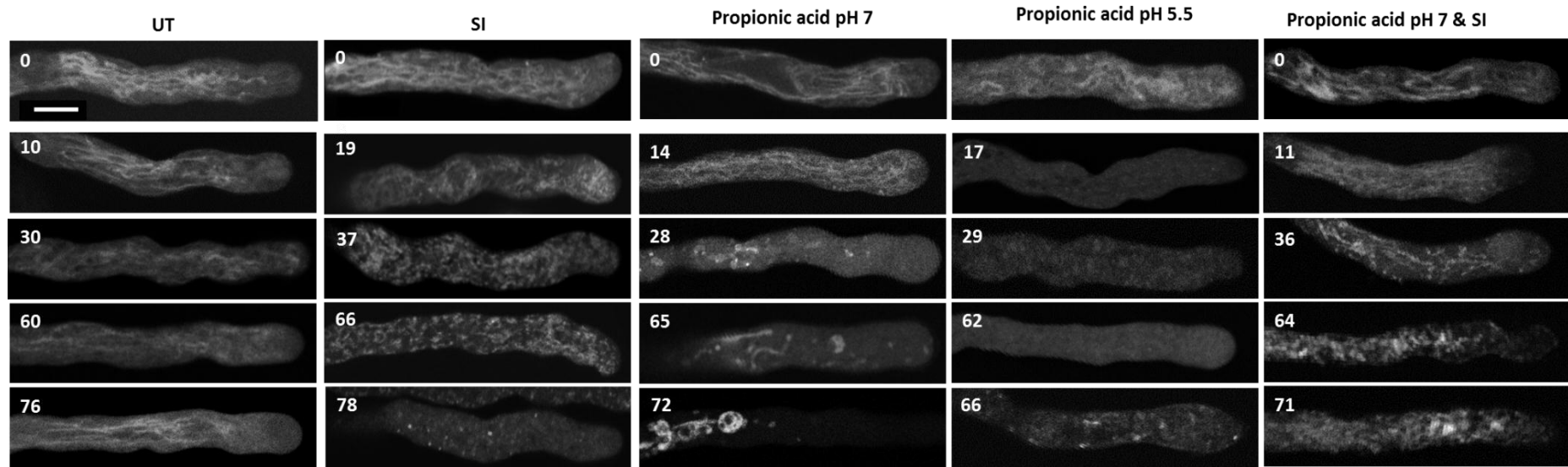
Figure 6.6. Artificial manipulation of cytosolic pH of pollen tube triggers alterations in vacuolar organization

Papaver pollen was incubated at T = 0 with either growth medium (untreated, UT), PrsS (SI), 50 mM propionic acid pH 7, 50 mM propionic acid pH 5.5 or pre-treated with 50 mM propionic acid pH 7 for 10 minutes prior to addition of PrsS (PPA pH 7 & SI). Pollen was labelled with c-DCFDA and imaged using a confocal microscope. Please note images shown under SI are the same as those shown in Figure 5.2. Scale bar = 10 μm.

Thus, this data suggests that by manipulating the cytosolic pH of the pollen tube, to ~pH 7 with propionic acid, the organization of the vacuole is altered, however such manipulation does not induce breakdown of the vacuole (Figure 6.6).

Pollen was treated with propionic acid pH 5.5, to artificially acidify the pollen tube to a similar pH of SI induced pollen tubes (see Chapter 5). Within 17 minute of treatment with propionic acid pH 5.5 there was a dramatic disintegration of the vacuolar signal, with no structures remaining (Figure 6.6). The breakdown of the vacuole in pollen treated with propionic acid pH 5.5 is comparable to the vacuolar breakdown of SI-induced pollen tubes, and may even be more extreme than SI-induced pollen after 78 minutes. The vacuolar signal in propionic acid pH 5.5 treated pollen did not recover during the 66 minute period in which pollen were imaged (Figure 6.6). These data suggest that acidification of the cytosol has an extreme effect on the organization and the stability of the vacuole in *Papaver* pollen tubes, and acidification of the cytosol may play a role in triggering vacuolar breakdown.

Pollen was also treated with propionic acid pH 7 for 10 minutes prior to SI induction to investigate whether blocking SI-induced acidification had an effect on vacuolar morphology and integrity. As shown in Figure 6.6, SI-induced pollen pre-treated with propionic acid pH 7 shows a slight reorganization of the vacuolar signal 11 minutes of SI induction, and the typical reticulate structure is not as well defined as that of untreated pollen at a similar time point. However, this reorganization is very similar to that of propionic acid pH 7 treated pollen, but not similar to SI-induced pollen, which had already undergone more extensive reorganization at a similar time point (Figure 6.6). Thereafter pollen treated with propionic acid pH 7 & SI continue to reorganize in to tight bundles of vacuolar signal, 36 minutes, and

aggregate in to bundles around 64 minutes, occupying large areas of the shank of the pollen tube (Figure 6.6). This aggregation of vacuolar signal did not resemble that of propionic acid pH 7 treated pollen, in which aggregates into tight bright bundles of vacuolar signal, nor does it resemble the breakdown observed in SI-induced pollen of a similar time point. Moreover, after 71 minutes of treatment with propionic acid pH 7 & SI there appeared to be no breakdown of the vacuole, but nor did there appear to be the typical reticulate structure of untreated pollen, instead the vacuole has reorganized into larger bundles which appear to be increasing in size over time. Thus, these data suggest that inhibition of SI-induced acidification prevent vacuole breakdown, but not reorganization. However, it is difficult to determine whether this reorganization is due to the presence of propionic acid pH 7, as similar reorganization is seen at early stages of the treatment, or where it is due to other SI-specific signals that are not regulated by a drop in cytosolic pH.

In summary, these data suggest that acidification of the cytosol may be upstream of SI-induced vacuolar breakdown, suggesting that there may be several sources of protons contributing to SI-induced acidification

6.3 DISCUSSION

Data presented in Chapter 5 showed that SI-induced acidification is rapid and extensive. Furthermore, weak acids can be used to manipulate the cytosolic pH of pollen tubes to mimic SI-induced acidification. In this chapter the vacuole has been investigated as a possible source and target of SI-induced acidification, providing the first insights into the spatial and temporal alterations of the vacuole during SI, and documenting the rapid reorganization and rupture of the vacuole. Vacuole breakdown is also mediated by increases in cytosolic Ca^{2+}. Furthermore, actin also plays a role in the reorganization, but not the breakdown of the vacuole. Artificial acidification of the pollen tube cytosol using weak acids also triggers vacuolar breakdown, suggesting the acidification could be upstream of vacuolar breakdown. These studies also provide the first evidence of SI-induced vacuolar breakdown and investigated some of the possible triggers involved.

6.3.1 SI-INDUCED VACUOLAR REORGANIZATION AND BREAKDOWN

The vacuole of pollen tubes has a different arrangement to that of other plant cells. Cells of leaf tissues contain a single large vacuole which occupies a large area of the cell (Kutsuna *et al.,* 2002). Imaging of Arabidopsis and lily pollen tubes' vacuoles revealed tubular, ribbon-like vacuole structures in the cytoplasm (Hicks et al., 2004; Lovy-Wheeler et al., 2007; Oda et al., 2009a). In addition, vacuolar membrane (VM) markers have been used in Arabidopsis, discovering structures termed 'bulbs', which are invaginations of intravacuolar sheets, these have been identified using various markers; γTIP–GFP, (Saito et al. 2002), GFP–AtVAM3 (Uemura et al. 2002, Kutsuna and Hasezawa 2005), AtTIP1-1–GFP (Boursiac et al. 2005),

BobTIP26-1–GFP (Reisen et al. 2005) and NtPT1 homolog– GFP (Escobar et al. 2003). It is thought these 'bulbs' may play a role as membrane reservoirs for rapid vacuolar expansion. Imaging of *Papaver* pollen tubes showed similar vacuolar organization to that of other species, consisting of a reticulate structure with long thin strands.

SI-induction in *Papaver* pollen tubes triggered rapid reorganization of the vacuole prior to its breakdown, with major alterations occurring within 30 minutes of SI induction. SI-induced vacuolar reorganization and breakdown in *Papaver* pollen tubes appear to be similar to that observed by Higaki *et al.,* (2007) during the HR response in cryptogein-induced cell death in tobacco BY-2 cells. During this response the vacuole undergoes major disruption in which 'bulb'-like structures are formed. In SI-induced *Papaver* pollen tubes the vacuole also aggregated in to bundles prior to breaking down. Moreover, in tobacco cells the disruption and bundling of cortical microtubules and actin microfilaments was also observed, during *Papaver* SI microtubules and the actin cytoskeleton are also disrupted and punctate actin foci are visible with 1 hr of the response (Poulter *et al.,* 2008; Snowman *et al.,* 2002). The next stage of vacuolar alteration in tobacco BY-2 cells included the formation of small spherical vacuoles. In the final stage the vacuolar membrane disintegrates just prior to PCD (Higaki *et al.,* 2007). In *Papaver* SI the vacuole also undergoes disintegration, suggesting similar to the HR in Tobacco vacuolar alterations may play a key role in the PCD-mediated responses, and perhaps a similar PCD-pathway exist. During xylem differentiation vacuolar reorganization is also occurs prior to tonoplast rupture. The rupture of the tonoplast is thought to release hydrolytic enzymes which fragment DNA resulting in cell death. Although the release of hydrolytic enzymes during HR and SI has yet to assessed it is presumed to

occur and this may play an important role in PCD and will be discussed further later on in relation to SI-induced vacuolar breakdown.

6.3.2 SI-INDUCED ACIDIFICATION IS UPSTREAM OF VACUOLE BREAKDOWN

The purpose of this chapter was to investigate the role of the vacuole as a potential source of protons during SI-induced cytosolic acidification. Data presented in this chapter has shown that SI induces vacuolar breakdown. The vacuole undergoes major reorganization within 10 minutes of induction, which coincided with cytosolic acidification (see Chapter 5 for details; Figure 6.7). Vacuolar breakdown is most prominent 30-70 minutes after SI induction which coincides with the cytosol reaching its most acidic point, pH 5.5 (Figure 6.7).
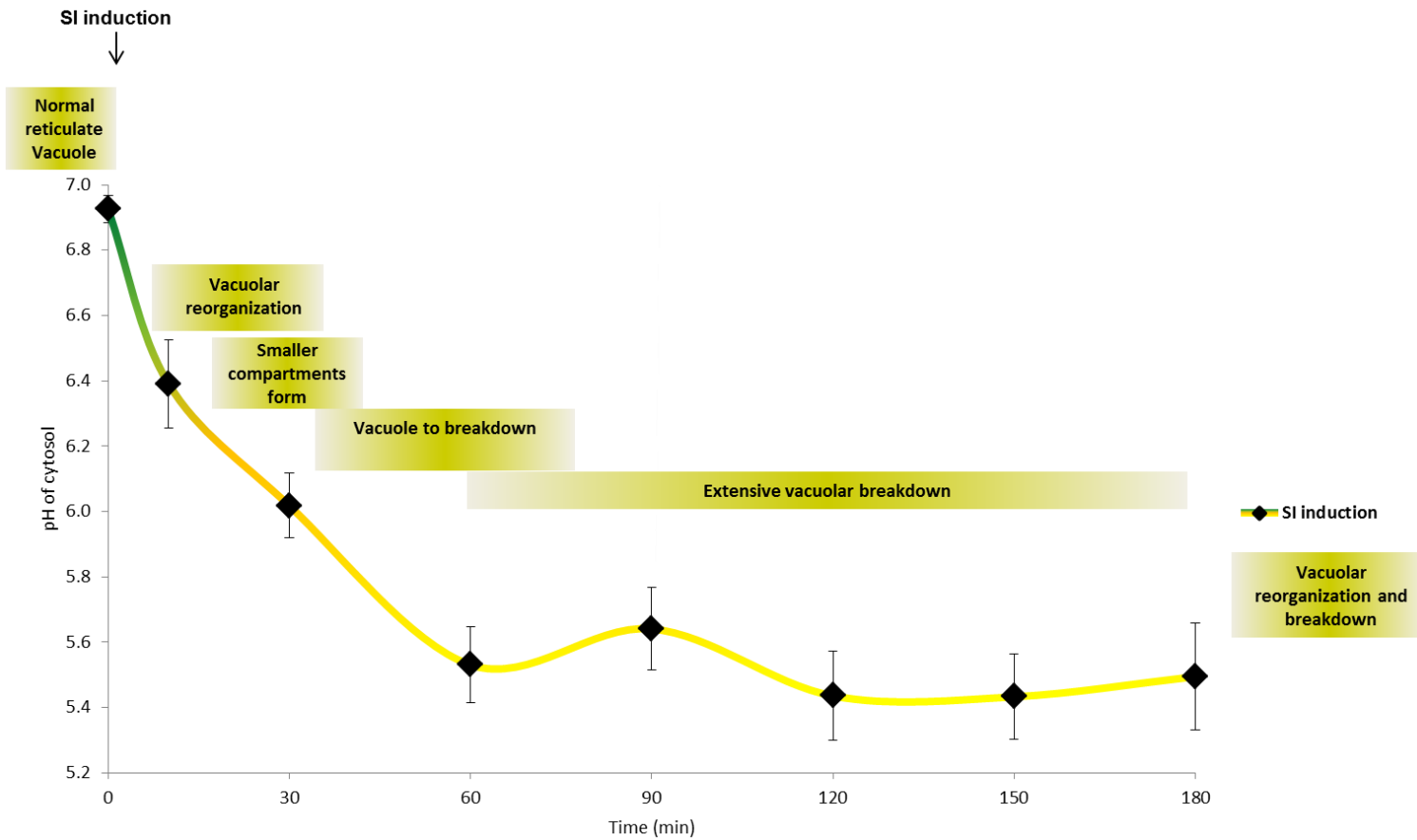
Figure 6.7 A model to show the temporal alteration in the SI-induced pollen tubes, highlighting the rapid acidification of the cytosol and vacuolar reorganization and breakdown.

This model shows the timings of SI-induced acidification in *Papaver* pollen tubes, as shown in Chapter 5 (yellow line with black marker). The timings of SI-induced vacuolar reorganization and breakdown are indicated and described in green boxes. Black arrow indicates the addition of PrsS.

As previously discussed, the vacuole is a very acidic organelle (Chapter 5). The pH of the vacuole in mung bean seedling roots is pH 5.6 (Nakamura 1992), furthermore in *Characean* cells (algae) the vacuole has been measured as pH 4.8 to 5.3 (Vorob'ev *et al.,* 1961). These data suggest that if the vacuole of *Papaver* pollen is of a similar pH, SI-induced vacuolar breakdown could cause the acidification of the cytosol to pH 5.5, and therefore play a role in scene for caspase-like activity, which have an optimal activity at pH 5 (Figure 6.7). This theory is supported by research in several different species in which vacuolar rupture is suspected to contribute to acidification of the cytosol, and is vacuolar rupture is used to mark the death of a cell (Jones *et al.,* 2001). Moreover, based on the temporal data of both SI-induced acidification and vacuolar reorganization, both events occur at similar time point and it is therefore difficult to determine which occurs first (Figure 6.7). Unfortunately at present we do not have tools to directly trigger the breakdown of the vacuole or block it. As a result we were unable to investigate whether the breakdown of the vacuole is essential for SI-induced acidification in *Papaver* pollen tubes. Alternative approaches were used to investigate the sequence of events leading to cytosolic acidification in SI-induced pollen tubes. As discussed in Chapter 5, the external medium in which *Papaver* pollen is grown is pH 5.5. Research has also shown that during the SI-response in *Papaver* pollen tubes there are alterations in Ca^{2+} and K^+ channel activities (Wu et al., 2011). It is possible that alterations channel activities or perhaps plasma membrane integrity, could result in the influx of protons from external medium into the cytosol, contributing to SI-induced acidification. This hypothesis would suggest that the vacuole may not be the only source of protons and acidification may occur prior to vacuolar breakdown. This hypothesis is further supported by data presented here in which the artificial acidification of the cytosol resulted

in the rapid reorganization and breakdown of the vacuole. Moreover, preventing SI-induced

acidification prevented vacuolar breakdown but not reorganization. These results

demonstrate that acidification of the cytosol is necessary for SI-induced vacuolar

breakdown, and therefore implying that other sources of protons play a role in SI-induced

acidification. However, as only a pH 7 and pH 5.5 buffer were used in the current studies, we

are unable to determine what level of acidification is required to trigger vacuolar

breakdown. It may be that a small pH change is sufficient to trigger vacuolar breakdown,

which in turn contributes to the overall acidification through the release of its acidic content

in to the cytosol. At present there are few studies in which the source of the cytosol

acidification has been investigated in such detail, and therefore this is something that

should be investigated further in the future. However, research has shown that during the

HR in suspension-cultured rice cells, cytosolic acidification occurs as the result of transient

membrane depolarization, in which there in an influx of H^+ and the efflux of K^+ immediately

after treatment with the elicitor (Ito et al., 1997). These data suggest that during the HR

acidification is due to alteration in membrane status, and this could also be the case during

SI-induced pollen tubes (see chapter 5 for further discussion).

Nevertheless although acidification of the cytosol plays a role in SI-induced vacuolar

breakdown, there is much evidence to suggest that the breakdown of the vacuole itself also

plays a role in acidifying the cytosol and therefore should not be disregarded. For example

as previously discussed in Chapter 5, during the HR response in cell culture of *Eschscholtzia*

californica (Californian poppy) elicitor (commercial bakers' yeast) treatments induced

acidification of the cytosol by 0.3 to 0.7 pH units, which coincided with an increase in

vacuolar pH by 0.2 to 0.4 pH units, occurring within 10 minutes of elicitor contact (Roos et

al., 1998; Roos et al., 2006). Roos *et al.,* (2006) also showed that during this response lysophosphatidylcholine (LPC) generated by phospholipase A_2 at the plasma membrane, triggered the activation of a tonoplast H^+/Na^+ antiporter which caused a transient increase of the vacuolar pH by increasing the Na^+ sensitivity of a Na^+-dependent proton efflux (Viehweger *et al.,* 2002). Moreover, during salt stress in tobacco cells treated with 500 mM NaCl the pH dropped from pH 7.3 to pH 5.85 in just 40 minutes, and coincided with a disrupted vacuolar compartment (Qiao *et al.,* 2002). Furthermore, the vacuole has also been suggested as a source of protons during auxin-triggered acidification of the cytoplasm guard cell protoplasts (Frohnmeyer *et al.,* 1998). Therefore the contribution of the vacuole as a source of protons during the SI induced acidification should be investigated in conjunction with examination of other sources of protons.

6.3.3 INCREASES IN INTRACELLULAR CA^{2+} TRIGGER VACUOLAR BREAKDOWN

Ca^{2+} is a known secondary messenger in many signalling cascades in both plant and animal systems (Hepler & Wayne, 1985; Trewavas & Gilroy, 1991). Transient increases in Ca^{2+} are shown in response to many biotic and abiotic stimuli (Hetherington & Brownlee, 2004; Rudd & Franklin-Tong, 1999). During the SI response in *Papaver* pollen tubes increases in $[Ca^{2+}]_{cyto}$ has been linked to a number of downstream events including alterations in the actin cytoskeleton and PCD (Bosch and Franklin-Tong, 2008; Snowman, 2000; Snowman et al., 2002). SI-induced increases in cytosolic calcium have been mimicked by use of the calcium ionophore A23187 to investigate the role of Ca^{2+} during the SI response (Snowman, 2000; Snowman et al., 2002; Wilkins et al., 2011). In order to determine whether Ca^{2+} was an

upstream mediator of vacuolar reorganization and breakdown, A23187 was used to increase the $[Ca^{2+}]_{cyto}$ to mimic SI-induced increases in Ca^{2+}, in conjunction with vacuolar labelling. Results presented here show that by artificially increasing the concentration of calcium in the pollen tube we were able to trigger vacuolar breakdown. Although vacuolar breakdown occurred much faster in A23187 treated pollen than during SI induced pollen, the changes in vacuole appearance were similar to those of SI-induced pollen tubes, suggesting the same method of vacuolar breakdown was induced, but perhaps activated at much faster than during an SI response. As calcium is already known to play a key role in SI, and is one of the earliest events triggered by SI, lying upstream of all the SI hallmark features, including cytosolic acidification (Chapter 5), it is not surprising that it also plays a role in vacuolar breakdown.

6.3.4 ACTIN ALTERATIONS TRIGGER VACUOLAR REORGANIZATION AND BREAKDOWN

As discussed Ca^{2+} plays a role in triggering vacuolar disintegration in SI-induced pollen tubes. In plants little is known about what other processes may act upstream of vacuolar breakdown, although some research has shown that the cytoskeleton could play a role in vacuolar morphogenesis (Kutsuna & Hasezawa, 2002, Mathur *et al*. 2003, Kutsuna *et al*. 2003, Higaki *et al*. 2006). In particular, cytoskeletal elements are known to be required for the formation and maturation of autophagic vacuoles (Jasionowski *et al.,* 1992). Pharmacological experiments have shown that actin and microtubules are essential for vacuolar membrane maintenance and nuclear positioning in synchronized tobacco BY-2 cells (Katsuna *et al.,* 1990). During embryogenesis plant cells undergo reorganization and

developmental PCD in order to reshape the embryo; this involves the breakdown of the vacuole and the mediation of meta-caspases (Filonova *et al.,* 2000b). It has also been suggested that actin-binding proteins may play a role in the maintenance of vacuolar structures (van der Honing *et al.,* 2007; Oda *et al.,* 2009). Moreover, the artificial disruption of F-actin bundles in Tobacco BY-2 Cells, by treatment with an actin polymerization inhibitor facilitates the disintegration of the bulb-like vacuole structures which are replaced by smaller vacuolar structures (Higaki *et al.,* 2006; Sheahan *et al.,* 2007).

Moreover, in other species actin acts both a sensory and mediator of cell death during stress and apoptotic events, translating stress signals into alterations in actin polymerization status, which can result in changes in cell morphogenesis (Desouza et al., 2012; Franklin-Tong and Gourlay, 2008). Examples include Fa*S*-mediated apoptosis in Jurkat T-cells, in which Jasp can stimulate apoptosis (Morley et al., 2003). Furthermore, actin stabilization resulted in the formation of distinct morphological and biochemical hallmarks of apoptosis, such as DNA fragmentation, chromatin condensation and caspase activation. Actin is therefore, implicates in playing a role in modulating apoptotic signals, and therefore executing cell death (Odaka et al., 2000; Suria et al., 1999).

In SI-induced *Papaver* pollen tubes, alterations of the cytoskeleton are observed, and both actin depolymerization and stabilization has been linked to initiating SI-PCD (Snowman *et al.,* 2002; Thomas *et al.,* 2006). Cortical microtubules also rapidly depolymerize in SI-induced incompatible pollen, and treatment with taxol, a microtubule stabilizing drug, alleviated SI-induced PCD (Poulter *et al.,* 2008). As discussed in Chapter 1, vacuolar rupture is a key feature of plant PCD, as alterations in actin dynamics are known to trigger PCD during an SI

response actin may also play a role in triggering vacuolar disruption. Data presented here show that both actin depolymerization and stabilization resulted in the reorganization of the vacuole in *Papaver* pollen tubes. However, unlike the SI-induced changes, alterations in actin status did not trigger vacuolar breakdown. These results suggest that changes in actin status may only result in a lack of structure or regulation of the vacuole morphology, and is not responsible for triggering the breakdown of the vacuole.

Similar results were shown in tobacco BY-2 cells, in which disruption of actin dynamics facilitated the reorganized of the vacuole, in which spherical vacuoles formed, but not the complete breakdown of the vacuole (Higaki et al., 2006; Kutsuna and Hasezawa, 2002). Moreover, during the HR in tobacco BY-2 cells, sequential *in vivo* imaging of the vacuole and cytoskeleton showed that during elicitor induced PCD, there is the reorganization of the vacuole and microfilaments, prior to vacuolar disruption and PCD (Higaki *et al.,* 2007). Furthermore, actin depolymerizing treatments during a HR response accelerated the transition from bulb-like vacuolar structure to a 'simple-shaped vacuole' with small spherical vacuoles and accelerated cell death. However, it was not shown whether alterations in actin dynamics induced the rupture of the vacuole (Higaki et al., 2007). Therefore, these results suggest that SI-induced vacuolar reorganization maybe regulated in a similar manner to HR-induced tobacco cells, as manipulation of actin dynamics in both species induced the reorganization of the vacuole but not the breakdown of the vacuole. However, the induction of cell death by either SI-induced Papaver pollen or by the addition of an elicitor in tobacco, triggered both the reorganization of the vacuole and its breakdown suggesting there must be another signal which is not mediated by actin to trigger breakdown of the vacuole.

6.3.5 OTHER POTENTIAL UPSTREAM MEDIATORS OF SI-INDUCED VACUOLAR BREAKDOWN

Data presented in this chapter has shown that SI triggers rapid reorganization and breakdown of the vacuole. In addition, both increases in $[Ca^{2+}]_{cyt}$ and artificial acidification triggers the rapid breakdown of the vacuole, however alterations in actin dynamics only triggered reorganization of the vacuole and not breakdown. Although vacuolar breakdown is a well-established PCD event, at present it is not known what is responsible for vacuolar rupture during plant PCD in any system and therefore this topic is of great interest and requires further investigation.

However, in viruS-induced HR in tobacco there is evidence that shows a vacuolar processing enzyme (VPE) maybe involved in HR-induced vacuolar breakdown (Hatsugai *et al.,* 2004). As discussed in Chapter 1, these VPEs are usually localised in the vacuole, require an acidic pH to be functionally active, and possess caspase-1-like activities. During the viruS-induced hypersensitive cell death VPE is thought to mediate the collapse of the vacuole, perhaps through loss of selective permeability of the tonoplast, resulting in the release of protons, and the release of degrading enzymes and perhaps causing acidification of the cytosol (Kuriyama *et al.,* 1999). However, more recent research has shown that this caspase-1-like activity is not required for vacuolar and plasma membrane fusion upon avirulent bacterial infection (Hatsugai et al., 2009). As discussed in the introduction chapter, a VPE has been identified in *Papaver* pollen tubes, PrVPE1, it has both minor DEVDase and IETDase activity and strong YVADase activity, all of which require an acidic pH for activity (Bosch et al., 2010). Although VPE localised to a compartment resembling the vacuole, it's activity was

not required for SI-induced PCD in *Papaver* pollen tubes. Therefore VPE activity is not implicated in mediating SI-induced PCD in a similar manner to that of cells undergoing the cell death in response to infection (Bosch et al., 2010). Thus, although VPE and its vacuolar localization suggested that investigation of vacuolar events in poppy SI might be a sensible avenue to follow, for other reasons, it does not shed light on mechanisms operating in the poppy system.

Research in tracheary element differentiation in *Cucurbita moschata* caspase-3/DEVDase-like activities are responsible for rupturing the tonoplast, triggering PCD (Hao et al., 2008). In addition in Arabidopsis *Pseudomonas syringae* induced HR there is the activation of proteasome subunit PBA1, which has caspase-3/DEVDase-like activity (Hatsugai et al., 2009). Hatsugai et al., showed that during this response membrane fusion of the tonoplast with the plasma membrane is linked to the release of vacuolar antimicrobial proteins into the extracellular spaces, and therefore defence of the cell (Hatsugai and Hara-Nishimura, 2010; Hatsugai et al., 2009). Moreover, the reduction in PBA1 activity abolished the collapse of the vacuole during PCD (Hatsugai et al., 2009; Pajerowska-Mukhtar and Dong, 2009). As discussed in the introduction chapter, there is significant increases in caspase-3-like activities during the SI response, with increases documented as early as 90 minutes after SI induction (Bosch and Franklin-Tong, 2007). At present we do not know the source of these activities, however the inhibition of SI-induced acidification also prevented caspase-3/DEVDase activities and vacuolar breakdown. Therefore the inhibition of caspase-3/DEVDase activity, such as those of PBA1 in Arabidopsis, may also prevent vacuolar breakdown in SI-induced pollen tubes. However, as caspase-3-like activities are only documented within 90 minutes of SI-induction, and vacuolar breakdown occurs within 60

minutes of SI induction, it is likely that caspase-3-like activities are not involved in this event. As a result their activity may only be due to the resultant acidification from vacuolar rupture.

During necrosis in *C. elegans* , cytoplasmic calcium overload is known to be upstream of intracellular acidification which is involved in modulating the function of executioner aspartyl proteases (Syntichaki et al., 2005). Furthermore, calcium overloading is thought to inhibit vacuolar H^+-ATPase activity and has been implicated in triggering intracellular acidification. Vacuolar ATPases (V-ATPases) have been identified as an important component in maintaining cellular homeostatus, by regulating cellular pH by pumping cytosolic protons into intracellular organelles. The inhibition of V-ATPases has been implicated in many cell death pathways through the resultant cytosolic acidification. Examples include both yeast cell death (Chan et al., 2012) and mammalian apoptotic cell death, including in several human cancer cell lines such as B-cell hybridoma cells (Nishihara et al., 1995; De Milito et al., 2007) and breast cancer (McHenry et al., 2010). When lysosomal V-ATPase was inhibited in these cells, lysosomal pH and permeability increased, resulted in the release of cathepsin D and activation of caspase (Nakashima et al., 2003). Moreover, in some events the mitochondria and lysosome might be together involved in V-ATPase-inhibitor-induced apoptosis via caspase pathway or RO*S*-dependant manner (Ishisaki et al., 1999; De Milito et al., 2007).

At present V-ATPase activities have not been investigated during the SI response in *Papaver* pollen tubes, however similarly to the studies mentioned above, the inhibition of a V-ATPase may result in the increased permeability of the plasma membrane or vacuole, and

contribute to cytosolic acidification, which in turn would create the optimal environment for proteases which have caspase-like activities. Therefore this avenue of research should be considered for future work, and may provide insight into possible mechanisms involved in SI-induced cytosolic acidification.

6.3.6 THE ROLE FOR SI-INDUCED VACUOLAR RUPTURE

So far, SI-induced vacuolar breakdown has been discussed in relation to acidification of the cytosol, however vacuolar breakdown may also have another role during the SI response. The collapse of the vacuole is thought to be regulated by the cell and not the result of metabolic rundown. For example, the breakdown of the vacuole is not associated with necrosis in plant cells, but appears to be regulated by a number of cell death pathways (van Doorn et al., 2011). As mentioned the vacuole is a source of many proteolytic enzymes that maybe involved in the degradation of the cell. In PCD events such as Anther Dehiscence in Tomato (*Solanum lycopersicum*), ricinosomes, which are precursor protease vesicles are thought to play a role in degrading the cell, are thought to deliver their enzymatic contents directly to the cytosol following vacuolar collapse (Rogers, 2005; Senatore et al., 2009). It is believed that the acidification of the cytosol results in the autocatalytic processing of the ricinosome enzyme KDEL-tailed cysteine proteinases that act in the final stages of corpse processing following cell death (Senatore *et al.,* 2009). Furthermore, in TE differentiation in Zinnia (*Zinnia elegans*), the vacuole undergoes rapid rupture resulting in the release of its hydrolytic content which is thought to assist in degrading the cell, resulting in a hollow corpse which serves as a water conductor. This rupture has also been linked to the

degradation of the nucleus (Kuriyama et al. 1999; Obara 2001; Rotari *et al.,* 2005). In

addition, studies have shown that an S1-type nuclease, *Zinnia* endonuclease 1 (ZEN1), which

accumulates in the vacuole, functions directly in nuclear DNA degradation during

programmed cell death (PCD) of TEs (Ito, 2002). Moreover, ZEN1 does not participate in the

degradation of the vacuole and is only active at an acidic pH, suggesting it is only active in

the vacuole or once the vacuole ruptures. Such a nuclease could also play a role in SI-PCD, in

which cytosolic acidification and vacuolar breakdown is a prominent feature. As the vacuole

appears to breakdown within 60 minutes of SI induction, if such as nuclease was active as

soon as it was released from the vacuole you would expect DNA fragmentation to occur

soon after. However, in Papaver SI significant DNA fragmentation is not documented until 4

hrs after SI-induction, with 70% of all SI-induced pollen tubes positively labelled for DNA

fragmentation after 14hrs of treatment. Therefore suggesting that there must be some

additional steps between vacuolar rupture and DNA fragmentation to account for this

significant delay in cell death, or SI-PCD does not trigger DNA fragmentation in a similar to

that of ZEN1 in TE differentiation.

The plant vacuole has been likened to the mammalian and yeast lysosome (Nilsson et al.,

2006; Sousa et al., 2011). During yeast lysosomal membrane permeabilization (LMP)

proteases such as cathepsins B, D and L are released into the cytosol and are known to

trigger a mitochondrial apoptotic cascade. Moreover, the vacuolar protease Pep4p,

orthologue of the human CatD, is released from the vacuole into the cytosol in response to

acetic acid (Sousa et al., 2011). Pep4p, is known to contribute to protein degradation in

yeast cells, and is associated with hydrogen peroxide-induced cell death (Marques et al.,

2006; Mason et al., 2005). At present we do not know if cathepsins play a role in the SI

response in *Papaver* pollen tubes, however the plant papain cysteine protease cathepsin B is required for the disease resistance hypersensitive response (Gilroy et al., 2007). Viru*S*-induced gene silencing (VIGS) of cathepsin B prevented programmed cell death (PCD) and compromised disease resistance, and therefore cathepsin could play a role in SI-induced PCD, and should be looked into in the future.

6.3.7 SUMMARY AND MODEL

In this chapter we have explored the role of the vacuole during the SI response in *Papaver* pollen tubes. Figure 6.8 shows a model based on data presented in this thesis (red arrows), and previously published data (yellow arrows), and identified potential pathways involving the breakdown of the vacuolar (white arrows with an orange outline). During an incompatible interaction between the secreted stigmatic protein, *Papaver rhoeas* stigmatic S (PrsS), interacts with *Papaver rhoeas* pollen S (PrpS), pollen receptor in a *S*-haplotype-specific manner, such as $PrsS_1$ binds to $PrpS_1$ (Figure 6.8; (Wheeler et al., 2010)). This interaction triggers alterations in channel activities, influx of K^+ and increases in cytosolic Ca^{2+} (Franklin-Tong et al., 1996; Franklin-Tong et al., 1997; Franklin-Tong et al., 2002).

Increases in cytosolic Ca^{2+} trigger rapid acidification of the cytosol, actin depolymerization, followed by actin foci formation, and vacuolar reorganization and breakdown (Figure 6.8). Both actin depolymerization and stabilization has been associated with vacuolar reorganization, but not breakdown. Treatments with weak acids have shown that artificial acidification is sufficient to trigger rapid vacuolar breakdown, suggesting acidification maybe upstream of vacuolar breakdown. Artificial acidification is also essential for caspase-like activities and actin foci formation.
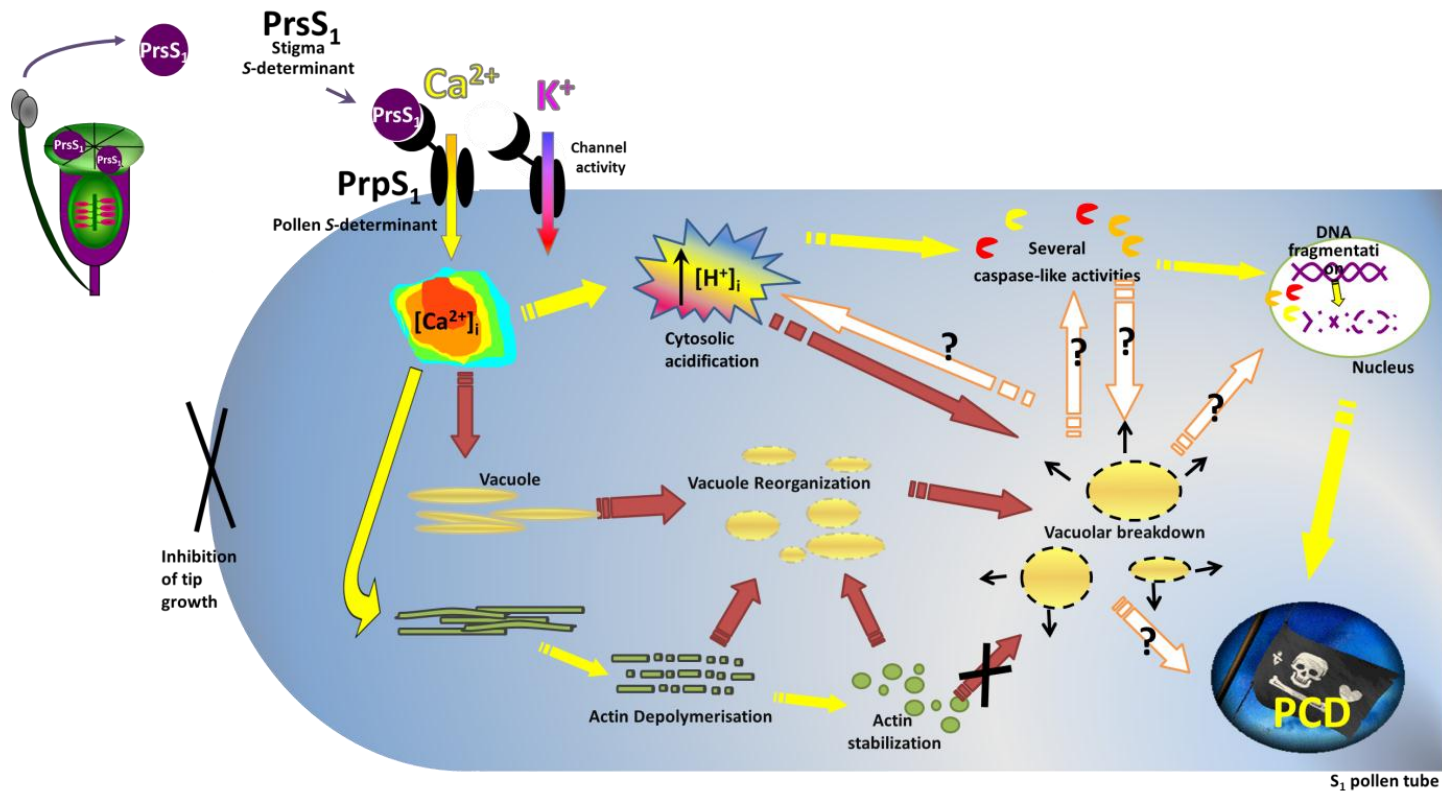
Figure 6.8 Model of the role of SI-induced vacuolar reorganization and breakdown in Papaver pollen tubes

A proposed model for the self-incompatibility mechanism in *Papaver rhoeas* highlighting data present in this chapter (indicated by red arrows). During an incompatible interaction secreted stigmatic protein, *Papaver rhoeas* stigmatic S (PrsS), interacts with *Papaver rhoeas pollen* S (PrpS), pollen receptor in a S haplotype-specific manner, such as $PrsS_1$ binds to $PrpS_1$. This incompatible interaction triggers a rapid influx of Ca^{2+}, which induces a signalling cascade, resulting in the inhibition of tip growth. Increases in Ca^{2+} trigger dramatic alterations in the action cytoskeleton, including the depolymerization of F-actin, which is later followed by stabilization of F-actin into actin foci. Furthermore, increases in Ca^{2+} trigger rapid acidification of the cytosol, moreover acidification of the cytosol is also essential for caspase-3/DEVDase-like activities which are known to translocate to the nucleus where DNA fragmentation occurs resulting in programmed cell death (PCD), ensuring the incompatible pollen does not start to grow again. Data presented in this chapter has identified SI-induced vacuolar reorganization and breakdown, which is also triggered by increases in intracellular Ca^{2+} and cytosolic acidification. Alterations in actin dynamics play a role in actin reorganization but are not involved in triggering vacuolar breakdown. Potential targets and mediators of SI-induced vacuolar breakdown are indicated by white arrows with an orange outline, these include caspase-like activities, DNA fragmentation and PCD.

It is expected that the breakdown of the vacuole results in the acidification of the cytosol, although it may not be the only source of protons during this event. Therefore vacuolar breakdown may also contribute the activation of caspase-like activities and therefore DNA fragmentation and PCD (Figure 6.8). Furthermore, as previously discussed vacuolar breakdown may be the result of caspase-like activities and therefore this avenue should be investigated further (Figure 6.8).

Although the data presented in this chapter has been identified as a significant event in SI-induced pollen tubes, it also raises many questions. Future studies should perhaps focus on trying to answer some of the following questions;

1. To what degree does vacuolar breakdown account for cytosolic acidification?

2. What are the targets of vacuolar breakdown, are there specific proteases that are released and play a role in PCD?

3. How is the vacuole broken down? Is it though caspase-like activities or alterations in channel activities or membrane potential?

CHAPTER 7: GENERAL

DISCUSSION

7.1 INTRODUCTION

Events described in this thesis have been incorporated in to a timeline to show temporally the significance of new data (depicted by black arrows) in relation to previously published data (Figure 7.1). Almost instantaneous alterations in channel activities and increases in $[Ca^{2+}]_{cyt}$ have been identified in SI-induced pollen tubes (Franklin-Tong et al., 1997; Franklin-Tong et al., 2002; Wu et al., 2011). Increases in $[Ca^{2+}]_{cyt}$ have been associated with many downstream events including p26 inhibition, which occurs within 90s of SI induction, and depolymerization of F-actin, which occurs within 2 minutes of SI induction (Geitmann et al., 2000; Rudd et al., 1996; Snowman, 2000; Snowman et al., 2002)(Figure 7.1). Furthermore, actin depolymerization has been linked to PCD (Thomas *et al.,* 2006). During SI microtubules also undergo rapid depolymerization, occurring within 2 minutes of SI-induction; furthermore, research has shown that actin depolymerization can trigger microtubule depolymerization but not vice versa, suggesting alterations in the microtubule status is downstream of SI-induced F-actin alterations (Poulter *et al.,* 2008) (Figure 7.1). Although microtubule depolymerization is not sufficient to induce PCD, blocking SI-induced microtubule depolymerization alleviated some caspase-3-like activities, suggesting microtubules may play a role in SI-PCD (Poulter *et al.,* 2008).

Data presented in this thesis has identified reactive oxygen species (ROS) as an important signalling molecule during the SI response in *Papaver* pollen tubes (Wilkins *et al.,* 2011) (Figure 7.1). SI-induced increases in ROS are documented as early at 6 minutes after addition of PrsS. Furthermore, increases in ROS are mediated by increases in Ca^{2+}, and have also been linked to downstream events including actin foci formation, which is identifiable

within 30 minutes of SI induction, and caspase-3-like activities which occur within 1 hr of SI

induction, but peaks at 5hrs (Bosch and Franklin-Tong, 2007; Bosch and Franklin-Tong, 2008;

Thomas et al., 2006; Wilkins et al., 2011) (Figure 7.1).
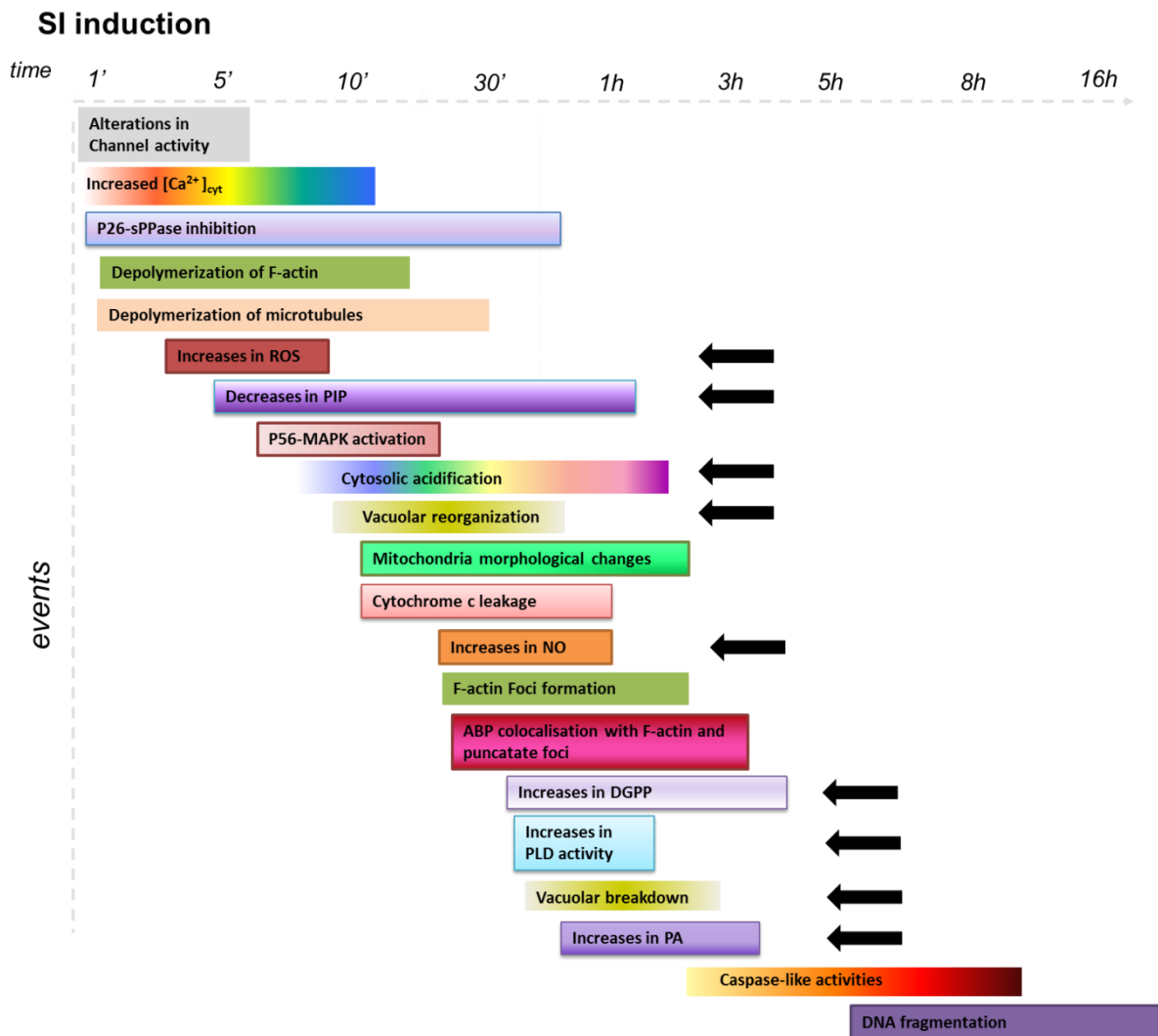
Figure 7.1. A timeline of SI-induced events characterised to date.

Figure shows the temporally SI-induced events in *Papaver* rhoeas pollen to help identify upstream and downstream targets of SI-induced events discussed in this thesis. Black arrows indicate data presented in this thesis.

Soon after ROS signalling begins there is a decrease in the phospholipid phosphatidylinositol

monophosphate (PIP; black arrow, Figure 7.1). At present we do not know what is

responsible for this decrease in PIP, or what its' role is during the SI response; therefore,

these future studies should focus on this to help us understand the relevance of these results. Potential roles and implications of a decrease in PIP levels are discussed in Chapter 4 (Figure 7.1). Another early event during the SI response in *Papaver* pollen tubes is the activation of the MAPK p56, occurring within 10 minutes of SI induction (Li et al., 2007; Rudd et al., 2003). Furthermore, p56 has been linked to downstream events such as increases in caspase-3-like activities and DNA fragmentation, and is mediated by increases in Ca^{2+} (Li et al., 2007; Rudd and Franklin-Tong, 2003; Rudd et al., 2003) (Figure 7.1).

Data presented in this thesis has also shown that acidification of the cytosol occurs within 10 minutes of SI-induction, and reaches its most acidic point, pH 5.5, within 1 hr (Figure 7.1; black arrow). However, due to limitation of the technique used to measure cytosolic pH, we were unable to measure pH of the cytosol prior to this time point (Figure 7.1). As discussed in Chapter 5, it may be that acidification of the cytosol occurs prior to this time point and therefore as more research is carried out on this topic it maybe that the timing of cytosolic acidification shifts. Despite this, data in this thesis has shown that acidification of the cytosol is essential for both caspase-3-like activities and actin foci formation. Furthermore, artificial acidification of the cytosol resulted in the breakdown of the acidic vacuole (Figure 7.1; black arrow). As discussed in Chapter 6, the vacuole was investigated as a potential source of protons responsible for SI-induced acidification, however research showed that acidification can also trigger breakdown of the vacuole, therefore placing acidification events upstream of vacuolar breakdown (Figure 7.1). As vacuolar breakdown is also expected to contribute to cytosolic acidification, future studies should focus on trying to determine to what extent vacuolar rupture contributes to cytosolic acidification. Is there an initial acidification

required to initiate vacuolar breakdown, and if so what is the source of these protons? These questions are discussed in Chapter 6 and are addressed later on in this chapter.

Interestingly, alterations in mitochondrial morphology and cytochrome c leakage also occur within 10 minutes of SI-induction (Geitmann et al., 2004a; Thomas and Franklin-Tong, 2004) (Figure 7.1). Temporal data suggests that both vacuolar and mitochondrial alterations occur at a similar time point; therefore we could hypothesise that a similar mechanism may be responsible for the breakdown of both organelles. Potential mediators are discussed in Chapter 6, and later on in this chapter.

Increases in the signalling messenger nitric oxide (NO) occur ~15 minutes after SI induction, and have been linked to both actin foci formation and caspase-3-like activities (Wilkins *et al.,* 2011) (Figure 7.1; black arrow). Furthermore, increases in Ca^{2+} was identified as an upstream mediator of NO signalling during SI (Wilkins *et al.,* 2011).

As mentioned previously, a significant event during the SI response in *Papaver* pollen tubes is the formation of actin foci (Thomas *et al.,* 2006). The formation of these foci has been linked to several secondary messengers including ROS and NO, however alterations in cytosolic pH also play a significant role in the formation of actin foci (Wilkins *et al.,* 2011). Furthermore, during the SI response these actin foci are decorated with two actin-binding proteins (ABPS), actin depolymerizing factor (ADF) and cyclase-associated protein (CAP). Co-localization of these ABPS with F-actin significantly increased within 10 minutes of SI-induction, and co-localised with actin foci within 30 minutes (Poulter et al., 2011; Poulter et al., 2010). Potential regulators of ABPs and actin foci are discussed later on in this chapter.

Within 20 minutes of SI induction there are significant increases in the phospholipid

diacylglycercol pyrophosphatase (DGPP) which is suspected to act as a signalling molecule

during plant stress (Figure 7.1; black arrow). Furthermore, data suggest that increases in

ROS maybe be upstream of this event (Figure 7.1). At present it is not known what is

downstream of DGPP. However, the addition of exogenous DGPP to pollen tubes may be

utilised in the future to investigate whether DGPP is involved in triggering some of the key SI

markers. For example confocal imaging of DPGG treated cell labelled c-DCFDA for live cell

imaging of the vacuole or fixed and stained with the actin dye rhodamine phalloidin (Rh-Ph),

could be used to investigate the role of DGPP increases on actin foci formation and vacuolar

breakdown.

In addition, after 30 minutes of SI-induction there were significant increases in

phospholipase D (PLD) activities (Figure 7.1; black arrow). PLD has been linked to

phosphatidic acid (PA) production in many systems so it was unsurprising that at a similar

time point there was a significant increase in PA levels in SI-induced pollen tubes (Figure 7.1;

black arrow). PA has been identified as a second messenger in many plant systems and

therefore its potential role in SI-induced pollen tubes is discussed in more detail in Chapter 4

and later on in this Chapter. Furthermore, vacuole breakdown also occurs within 30 minutes

of SI induction (Figure 7.1). As mentioned, acidification of the cytosol appears to be

upstream of vacuolar breakdown, as are increases in Ca^{2+}; however, alterations in actin

dynamics were not involved in vacuolar breakdown, although they may play a role in

vacuolar organization. 1 hr after SI induction increases in caspase-3-like activities occur,

peaking at 5 hrs post-induction (Bosch and Franklin-Tong, 2007) Figure 7.1). Finally, DNA

fragmentation has been documented after 4 hrs of SI-induction, and continued to increase for 10 hrs (Bosch and Franklin-Tong, 2008; Bosch et al., 2008; Jordan et al., 2000).

7.2 TEASING OUT A NETWORK OF SIGNALS

As discussed during this thesis, we have identified several new signalling molecules during the SI response: ROS, NO and several phospholipids. Although this thesis has answered many questions regarding signalling pathways during the SI response, it has also helped identify a new set of potential links within the SI signalling network; these are summarized in Figure 7.2. This model is based upon the data from previously published work on *Papaver* SI response and from data collected during this thesis, (Figure 7.2; yellow arrows). However, new untested targets and pathways during the SI response are indicated by blue arrows, and are based on current literature in other species and systems. These potential pathways will be discussed further with reference to future experimental design and hypotheses.

In particular, two major pathways have been selected as promising topics for future experiments. These pathways are interlinked and contain many components, however, for the purpose of this chapter I will discuss them separately; these are the ROS signalling pathway and the acidification and vacuole breakdown pathway (Figure 7.2). Although data presented during this thesis has made ground breaking advances in both understanding ROS signalling and the role of pH in SI-PCD, many questions remain to be investigated. Some of this will be discussed in this section.
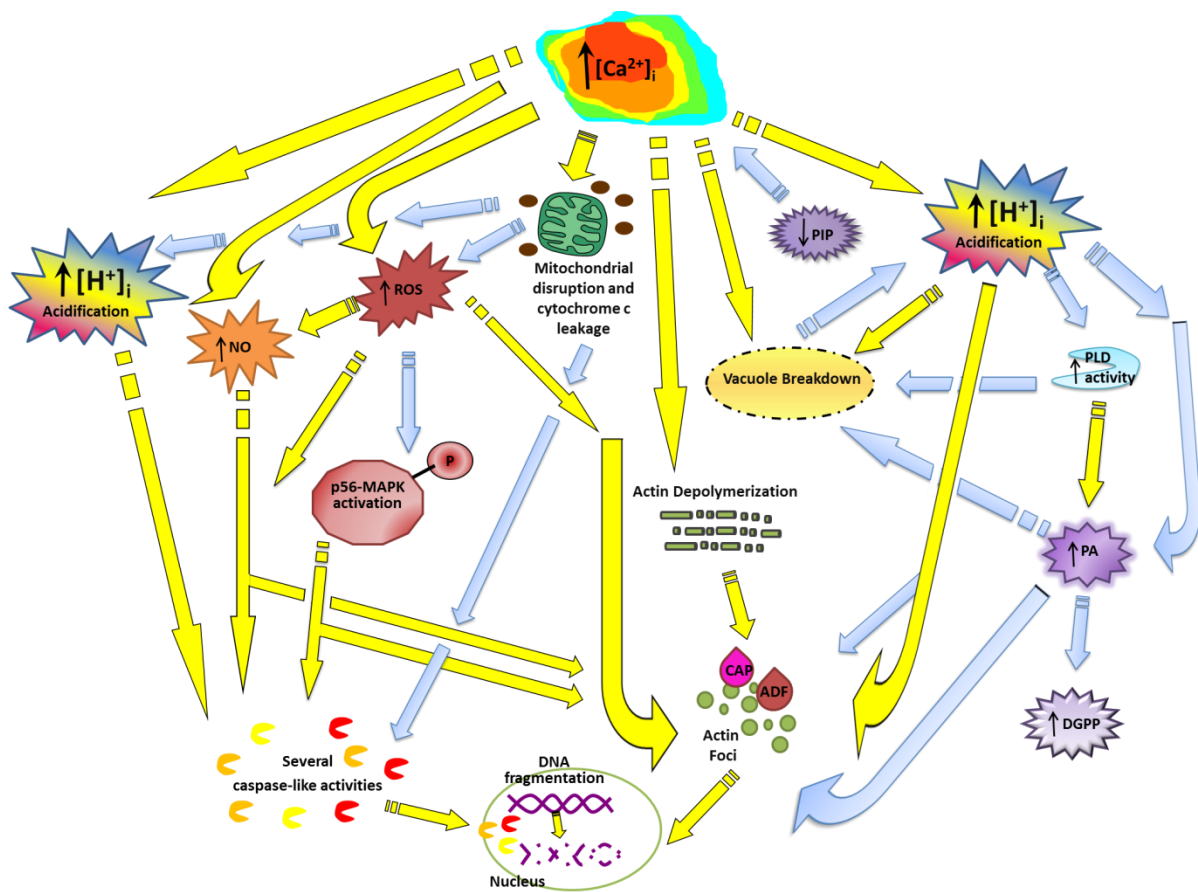
Figure 7.2 A model of Potential SI signalling network in *Papaver* pollen tubes.

Yellow arrows indicate pathways which have been characterized either in this thesis of previously published data. Blue arrows indicate potential pathways were may be of interest for further research.

7.2.1 ROS signalling pathway

Papaver SI triggers almost instantaneous increases in cytosolic Ca^{2+} (Franklin-Tong *et al.,* 1997) (Figure 7.2). These increases in Ca^{2+} trigger transient increases in ROS (Chapter 3; Wilkins *et al.,* 2011)(Figure 7.2). Although live cell imaging of SI events has shown that increases in ROS occur at the membrane of organelles which resemble mitochondria, during the studies presented in this thesis, the localization of ROS production was not thoroughly investigated. Evidence from other systems suggests that the site of intracellular ROS

production influences its signalling role (Foyer and Noctor, 2005; Laloi et al., 2004). We hypothesize that the SI-induced ROS is organelle-derived, and mitochondria are of particular interest (Figure 7.2). To investigate further the origin of SI-induced increases in ROS, co-localization studies of ROS and specific organelles should be undertaken. Such experiments would help to identify the source of ROS and further our understanding of RO*S*-induced signalling events. Imaging could be carried out using probes such as HyPer (a H_2O_2 reporter)(Swanson et al., 2011) which could be introduced into poppy pollen tubes using a biolistic approach and incubated with a live cell imaging probe for mitochondria, such as CMXRos (Bothwell et al., 2006). Furthermore, recent research has shown that the *Papaver rhoeas* pollen *S*-determinant (PrpS) can be expressed in Arabidopsis, and addition of *Papaver rhoeas* stigmatic S protein (PrsS) is able to induced *Papaver* specific SI-PCD in this system (de Graaf et al., 2012). Therefore, using these lines crossed with a genetically-encoded biosensor such as HyPer could help us to determine the localization of ROS during the SI response. Particularly as HyPer has been successfully targeted to peroxisomes in Arabidopsis (Costa et al., 2010), which could also be involved in SI-induced increases in ROS.

Another pressing question is what is the molecular basis for ROS production? Research presented in this thesis has shown that the NADPH oxidase inhibitor DPI, is able to prevent SI-induced caspase-3-like activities (Figure 7.2). Therefore, these data suggest that SI-induced ROS signalling, may be produced by an NADPH oxidase. As discussed in Chapter 3, NADPH oxidase is usually localised at the plasma membrane, and as ROS increases appear to be organelle derived, it suggests that there could be several sources of ROS during the SI response. To determine the localization of *Papaver* NADPH oxidase, immunolocalisation experiments could be carried out; however, several other species have shown that NADPH

oxidase resides at the plasma membrane in pollen tubes (Potocký et al., 2007). These data suggest that NADPH oxidase is not responsible for the ROS increases localised in organelles. However, to investigate whether NADPH oxidase plays a role in SI-induced increases in ROS, antisense oligonucleotides for NADPH oxidase could be used to block NADPH oxidase activities in conjunction with live cell imaging of ROS during an SI response. Furthermore, there are several NADPH oxidase knockout lines in Arabidopsis which could be crossed with the PrpS Aradidopsis lines to investigate the role of NADPH oxidase activity during the SI response.

Data presented in this thesis has also identified caspase-3-like activities as a target of SI-induced increase in ROS (Figure 7.2). At present we do not know how ROS increases trigger this response. As previously discussed, caspase-3-like activities require an acidic environment to be functionally active (Figure 7.2). Based on temporal data, cytosolic acidification occurs at a very similar time point to SI-induced increases in ROS (Figure 7.2). This raises the question 'Are the events which trigger acidification of the cytosol also involved in triggering increases in ROS?'. As mentioned, mitochondria are suspected as a source of SI-induced increase in ROS. Mitochondria also store protons, and therefore disruption mitochondria, perhaps in the form of ROS production, may result in the leakage of protons which may also contribute to SI-induced acidification (Figure 7.2). The link between mitochondrial leakage and intracellular acidification has already been documented in several species including *Caenorhabditis elegans* and mammalian cells (Johnson and Nehrke, 2010). Therefore, future studies should investigate the role of the mitochondria as this may help us understand how ROS is generated and further our understanding of how SI-induced acidification occurs. Anticancer drugs, such as betulinic acid (BetA) and cyclosporin

A (CsA) could be used to trigger or block mitochondria permeability transition pore (PTP) opening, and therefore could be used to investigate whether alterations in mitochondria permeability triggers increases in ROS or contributed to acidification of the cytosol.

Furthermore, evidence suggests that there may be crosstalk between NADPH oxidase and mitochondria-derived ROS (Desouki et al., 2005; Wenzel et al., 2008; Wosniak et al., 2009). However, as previously discussed, if NADPH oxidase plays a role in SI-induced increase in ROS at the mitochondria, knockout lines of NADPH oxidase or oligonucleotides for NADPH oxidase could be used in conjunction with pH imaging to determine whether inhibiting NADPH oxidase prevents SI-induced acidification. These experiments would help to determine whether the activation of NADPH oxidase-derived ROS plays a role in SI-induced acidification.

Research has also shown that during SI the mitochondria leaks cytochrome c, (Thomas and Franklin-Tong, 2004) (Figure 7.2). Data from heat shock-induced cell death in tobacco suggest that cytochrome c is released in a ROS-dependent manner (Vacca *et al.,* 2006). Therefore, SI-induced increases in ROS, which probably originate at the mitochondria, may trigger cytochrome c leakage (Figure 7.2). Moreover, in heat shock-induced cells cytochrome c leakage has also been linked to increases in caspase-3-like activities and therefore cell death (Balk et al., 2003; Balk et al., 1999) (Figure 7.2). At present it is not known if caspase-like activities in *Papaver* pollen tubes are activated by cytochrome c and is therefore identified as a possible link in Figure 7.2. However, increases in ROS and NO have been linked to SI-induced increases in caspase-3-like activities suggesting there could be a pathway in which ROS triggers cytochrome c leakage, resulting in the activation of caspase-

3-like activities and therefore cell death. However, at present this is no evidence that cytochrome c is a direct activator of caspase-like activities in plant cells.

Cytochrome c leakage occurs during Zinnia tracheary element development PCD. However, if vacuolar rupture is prevented with Ca^{2+} inhibitors after cytochrome c leakage has occurred, cytochrome c was not sufficient to induce PCD (Yu et al., 2002). However, data presented in this thesis has shown that without acidification of the cytosol caspase-like activities are not triggered. As vacuolar rupture and presumably cytosolic pH alterations are inhibited it suggests that caspase-like activities would not active with or with cytochrome c leakage. However breakdown of the mitochondria may contribute to cytosolic acidification, the vacuole is a much larger organelle and therefore it may be that mitochondria acidification may not be sufficient to create the correct environment for caspase-3-like activities. Therefore to investigate whether cytochrome c does play a role in triggering caspase-3-like activities, pollen tubes should be treated with an inhibitor of cytochrome c leakage, such as CsA, and the pH of the pollen tube manipulated to pH 5.5 with propionic acid (as described in Chapter 5 &6), and caspase-like activities could be monitored with a caspase detection probe as described in Chapter 2.

Another possible role of ROS could be the activation of MAPKs (Figure 7.2). SI induced the activation of p56-MAPK has been linked to DNA fragmentation (Li et al., 2007; Rudd et al., 2003). During a pathogen response in root hairs, increases in ROS have been linked to the activation of a serine/threonine kinase *OXIDATIVE SIGNAL-INDUCIBLE1* (OXI1) (Rentel *et al.,* 2004). In turn, OXI1 activates MAPK 3 & 6 which are involved in basal resistant to a pathogen. At present we do not know if OXI1 also plays a role in *Papaver* SI events, however

these data suggest that ROS could play a role in the activation of MAPK during a cell death event, and therefore isa possible pathway to be investigated in the future (Figure 7.2). During the studies presented in this thesis ROS signalling was investigated during the SI response. However, exogenous ROS was not added to pollen tubes to investigate downstream signalling events. This technique could be used to investigate whether ROS is upstream of p56 activation by in gel kinase assay of ROS treated pollen tubes. Furthermore inhibitors of ROS, such as tempol or DPI, could be used in conjunction with an SI treatment to block ROS signalling and monitor whether this affects p56 activity.

7.2.3 Acidification and vacuole breakdown pathway

Research presented in this thesis has shown that during the SI response there is significant acidification of the cytosol (Chapter 5). Moreover, this acidification is mediated by increases in cytosolic Ca^{2+} (Figure 7.2). As discussed in Chapter 5, there are several possible sources of protons which could contribute to cytosolic acidification, namely the vacuole. Data showed that during the SI response there was rapid reorganization and breakdown of the acidic vacuole, and was therefore suspected to contributing to SI induced cytosolic acidification (Chapter 6)(Figure 7.2). However, further investigation showed that artificial acidification of the cytosol was sufficient to trigger vacuolar breakdown. Unfortunately the cytosol was artificially acidified to pH 5.5 or maintained at pH 7, and other pHs were not tested. Artificial acidification of the cytosol using a range of pH buffers will help to identify whether there is a specific level of acidification needed to trigger vacuolar breakdown. In turn these experiments would help us to further understand the role of SI-induced signalling events

involved acidification of the cytosol, and potentially identify the mechanism involved in triggering vacuolar rupture.

At present these data suggest that another source of protons maybe involved in acidification of the cytosol. As discussed in Chapter 5, during the SI response there are significant alterations in channel activities (Wu et al., 2011). The SI-activated conductance is permeable to the divalent cation, Ca^{2+}, and the monovalent ion K^+, however H^+ currents were not investigated. Whole-cell patch clamping of pollen protoplasts could be used to monitor H^+ currents during an SI response, and assess whether an influx of H^+ from external medium could contributes to SI-induced cytosolic acidification.

As previously discussed in Chapter 6, vacuolar breakdown is a common event during plant PCD. Studies presented here we have shown that SI induction, increases in Ca^{2+} and artificial acidification of the cytosol are sufficient to induced vacuolar breakdown (Figure 7.2). A present the mechanism involved in triggering vacuolar rupture is not yet known in any species or event, and therefore this topic is of considerable interest and should be pursued further during *Papaver* SI. As discussed, SI-induced vacuolar breakdown may be regulated in a pH-dependent manner. Data presented in this thesis has shown that during the SI response there are significant increases in PLD activities (Figure 7.2). At present we do not know which PLDs are present in *Papaver* pollen tubes, however research has shown that the pH sensitive PLDα, plays a role in membrane tethering (Bargmann and Munnik, 2006; Munnik and Musgrave, 2001; Pappan and Wang, 1999). Moreover, data from castor bean leaf and seedling tissues suggests PLD is localised to the vacuole (Xu *et al.,* 1996). We therefore hypothesise that during the SI response, acidification of the cytosol may result in

the pH-dependent activation of PLD, which could be responsible for the breakdown of the vacuole, though destabilization of the tonoplast (Figure 7.2).

However, another example of lysosomal membrane permeability (LMP)-induced cell death suggests that phosphatidic acid (PA), the product of PLD activities, is involved in the destabilised the lysosome from rat livers, through increased permeability to K^+ and H^+ (Yi *et al.,* 2006). These data suggest that PA could also play a role in membrane destabilization during SI in *Papaver* pollen tubes (Figure 7.2). PA increases within 40 minutes of SI induction, which is a similar time point to which vacuolar breakdown begins and therefore this could be a potential role for PA increase during this response. Addition of exogenous PA to *Papaver* pollen tubes labelled with the vacuolar probe c-DCFDA, would help to investigate this potential link.

Recently there has been evidence to suggest that PA, could also play a role as a pH biosensor (Shin and Loewen, 2011). Data has shown that due to the pKa of PA, it is able to change its protonation state in response to changes in intracellular pH, becoming more protonated in acidic environments. These changes in PA protonation state can be sensed by protein effectors which led to a signalling response (Shin and Loewen, 2011). In yeast cells, during both glucose starvation and acid stress in hypomorphic mutants of the plasma membrane proton ATPase, *Pma,* acidification of the cytosol occurs. This acidification altered the protonation state of PA at the endoplasmic reticulum (ER), which lead to the release of the transcriptional repressor Opi1 (Young et al., 2010b). Opi1 translocate to the nucleus where it is involved in repressing the transcription of many genes, facilitating global repression of lipid metabolism and therefore prevent the synthesis of new membranes

which would be required for cell growth (Carman and Henry, 2007; Loewen et al., 2004; Young et al., 2010b). These data suggest that PA could potentially act as an intermediate sensor for SI-induced acidification (Figure 7.2). Investigation into the role of pH in PA signalling during the SI response could be carried out by artificially acidifying pollen tubes with propionic acid (as described in Chapter 5&6), and monitoring PA levels through lipid extractions described in Chapter 2.

Throughout this thesis actin foci have been used as a key marker of the SI response. Research has shown that increases in Ca^{2+}, ROS, NO, and acidification of the cytosol, all play a role in mediating SI-induced actin foci formation (Geitmann et al., 2000; Snowman et al., 2002; Wilkins et al., 2011)(Chapter 3 & 5). As previously discussed actin foci are decorated with ABPs, ADF and CAP (Poulter et al., 2011; Poulter et al., 2010), and therefore perhaps upstream mediators of actin foci are interacting with these ABP to induce their formation. Research has shown that the ABP, ADF, is pH-sensitive. As discussed in Chapter 5, in an acidic environment ADF co-localizes with actin filaments, and when the pH was increased, ADF resumes it depolymerizing role (Bernstein et al., 2000; Gungabissoon et al., 1998; Hawkins et al., 1993). We therefore hypothesise that SI-induced acidification manipulates ADF activity which in turn mediated actin foci formation (Figure 7.2). Experimentally this theory could be tested by using propionic acid to artificially manipulate cytosolic pH of the pollen tube, and co-localisation of actin foci with ADF could be monitored through immunolocalisation studies.

As discussed in Chapter 4, another potential mediator of SI-induced actin foci is the phospholipid PA (Figure 7.2). PA is known to bind capping protein (CP), inhibiting its activity,

resulting in increases in filament elongation and density in Arabidopsis (Huang, 2006; Li et al., 2012). At present we do not know if CP is associated with actin foci during the SI response in *Papaver* pollen tubes, however this research such actin could be a potential target of PA signalling. Immunolocalisation studies of CP during the SI response followed by exogenous PA treatments could be used to investigate whether CP is associated with SI-induced actin foci.

Another key marker of PCD during the SI response is capsase-3-like activities (Chapter 3, 5 & 6) (Bosch and Franklin-Tong, 2007). Data presented in this thesis has shown that cytosolic acidification occurs within an 1 hr of SI induction, and previous data has shown that caspase-3-like peak at 5 hrs (Bosch and Franklin-Tong, 2007). These data suggest there must be intermediate events, which account for the delay in caspase-3-like activities during the SI response. The most obvious conclusion is that caspase-3-like activities are compartmentalized during the initial acidification and are only released at a later time point. Imaging of caspase-3-like activities has shown that they are cytosolic within 2 hours for SI induction (Bosch and Franklin-Tong, 2007). Therefore these results suggest that the delay in caspase-3-like activities is not due to compartmentalization and therefore perhaps something is inhibiting their activity, or perhaps they are part of a strict signalling cascade, which could be linked to cytochrome c leakage as previously discussed.

7.3 COMPARISON WITH EVENTS IN OTHER SI SPECIES

As discussed, data presented in this thesis has shown that during the SI response in *Papaver* pollen tubes there are increases in ROS and NO, the formation of actin foci and increases in

caspase-3-like activities, and vacuolar breakdown. These SI-induced events have been investigated in *S*-RNase and SRK/SP11 (Brassica) based SI systems and similarities between these systems will be discussed here.

During an SI response in olive (*Olea europaea* L.) papillar cells, cell death is associated with increases in both $O_2^{\cdot-}$ and NO (Serrano *et al.,* 2012). Data presented suggested that a peroxynitrite was formed as the result of a reaction between $O^{2\cdot-}$ and NO. This peroxynitrite was associated with protein nitration, and PCD. However, as yet detailed temporal and spatial data of $O_2^{\cdot-}$ and NO generation is yet to be shown. As discussed in Chapter 3, during the SI response in *Papaver* pollen tubes there are significant increase in NO within 20 minutes of SI induction. Although we did not specifically examine O_2^- levels in *Papaver* pollen, similarly to olive SI, increases in NO were also associated with PCD. Unfortunately at present live cell imaging of olive SI-induced ROS decrease has not been presented and therefore it is difficult to comment on their results.

During *S*-RNAse-SI in *Pyrus* pollen tubes there was a disruption of tip-localized ROS, which was associated with a decrease in ROS formation at the mitochondria and cell walls (Wang *et al.,* 2010). This is very different to SI-induced *Papaver* pollen where SI induction was associated with a rapid, but transient increase in ROS (Wilkins *et al.,* 2011). Wang *et al.,* (2010) also suggested that disruption of ROS production at the mitochondria was due to alterations in mitochondria, including membrane potential collapse, cytochrome c leakage and swelling (Wang *et al.,* 2009). However, the reduction in ROS production at the cell wall was suspected to be due to a decrease in NADPH activity. During *Papaver* SI, ROS increases were associated with an organelle which resembled the mitochondria, and was not

associated with a decrease in ROS levels. Moreover, inhibitors of NADPH oxidase were used to rescue SI-induced *Papaver* pollen from actin foci formation and caspase-3-like activities and therefore PCD. Furthermore, During Pyrus SI disruption of ROS also results in the apparent depolymerization of actin cytoskeleton. Interestingly in *Papaver* SI ROS increases were responsible for inducing actin polymerization in to actin foci. When SI-induced actin alterations are compared in both *Pyrus* and *Papaver* pollen the actin formation actually looks very similar despite different classification.

In summary, both *Papaver* and Olive SI showed increase in a NO, moreover *Papaver* SI also showed an increase in ROS, which was associated with PCD. However, *S*-RNase based SI suggested reduction in tip-localized ROS triggered cell death, which is very different to SI-induced responses in *Papaver* pollen. Interestingly despite the opposite observations of ROS levels, both systems have shown there are alterations in actin during SI and PCD is triggered as a result of these ROS alterations.

In addition, another similarity between the different SI systems is induction of vacuolar breakdown. During *S*-RNase SI, vacuolar breakdown is thought to be key feature (Goldraij et al., 2006; Meng et al., 2009). As discussed in Chapter 1, it is thought that non-self-*S*-RNases are compartmentalized to prevent degradation of pollen tube RNAs. However, during an incompatible interaction compartmentalised self- *S*-RNases are released from the vacuole, allowing the degradation of self-RNAs leading to cell death. The release of self- *S*-RNases is thought to be due to rupture of the vacuolar compartment (Goldraij et al., 2006; McClure, 2006; Meng et al., 2009). At present, live cell imaging of vacuolar breakdown has yet to be shown during *S*-RNase-based SI and therefore it is difficult to compare this event with

Papaver SI-induced vacuolar breakdown. However, during an incompatible SI response in papilla cells of *Brassica rapa,* disruption of the vacuole network has been observed (Iwano et al., 2007). However, temporal data was not collected to it is difficult to determine whether vacuolar breakdown in this system is similar to that of SI induced *Papaver* pollen tubes. Despite this these data suggest that the vacuolar breakdown is a significant event in both gametophytic and sporophytic SI response. Although it is still unknown what mediates vacuole breakdown in all SI systems, and plant cells in general, data presented here suggest a possible similarities in mechanism may exist in different SI systems, despite the different *S*-determinant.

In summary, although there many difference between the different SI systems, such as *S*-determinants, recent research has identified several common features including alterations in NO and ROS levels, and vacuolar breakdown. Future studies identifying common factors between these different SI systems will help us to further our understanding of key PCD events in plant reproduction.

7.4 SUMMARY

Data presented in this thesis has made considerable progress in our understanding of SI-induced signalling mechanisms in *Papaver* pollen tubes. Figure 7.3 is a model based on SI-induced events to date. These included increases in both ROS and NO (Chapter 3), and alterations in phospholipid levels and phospholipase D activities (Chapter 4). SI –induced cytosolic acidification (Chapter 5) and vacuolar reorganization and breakdown (Chapter 6).
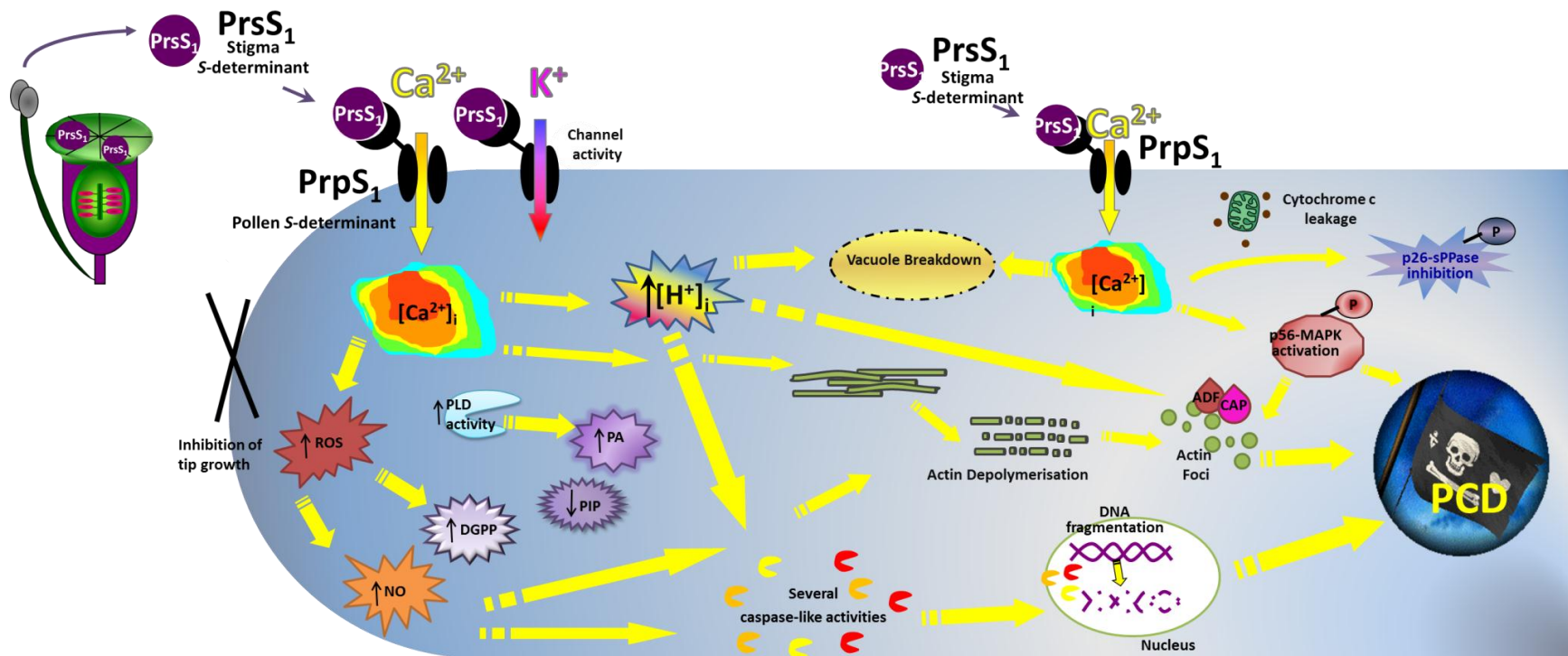
S₁ pollen tube

Figure

7.3. Model of SI in *Papaver* rhoeas pollen based on data presented in the thesis and previously publish data.

A proposed model for the self-incompatibility mechanism in *Papaver rhoeas*. During an incompatible interaction secreted stigmatic protein, *Papaver rhoeas* stigmatic S (PrsS), interacts with *Papaver rhoeas pollen* S (PrpS), pollen receptor in a S haplotype-specific manner, such as $PrsS_1$ binds to $PrpS_1$. This incompatible interaction triggers a rapid influx of Ca^{2+}, which induces a signalling cascade, resulting in the inhibition of tip growth. Increases in Ca^{2+} trigger dramatic alterations in the action cytoskeleton, including the depolymerization of F-actin, which is later followed by stabilisation of F-actin into actin foci, which are decorated with actin binding proteins (ABPS), actin-depolymerizing factor (ADF) and cyclase-associated protein (CAP). Increases in cytosolic Ca^{2+} also trigger transient increases in both reactive oxygen species (ROS) and nitric oxide (NO). These increases were linked to actin foci formation and caspase-3-like activities. Moreover, there are alterations in channel activity and acidification of the cytosol and the release of cytochrome c which is involved in programmed cell death (PCD). Furthermore SI-induced rapid acidification of the cytosol which is linked to vacuolar breakdown, actin foci formation and caspase-3-lika activities. Furthermore, there is the activation of caspase-like activities which are known to translocate to the nucleus where DNA fragmentation occurs resulting in PCD, ensuring the incompatible pollen does not start to grow again. There is also the phosphorylation and inactivation of soluble inorganic pyrophosphatases (sPPases) Pr-p26.1a/b, and the phosphorylation and activation of mitogen activated protein kinases (MAPK) p56 which may signal to PCD. In addition SI-induced led the alterations in phospholipid activities, most notably increases in phosphatidic acid (PA) and diacylglycercol pyrophosphatase (DGPP), and decrease in phosphatidylinositol monophosphate (PIP). Furthermore increases in phospholipase D activity has been linked to SI-induced increase in PA, and increases in ROS may have a role in SI-induced increases in DGPP

243

CHAPTER 8: LIST OF

REFERENCES

Ahmad, K.A., K.B. Iskandar, J.L. Hirpara, M.-V. Clement, and S. Pervaiz. 2004. Hydrogen Peroxide-Mediated Cytosolic Acidification Is a Signal for Mitochondrial Translocation of Bax during Drug-Induced Apoptosis of Tumor Cells. *Cancer Res*. 64:7867-7878.

Allwood, E.G. 2002. Regulation of the Pollen-Specific Actin-Depolymerizing Factor LlADF1. *The Plant Cell Online*. 14:2915-2927.

Apel, K., and H. Hirt. 2004. REACTIVE OXYGEN SPECIES: Metabolism, Oxidative Stress, and Signal Transduction. *Annual Review of Plant Biology*. 55:373-399.

Asai, S., K. Ohta, and H. Yoshioka. 2008. MAPK Signaling Regulates Nitric Oxide and NADPH Oxidase-Dependent Oxidative Bursts in Nicotiana benthamiana. *The Plant Cell Online*. 20:1390-1406.

Asai, S., and H. Yoshioka. 2008. The role of radical burst via MAPK signaling in plant immunity. *Plant Signal Behav*. 3:920-922.

Auh, C.K., and T.M. Murphy. 1995. Plasma Membrane Redox Enzyme Is Involved in the Synthesis of O2- and H2O2 by Phytophthora Elicitor-Stimulated Rose Cells. *Plant Physiology*. 107:1241-1247.

Balk, J., S.K. Chew, C.J. Leaver, and P.F. McCabe. 2003. The intermembrane space of plant mitochondria contains a DNase activity that may be involved in programmed cell death. *Plant J*. 34:573-583.

Balk, J., C.J. Leaver, and P.F. McCabe. 1999. Translocation of cytochrome c from the mitochondria to the cytosol occurs during heat-induced programmed cell death in cucumber plants. *FEBS Letters*. 463:151-154.

Banks, D.F. 1966. Organic Polyvalent Iodine Compounds. *Chem. Rev*. 66:243–266.

Bargmann, B.O., A.M. Laxalt, B. ter Riet, C. Testerink, E. Merquiol, A. Mosblech, A. Leon-Reyes, C.M. Pieterse, M.A. Haring, I. Heilmann, D. Bartels, and T. Munnik. 2009a. Reassessing the role of phospholipase D in the Arabidopsis wounding response. *Plant, Cell & Environment*. 32:837-850.

Bargmann, B.O., A.M. Laxalt, B. ter Riet, B. van Schooten, E. Merquiol, C. Testerink, M.A. Haring, D. Bartels, and T. Munnik. 2009b. Multiple PLDs required for high salinity and water deficit tolerance in plants. *Plant Cell Physiol*. 50:78-89.

Bargmann, B.O., and T. Munnik. 2006. The role of phospholipase D in plant stress responses. *Current Opinion in Plant Biology*. 9:515-522.

Bargmann, B.O.R., A.M. Laxalt, B. ter Riet, E. Schouten, W. van Leeuwen, H.L. Dekker, C.G. de Koster, M.A. Haring, and T. Munnik. 2006. LePLD beta 1 activation and relocalization in suspension-cultured tomato cells treated with xylanase. *Plant J*. 45:358-368.

Barry, M.A., and A. Eastman. 1992. Endonuclease activation during apoptosis: The role of cytosolic Ca2+ and pH. *Biochemical and Biophysical Research Communications*. 186:782-789.

Belenghi, B., M. Salomon, and A. Levine. 2004. Caspase-like activity in the seedlings of Pisum sativum eliminates weaker shoots during early vegetative development by induction of cell death. *Journal of Experimental Botany*. 55:889-897.

Beligni, M.V., and L. Lamattina. 2000. Nitric oxide stimulates seed germination and de-etiolation, and inhibits hypocotyl elongation, three light-inducible responses in plants. *Planta*. 210:215-221.

Bernstein, B.W., W.B. Painter, H. Chen, L.S. Minamide, H. Abe, and J.R. Bamburg. 2000. Intracellular pH modulation of ADF/cofilin proteins. *Cell Motility and the Cytoskeleton*. 47:319-336.

Bethke, P.C. 2004. Apoplastic Synthesis of Nitric Oxide by Plant Tissues. *The Plant Cell Online*. 16:332-341.

Bethke, P.C., M.R. Badger, and R.L. Jones. 2004. Apoplastic Synthesis of Nitric Oxide by Plant Tissues. *The Plant Cell Online*. 16:332-341.

Bhattacharjee, S. 2012. The Language of Reactive Oxygen Species Signaling in Plants. *Journal of Botany*. 2012.

Bibikova, T.N., T. Jacob, I. Dahse, and S. Gilroy. 1998. Localized changes in apoplastic and cytoplasmic pH are associated with root hair development in Arabidopsis thaliana. *Development*. 125:2925-2934.

Bibikova, T.N., A. Zhigilei, and S. Gilroy. 1997. Root hair growth in Arabidopsis thaliana is directed by calcium and an endogenous polarity. *Planta*. 203:495-505.

Bollhöner, B., J. Prestele, and H. Tuominen. 2012. Xylem cell death: emerging understanding of regulation and function. *Journal of Experimental Botany*. 63:1081-1094.

Bosch, M., and V.E. Franklin-Tong. 2007. Temporal and spatial activation of caspase-like enzymes induced by self-incompatibility in Papaver pollen. *Proceedings of the National Academy of Sciences*. 104:18327-18332.

Bosch, M., and V.E. Franklin-Tong. 2008. Self-incompatibility in Papaver: signalling to trigger PCD in incompatible pollen. *Journal of Experimental Botany*. 59:481-490.

Bosch, M., N.S. Poulter, R.M. Perry, K.A. Wilkins, and V.E. Franklin-Tong. 2010. Characterization of a legumain/vacuolar processing enzyme and YVADase activity in Papaver pollen. *Plant Molecular Biology*. 74:381-393.

Bosch, M., N.S. Poulter, S. Vatovec, and V.E. Franklin-Tong. 2008. Initiation of Programmed Cell Death in Self-Incompatibility: Role for Cytoskeleton Modifications and Several Caspase-Like Activities. *Molecular Plant*. 1:879-887.

Bothwell, J.H.F., C. Brownlee, A.M. Hetherington, C.K.Y. Ng, G.L. Wheeler, and M.R. McAinsh. 2006. Biolistic delivery of Ca^{2+} dyes into plant and algal cells. *The Plant Journal*. 46:327-335.

Bower, M.S., D.D. Matias, E. FernandesCarvalho, M. Mazzurco, T.S. Gu, S.J. Rothstein, and D.R. Goring. 1996. Two members of the thioredoxin-h family interact with the kinase domain of a Brassica S locus receptor kinase. *Plant Cell*. 8:1641-1650.

Bozhkov, P.V., L.H. Filonova, M.F. Suarez, A. Helmersson, A.P. Smertenko, B. Zhivotovsky, and S. von Arnold. 2003. VEIDase is a principal caspase-like activity involved in plant programmed cell death and essential for embryonic pattern formation. *Cell Death Differ*. 11:175-182.

Bradford, M.M. 1976. A rapid and sensitive method for the quantitation of microgram quantities of protein utilizing the principle of protein-dye binding. *Analytical Biochemistry*. 72:248-254.

Bradley, D.J., P. Kjellbom, and C.J. Lamb. 1992. Elicitor- and wound-induced oxidative cross-linking of a proline-rich plant cell wall protein: a novel, rapid defense response. *Cell*. 70:21-30.

Brewbaker, J.L., and N. Shapiro. 1959. HOMOZYGOSITY AND S GENE MUTATION. *Nature*. 183:1209-1210.

Bubb, M.R., A.M.J. Senderowicz, E.A. Sausville, K.L.K. Duncan, and E.D. Korn. 1994. JASPLAKINOLIDE, A CYTOTOXIC NATURAL PRODUCT, INDUCES ACTIN POLYMERIZATION AND COMPETITIVELY INHIBITS THE BINDING OF PHALLOIDIN TO F-ACTIN. *Journal of Biological Chemistry*. 269:14869-14871.

Cabrillac, D., J.M. Cock, C. Dumas, and T. Gaude. 2001. The S-locus receptor kinase is inhibited by thioredoxins and activated by pollen coat proteins. *Nature*. 410:220-223.

Cardenas, L. 2009. New findings in the mechanisms regulating polar growth in root hair cells. *Plant Signal Behav*. 4:4-8.

Carlier, M.F., V. Laurent, J. Santolini, R. Melki, D. Didry, G.X. Xia, Y. Hong, N.H. Chua, and D. Pantaloni. 1997. Actin depolymerizing factor (ADF/cofilin) enhances the rate of filament turnover: implication in actin-based motility. *The Journal of Cell Biology*. 136:1307-1322.

Carman, G.M., and S.A. Henry. 2007. Phosphatidic Acid Plays a Central Role in the Transcriptional Regulation of Glycerophospholipid Synthesis in Saccharomyces cerevisiae. *Journal of Biological Chemistry*. 282:37293-37297.

Carol, R.J., and L. Dolan. 2006. The role of reactive oxygen species in cell growth: lessons from root hairs. *Journal of Experimental Botany*. 57:1829-1834.

Carol, R.J., S. Takeda, P. Linstead, M.C. Durrant, H. Kakesova, P. Derbyshire, S. Drea, V. Zarsky, and L. Dolan. 2005. A RhoGDP dissociation inhibitor spatially regulates growth in root hair cells. *Nature*. 438:1013-1016.

Chan, C.Y., C. Prudom, S.M. Raines, S. Charkhzarrin, S.D. Melman, L.P. De Haro, C. Allen, S.A. Lee, L.A. Sklar, and K.J. Parra. 2012. Inhibitors of V-ATPase proton transport reveal uncoupling functions of tether linking cytosolic and membrane domains of V0 subunit a (Vph1p). *J Biol Chem*. 287:10236-10250.

Cheung, A.Y., and H.-m. Wu. 2008. Structural and Signaling Networks for the Polar Cell Growth Machinery in Pollen Tubes. *Annual Review of Plant Biology*. 59:547-572.

Chookajorn, T., A. Kachroo, D.R. Ripoll, A.G. Clark, and J.B. Nasrallah. 2004. Specificity determinants and diversification of the Brassica self-incompatibility pollen ligand. *P Natl Acad Sci USA*. 101:911-917.

Clarke, A., R. Desikan, R.D. Hurst, J.T. Hancock, and S.J. Neill. 2000. NO way back: nitric oxide and programmed cell death in Arabidopsis thaliana suspension cultures. *The Plant Journal*. 24:667-677.

Coffeen, W.C., and T.J. Wolpert. 2004. Purification and characterization of serine proteases that exhibit caspase-like activity and are associated with programmed cell death in Avena sativa. *Plant Cell*. 16:857-873.

Correa-Aragunde, N., M. Graziano, and L. Lamattina. 2004. Nitric oxide plays a central role in determining lateral root development in tomato. *Planta*. 218:900-905.

Correa-Aragunde, N., C. Lombardo, and L. Lamattina. 2008. Nitric oxide: an active nitrogen molecule that modulates cellulose synthesis in tomato roots. *New Phytol*. 179:386-396.

Costa, A., I. Drago, S. Behera, M. Zottini, P. Pizzo, J.I. Schroeder, T. Pozzan, and F.L. Schiavo. 2010. H_2O_2 in plant peroxisomes: an in vivo analysis uncovers a Ca^{2+}-dependent scavenging system. *The Plant Journal*. 62:760-772.

Danon, A., V. Delorme, N. Mailhac, and P. Gallois. 2000. Plant programmed cell death: A common way to die. *Plant Physiology and Biochemistry*. 38:647-655.

Daugirdas, J.T., J. Arrieta, M. Ye, G. Flores, and D.C. Battle. 1995. Intracellular acidification associated with changes in free cytosolic calcium. Evidence for Ca2+/H+ exchange via a plasma membrane Ca(2+)-ATPase in vascular smooth muscle cells. *The Journal of Clinical Investigation*. 95:1480-1489.

Davis, L.E., A.G. Stephenson, and J.A. Winsor. 1987. POLLEN COMPETITION IMPROVES PERFORMANCE AND REPRODUCTIVE OUTPUT OF THE COMMON ZUCCHINI SQUASH UNDER FIELD CONDITIONS. *Journal of the American Society for Horticultural Science*. 112:712-716.

de Graaf, B.H., J.J. Rudd, M.J. Wheeler, R.M. Perry, E.M. Bell, K. Osman, F.C. Franklin, and V.E. Franklin-Tong. 2006. Self-incompatibility in Papaver targets soluble inorganic pyrophosphatases in pollen. *Nature*. 444:490-493.

de Graaf, B.H., S. Vatovec, J.A. Juarez-Diaz, L. Chai, K. Kooblall, K.A. Wilkins, H. Zou, T. Forbes, F.C. Franklin, and V.E. Franklin-Tong. 2012. The Papaver self-incompatibility pollen S-determinant, PrpS, functions in Arabidopsis thaliana. *Curr Biol*. 22:154-159.

de Jong, C.F., A.M. Laxalt, B.O. Bargmann, P.J. de Wit, M.H. Joosten, and T. Munnik. 2004. Phosphatidic acid accumulation is an early response in the Cf-4/Avr4 interaction. *The Plant journal : for cell and molecular biology*. 39:1-12.

Delledonne, M. 2005. NO news is good news for plants. *Current Opinion in Plant Biology*. 8:390-396.

den Hartog, M., A. Musgrave, and T. Munnik. 2001. Nod factor-induced phosphatidic acid and diacylglycerol pyrophosphate formation: a role for phospholipase C and D in root hair deformation. *The Plant journal : for cell and molecular biology*. 25:55-65.

den Hartog, M., N. Verhoef, and T. Munnik. 2003. Nod factor and elicitors activate different phospholipid signaling pathways in suspension-cultured alfalfa cells. *Plant Physiology*. 132:311-317.

Desouki, M.M., M. Kulawiec, S. Bansal, G.C. Das, and K.K. Singh. 2005. Cross talk between mitochondria and superoxide generating NADPH oxidase in breast and ovarian tumors. *Cancer Biol Ther*. 4:1367-1373.

Desouza, M., P.W. Gunning, and J.R. Stehn. 2012. The actin cytoskeleton as a sensor and mediator of apoptosis. *Bioarchitecture*. 2:75-87.

Dhonukshe, P., A.M. Laxalt, J. Goedhart, T.W.J. Gadella, and T. Munnik. 2003. Phospholipase D Activation Correlates with Microtubule Reorganization in Living Plant Cells. *The Plant Cell Online*. 15:2666-2679.

Dittrich, H., and T.M. Kutchan. 1991. Molecular cloning, expression, and induction of berberine bridge enzyme, an enzyme essential to the formation of benzophenanthridine alkaloids in the response of plants to pathogenic attack. *Proceedings of the National Academy of Sciences*. 88:9969-9973.

Drew, M.C., C.J. He, and P.W. Morgan. 2000. Programmed cell death and aerenchyma formation in roots. *Trends in Plant Science*. 5:123-127.

Drobak, B.K., P.A.C. Watkins, R. Valenta, S.K. Dove, C.W. Lloyd, and C.J. Staiger. 1994. INHIBITION OF PLANT PLASMA-MEMBRANE PHOSPHOINOSITIDE PHOSPHOLIPASE-C BY THE ACTIN-BINDING PROTEIN, PROFILIN. *Plant J*. 6:389-400.

Elmayan, T., and F. Simon-Plas. 2007. Regulation of plant NADPH oxidase. *Plant Signal Behav*. 2:505-507.

Elmore, S. 2007. Apoptosis: A Review of Programmed Cell Death. *Toxicologic Pathology*. 35:495-516.

Enari, M., H. Sakahira, H. Yokoyama, K. Okawa, A. Iwamatsu, and S. Nagata. 1998. A caspase-activated DNase that degrades DNA during apoptosis, and its inhibitor ICAD. *Nature*. 391:43-50.

England, B.K., J.L. Chastain, and W.E. Mitch. 1991. Abnormalities in protein synthesis and degradation induced by extracellular pH in BC3H1 myocytes. *American Journal of Physiology - Cell Physiology*. 260:C277-C282.

Fais, S. 2010. Proton pump inhibitor-induced tumour cell death by inhibition of a detoxification mechanism. *Journal of Internal Medicine*. 267:515-525.

Fan, L., S. Zheng, and X. Wang. 1997. Antisense Suppression of Phospholipase D[alpha] Retards Abscisic Acid[mdash] and Ethylene-Promoted Senescence of Postharvest Arabidopsis Leaves. *The Plant Cell Online*. 9:2183-2196.

Fasano, J.M., G.D. Massa, and S. Gilroy. 2002. Ionic Signaling in Plant Responses to Gravity and Touch. *Journal of Plant Growth Regulation*. 21:71-88.

Fasano, J.M., S.J. Swanson, E.B. Blancaflor, P.E. Dowd, T.H. Kao, and S. Gilroy. 2001. Changes in root cap pH are required for the gravity response of the Arabidopsis root. *The Plant cell*. 13:907-921.

Feijo, J.A., J. Sainhas, G.R. Hackett, J.G. Kunkel, and P.K. Hepler. 1999. Growing pollen tubes possess a constitutive alkaline band in the clear zone and a growth-dependent acidic tip. *J Cell Biol*. 144:483-496.

Feijo, J.A., J. Sainhas, T. Holdaway-Clarke, M.S. Cordeiro, J.G. Kunkel, and P.K. Hepler. 2001. Cellular oscillations and the regulation of growth: the pollen tube paradigm. *BioEssays : news and reviews in molecular, cellular and developmental biology*. 23:86-94.

Felle, H.H. 2001. pH: Signal and Messenger in Plant Cells. *Plant Biology*. 3:577-591.

Ferri, K.F., and G. Kroemer. 2001. Organelle-specific initiation of cell death pathways. *Nature Cell Biology*. 3:E255-E263.

Foote, H.C.C., J.P. Ride, V.E. Franklintong, E.A. Walker, M.J. Lawrence, and F.C.H. Franklin. 1994. CLONING AND EXPRESSION OF A DISTINCTIVE CLASS OF SELF-INCOMPATIBILITY (S) GENE FROM PAPAVER-RHOEAS L. *P Natl Acad Sci USA*. 91:2265-2269.

Foreman, J., V. Demidchik, J.H.F. Bothwell, P. Mylona, H. Miedema, M.A. Torres, P. Linstead, S. Costa, C. Brownlee, J.D.G. Jones, J.M. Davies, and L. Dolan. 2003. Reactive oxygen species produced by NADPH oxidase regulate plant cell growth. *Nature*. 422:442-446.

Foyer, C.H., and G. Noctor. 2005. Redox Homeostasis and Antioxidant Signaling: A Metabolic Interface between Stress Perception and Physiological Responses. *Plant Cell* 17:1866-1875.

Franklin-Tong, N., and C. Franklin. 1993. Gametophytic self-incompatibility: Contrasting mechanisms for Nicotiana and Papaver. *Trends in Cell Biology*. 3:340-345.

Franklin-Tong, V.E. 1999. Signaling and the modulation of pollen tube growth. *Plant Cell*. 11:727-738.

Franklin-Tong, V.E., B.K. Drobak, A.C. Allan, P. Watkins, and A.J. Trewavas. 1996. Growth of Pollen Tubes of Papaver rhoeas Is Regulated by a Slow-Moving Calcium Wave Propagated by Inositol 1,4,5-Trisphosphate. *The Plant cell*. 8:1305-1321.

Franklin-Tong, Vernonica E., and Campbell W. Gourlay. 2008. A role for actin in regulating apoptosis/programmed cell death: evidence spanning yeast, plants and animals. *Biochemical Journal*. 413:389.

Franklin-Tong, V.E., G. Hackett, and P.K. Hepler. 1997. Ratio-imaging of Ca-i(2+) in the self-incompatibility response in pollen tubes of Papaver rhoeas. *Plant J*. 12:1375-1386.

Franklin-Tong, V.E., T.L. Holdaway-Clarke, K.R. Straatman, J.G. Kunke, and P.K. Hepler. 2002. Involvement of extracellular calcium influx in the self-incompatibility response of Papaver rhoeas. *Plant J*. 29:333-345.

Fricker, M.D., N.S. White, and G. Obermeyer. 1997. pH gradients are not associated with tip growth in pollen tubes of Lilium longiflorum. *Journal of Cell Science*. 110:1729-1740.

Fukuda, H. 1997. Tracheary Element Differentiation. *Plant Cell*. 9:1147-1156.

Fukuda, H. 2000. Programmed cell death of tracheary elements as a paradigm in plants. *Plant Molecular Biology*. 44:245-253.

Furlong, I.J., R. Ascaso, A. Lopez Rivas, and M.K. Collins. 1997. Intracellular acidification induces apoptosis by stimulating ICE-like protease activity. *Journal of Cell Science*. 110 (Pt 5):653-661.

Gao, C., D. Xing, L. Li, and L. Zhang. 2008a. Implication of reactive oxygen species and mitochondrial dysfunction in the early stages of plant programmed cell death induced by ultraviolet-C overexposure. *Planta*. 227:755-767.

Gao, C., L. Zhang, F. Wen, and D. Xing. 2008b. Sorting out the role of reactive oxygen species during plant programmed cell death induced by ultraviolet-C overexposure. *Plant Signal Behav*. 3:197-198.

Gapper, C., and L. Dolan. 2006. Control of Plant Development by Reactive Oxygen Species. *Plant Physiology*. 141:341-345.

Gardiner, J., D.A. Collings, J.D.I. Harper, and J. Marc. 2003. The Effects of the Phospholipase D-Antagonist 1-Butanol on Seedling Development and Microtubule Organisation in Arabidopsis. *Plant and Cell Physiology*. 44:687-696.

Gardiner, J.C., J.D.I. Harper, N.D. Weerakoon, D.A. Collings, S. Ritchie, S. Gilroy, R.J. Cyr, and J. Marc. 2001. A 90-kD Phospholipase D from Tobacco Binds to Microtubules and the Plasma Membrane. *The Plant Cell Online*. 13:2143-2158.

Geitmann, A., V.E. Franklin-Tong, and A.C. Emons. 2004a. The self-incompatibility response in Papaver rhoeas pollen causes early and striking alterations to organelles. *Cell Death and Differentiation*. 11:812-822.

Geitmann, A., W. McConnaughey, I. Lang-Pauluzzi, V.E. Franklin-Tong, and A.M.C. Emons. 2004b. Cytomechanical properties of Papaver pollen tubes are altered after self-incompatibility challenge. *Biophys J*. 86:3314-3323.

Geitmann, A., B.N. Snowman, A.M.C. Emons, and V.E. Franklin-Tong. 2000. Alterations in the actin cytoskeleton of pollen tubes are induced by the self-incompatibility reaction in Papaver rhoeas. *Plant Cell*. 12:1239-1251.

Gibbon, B.C., D.R. Kovar, and C.J. Staiger. 1999. Latrunculin B has different effects on pollen germination and tube growth. *Plant Cell*. 11:2349-2363.

Gibbon, B.C., and D.L. Kropf. 1994. Cytosolic pH Gradients Associated with Tip Growth. *Science*. 263:1419-1421.

Gilroy, E.M., I. Hein, R. van der Hoorn, P.C. Boevink, E. Venter, H. McLellan, F. Kaffarnik, K. Hrubikova, J. Shaw, M. Holeva, E.C. Lopez, O. Borras-Hidalgo, L. Pritchard, G.J. Loake, C. Lacomme, and P.R. Birch. 2007. Involvement of cathepsin B in the plant disease resistance hypersensitive response. *The Plant journal : for cell and molecular biology*. 52:1-13.

Goldraij, A., K. Kondo, C.B. Lee, C.N. Hancock, M. Sivaguru, S. Vazquez-Santana, S. Kim, T.E. Phillips, F. Cruz-Garcia, and B. McClure. 2006. Compartmentalization of S-RNase and HT-B degradation in self-incompatible Nicotiana. *Nature*. 439:805-810.

Goossens, J.F., J.P. Henichart, L. Dassonneville, M. Facompre, and C. Bailly. 2000. Relation between intracellular acidification and camptothecin-induced apoptosis in leukemia cells. *Eur J Pharm Sci*. 10:125-131.

Gottlieb, R.A. 1996. Cell acidification in apoptosis. *Apoptosis*. 1:40-48.

Grant, J.J., B.-W. Yun, and G.J. Loake. 2000. Oxidative burst and cognate redox signalling reported by luciferase imaging: identification of a signal network that functions independently of ethylene, SA and Me-JA but is dependent on MAPKK activity. *The Plant Journal*. 24:569-582.

Greenberg, J.T., and N. Yao. 2004. The role and regulation of programmed cell death in plant–pathogen interactions. *Cellular Microbiology*. 6:201-211.

Groover, A., N. DeWitt, A. Heidel, and A. Jones. 1997. Programmed cell death of plant tracheary elements: Differentiating in vitro. *Protoplasma*. 196:197-211.

Grun, S. 2006. Nitric oxide and gene regulation in plants. *Journal of Experimental Botany*. 57:507-516.

Gu, T.S., M. Mazzurco, W. Sulaman, D.D. Matias, and D.R. Goring. 1998. Binding of an arm repeat protein to the kinase domain of the S-locus receptor kinase. *P Natl Acad Sci USA*. 95:382-387.

Guern, J., H. Felle, Y. Mathieu, and A. Kurkdjian. 1991. Regulation of Intracellular Ph in Plant-Cells. *International Review of Cytology-a Survey of Cell Biology*. 127:111-173.

Gunawardena, A.H.L.A.N., J.S. Greenwood, and N.G. Dengler. 2004. Programmed Cell Death Remodels Lace Plant Leaf Shape during Development. *The Plant Cell Online*. 16:60-73.

Gungabissoon, R.A., C.-J. Jiang, B.K. Drøbak, S.K. Maciver, and P.J. Hussey. 1998. Interaction of maize actin-depolymerising factor with actin and phosphoinositides and its inhibition of plant phospholipase C. *The Plant Journal*. 16:689-696.

Guo, F.Q., M. Okamoto, and N.M. Crawford. 2003. Identification of a plant nitric oxide synthase gene involved in hormonal signaling. *Science*. 302:100-103.

Ha, K.S., and J.H. Exton. 1993. Activation of actin polymerization by phosphatidic acid derived from phosphatidylcholine in IIC9 fibroblasts. *The Journal of Cell Biology*. 123:1789-1796.

Haffani, Y.Z., T. Gaude, J.M. Cock, and D.R. Goring. 2004. Antisense suppression of thioredoxin h mRNA in Brassica napus cv. Westar pistils causes a low level constitutive pollen rejection response. *Plant Molecular Biology*. 55:619-630.

Han, G.S., C.N. Johnston, and G.M. Carman. 2004. Vacuole membrane topography of the DPP1-encoded diacylglycerol pyrophosphate phosphatase catalytic site from Saccharomyces cerevisiae. *J Biol Chem*. 279:5338-5345.

Han, J.J., W. Lin, Y. Oda, K.M. Cui, H. Fukuda, and X.Q. He. 2012. The proteasome is responsible for caspase-3-like activity during xylem development. *The Plant journal : for cell and molecular biology*.

Hanaoka, H., T. Noda, Y. Shirano, T. Kato, H. Hayashi, D. Shibata, S. Tabata, and Y. Ohsumi. 2002. Leaf senescence and starvation-induced chlorosis are accelerated by the disruption of an Arabidopsis autophagy gene. *Plant Physiol*. 129:1181-1193.

Hao, X., J. Qian, S. Xu, X. Song, and J. Zhu. 2008. Location of caspase 3-like protease in the development of sieve element and tracheary element of stem in Cucurbita moschata. *Journal of Integrative Plant Biology*. 50:1499-1507.

Hara-Nishimura, I., and N. Hatsugai. 2011. The role of vacuole in plant cell death. *Cell Death and Differentiation*. 18:1298-1304.

Hara-Nishimura, I., N. Hatsugai, S. Nakaune, M. Kuroyanagi, and M. Nishimura. 2005. Vacuolar processing enzyme: an executor of plant cell death. *Current Opinion in Plant Biology*. 8:404-408.

Hara-Nishimura, I., K. Inoue, and M. Nishimura. 1991. A unique vacuolar processing enzyme responsible for conversion of several proprotein precursors into the mature forms. *FEBS Letters*. 294:89-93.

Hara-Nishimura, I., Y. Takeuchi, and M. Nishimura. 1993. Molecular characterization of a vacuolar processing enzyme related to a putative cysteine proteinase of Schistosoma mansoni. *The Plant cell*. 5:1651-1659.

Hatsugai, N. 2004. A Plant Vacuolar Protease, VPE, Mediates Virus-Induced Hypersensitive Cell Death. *Science*. 305:855-858.

Hatsugai, N., and I. Hara-Nishimura. 2010. Two vacuole-mediated defense strategies in plants. *Plant Signal Behav*. 5:1568-1570.

Hatsugai, N., S. Iwasaki, K. Tamura, M. Kondo, K. Fuji, K. Ogasawara, M. Nishimura, and I. Hara-Nishimura. 2009. A novel membrane fusion-mediated plant immunity against bacterial pathogens. *Genes & Development*. 23:2496-2506.

Hatsugai, N., M. Kuroyanagi, K. Yamada, T. Meshi, I. Hara-Nishimura, and M. Nishimura. 2004. Vacuolar processing enzyme exhibiting caspase-1-like activity is involved in TMV-induced hypersensitive cell death in tobacco. *Plant and Cell Physiology*. 45:S143-S143.

Hatsugai, N., M. Kuroyanagi, K. Yamada, T. Meshi, I. Hara-Nishimura, and M. Nishimura. 2005. A VPE exhibiting caspase-1 activity regulates virus-induced hypersensitive cell death. *Plant and Cell Physiology*. 46:S47-S47.

Hawkins, M., B. Pope, S.K. Maciver, and A.G. Weeds. 1993. Human actin depolymerizing factor mediates a pH-sensitive destruction of actin filaments. *Biochemistry-Us*. 32:9985-9993.

He, J.-M., X.-L. Bai, R.-B. Wang, B. Cao, and X.-P. She. 2007. The involvement of nitric oxide in ultraviolet-B-inhibited pollen germination and tube growth of Paulownia tomentosa in vitro. *Physiologia Plantarum*. 131:273-282.

Hepler, P.K., J.G. Kunkel, C.M. Rounds, and L.J. Winship. 2012. Calcium entry into pollen tubes. *Trends in Plant Science*. 17:32-38.

Heslop-Harrison, J., and Y. Heslop-Harrison. 1985. Surfaces and secretions in the pollen-stigma interaction: a brief review. *J Cell Sci Suppl*. 2:287-300.

Hetherington, A.M., and C. Brownlee. 2004. The generation of Ca2+ signals in plants. *Annual Review of Plant Biology*. 55:401-427.

Hetherington, A.M., J.E. Gray, C.P. Leckie, M.R. McAinsh, C. Ng, C. Pical, A.J. Priestley, I. Staxén, and A.A.R. Webb. 1998. The control of specificity in guard cell signal transduction. *Philosophical Transactions of the Royal Society of London. Series B: Biological Sciences*. 353:1489-1494.

Hicks, G.R., E. Rojo, S.H. Hong, D.G. Carter, and N.V. Raikhel. 2004. Geminating pollen has tubular vacuoles, displays highly dynamic vacuole biogenesis, and requires VACUOLESS1 for proper function. *Plant Physiology*. 134:1227-1239.

Higaki, T., T. Goh, T. Hayashi, N. Kutsuna, Y. Kadota, S. Hasezawa, T. Sano, and K. Kuchitsu. 2007. Elicitor-Induced Cytoskeletal Rearrangement Relates to Vacuolar Dynamics and Execution of Cell Death: In Vivo Imaging of Hypersensitive Cell Death in Tobacco BY-2 Cells. *Plant and Cell Physiology*. 48:1414-1425.

Higaki, T., N. Kutsuna, E. Okubo, T. Sano, and S. Hasezawa. 2006. Actin Microfilaments Regulate Vacuolar Structures and Dynamics: Dual Observation of Actin Microfilaments and Vacuolar Membrane in Living Tobacco BY-2 Cells. *Plant and Cell Physiology*. 47:839-852.

Hirano, A. 1994. Hirano bodies and related neuronal inclusions. *Neuropathology and Applied Neurobiology*. 20:3-11.

Hirpara, J.L., M.-V. Clément, and S. Pervaiz. 2001. Intracellular Acidification Triggered by Mitochondrial-derived Hydrogen Peroxide Is an Effector Mechanism for Drug-induced Apoptosis in Tumor Cells. *Journal of Biological Chemistry*. 276:514-521.

Hiscock, S.J., and U. Kues. 1999. Cellular and molecular mechanisms of sexual incompatibility in plants and fungi. *International Review of Cytology - a Survey of Cell Biology, Vol 193*. 193:165-295.

Hiscock, S.J., and S.M. McInnis. 2003. The diversity of self-incompatibility systems in flowering plants. *Plant Biology*. 5:23-32.

Hiscock, S.J., and D.A. Tabah. 2003. The different mechanisms of sporophytic self-incompatibility. *Philosophical Transactions of the Royal Society B: Biological Sciences*. 358:1037-1045.

Holdaway-Clarke, T.L., J.A. Feijo, G.R. Hackett, J.G. Kunkel, and P.K. Hepler. 1997. Pollen Tube Growth and the Intracellular Cytosolic Calcium Gradient Oscillate in Phase while Extracellular Calcium Influx Is Delayed. *The Plant cell*. 9:1999-2010.

Holdaway-Clarke, T.L., N.M. Weddle, S. Kim, A. Robi, C. Parris, J.G. Kunkel, and P.K. Hepler. 2003. Effect of extracellular calcium, pH and borate on growth oscillations in Lilium formosanum pollen tubes. *Journal of Experimental Botany*. 54:65-72.

Hua, Z.H., and T.H. Kao. 2006. Identification and characterization of components of a putative Petunia S-locus F-box-containing E3 ligase complex involved in S-RNase-based self-incompatability. *Plant Cell*. 18:2531-2553.

Huang, S. 2006. Phosphatidic Acid Inhibits Arabidopsis Actin Capping Protein. *Sci. STKE*. 2006:tw115-.

Huang, S., L. Blanchoin, D.R. Kovar, and C.J. Staiger. 2003. Arabidopsis capping protein (AtCP) is a heterodimer that regulates assembly at the barbed ends of actin filaments. *J Biol Chem*. 278:44832-44842.

Huang, S., L. Gao, L. Blanchoin, and C.J. Staiger. 2006. Heterodimeric capping protein from Arabidopsis is regulated by phosphatidic acid. *Molecular Biology of the Cell*. 17:1946-1958.

Huang, W.C., P. Swietach, R.D. Vaughan-Jones, O. Ansorge, and M.D. Glitsch. 2008. Extracellular acidification elicits spatially and temporally distinct Ca2+ signals. *Curr Biol*. 18:781-785.

Ichimonji, I., H. Tomura, C. Mogi, K. Sato, H. Aoki, T. Hisada, K. Dobashi, T. Ishizuka, M. Mori, and F. Okajima. 2010. Extracellular acidification stimulates IL-6 production and Ca2+ mobilization through proton-sensing OGR1 receptors in human airway smooth muscle cells. *American Journal of Physiology - Lung Cellular and Molecular Physiology*. 299:L567-L577.

Ioerger, T.R., J.R. Gohlke, B. Xu, and T.H. Kao. 1991. PRIMARY STRUCTURAL FEATURES OF THE SELF-INCOMPATIBILITY PROTEIN IN SOLANACEAE. *Sexual Plant Reproduction*. 4:81-87.

Ito, J. 2002. ZEN1 Is a Key Enzyme in the Degradation of Nuclear DNA during Programmed Cell Death of Tracheary Elements. *The Plant Cell Online*. 14:3201-3211.

Ito, Y., H. Kaku, and N. Shibuya. 1997. Identification of a high-affinity binding protein for N-acetylchitooligosaccharide elicitor in the plasma membrane of suspension-cultured rice cells by affinity labeling. *The Plant Journal*. 12:347-356.

Iwano, M., H. Shiba, K. Matoba, T. Miwa, M. Funato, T. Entani, P. Nakayama, H. Shimosato, A. Takaoka, A. Isogai, and S. Takayama. 2007. Actin Dynamics in Papilla Cells of Brassica rapa during Self- and Cross-Pollination. *Plant Physiology*. 144:72-81.

Jacob, T., S. Ritchie, S.M. Assmann, and S. Gilroy. 1999. Abscisic acid signal transduction in guard cells is mediated by phospholipase D activity. *Proceedings of the National Academy of Sciences*. 96:12192-12197.

Jeannette, E., S. Paradis, and C. Zalejski. 2010. Diacylglycerol Pyrophosphate, A Novel Plant Signaling Lipid. Lipid Signaling in Plants. Vol. 16. T. Munnik, editor. Springer Berlin / Heidelberg. 263-276.

Johannes, E., D.A. Collings, J.C. Rink, and N.S. Allen. 2001. Cytoplasmic pH Dynamics in Maize Pulvinal Cells Induced by Gravity Vector Changes. *Plant Physiology*. 127:119-130.

Johnson, D., and K. Nehrke. 2010. Mitochondrial Fragmentation Leads to Intracellular Acidification in Caenorhabditis elegans and Mammalian Cells. *Molecular Biology of the Cell*. 21:2191-2201.

Jones, M.A., M.J. Raymond, Z. Yang, and N. Smirnoff. 2007. NADPH oxidase-dependent reactive oxygen species formation required for root hair growth depends on ROP GTPase. *Journal of Experimental Botany*. 58:1261-1270.

Jordan, N.D., F.C.H. Franklin, and V.E. Franklin-Tong. 2000. Evidence for DNA fragmentation triggered in the self-incompatibility response in pollen of Papaver rhoeas. *Plant J*. 23:471-479.

Jung, J.-Y., Y.-W. Kim, J.M. Kwak, J.-U. Hwang, J. Young, J.I. Schroeder, I. Hwang, and Y. Lee. 2002. Phosphatidylinositol 3- and 4-Phosphate Are Required for Normal Stomatal Movements. *The Plant Cell Online*. 14:2399-2412.

Jyothi, G., A. Surolia, and K. Easwaran. 1994. A23187—Channel behaviour: Fluorescence study. *Journal of Biosciences*. 19:277-282.

Kader, M.A., and S. Lindberg. 2010. Cytosolic calcium and pH signaling in plants under salinity stress. *Plant Signal Behav*. 5:233-238.

Kader, M.A., S. Lindberg, T. Seidel, D. Golldack, and V. Yemelyanov. 2007. Sodium sensing induces different changes in free cytosolic calcium concentration and pH in salt-tolerant and -sensitive rice (Oryza sativa) cultivars. *Physiologia Plantarum*. 130:99-111.

Kakeda, K., N.D. Jordan, A. Conner, J.P. Ride, V.E. Franklin-Tong, and F.C.H. Franklin. 1998. Identification of residues in a hydrophilic loop of the Papaver rhoeas S protein that play a crucial role in recognition of incompatible pollen. *Plant Cell*. 10:1723-1731.

Kakita, M., K. Murase, M. Iwano, T. Matsumoto, M. Watanabe, H. Shiba, A. Isogai, and S. Takayama. 2007. Two distinct forms of M-locus protein kinase localize to the plasma membrane and interact directly with S-Locus receptor kinase to transduce self-incompatibility signaling in Brassica rapa. *Plant Cell*. 19:3961-3973.

Katsuhara, M., K. Kuchitsu, K. Takeshige, and M. Tazawa. 1989. Salt Stress-Induced Cytoplasmic Acidification and Vacuolar Alkalization in Nitellopsis obtusa Cells : In VivoP-Nuclear Magnetic Resonance Study. *Plant Physiology*. 90:1102-1107.

Keller, T., H.G. Damude, D. Werner, P. Doerner, R.A. Dixon, and C. Lamb. 1998. A plant homolog of the neutrophil NADPH oxidase gp91phox subunit gene encodes a plasma membrane protein with Ca2+ binding motifs. *Plant Cell*. 10:255-266.

Kerscher, O., R. Felberbaum, and M. Hochstrasser. 2006. Modification of proteins by ubiquitin and ubiquitin-like proteins. *Annual Review of Cell and Developmental Biology*. 22:159-180.

Kim, M., J.W. Ahn, U.H. Jin, D. Choi, K.H. Paek, and H.S. Pai. 2003. Activation of the programmed cell death pathway by inhibition of proteasome function in plants. *J Biol Chem*. 278:19406-19415.

Kinoshita, T., K. Yamada, N. Hiraiwa, M. Kondo, M. Nishimura, and I. Hara-Nishimura. 1999. Vacuolar processing enzyme is up-regulated in the lytic vacuoles of vegetative tissues during senescence and under various stressed conditions. *The Plant Journal*. 19:43-53.

Klionsky, D.J., and S.D. Emr. 2000. Autophagy as a regulated pathway of cellular degradation. *Science*. 290:1717-1721.

Kooijman, E.E., V. Chupin, B. De Kruijff, and K.N.J. Burger. 2003. Modulation of Membrane Curvature by Phosphatidic Acid and Lysophosphatidic Acid. *Traffic*. 4:162-174.

Kopyra, M., and E.A. Gwózdz. 2003. Nitric oxide stimulates seed germination and counteracts the inhibitory effect of heavy metals and salinity on root growth of Lupinus luteus. *Plant Physiology and Biochemistry*. 41:1011-1017.

Kroemer, G., L. Galluzzi, P. Vandenabeele, J. Abrams, E.S. Alnemri, E.H. Baehrecke, M.V. Blagosklonny, W.S. El-Deiry, P. Golstein, D.R. Green, M. Hengartner, R.A. Knight, S. Kumar, S.A. Lipton, W. Malorni, G. Nunez, M.E. Peter, J. Tschopp, J. Yuan, M. Piacentini, B. Zhivotovsky, and G. Melino. 2009. Classification of cell death: recommendations of the Nomenclature Committee on Cell Death 2009. *Cell Death and Differentiation*. 16:3-11.

Kubo, K., T. Entani, A. Takara, N. Wang, A.M. Fields, Z. Hua, M. Toyoda, S. Kawashima, T. Ando, A. Isogai, T.H. Kao, and S. Takayama. 2010. Collaborative non-self recognition system in S-RNase-based self-incompatibility. *Science*. 330:796-799.

Kuriyama, H. 1999. Loss of tonoplast integrity programmed in tracheary element differentiation. *Plant Physiology*. 121:763-774.

Kuroyanagi, M., K. Yamada, N. Hatsugai, M. Kondo, M. Nishimura, and I. Hara-Nishimura. 2005. Vacuolar processing enzyme is essential for mycotoxin-induced cell death in Arabidopsis thaliana. *J Biol Chem*. 280:32914-32920.

Kuroyanagi, M., K. Yamada, M. Nishimura, and I. Hara-Nishimura. 2002. The function of vacuolar enzyme(s) on programmed cell death in higher plants. *Plant and Cell Physiology*. 43:S216-S216.

Kurup, S., J.P. Ride, N. Jordan, G. Fletcher, V.E. Franklin-Tong, and F.C.H. Franklin. 1998. Identification and cloning of related self-incompatibility S-genes in Papaver rhoeas and Papaver nudicaule. *Sexual Plant Reproduction*. 11:192-198.

Kutsuna, N., and S. Hasezawa. 2002. Dynamic organization of vacuolar and microtubule structures during cell cycle progression in synchronized tobacco BY-2 cells. *Plant and Cell Physiology*. 43:965-973.

Kwak, J.M., V. Nguyen, and J.I. Schroeder. 2006. The role of reactive oxygen species in hormonal responses. *Plant Physiology*. 141:323-329.

Lai, Z., W.S. Ma, B. Han, L.Z. Liang, Y.S. Zhang, G.F. Hong, and Y.B. Xue. 2002. An F-box gene linked to the self-incompatibility (S) locus of Antirrhinum is expressed specifically in pollen and tapetum. *Plant Molecular Biology*. 50:29-42.

Laloi, C., K. Apel, and A. Danon. 2004. Reactive oxygen signalling: the latest news. *Current Opinion in Plant Biology*. 7:323-328.

Lam, E., N. Kato, and M. Lawton. 2001. Programmed cell death, mitochondria and the plant hypersensitive response. *Nature*. 411:848-853.

Lanteri, M.L., A.M. Laxalt, and L. Lamattina. 2008. Nitric Oxide Triggers Phosphatidic Acid Accumulation via Phospholipase D during Auxin-Induced Adventitious Root Formation in Cucumber. *Plant Physiology*. 147:188-198.

Latchoumycandane, C., G.K. Marathe, R. Zhang, and T.M. McIntyre. 2012. Oxidatively truncated phospholipids are required agents of TNFα induced apoptosis. *Journal of Biological Chemistry*.

Lawrence, M.J. 1975. GENETICS OF SELF-INCOMPATIBILITY IN PAPAVER-RHOEAS. *Proceedings of the Royal Society of London Series B-Biological Sciences*. 188:275-&.

Laxalt, A.M., and T. Munnik. 2002. Phospholipid signalling in plant defence. *Current Opinion in Plant Biology*. 5:332-338.

Laxalt, A.M., N. Raho, A.T. Have, and L. Lamattina. 2007. Nitric oxide is critical for inducing phosphatidic acid accumulation in xylanase-elicited tomato cells. *J Biol Chem*. 282:21160-21168.

Lecourieux, D., C. Mazars, N. Pauly, R. Ranjeva, and A. Pugin. 2002. Analysis and Effects of Cytosolic Free Calcium Increases in Response to Elicitors in Nicotiana plumbaginifolia Cells. *The Plant Cell Online*. 14:2627-2641.

Lee, S., H. Hirt, and Y. Lee. 2001. Phosphatidic acid activates a wound-activated MAPK in Glycine max. *The Plant journal : for cell and molecular biology*. 26:479-486.

Lee, S., J. Park, and Y. Lee. 2003. Phosphatidic acid induces actin polymerization by activating protein kinases in soybean cells. *Mol Cells*. 15:313-319.

Lee, Y., G. Bak, Y. Choi, W.-I. Chuang, H.-T. Cho, and Y. Lee. 2008a. Roles of Phosphatidylinositol 3-Kinase in Root Hair Growth. *Plant Physiology*. 147:624-635.

Lee, Y., Y.B. Choi, S. Suh, J. Lee, S.M. Assmann, C.O. Joe, J.F. Kelleher, and R.C. Crain. 1996. Abscisic Acid-Induced Phosphoinositide Turnover in Guard Cell Protoplasts of Vicia faba. *Plant Physiology*. 110:987-996.

Lee, Y., E.S. Kim, Y. Choi, I. Hwang, C.J. Staiger, and Y.Y. Chung. 2008b. The Arabidopsis phosphatidylinositol 3-kinase is important for pollen development. *Plant Physiology*. 147:1886-1897.

Leshem, Y., L. Seri, and A. Levine. 2007. Induction of phosphatidylinositol 3-kinase-mediated endocytosis by salt stress leads to intracellular production of reactive oxygen species and salt tolerance. *The Plant Journal*. 51:185-197.

Levine, A., R.I. Pennell, M.E. Alvarez, R. Palmer, and C. Lamb. 1996. Calcium-mediated apoptosis in a plant hypersensitive disease resistance response. *Curr Biol*. 6:427-437.

Levine, A., R. Tenhaken, R. Dixon, and C. Lamb. 1994. H2O2 from the oxidative burst orchestrates the plant hypersensitive disease resistance response. *Cell*. 79:583-593.

Levine, B., and G. Kroemer. 2009. Autophagy in aging, disease and death: the true identity of a cell death impostor. *Cell Death and Differentiation*. 16:1-2.

Li, J., J.L. Henty-Ridilla, S. Huang, X. Wang, L. Blanchoin, and C.J. Staiger. 2012. Capping Protein Modulates the Dynamic Behavior of Actin Filaments in Response to Phosphatidic Acid in Arabidopsis. *The Plant cell*.

Li, M., Y. Hong, and X. Wang. 2009. Phospholipase D- and phosphatidic acid-mediated signaling in plants. *Biochim Biophys Acta*. 1791:927-935.

Li, S., J. Samaj, and V.E. Franklin-Tong. 2007. A Mitogen-Activated Protein Kinase Signals to Programmed Cell Death Induced by Self-Incompatibility in Papaver Pollen. *Plant Physiology*. 145:236-245.

Li, W., M. Li, W. Zhang, R. Welti, and X. Wang. 2004. The plasma membrane-bound phospholipase Ddelta enhances freezing tolerance in Arabidopsis thaliana. *Nat Biotechnol*. 22:427-433.

Liszkay, A., E. van der Zalm, and P. Schopfer. 2004. Production of reactive oxygen intermediates (O(2)(.-), H(2)O(2), and (.)OH) by maize roots and their role in wall loosening and elongation growth. *Plant Physiol*. 136:3114-3123; discussion 3001.

Liu, D., G. Martino, M. Thangaraju, M. Sharma, F. Halwani, S.-H. Shen, Y.C. Patel, and C.B. Srikant. 2000. Caspase-8-mediated Intracellular Acidification Precedes Mitochondrial Dysfunction in Somatostatin-induced Apoptosis. *Journal of Biological Chemistry*. 275:9244-9250.

Loewen, C.J., M.L. Gaspar, S.A. Jesch, C. Delon, N.T. Ktistakis, S.A. Henry, and T.P. Levine. 2004. Phospholipid metabolism regulated by a transcription factor sensing phosphatidic acid. *Science*. 304:1644-1647.

Lombardo, M.C., M. Graziano, J.C. Polacco, and L. Lamattina. 2006. Nitric oxide functions as a positive regulator of root hair development. *Plant Signal Behav*. 1:28-33.

Lovy-Wheeler, A., L. Cardenas, J.G. Kunkel, and P.K. Hepler. 2007. Differential organelle movement on the actin cytoskeleton in lily pollen tubes. *Cell Motility and the Cytoskeleton*. 64:217-232.

Lovy-Wheeler, A., J.G. Kunkel, E.G. Allwood, P.J. Hussey, and P.K. Hepler. 2006. Oscillatory increases in alkalinity anticipate growth and may regulate actin dynamics in pollen tubes of lily. *The Plant cell*. 18:2182-2193.

Lowe, S.W., and A.W. Lin. 2000. Apoptosis in cancer. *Carcinogenesis*. 21:485-495.

Luu, D.T., X.K. Qin, D. Morse, and M. Cappadocia. 2000. S-RNase uptake by compatible pollen tubes in gametophytic self-incompatibility. *Nature*. 407:649-651.

MacRobbie, E.A.C. 2000. ABA activates multiple Ca2+ fluxes in stomatal guard cells, triggering vacuolar K+(Rb+) release. *Proceedings of the National Academy of Sciences*. 97:12361-12368.

Malhó, R. 2006. The pollen tube a cellular and molecular perspective. Springer, Berlin; New York.

Malho, R., Q. Liu, D. Monteiro, C. Rato, L. Camacho, and A. Dinis. 2006. Signalling pathways in pollen germination and tube growth. *Protoplasma*. 228:21-30.

Malho, R., N.D. Read, M.S. Pais, and A.J. Trewavas. 1994. Role of Cytosolic-Free Calcium in the Reorientation of Pollen-Tube Growth. *Plant J*. 5:331-341.

Malho, R., and A.J. Trewavas. 1996. Localized Apical Increases of Cytosolic Free Calcium Control Pollen Tube Orientation. *The Plant cell*. 8:1935-1949.

Marques, M., D. Mojzita, M.A. Amorim, T. Almeida, S. Hohmann, P. Moradas-Ferreira, and V. Costa. 2006. The Pep4p vacuolar proteinase contributes to the turnover of oxidized proteins but PEP4 overexpression is not sufficient to increase chronological lifespan in Saccharomyces cerevisiae. *Microbiology*. 152:3595-3605.

Maselli, A.G., R. Davis, R. Furukawa, and M. Fechheimer. 2002. Formation of Hirano bodies in Dictyostelium and mammalian cells induced by expression of a modified form of an actin-crosslinking protein. *Journal of Cell Science*. 115:1939-1949.

Mason, D.A., N. Shulga, S. Undavai, E. Ferrando-May, M.F. Rexach, and D.S. Goldfarb. 2005. Increased nuclear envelope permeability and Pep4p-dependent degradation of nucleoporins during hydrogen peroxide-induced cell death. *FEMS Yeast Res*. 5:1237-1251.

Mathur, J., N. Mathur, B. Kernebeck, and M. Hulskamp. 2003. Mutations in actin-related proteins 2 and 3 affect cell shape development in Arabidopsis. *Plant Cell*. 15:1632-1645.

Matsuyama, S., and J.C. Reed. 2000. Mitochondria-dependent apoptosis and cellular pH regulation. *Cell Death and Differentiation*. 7:1155-1165.

Matveeva, N.P., D.S. Andreyuk, O.O. Voitsekh, and I.P. Ermakov. 2003. Regulatory changes in the intracellular pH and Cl- efflux at early stages of pollen grain germination in vitro. *Russ J Plant Physl+*. 50:318-323.

McClure, B. 2004. S-RNase and SLF determine S-haplotype-specific pollen recognition and rejection. *Plant Cell*. 16:2840-2847.

McClure, B. 2006. New views of S-RNase-based self-incompatibility. *Current Opinion in Plant Biology*. 9:639-646.

McClure, B., F. Cruz-Garcia, and C. Romero. 2011. Compatibility and incompatibility in S-RNase-based systems. *Annals of Botany*. 108:647-658.

McClure, B.A., F. Cruz-Garcia, B. Beecher, and W. Sulaman. 2000. Factors affecting inter- and intraspecific pollen rejection in Nicotiana. *Annals of Botany*. 85:113-123.

McClure, B.A., and V. Franklin-Tong. 2006. Gametophytic self-incompatibility: understanding the cellular mechanisms involved in "self" pollen tube inhibition. *Planta*. 224:233-245.

McClure, B.A., J.E. Gray, M.A. Anderson, and A.E. Clarke. 1990. Self-incompatibility in Nicotiana alata involves degradation of pollen rRNA. *Nature*. 347:757-760.

McCubbin, A.G., and T.H. Kao. 2000. Molecular recognition and response in pollen and pistil interactions. *Annual Review of Cell and Developmental Biology*. 16:333-364.

McInnis, S.M., R. Desikan, J.T. Hancock, and S.J. Hiscock. 2006. Production of reactive oxygen species and reactive nitrogen species by angiosperm stigmas and pollen: potential signalling crosstalk? *New Phytol*. 172:221-228.

Meijer, H.J., S.A. Arisz, J.A. Van Himbergen, A. Musgrave, and T. Munnik. 2001. Hyperosmotic stress rapidly generates lyso-phosphatidic acid in Chlamydomonas. *The Plant journal : for cell and molecular biology*. 25:541-548.

Meijer, H.J., and T. Munnik. 2003. Phospholipid-based signaling in plants. *Annual Review of Plant Biology*. 54:265-306.

Meisenholder, G.W., S.J. Martin, D.R. Green, J. Nordberg, B.M. Babior, and R.A. Gottlieb. 1996. Events in Apoptosis. *Journal of Biological Chemistry*. 271:16260-16262.

Meng, X., Z. Hua, N. Wang, A.M. Fields, P.E. Dowd, and T.H. Kao. 2009. Ectopic expression of S-RNase of Petunia inflata in pollen results in its sequestration and non-cytotoxic function. *Sexual Plant Reproduction*. 22:263-275.

Messerli, M.A., and K.R. Robinson. 2003. Ionic and osmotic disruptions of the lily pollen tube oscillator: testing proposed models. *Planta*. 217:147-157.

Michard, E., F. Alves, and J.A. Feijo. 2009. The role of ion fluxes in polarized cell growth and morphogenesis: the pollen tube as an experimental paradigm. *The International Journal of Developmental Biology*. 53:1609-1622.

Mino, M., N. Murata, S. Date, and M. Inoue. 2007. Cell death in seedlings of the interspecific hybrid of Nicotiana gossei and N. tabacum; possible role of knob-like bodies formed on tonoplast in vacuolar-collapse-mediated cell death. *Plant Cell Reports*. 26:407-419.

Mishra, G., W. Zhang, F. Deng, J. Zhao, and X. Wang. 2006. A bifurcating pathway directs abscisic acid effects on stomatal closure and opening in Arabidopsis. *Science*. 312:264-266.

Mittler, R., S. Vanderauwera, M. Gollery, and F. Van Breusegem. 2004. Reactive oxygen gene network of plants. *Trends in Plant Science*. 9:490-498.

Monshausen, G.B., T.N. Bibikova, M.A. Messerli, C. Shi, and S. Gilroy. 2007. Oscillations in extracellular pH and reactive oxygen species modulate tip growth of Arabidopsis root hairs. *P Natl Acad Sci USA*. 104:20996-21001.

Monshausen, G.B., N.D. Miller, A.S. Murphy, and S. Gilroy. 2011. Dynamics of auxin-dependent Ca2+ and pH signaling in root growth revealed by integrating high-resolution imaging with automated computer vision-based analysis. *The Plant journal : for cell and molecular biology*. 65:309-318.

Monteiro, D., P. Castanho Coelho, C. Rodrigues, L. Camacho, H. Quader, and R. Malhó. 2005a. Modulation of endocytosis in pollen tube growth by phosphoinositides and phospholipids. *Protoplasma*. 226:31-38.

Monteiro, D., Q. Liu, S. Lisboa, G.E.F. Scherer, H. Quader, and R. Malhó. 2005b. Phosphoinositides and phosphatidic acid regulate pollen tube growth and reorientation through modulation of [Ca2+]c and membrane secretion. *Journal of Experimental Botany*. 56:1665-1674.

Morimoto, H., and T. Shimmen. 2008. Primary effect of bromoxynil to induce plant cell death may be cytosol acidification. *J Plant Res*. 121:227-233.

Morley, S.C., G.P. Sun, and B.E. Bierer. 2003. Inhibition of actin polymerization enhances commitment to and execution of apoptosis induced by withdrawal of trophic support. *Journal of Cellular Biochemistry*. 88:1066-1076.

Munnik, T. 2001. Phosphatidic acid: An emerging plant lipid second messenger. *Trends in Plant Science*. 6:227-233.

Munnik, T., S.A. Arisz, T. De Vrije, and A. Musgrave. 1995. G Protein Activation Stimulates Phospholipase D Signaling in Plants. *The Plant cell*. 7:2197-2210.

Munnik, T., T. de Vrije, R.F. Irvine, and A. Musgrave. 1996. Identification of diacylglycerol pyrophosphate as a novel metabolic product of phosphatidic acid during G-protein activation in plants. *J Biol Chem*. 271:15708-15715.

Munnik, T., R.F. Irvine, and A. Musgrave. 1994. Rapid turnover of phosphatidylinositol 3-phosphate in the green alga Chlamydomonas eugametos: signs of a phosphatidylinositide 3-kinase signalling pathway in lower plants? *Biochem J*. 298 (Pt 2):269-273.

Munnik, T., R.F. Irvine, and A. Musgrave. 1998. Phospholipid signalling in plants. *Biochim Biophys Acta*. 1389:222-272.

Munnik, T., and H.J. Meijer. 2001. Osmotic stress activates distinct lipid and MAPK signalling pathways in plants. *FEBS Letters*. 498:172-178.

Munnik, T., H.J. Meijer, B. Ter Riet, H. Hirt, W. Frank, D. Bartels, and A. Musgrave. 2000. Hyperosmotic stress stimulates phospholipase D activity and elevates the levels of phosphatidic acid and diacylglycerol pyrophosphate. *The Plant journal : for cell and molecular biology*. 22:147-154.

Munnik, T., and A. Musgrave. 2001. Phospholipid signaling in plants: holding on to phospholipase D. *Sci STKE*. 2001:pe42.

Munnik, T., and E. Nielsen. 2011. Green light for polyphosphoinositide signals in plants. *Current Opinion in Plant Biology*.

Munnik, T., and C. Testerink. 2009. Plant phospholipid signaling: "in a nutshell". *J Lipid Res*. 50 Suppl:S260-265.

Murase, K., H. Shiba, M. Iwano, F.S. Che, M. Watanabe, A. Isogai, and S. Takayama. 2004. A membrane-anchored protein kinase involved in Brassica self-incompatibility signaling. *Science*. 303:1516-1519.

Murfett, J., T.L. Atherton, B. Mou, C.S. Gasser, and B.A. McClure. 1994. S-RNAse expressed in transgenic Nicotiana causes S-allel-specific pollen rejection. *Nature*. 367:563-566.

Nakagami, H., A. Pitzschke, and H. Hirt. 2005. Emerging MAP kinase pathways in plant stress signalling. *Trends in Plant Science*. 10:339-346.

Nakaune, S., K. Yamada, M. Kondo, T. Kato, S. Tabata, M. Nishimura, and I. Hara-Nishimura. 2005. A vacuolar processing enzyme, deltaVPE, is involved in seed coat formation at the early stage of seed development. *The Plant cell*. 17:876-887.

Nakaune, S., K. Yamada, M. Kondo, M. Nishimura, and I. Nishimura. 2004. Arabidopsis delta VPE is involved in programmed cell death of limited cell layers, the purpose of which is to a form seed coat. *Plant and Cell Physiology*. 45:S64-S64.

Neill, S.J., R. Desikan, and J.T. Hancock. 2003. Nitric oxide signalling in plants. *New Phytologist*. 159:11-35.

Ng, C.K., and M.R. McAinsh. 2003. Encoding specificity in plant calcium signalling: hot-spotting the ups and downs and waves. *Ann Bot*. 92:477-485.

Nilsson, C., U. Johansson, A.-C. Johansson, K. Kågedal, and K. Öllinger. 2006. Cytosolic acidification and lysosomal alkalinization during TNF-α induced apoptosis in U937 cells. *Apoptosis*. 11:1149-1159.

Nilsson, C., K. Kågedal, U. Johansson, and K. Öllinger. 2004. Analysis of cytosolic and lysosomal pH in apoptotic cells by flow cytometry. *Methods in Cell Science*. 25:185-194.

Obara, K., H. Kuriyama, and H. Fukuda. 2001. Direct evidence of active and rapid nuclear degradation triggered by vacuole rupture during programmed cell death in Zinnia. *Plant Physiology*. 125:615-626.

Ockendon, D.J. 2000. The S-allele collection of Brassica oleracea. *Proceedings of the Third International Symposium on Brassicas and Twelfth Crucifer Genetics Workshop*:25-30.

Oda, Y., T. Higaki, S. Hasezawa, and N. Kutsuna. 2009a. Chapter 3 New Insights into Plant Vacuolar Structure and Dynamics. *In* International Review of Cell and Molecular Biology. Vol. Volume 277. W.J. Kwang, editor. Academic Press. 103-135.

Oda, Y., A. Hirata, T. Sano, T. Fujita, Y. Hiwatashi, Y. Sato, A. Kadota, M. Hasebe, and S. Hasezawa. 2009b. Microtubules Regulate Dynamic Organization of Vacuoles in Physcomitrella patens. *Plant and Cell Physiology*. 50:855-868.

Odaka, C., M.L. Sanders, and P. Crews. 2000. Jasplakinolide induces apoptosis in various transformed cell lines by a caspase-3-like protease-dependent pathway. *Clin Diagn Lab Immunol*. 7:947-952.

Okuda, S., H. Tsutsui, K. Shiina, S. Sprunck, H. Takeuchi, R. Yui, R.D. Kasahara, Y. Hamamura, A. Mizukami, D. Susaki, N. Kawano, T. Sakakibara, S. Namiki, K. Itoh, K. Otsuka, M. Matsuzaki, H. Nozaki, T. Kuroiwa, A. Nakano, M.M. Kanaoka, T. Dresselhaus, N. Sasaki, and T. Higashiyama. 2009. Defensin-like polypeptide LUREs are pollen tube attractants secreted from synergid cells. *Nature*. 458:357-361.

Otto, G.P., M.Y. Wu, N. Kazgan, O.R. Anderson, and R.H. Kessin. 2003. Macroautophagy is required for multicellular development of the social amoeba Dictyostelium discoideum. *Journal of Biological Chemistry*. 278:17636-17645.

Pagnussat, G.C., M.L. Lanteri, M.C. Lombardo, and L. Lamattina. 2004. Nitric oxide mediates the indole acetic acid induction activation of a mitogen-activated protein kinase cascade involved in adventitious root development. *Plant Physiology*. 135:279-286.

Pajerowska-Mukhtar, K., and X. Dong. 2009. A kiss of death--proteasome-mediated membrane fusion and programmed cell death in plant defense against bacterial infection. *Genes & Development*. 23:2449-2454.

Palissot, V., R. Belhoussine, Y. Carpentier, S. Sebille, H. Morjani, M. Manfait, and J. Dufer. 1998. Resistance to Apoptosis Induced by Topoisomerase I Inhibitors in Multidrug-Resistant HL60 Leukemic Cells. *Biochemical and Biophysical Research Communications*. 245:918-922.

Pappan, K., and X. Wang. 1999. Plant Phospholipase D[alpha] Is an Acidic Phospholipase Active at Near-Physiological Ca2+ Concentrations. *Archives of Biochemistry and Biophysics*. 368:347-353.

Papuga, J., C. Hoffmann, M. Dieterle, D. Moes, F. Moreau, S. Tholl, A. Steinmetz, and C. Thomas. 2010. Arabidopsis LIM Proteins: A Family of Actin Bundlers with Distinct Expression Patterns and Modes of Regulation. *The Plant Cell Online*. 22:3034-3052.

Park, H.J., C.M. Makepeace, J.C. Lyons, and C.W. Song. 1996. Effect of intracellular acidity and ionomycin on apoptosis in HL-60 cells. *Eur J Cancer*. 3:540-546.

Park, J., Y. Gu, Y. Lee, and Z. Yang. 2004. Phosphatidic acid induces leaf cell death in Arabidopsis by activating the Rho-related small G protein GTPase-mediated pathway of reactive oxygen species generation. *Plant Physiology*. 134:129-136.

Pennell, R.I., and C. Lamb. 1997. Programmed cell death in plants. *Plant Cell*. 9:1157-1168.

Pérez-Sala, D., D. Collado-Escobar, and F. Mollinedo. 1995. Intracellular Alkalinization Suppresses Lovastatin-induced Apoptosis in HL-60 Cells through the Inactivation of a pH-dependent Endonuclease. *Journal of Biological Chemistry*. 270:6235-6242.

Peters, N.T., K.O. Logan, A.C. Miller, and D.L. Kropf. 2007. Phospholipase D Signaling Regulates Microtubule Organization in the Fucoid Alga Silvetia compressa. *Plant and Cell Physiology*. 48:1764-1774.

Pical, C., T. Westergren, S.K. Dove, C. Larsson, and M. Sommarin. 1999. Salinity and Hyperosmotic Stress Induce Rapid Increases in Phosphatidylinositol 4,5-Bisphosphate, Diacylglycerol Pyrophosphate, and Phosphatidylcholine in Arabidopsis thaliana Cells. *Journal of Biological Chemistry*. 274:38232-38240.

Pierson, E.S., D.D. Miller, D.A. Callaham, J. van Aken, G. Hackett, and P.K. Hepler. 1996. Tip-localized calcium entry fluctuates during pollen tube growth. *Dev Biol*. 174:160-173.

Pleskot, R., P. Pejchar, R. Bezvoda, I.K. Lichtscheidl, M. Wolters-Arts, J. Marc, V. Žárský , and M. Potocký. 2012. Turnover of phosphatidic acid through distinct signalling pathways affects multiple aspects of tobacco pollen tube tip growth. *Frontiers in Plant Science*. 3.

Pleskot, R., M. Potocky, P. Pejchar, J. Linek, R. Bezvoda, J. Martinec, O. Valentova, Z. Novotna, and V. Zarsky. 2010. Mutual regulation of plant phospholipase D and the actin cytoskeleton. *The Plant journal : for cell and molecular biology*. 62:494-507.

Potocký, M., M. Eliáš, B. Profotová, Z. Novotná, O. Valentová, and V. Žárský. 2003. Phosphatidic acid produced by phospholipase D is required for tobacco pollen tube growth. *Planta*. 217:122-130.

Potocký, M., M.A. Jones, R. Bezvoda, N. Smirnoff, and V. Žárský. 2007. Reactive oxygen species produced by NADPH oxidase are involved in pollen tube growth. *New Phytologist*. 174:742-751.

Poulter, N.S., M. Bosch, and V.E. Franklin-Tong. 2011. Proteins implicated in mediating self-incompatibility-induced alterations to the actin cytoskeleton of Papaver pollen. *Annals of Botany*.

Poulter, N.S., C.J. Staiger, J.Z. Rappoport, and V.E. Franklin-Tong. 2010. Actin-Binding Proteins Implicated in the Formation of the Punctate Actin Foci Stimulated by the Self-Incompatibility Response in Papaver. *Plant Physiology*. 152:1274-1283.

Poulter, N.S., S. Vatovec, and V.E. Franklin-Tong. 2008. Microtubules Are a Target for Self-Incompatibility Signaling in Papaver Pollen. *Plant Physiology*. 146:1358-1367.

Prado, A.M., R. Colaco, N. Moreno, A.C. Silva, and J.A. Feijo. 2008. Targeting of Pollen Tubes to Ovules Is Dependent on Nitric Oxide (NO) Signaling. *Molecular Plant*. 1:703-714.

Prado, A.M., D.M. Porterfield, and J.A. Feijo. 2004. Nitric oxide is involved in growth regulation and re-orientation of pollen tubes. *Development*. 131:2707-2714.

Qiao, H., F. Wang, L. Zhao, J.L. Zhou, Z. Lai, Y.S. Zhang, T.P. Robbins, and Y.B. Xue. 2004. The F-Box protein AhSLF-S-2 controls the pollen function of S-RNase-based self-incompatibility. *Plant Cell*. 16:2307-2322.

Raff, M. 1998. Cell suicide for beginners. *Nature*. 396:119-122.

Raho, N., L. Ramirez, M.L. Lanteri, G. Gonorazky, L. Lamattina, A. ten Have, and A.M. Laxalt. 2011. Phosphatidic acid production in chitosan-elicited tomato cells, via both phospholipase D and phospholipase C/diacylglycerol kinase, requires nitric oxide. *Journal of Plant Physiology*. 168:534-539.

Rathore, K.S., R.J. Cork, and K.R. Robinson. 1991. A cytoplasmic gradient of Ca2+ is correlated with the growth of lily pollen tubes. *Dev Biol*. 148:612-619.

Reichler, S.A., J. Torres, A.L. Rivera, V.A. Cintolesi, G. Clark, and S.J. Roux. 2009. Intersection of two signalling pathways: extracellular nucleotides regulate pollen germination and pollen tube growth via nitric oxide. *Journal of Experimental Botany*. 60:2129-2138.

Renew, S., E. Heyno, P. Schopfer, and A. Liszkay. 2005. Sensitive detection and localization of hydroxyl radical production in cucumber roots and Arabidopsis seedlings by spin trapping electron paramagnetic resonance spectroscopy. *The Plant Journal*. 44:342-347.

Rentel, M.C., D. Lecourieux, F. Ouaked, S.L. Usher, L. Petersen, H. Okamoto, H. Knight, S.C. Peck, C.S. Grierson, H. Hirt, and M.R. Knight. 2004. OXI1 kinase is necessary for oxidative burst-mediated signalling in Arabidopsis. *Nature*. 427:858-861.

Reynolds, J.E., J. Li, R.W. Craig, and A. Eastman. 1996. BCL-2 and MCL-1 Expression in Chinese Hamster Ovary Cells Inhibits Intracellular Acidification and Apoptosis Induced by Staurosporine. *Exp Cell Res*. 225:430-436.

Riedl, S.J., and Y.G. Shi. 2004. Molecular mechanisms of caspase regulation during apoptosis. *Nature Reviews Molecular Cell Biology*. 5:897-907.

Robson, G.D., E. Prebble, A. Rickers, S. Hosking, D.W. Denning, A.P.J. Trinci, and W. Robertson. 1996. Polarized Growth of Fungal Hyphae Is Defined by an Alkaline pH Gradient. *Fungal Genetics and Biology*. 20:289-298.

Rodríguez-Serrano, M., I. Bárány, D. Prem, M.-J. Coronado, M.C. Risueño, and P.S. Testillano. 2011. NO, ROS, and cell death associated with caspase-like activity increase in stress-induced microspore embryogenesis of barley. *Journal of Experimental Botany*.

Rodríguez, A.A., K.A. Grunberg, and E.L. Taleisnik. 2002. Reactive Oxygen Species in the Elongation Zone of Maize Leaves Are Necessary for Leaf Extension. *Plant Physiology*. 129:1627-1632.

Rogers, H.J. 2005. Programmed Cell Death in Floral Organs: How and Why do Flowers Die? *Annals of Botany*. 97:309-315.

Rojo, E., R. Martín, C. Carter, J. Zouhar, S. Pan, J. Plotnikova, H. Jin, M. Paneque, J.J. Sánchez-Serrano, and B. Baker. 2004. VPEγ Exhibits a Caspase-like Activity that Contributes to Defense against Pathogens. *Current Biology*. 14:1897-1906.

Romero-Puertas, M.C., M. Perazzolli, E.D. Zago, and M. Delledonne. 2004. Nitric oxide signalling functions in plant-pathogen interactions. *Cellular Microbiology*. 6:795-803.

Roos, W., S. Evers, M. Hieke, M. Tschope, and B. Schumann. 1998. Shifts of intracellular pH distribution as a part of the signal mechanism leading to the elicitation of benzophenanthridine alkaloids - Phytoalexin biosynthesis in cultured cells of Eschscholtzia californica. *Plant Physiology*. 118:349-364.

Roos, W., K. Viehweger, B. Dordschbal, B. Schumann, S. Evers, J. Steighardt, and W. Schwartze. 2006. Intracellular pH signals in the induction of secondary pathways – The case of Eschscholzia californica. *Journal of Plant Physiology*. 163:369-381.

Rubinstein, B. 2000. Regulation of cell death in flower petals. *Plant Molecular Biology*. 44:303-318.

Rudd, J.J., and V.E. Franklin-Tong. 2003. Signals and targets of the self-incompatibility response in pollen of Papaver rhoeas. *Journal of Experimental Botany*. 54:141-148.

Rudd, J.J., F. Franklin, J.M. Lord, and V.E. Franklin-Tong. 1996. Increased Phosphorylation of a 26-kD Pollen Protein Is Induced by the Self-Incompatibility Response in Papaver rhoeas. *The Plant cell*. 8:713-724.

Rudd, J.J., K. Osman, F.C.H. Franklin, and V.E. Franklin-Tong. 2003. Activation of a putative MAP kinase in pollen is stimulated by the self-incompatibility (SI) response. *FEBS Letters*. 547:223-227.

Sage, T.L., and F.B. Sampson. 2003. Evidence for ovarian self-incompatibility as a cause of self-sterility in the relictual woody angiosperm, Pseudowintera axillaris (Winteraceae). *Annals of Botany*. 91:807-816.

Sagot, I., B. Pinson, B. Salin, and B. Daignan-Fornier. 2006. Actin Bodies in Yeast Quiescent Cells: An Immediately Available Actin Reserve? *Molecular Biology of the Cell*. 17:4645-4655.

Samuel, M.A., J.N. Salt, S.H. Shiu, and D.R. Goring. 2006. Multifunctional arm repeat domains in plants. *International Review of Cytology - a Survey of Cell Biology, Vol 253*. 253:1-+.

Sanders, D., C. Brownlee, and J.F. Harper. 1999. Communicating with calcium. *Plant Cell*. 11:691-706.

Sang, Y., D. Cui, and X. Wang. 2001. Phospholipase D and phosphatidic acid-mediated generation of superoxide in Arabidopsis. *Plant Physiol*. 126:1449-1458.

Sanmartín, M., L. Jaroszewski, N.V. Raikhel, and E. Rojo. 2005. Caspases. Regulating Death Since the Origin of Life. *Plant Physiology*. 137:841-847.

Schachtman, D.P., and J.Q.D. Goodger. 2008. Chemical root to shoot signaling under drought. *Trends in Plant Science*. 13:281-287.

Schopfer, C.R., M.E. Nasrallah, and J.B. Nasrallah. 1999. The male determinant of self-incompatibility in Brassica. *Science*. 286:1697-1700.

Scott, A.C., and N.S. Allen. 1999. Changes in Cytosolic pH within Arabidopsis Root Columella Cells Play a Key Role in the Early Signaling Pathway for Root Gravitropism. *Plant Physiology*. 121:1291-1298.

Senatore, A., C.P. Trobacher, and J.S. Greenwood. 2009. Ricinosomes Predict Programmed Cell Death Leading to Anther Dehiscence in Tomato. *Plant Physiology*. 149:775-790.

Serrano, I., M.C. Romero-Puertas, M. Rodriguez-Serrano, L.M. Sandalio, and A. Olmedilla. 2012. Peroxynitrite mediates programmed cell death both in papillar cells and in self-incompatible pollen in the olive (Olea europaea L.). *Journal of Experimental Botany*. 63:1479-1493.

Sharma, K., and C.B. Srikant. 1998. G Protein Coupled Receptor Signaled Apoptosis Is Associated with Activation of a Cation Insensitive Acidic Endonuclease and Intracellular Acidification. *Biochemical and Biophysical Research Communications*. 242:134-140.

Sheahan, M.B., R.J. Rose, and D.W. McCurdy. 2007. Actin-filament-dependent remodeling of the vacuole in cultured mesophyll protoplasts. *Protoplasma*. 230:141-152.

Shiba, H., S. Takayama, M. Iwano, H. Shimosato, M. Funato, T. Nakagawa, F.S. Che, G. Suzuki, M. Watanabe, K. Hinata, and A. Isogai. 2001. A pollen coat protein, SP11/SCR, determines the pollen S-specificity in the self-incompatibility of Brassica species. *Plant Physiology*. 125:2095-2103.

Shimosato, H., N. Yokota, H. Shiba, M. Iwano, T. Entani, F.S. Che, M. Watanabe, A. Isogai, and S. Takayama. 2007. Characterization of the SP11/SCR high-affinity binding site involved in self/nonself recognition in Brassica self-incompatibility. *Plant Cell*. 19:107-117.

Shin, J.J., and C.J. Loewen. 2011. Putting the pH into phosphatidic acid signaling. *BMC Biol*. 9:85.

Sijacic, P., X. Wang, A.L. Skirpan, Y. Wang, P.E. Dowd, A.G. McCubbin, S. Huang, and T.H. Kao. 2004. Identification of the pollen determinant of S-RNase-mediated self-incompatibility. *Nature*. 429:302-305.

Silva, N.F., and D.R. Goring. 2001. Mechanisms of self-incompatibility in flowering plants. *Cell Mol Life Sci*. 58:1988-2007.

Simon, S., D. Roy, and M. Schindler. 1994. Intracellular pH and the control of multidrug resistance. *Proceedings of the National Academy of Sciences*. 91:1128-1132.

Smart, C.M. 1994. GENE-EXPRESSION DURING LEAF SENESCENCE. *New Phytologist*. 126:419-448.

Snowman, B. 2000. Signalling and the Cytoskeleton of Pollen Tubes of Papaver rhoeas. *Annals of Botany*. 85:49-57.

Snowman, B.N., D.R. Kovar, G. Shevchenko, V.E. Franklin-Tong, and C.J. Staiger. 2002. Signal-mediated depolymerization of actin in pollen during the self-incompatibility response. *Plant Cell*. 14:2613-2626.

Sousa, M.J., F. Azevedo, A. Pedras, C. Marques, O.P. Coutinho, A. Preto, H. Geros, S.R. Chaves, and M. Corte-Real. 2011. Vacuole-mitochondrial cross-talk during apoptosis in yeast: a model for understanding lysosome-mitochondria-mediated apoptosis in mammals. *Biochemical Society Transactions*. 39:1533-1537.

Staiger, C.J., N.S. Poulter, J.L. Henty, V.E. Franklin-Tong, and L. Blanchoin. 2010. Regulation of actin dynamics by actin-binding proteins in pollen. *Journal of Experimental Botany*. 61:1969-1986.

Stein, J.C., B. Howlett, D.C. Boyes, M.E. Nasrallah, and J.B. Nasrallah. 1991. Molecular Cloning of a Putative Receptor Protein-Kinase Gene Encoded at the Self-Incompatibility Locus of Brassica oleracea. *P Natl Acad Sci USA*. 88:8816-8820.

Stone, S.L., E.M. Anderson, R.T. Mullen, and D.R. Goring. 2003. ARC1 is an E3 ubiquitin ligase and promotes the ubiquitination of proteins during the rejection of self-incompatible Brassica pollen. *Plant Cell*. 15:885-898.

Stone, S.L., M. Arnoldo, and D.R. Goring. 1999. A breakdown of Brassica self-incompatibility in ARC1 antisense transgenic plants. *Science*. 286:1729-1731.

Straatman, K.R., S.K. Dove, T. Holdaway-Clarke, P.K. Hepler, J.G. Kunkel, and V.E. Franklin-Tong. 2001. Calcium signalling in pollen of Papaver rhoeas undergoing the self-incompatibility (SI) response. *Sexual Plant Reproduction*. 14:105-110.

Suria, H., L.A. Chau, E. Negrou, D.J. Kelvin, and J. Madrenas. 1999. Cytoskeletal disruption induces T cell apoptosis by a caspase-3 mediated mechanism. *Life Sciences*. 65:2697-2707.

Suzuki, G., N. Kai, T. Hirose, K. Fukui, T. Nishio, S. Takayama, A. Isogai, M. Watanabe, and K. Hinata. 1999. Genomic organization of the S locus: Identification and characterization of genes in SLG/SRK region of S-9 haplotype of Brassica campestris (syn. rapa). *Genetics*. 153:391-400.

Swanson, S.J., W.G. Choi, A. Chanoca, and S. Gilroy. 2011. In vivo imaging of Ca2+, pH, and reactive oxygen species using fluorescent probes in plants. *Annual Review of Plant Biology*. 62:273-297.

Syntichaki, P., C. Samara, and N. Tavernarakis. 2005. The Vacuolar H+-ATPase Mediates Intracellular Acidification Required for Neurodegeneration in C. elegans. *Curr Biol*. 15:1249-1254.

Takasaki, T., K. Hatakeyama, G. Suzuki, M. Watanabe, A. Isogai, and K. Hinata. 2000. The S receptor kinase determines self-incompatibility in Brassica stigma. *Nature*. 403:913-916.

Takayama, S., and A. Isogai. 2005. Self-incompatibility in plants. *Annual Review of Plant Biology*. 56:467-489.

Takayama, S., H. Shimosato, H. Shiba, M. Funato, F.S. Che, M. Watanabe, M. Iwano, and A. Isogai. 2001. Direct ligand-receptor complex interaction controls Brassica self-incompatibility. *Nature*. 413:534-538.

Taylor, L.P., and P.K. Hepler. 1997. Pollen Germination and Tube Growth. *Annual Review of Plant Physiology and Plant Molecular Biology*. 48:461-491.

Testerink, C., and T. Munnik. 2005. Phosphatidic acid: a multifunctional stress signaling lipid in plants. *Trends in Plant Science*. 10:368-375.

Testerink, C., and T. Munnik. 2011. Molecular, cellular, and physiological responses to phosphatidic acid formation in plants. *Journal of Experimental Botany*. 62:2349-2361.

Thangaraju, M., K. Sharma, B. Leber, D.W. Andrews, S.-H. Shen, and C.B. Srikant. 1999a. Regulation of Acidification and Apoptosis by SHP-1 and Bcl-2. *Journal of Biological Chemistry*. 274:29549-29557.

Thangaraju, M., K. Sharma, D. Liu, S.-H. Shen, and C.B. Srikant. 1999b. Interdependent Regulation of Intracellular Acidification and SHP-1 in Apoptosis. *Cancer Res*. 59:1649-1654.

Thomas, S., K. Osman, B.H.J. de Graaf, G. Shevchenko, M. Wheeler, C. Franklin, and N. Franklin-Tong. 2003. Investigating mechanisms involved in the self-incompatibility response in Papaver rhoeas. *Philos T Roy Soc B*. 358:1033-1036.

Thomas, S.G., and V.E. Franklin-Tong. 2004. Self-incompatibility triggers programmed cell death in Papaver pollen. *Nature*. 429:305-309.

Thomas, S.G., S. Huang, S. Li, C.J. Staiger, and V.E. Franklin-Tong. 2006. Actin depolymerization is sufficient to induce programmed cell death in self-incompatible pollen. *The Journal of Cell Biology*. 174:221-229.

Torres, M.A., J.D. Jones, and J.L. Dangl. 2006. Reactive oxygen species signaling in response to pathogens. *Plant Physiology*. 141:373-378.

Torres, M.A., H. Onouchi, S. Hamada, C. Machida, K.E. Hammond-Kosack, and J.D.G. Jones. 1998. Six Arabidopsis thaliana homologues of the human respiratory burst oxidase (gp91phox). *The Plant Journal*. 14:365-370.

Tuteja, N., and S.K. Sopory. 2008. Plant signaling in stress: G-protein coupled receptors, heterotrimeric G-proteins and signal coupling via phospholipases. *Plant Signal Behav*. 3:79-86.

Vacca, R.A., D. Valenti, A. Bobba, R.S. Merafina, S. Passarella, and E. Marra. 2006. Cytochrome c Is Released in a Reactive Oxygen Species-Dependent Manner and Is Degraded via Caspase-Like Proteases in Tobacco Bright-Yellow 2 Cells en Route to Heat Shock-Induced Cell Death. *Plant Physiology*. 141:208-219.

van der Luit, A.H., T. Piatti, A. van Doorn, A. Musgrave, G. Felix, T. Boller, and T. Munnik. 2000. Elicitation of Suspension-Cultured Tomato Cells Triggers the Formation of Phosphatidic Acid and Diacylglycerol Pyrophosphate. *Plant Physiology*. 123:1507-1516.

van Doorn, W.G. 2005. Plant programmed cell death and the point of no return. *Trends in Plant Science*. 10:478-483.

van Doorn, W.G., E.P. Beers, J.L. Dangl, V.E. Franklin-Tong, P. Gallois, I. Hara-Nishimura, A.M. Jones, M. Kawai-Yamada, E. Lam, J. Mundy, L.A.J. Mur, M. Petersen, A. Smertenko, M. Taliansky, F. Van Breusegem, T. Wolpert, E. Woltering, B. Zhivotovsky, and P.V. Bozhkov. 2011. Morphological classification of plant cell deaths. *Cell Death Differ*. 18:1241-1246.

van Doorn, W.G., and E.J. Woltering. 2005. Many ways to exit? Cell death categories in plants. *Trends in Plant Science*. 10:117-122.

Vardar, F., and M. Unal. 2012. Ultrastructural aspects and programmed cell death in the tapetal cells of Lathyrus undulatus Boiss. *Acta Biol Hung*. 63:52-66.

Vercher, Y., A. Molowny, and J. Carbonell. 1987. GIBBERELLIC-ACID EFFECTS ON THE ULTRASTRUCTURE OF ENDOCARP CELLS OF UNPOLLINATED OVARIES OF PISUM-SATIVUM. *Physiologia Plantarum*. 71:302-308.

Vidali, L., C.M. Rounds, P.K. Hepler, and M. Bezanilla. 2009. Lifeact-mEGFP reveals a dynamic apical F-actin network in tip growing plant cells. *PLoS ONE*. 4:e5744.

Walker, E.A., J.P. Ride, S. Kurup, V.E. FranklinTong, M.J. Lawrence, and F.C.H. Franklin. 1996. Molecular analysis of two functional homologues of the S-3 allele of the Papaver rhoeas self-incompatibility gene isolated from different populations. *Plant Molecular Biology*. 30:983-994.

Wang, C.L., J. Wu, G.H. Xu, Y.B. Gao, G. Chen, J.Y. Wu, H.Q. Wu, and S.L. Zhang. 2010. S-RNase disrupts tip-localized reactive oxygen species and induces nuclear DNA degradation in incompatible pollen tubes of Pyrus pyrifolia. *Journal of Cell Science*. 123:4301-4309.

Wang, C.L., G.H. Xu, X.T. Jiang, G. Chen, J. Wu, H.Q. Wu, and S.L. Zhang. 2009. S-RNase triggers mitochondrial alteration and DNA degradation in the incompatible pollen tube of Pyrus pyrifolia in vitro. *The Plant journal : for cell and molecular biology*. 57:220-229.

Wang, H.J., A.R. Wan, and G.Y. Jauh. 2008. An Actin-Binding Protein, LlLIM1, Mediates Calcium and Hydrogen Regulation of Actin Dynamics in Pollen Tubes. *Plant Physiology*. 147:1619-1636.

Wang, X. 2005. Regulatory Functions of Phospholipase D and Phosphatidic Acid in Plant Growth, Development, and Stress Responses. *Plant Physiology*. 139:566-573.

Wang, Y.F., L.M. Fan, W.Z. Zhang, W. Zhang, and W.H. Wu. 2004. Ca2+-permeable channels in the plasma membrane of Arabidopsis pollen are regulated by actin microfilaments. *Plant Physiology*. 136:3892-3904.

Watanabe, M., T. Takasaki, K. Toriyama, S. Yamakawa, A. Isogai, A. Suzuki, and K. Hinata. 1994. A high-degree of homology exists between the protein encoded by SLG and the S-receptor deomain encoded by SRK in self-incompatible brassica campestris l. *Plant and Cell Physiology*. 35:1221-1229.

Watanabe, N., and E. Lam. 2004. Recent advance in the study of caspase-like proteases and Bax inhibitor-1 in plants: their possible roles as regulator of programmed cell death. *Molecular Plant Pathology*. 5:65-70.

Wenzel, P., H. Mollnau, M. Oelze, E. Schulz, J.M.D. Wickramanayake, J. Muller, S. Schuhmacher, M. Hortmann, S. Baldus, T. Gori, R.P. Brandes, T. Munzel, and A. Daiber. 2008. First evidence for a crosstalk between mitochondrial and NADPH oxidase-derived reactive oxygen species in nitroglycerin-triggered vascular dysfunction. *Antioxid Redox Signal*. 10:1435-1447.

Wheeler, M.J., B.H. de Graaf, N. Hadjiosif, R.M. Perry, N.S. Poulter, K. Osman, S. Vatovec, A. Harper, F.C. Franklin, and V.E. Franklin-Tong. 2009. Identification of the pollen self-incompatibility determinant in Papaver rhoeas. *Nature*. 459:992-995.

Wheeler, M.J., S. Vatovec, and V.E. Franklin-Tong. 2010. The pollen S-determinant in Papaver: comparisons with known plant receptors and protein ligand partners. *Journal of Experimental Botany*. 61:2015-2025.

Wilkins, K.A., J. Bancroft, M. Bosch, J. Ings, N. Smirnoff, and V.E. Franklin-Tong. 2011. Reactive oxygen species and nitric oxide mediate actin reorganization and programmed cell death in the self-incompatibility response of papaver. *Plant Physiology*. 156:404-416.

Wissing, J.B., and H. Behrbohm. 1993. Phosphatidate Kinase, a Novel Enzyme in Phospholipid Metabolism (Purification, Subcellular Localization, and Occurrence in the Plant Kingdom). *Plant Physiology*. 102:1243-1249.

Wolf, B.B., M. Schuler, W. Li, B. Eggers-Sedlet, W. Lee, P. Tailor, P. Fitzgerald, G.B. Mills, and D.R. Green. 2001. Defective cytochrome c-dependent caspase activation in ovarian cancer cell lines due to diminished or absent apoptotic protease activating factor-1 activity. *Journal of Biological Chemistry*. 276:34244-34251.

Wolf, C.M., and A. Eastman. 1999. Intracellular Acidification during Apoptosis Can Occur in the Absence of a Nucleus. *Biochemical and Biophysical Research Communications*. 254:821-827.

Wolf, C.M., J.E. Reynolds, S.J. Morana, and A. Eastman. 1997. The Temporal Relationship between Protein Phosphatase, ICE/CED-3 Proteases, Intracellular Acidification, and DNA Fragmentation in Apoptosis. *Exp Cell Res*. 230:22-27.

Woltering, E.J. 2004. Death proteases come alive. *Trends in Plant Science*. 9:469-472.

Wosniak, J., Jr., C.X. Santos, A.J. Kowaltowski, and F.R. Laurindo. 2009. Cross-talk between mitochondria and NADPH oxidase: effects of mild mitochondrial dysfunction on angiotensin II-mediated increase in Nox isoform expression and activity in vascular smooth muscle cells. *Antioxid Redox Signal*. 11:1265-1278.

Wright, H., W.G. van Doorn, and A.H.L.A.N. Gunawardena. 2009. In Vivo Study of Developmental Programmed Cell Death Using the Lace Plant (Aponogeton Madagascariensis; Aponogetonaceae) Leaf Model System. *Am J Bot*. 96:865-876.

Wu, J., S. Wang, Y. Gu, S. Zhang, S.J. Publicover, and V.E. Franklin-Tong. 2011. Self-incompatibility in papaver rhoeas activates nonspecific cation conductance permeable to Ca2+ and K+. *Plant Physiology*. 155:963-973.

Xu, L., A.Q. Paulsen, S.B. Ryu, and X. Wang. 1996. Intracellular Localization of Phospholipase D in Leaves and Seedling Tissues of Castor Bean. *Plant Physiology*. 111:101-107.

Xu, Q., and L. Zhang. 2009. Plant caspase-like proteases in plant programmed cell death. *Plant Signal Behav*. 4:902-904.

Xue, Y.B., R. Carpenter, H.G. Dickinson, and E.S. Coen. 1996. Origin of allelic diversity in antirrhinum S locus RNases. *Plant Cell*. 8:805-814.

Yakimova, E.T., V.M. Kapchina-Toteva, and E.J. Woltering. 2007. Signal transduction events in aluminum-induced cell death in tomato suspension cells. *Journal of Plant Physiology*. 164:702-708.

Yamada, K., M. Nishimura, and I. Hara-Nishimura. 2004. The slow wound-response of gamma VPE is regulated by endogenous salicylic acid in Arabidopsis. *Planta*. 218:599-605.

Yamaguchi, T., E. Minami, J. Ueki, and N. Shibuya. 2005. Elicitor-induced activation of phospholipases plays an important role for the induction of defense responses in suspension-cultured rice cells. *Plant and Cell Physiology*. 46:579-587.

Yamamoto-Katou, A., S. Katou, H. Yoshioka, N. Doke, and K. Kawakita. 2006. Nitrate Reductase is Responsible for Elicitin-induced Nitric Oxide Production in Nicotiana benthamiana. *Plant and Cell Physiology*. 47:726-735.

Yamaoka, N., S. Yoshida, E. Motoyama, Y. Takeuchi, Y. Takada, and N. Fukunaga. 2000. Resistance Induction in Barley Coleoptile Cells by Intracellular pH Decline. *Plant and Cell Physiology*. 41:1321-1326.

Yang, S.L., and K.-R. Chung. 2012. The NADPH oxidase-mediated production of hydrogen peroxide (H2O2) and resistance to oxidative stress in the necrotrophic pathogen Alternaria alternata of citrus. *Molecular Plant Pathology*:no-no.

Yarmola, E.G., T. Somasundaram, T.A. Boring, I. Spector, and M.R. Bubb. 2000. Actin-Latrunculin A Structure and Function. *Journal of Biological Chemistry*. 275:28120-28127.

Ye, Y.U.N., Z.H.E. Li, and D.A. Xing. 2012. Nitric oxide promotes MPK6-mediated caspase-3-like activation in cadmium-induced Arabidopsis thaliana programmed cell death. *Plant, Cell & Environment*:no-no.

Yi, Y.P., X. Wang, G. Zhang, T.S. Fu, and G.J. Zhang. 2006. Phosphatidic acid osmotically destabilizes lysosomes through increased permeability to K+ and H+. *Gen Physiol Biophys*. 25:149-160.

Yonezawa, N., E. Nishida, S. Koyasu, S. Maekawa, Y. Ohta, I. Yahara, and H. Sakai. 1987. Distribution among tissues and intracellular localization of cofilin, a 21kDa actin-binding protein. *Cell Struct Funct*. 12:443-452.

Yoshimori, T. 2004. Autophagy: a regulated bulk degradation process inside cells. *Biochemical and Biophysical Research Communications*. 313:453-458.

Yoshioka, H., N. Numata, K. Nakajima, S. Katou, K. Kawakita, O. Rowland, J.D.G. Jones, and N. Doke. 2003. Nicotiana benthamiana gp91phox Homologs NbrbohA and NbrbohB Participate in H2O2 Accumulation and Resistance to Phytophthora infestans. *The Plant Cell Online*. 15:706-718.

Young, B., R. Wightman, R. Blanvillain, S.B. Purcel, and P. Gallois. 2010a. pH-sensitivity of YFP provides an intracellular indicator of programmed cell death. *Plant Methods*. 6:27.

Young, B.P., J.J. Shin, R. Orij, J.T. Chao, S.C. Li, X.L. Guan, A. Khong, E. Jan, M.R. Wenk, W.A. Prinz, G.J. Smits, and C.J. Loewen. 2010b. Phosphatidic acid is a pH biosensor that links membrane biogenesis to metabolism. *Science*. 329:1085-1088.

Young, M.E., J.A. Cooper, and P.C. Bridgman. 2004. Yeast actin patches are networks of branched actin filaments. *The Journal of Cell Biology*. 166:629-635.

Young, S.A., X. Wang, and J.E. Leach. 1996. Changes in the Plasma Membrane Distribution of Rice Phospholipase D during Resistant Interactions with Xanthomonas oryzae pv oryzae. *The Plant Cell Online*. 8:1079-1090.

Yu, L., J. Nie, C. Cao, Y. Jin, M. Yan, F. Wang, J. Liu, Y. Xiao, Y. Liang, and W. Zhang. 2010. Phosphatidic acid mediates salt stress response by regulation of MPK6 in Arabidopsis thaliana. *New Phytol*. 188:762-773.

Yu, X.H., T.D. Perdue, Y.M. Heimer, and A.M. Jones. 2002. Mitochondrial involvement in tracheary element programmed cell death. *Cell Death and Differentiation*. 9:189-198.

Zalejski, C., S. Paradis, R. Maldiney, Y. Habricot, E. Miginiac, J.-P. Rona, and E. Jeannette. 2006. Induction of Abscisic Acid-Regulated Gene Expression by Diacylglycerol Pyrophosphate Involves Ca2+ and Anion Currents in Arabidopsis Suspension Cells. *Plant Physiology*. 141:1555-1562.

Zalejski, C., Z. Zhang, A.-L. Quettier, R. Maldiney, M. Bonnet, M. Brault, C. Demandre, E. Miginiac, J.-P. Rona, B. Sotta, and E. Jeannette. 2005. Diacylglycerol pyrophosphate is a second messenger of abscisic acid signaling in Arabidopsis thaliana suspension cells. *The Plant Journal*. 42:145-152.

Zhang, L., Q. Xu, D. Xing, C. Gao, and H. Xiong. 2009a. Real-time detection of caspase-3-like protease activation in vivo using fluorescence resonance energy transfer during plant programmed cell death induced by ultraviolet C overexposure. *Plant Physiology*. 150:1773-1783.

Zhang, S.Q., and D.F. Klessig. 2001. MAPK cascades in plant defense signaling. *Trends in Plant Science*. 6:520-527.

Zhang, W., C. Qin, J. Zhao, and X. Wang. 2004. Phospholipase Dα1-derived phosphatidic acid interacts with ABI1 phosphatase 2C and regulates abscisic acid signaling. *P Natl Acad Sci USA*. 101:9508-9513.

Zhang, W., C. Wang, C. Qin, T. Wood, G. Olafsdottir, R. Welti, and X. Wang. 2003. The oleate-stimulated phospholipase D, PLDdelta, and phosphatidic acid decrease H2O2-induced cell death in Arabidopsis. *The Plant cell*. 15:2285-2295.

Zhang, Y., H. Zhu, Q. Zhang, M. Li, M. Yan, R. Wang, L. Wang, R. Welti, W. Zhang, and X. Wang. 2009b. Phospholipase Dα1 and Phosphatidic Acid Regulate NADPH Oxidase Activity and Production of Reactive Oxygen Species in ABA-Mediated Stomatal Closure in Arabidopsis. *The Plant Cell Online*. 21:2357-2377.

Zhou, D., W. Luini, S. Bernasconi, L. Diomede, M. Salmona, A. Mantovani, and S. Sozzani. 1995. Phosphatidic Acid and Lysophosphatidic Acid Induce Haptotactic Migration of Human Monocytes. *Journal of Biological Chemistry*. 270:25549-25556.

Zhu, J.-K. 2003. Regulation of ion homeostasis under salt stress. *Current Opinion in Plant Biology*. 6:441-445.

Zonia, L., and T. Munnik. 2004. Osmotically induced cell swelling versus cell shrinking elicits specific changes in phospholipid signals in tobacco pollen tubes. *Plant Physiology*. 134:813-823.

APPENDIX I
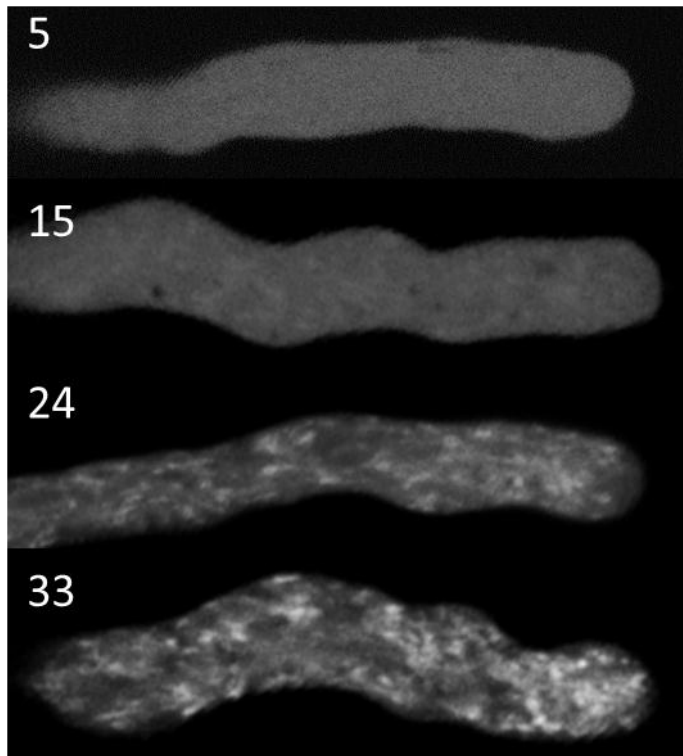
Supplemental Figure 1: BCECF AM is sequestered in to organelles of *Papaver* pollen tubes after 30 min incubation

Pollen tubes were stained with 1µM BCECF AM for a minimum of 5 minutes before imaging using a Leica confocal microscope. Numbers refer to the length of time (min) that the pollen tube was incubated with the pH indicator BECEF AM.
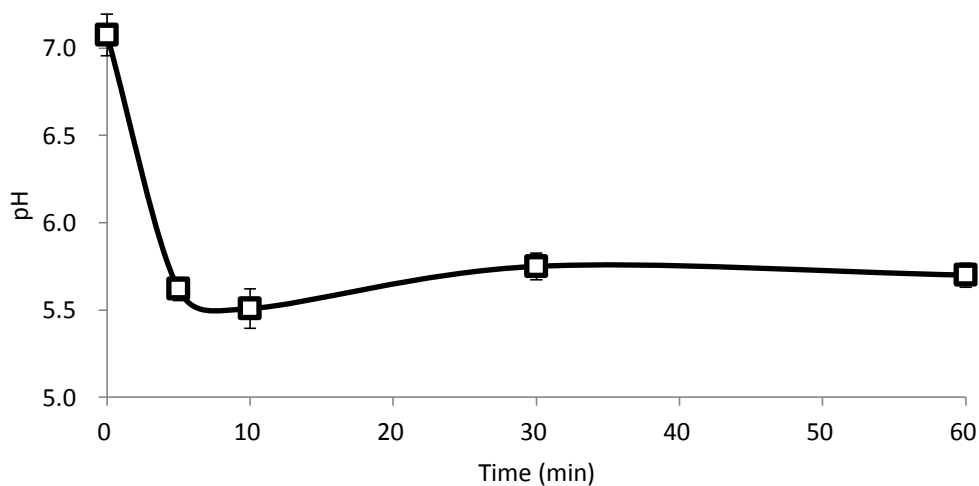
Supplemental Figure 2: Artificial acidification of pollen tubes with 100 mM sodium acetate pH 5.5.

Papaver pollen was loaded with 60 µM BCECF AM either prior to the addition of 100 mM sodium acetate (NaOAc). Ratiometric imaging of loaded cells was carried out with a confocal microscope. A ratio value was calculated for the pair of images and a pH value was calculated using a calibration curve. Within 5 min of NaOAc there is asignificant acidification of the cytosol, and over the 60 min period there was no significant recovery of cytosol pH. N=11.

APPENDIX II

Published papers

de Graaf BH, Vatovec S, Juárez-Díaz JA, Chai L, Kooblall K, **Wilkins KA**, Zou H, Forbes T, Franklin FC, Franklin-Tong VE (2012). The *Papaver* self-incompatibility pollen S-determinant, PrpS, functions in *Arabidopsis thaliana*, *Curr Biol*, **24;22(2):**154-9.

My contribution: I carried out confocal imaging of *Arabidopsis* pollen labelled with the actin probe rhodamine phallioidin and organized the figure and wrote the legend. I also proof-read the manuscript before submission.

Bosch M, Poulter NS, Perry RM, **Wilkins KA**, Franklin-Tong VE (2010). Characterization of a legumain/vacuolar processing enzyme and YVADase activity in *Papaver* pollen, *Plant Mol Biol.* **74 (4-5)**:381-93.

My contribution: I carried out confocal imaging of *Papaver* pollen tubes labelled with a probe FAM-YVAD-FAM which labels pollen with caspase-1-like activities. I also organized the figure and proof-read the manuscript before submission.